Impacts of Climate Change and Land-use Change on the Water Resources of the Upper Kharun Catchment, Chhattisgarh, India

Inaugural – Dissertation

zur

Erlangung des Grades
Doktor-Ingenieur
(Dr.-Ing.)

der
Landwirtschaftlichen Fakultät
der

Rheinischen Friedrich-Wilhelms-Universität
zu Bonn

Navneet Kumar
aus
Patna, Indien

Gedruckt mit der Unterstützung des Deutschen Akademischen Austauschdienstes (DAAD)

1. Referent: Prof. Dr. Janos J. Bogardi

2. Referent: Prof. Dr. Jürgen Kusche

Tag der Promotion: 10.09.2014

Erscheinungsjahr: 2014

Diese Dissertation ist auf dem Hochschulschriftenserver der ULB Bonn http://hss.ulb.uni-bonn.de/diss_online elektronisch publiziert

ABSTRACT

The Upper Kharun Catchment (UKC) is one of the most important, economically sound and highly populated watersheds of Chhattisgarh state in India. It covers diverse land-use types: urban, rural, agricultural, forest and industrial areas. The study area is a part of the newly formed state, which was established in 2000 and is characterized by considerable population growth and expansion of urban areas, industrialization, and irrigation areas and facilities for meeting the increasing food demand. Furthermore, the government has planned the formation of the new capital city. The planning unit is partly in the study area, and hence there is an urgent need to estimate the impact of future land-use change on the water resources of UKC, and to consider whether and to which degree the intensification of irrigated agriculture is putting the groundwater resources of the UKC at risk of over-exploitation that might lead to a major water crisis in near future.

Climate change is likely to severely affect the surface and groundwater resources due to changes in precipitation and evapotranspiration and their spatio-temporal distribution. The impact of future climate change may be felt more severely in the study area, which is already under stress due to the current population increase and associated demands for energy, freshwater and food. In spite of the uncertainties about the precise magnitude of climate change and its possible impacts, particularly on regional scales, measures must be taken to anticipate, mitigate and/or adapt to its adverse effects on surface and ground-water availability.

There is no research documented in literature related to climate change and land-use change impacts on water resources of the UKC. Hence, an attempt is made to overcome these shortcomings and to run the Soil Water Assessment Tool (SWAT) with high resolution input data taking irrigation issues relevant in the UKC explicitly into account. For this purpose, the climate scenarios of the PRECIS regional climate model were bias corrected to station level, and land-use maps of 1991, 2001, 2011 and 2021 were prepared with details of surface and groundwater-irrigated areas. The results of the study provide the base for framing strategies for water resource management in the study area.

The trend analyses show that the overall rainfall trend for the UKC increased at a rate of 1.94 mm per annum at $p=0.033$ level of significance from 1961-2011. No statistically significant change in rainfall in the month of peak rainfall was observed. Mid July remains the period of peak rainfall over the years (1961-2011). There was no significant trend for mean annual temperature. However, slight increase in temperature was detected in specific months.

The bias-corrected PRECIS RCM scenarios show an increasing trend for both mean annual rainfall and temperature (except for the q0 and q1 scenarios for the 2020s, where there is a decrease in annual rainfall compared to the baseline). The mean monthly rainfall increases for all scenarios, except for the month of June, where a significant decrease in rainfall is predicted.

The main land-use change pattern between 1991 and 2011 shows a significant increase in urban areas by 4.67%, decrease in wasteland by 3.76%, increase in area under two-season crops by 5.43 %, while 5.67% of the area is under more than two-season crops with paddy as a summer crop. The two and more than two-season crops are irrigated by groundwater sources. The land-use scenario of 2021 shows a further increase in built-up area by 2.6% compared to 2011. Also, the groundwater-irrigated area with two-season crops is expected to increase by 24.25% and the area with more than two-season crops with summer paddy by 12.57%, which indicates an excessive increase in groundwater irrigation for some villages in the UKC and unsustainable use of the precious groundwater resources.

On the UKC scale, the impact of land-use change on different water balance components is small. There is a decreasing trend of annual discharge, water yield and groundwater contribution to streamflow, and an increasing trend of annual surface runoff and actual evapotranspiration over the decades. The impact on water resources is significant and clearly visible at sub-catchment level, where an increasing trend for urban areas can be observed. Based on the bias-corrected climate scenarios q0, q1 and q14, changes in the main water balance components were simulated with the SWAT model.

The simulated annual discharge for the 2020s ranged between 25.9% decrease to 23.6% increase depending on the PRECIS scenario. For the 2050s, discharged ranges between 17.6% decrease to 39.4% increase, and for the 2080s an increase in the range of 16.3% to 63.7% is simulated.

The annual surface runoff for the 2020s ranges between 28.8% decrease to 26.8% increase. For the 2050s, predictions vary between 17.9% decrease to 44.1% increase, whereas for the 2080s an increase in the range of 19.5% to 69.6% is expected.

The annual percolation for the 2020s is estimated to range between 12.8% decrease to 8.7% increase. Predictions for the 2050s range between 10.3% decrease to 15.4% increase, and for the 2080s between 0.3% decrease and 13.7% increase.

The annual groundwater contribution to streamflow for the 2020s is expected in the range of 7.0% decrease to 14.7% increase. Predictions for the 2050s range from 13.3% decrease to 64.7% increase, and for the 2080s between 10.4% decrease and 59.1% increase. Scenario Q1 shows a decrease in annual groundwater contribution to streamflow in all time steps.

ZUSAMMENFASSUNG

Das obere Kharun-Einzugsgebiet (UKC) ist eines der wichtigsten, wirtschaftlich bedeutsamen und dicht besiedelten Einzugsgebiete im indischen Bundesstaat Chhattisgarh. Es enthält vielfältige Landnutzungstypen: bebaute städtische und ländliche Flächen, Landwirtschaft, Wald und Industriegebiete. Das Untersuchungsgebiet ist ein Teil des im Jahr 2000 neu gebildeten Bundesstaates. Die Entstehung des Bundesstaates führt zu dynamischen Entwicklungen: erhebliches Bevölkerungswachstum und Ausdehnung der bebauten Flächen, Industrialisierung und Erweiterung der Bewässerungsflächen/-einrichtungen, um den steigenden Nahrungsmittelbedarf zu decken. Darüber hinaus hat die Regierung den Aufbau einer Hauptstadt für den neuen Bundesstaat geplant. Diese Planungseinheit fällt teilweise in das Untersuchungsgebiet, und somit ergibt sich die dringende Notwendigkeit, die Auswirkungen künftiger Landnutzungsänderung auf die Wasserressourcen des UKC einzuschätzen. Eine wichtige Frage besteht in diesem Zusammenhang darüber hinaus darin, ob und in welchem Ausmaß die Intensivierung der Bewässerungslandwirtschaft zu einer Gefährdung der Grundwasserressourcen durch Übernutzung im UKC führen kann und eine Wasserkrise in naher Zukunft bedingen könnte.

Der Klimawandel lässt deutliche Auswirkungen auf die Oberflächen- und Grundwasserressourcen erwarten, und zwar aufgrund von Änderungen in Niederschlag und Evapotranspiration und deren räumlich-zeitlicher Verteilung. Diese Auswirkungen sind für das Untersuchungsgebiet deswegen relevant, weil es bereits aufgrund des aktuellen Bevölkerungswachstums und den damit verbundenen Anforderungen an die Versorgung mit Energie, Wasser und Nahrungsmitteln unter Stress steht. Trotz der – insbesondere auf der regionalen Ebene bestehenden - Unsicherheiten über das genaue Ausmaß des Klimawandels und seiner möglichen Auswirkungen, müssen Maßnahmen ergriffen werden, um negative Auswirkungen auf die Oberflächen- und Grundwasserressourcen vorherzusehen, zu mildern und/oder Anpassungsstrategien zu entwickeln.

Die Literatur dokumentiert keine Forschungen im oberen Kharun-Einzugsgebiet zu den Auswirkungen von Klimawandel und Landnutzungsänderungen auf die Wasserressourcen. Diese Studie stellt den Versuch dar, dieses Defizit abzubauen. Dazu wird das Einzugsgebietsmodell SWAT genutzt, und zwar mit hoch-aufgelösten Eingangsdaten sowie expliziter Berücksichtigung der im UKC relevanten Aspekte der Bewässerung. Zu diesem Zweck wurden die Klimaszenarien des regionalen Klimamodell PRECIS auf Stationsebene Schiefe-korrigiert und detaillierte Karten der Landnutzung für 1991, 2001, 2011 und 2021 erstellt, wobei die mit Oberflächen-und Grundwasser bewässerten Flächen besondere Berücksichtigung fanden. Die Ergebnisse der Studie liefern die Grundlage für die Konzeption von Strategien für Wasserbewirtschaftung im Untersuchungsgebiet.

Ein wichtiges Ergebnis der Trendanalysen besteht darin, dass die Jahressumme des Niederschlags für das UKC zwischen 1961-2011 mit einer Rate von 1,94 mm pro Jahr ($p = 0,033$ Signifikanzniveau) zugenommen hat, wohingegen beim Jahresmittelwert der Temperatur kein signifikanter Trend festgestellt wurde. Es ergaben sich jedoch geringe Zunahmen der Temperatur in Bezug auf einige Monate. Es gibt keine statistisch signifikante Veränderung des Niederschlags in dem Monat mit den höchsten Niederschlägen. Mitte Juli bleibt der Zeitraum des Spitzenniederschlags in den Jahren 1961-2011.

Der Schiefe-korrigierten PRECIS RCM Szenarien zeigen eine steigende Tendenz sowohl für die mittlere jährliche Niederschlagsmenge und die Temperatur (mit Ausnahme der 2020er Jahre und die q0 und q1 Szenarien, die einen Rückgang des Jahresniederschlags im Vergleich zum Referenzwert angeben). Der mittlere monatliche Niederschlag steigt für alle Szenarien, mit Ausnahme des Monats Juni, wo eine signifikante Abnahme der Niederschläge vorhergesagt wird.

Die Muster der Landnutzungsänderungen zwischen 1991 und 2011 bestehen in einem deutlichen Anstieg der bebauten Gebiete (4,67%), einer Abnahme des Ödlands (3,76%) und in klaren Ausweitungen der Flächen mit jährlich zwei (5,43%) oder mehr (5,67%) Anbaukulturen und mit Reis als Sommer-Kultur. Diese zwei- oder mehrfach genutzten Flächen werden mit Grundwasser bewässert. Ein realistisches Szenario der künftigen Landnutzung für 2021 zeigt einen weiteren Anstieg der bebauten Fläche um 2,6% im Vergleich zu 2011. Es wird auch eine weitere Zunahme der mit Grundwasser bewässerten zwei- oder mehrfach genutzten Anbaufläche erwartet, und zwar um 24,25% (zweifach) und 12,57% (drei Kulturen mit Reis im Sommer). Dies führt zu einem übermäßigen Anstieg der Grundentnahmen für Bewässerungszwecke in einigen Dörfern des UKC und wirft die Frage der nachhaltigen Nutzung der kostbaren Grundwasserressourcen auf.

Auf der Ebene des Gesamteinzugsgebietes bleiben die simulierten Auswirkungen der Landnutzungsänderungen auf relevante Komponenten des Wasserhaushalts eher gering. Es wird ein abnehmender Trend des jährlichen Gesamt-Abflusses und des Beitrags des Grundwassers zum Abfluss berechnet, wohingegen die Simulationen steigende Trends bei Oberflächenabfluss und aktueller Evapotranspiration über die Jahrzehnte anzeigen. Dagegen ist der von Änderungen der Landnutzung auf den Wasserhaushalt ausgehende Einfluss signifikant und deutlich sichtbar auf der Ebene von Teileinzugsgebieten des UKC. Den klarsten Anstieg des Oberflächenabflusses im Laufe der Jahrzehnte wurde für die Teileinzugsgebiete berechnet, die einen zunehmenden Trend für bebaute Flächen aufweisen.
Auf der Grundlage unterschiedlicher Schiefe-korrigierter Klimaszenarien (q0, q1 und q14) wurden Änderungen in den relevanten Komponenten des Wasserhaushalts mit dem SWAT-Modell simuliert.
Der jährliche Abfluss für die 2020er Jahre schwankt in Abhängigkeit von dem als SWAT-Input verwendeten PRECIS Klimaszenario zwischen 25,9% Abnahme und 23,6% Erhöhung. Für 2050 liegt der simulierte Abfluss zwischen einer Abnahme um 17,6% und einer Zunahme um 39,4%. Dagegen führen die Simulationen für 2080 durchweg zu Anstiegen und zwar im Bereich von 16,3% auf 63,7%.
Für den jährlichen Oberflächenabfluss in den 2020er Jahren wird ein Korridor zwischen einer Abnahme um 28,8% und einem Anstieg um 26,8% berechnet. Für 2050 schwanken die Vorhersagen zwischen 17,9% Rückgang und 44,1% Steigerung, wohingegen für 2080 generell steigenden Tendenzen im Bereich von 19,5% bis 69,6% erwartet werden.
In Bezug auf die jährliche Versickerung weisen die Simulationsergebnisse eine Bandbreite zwischen 12,8% Abnahme und einem Anstieg um 8,7%. Prognosen für 2050 differieren zwischen 10,3% Rückgang und 15,4% Steigerung, und für 2080 liegen sie im Bereich von 0,3% Abnahme und einem Anstieg um 13,7%.
Die Simulationen des jährlichen Grundwasserbeitrags zum Abfluss für die 2020er Jahre bewegen sich zwischen einem Absinken um 7,0% und einer Steigerung um 14,7%. Prognosen für 2050 reichen von 13,3% Abnahme bis auf 64,7% Steigerung, und für 2080 werden ein Rückgang um 10,4% und eine Zunahme um 59,1% zu geschätzt. Das Szenario Q1 führt in Bezug auf alle Simulationszeiten (im Vergleich mit dem Referenzzeitraum) zu Abnahmen des Grundwasserbeitrags zum Abfluss.

TABLE OF CONTENTS

ACKNOWLEDGEMENTS

LIST OF ACRONYMS AND ABBREVIATIONS

AGCM	Atmospheric General Circulation Model
AOGCM	Atmosphere Ocean General Circulation Model
ARMA	Auto Regressive Moving Average
ARS	Agricultural Research Station
CGWB	Central Ground Water Board
CUSUM	Cumulative Sum
CWC	Central Water Commission
DEM	Digital Elevation Model
DLR	Deutsches Zentrum für Luft- und Raumfahrt
EPCO	Plant Uptake Compensation Factor
ERDAS	Earth Resources Data Analysis System
ESCO	Soil Evaporation Compensation Factor
ETM+	Enhanced Thematic Mapper Plus
FAO	Food and Agricultural Organization
GCM	General Circulation Model
GEC	Groundwater Resource Estimation Committee
GHG	Greenhouse Gas
GIS	Geographical Information Systems
GLCF	Global Land Cover Facility
GPS	Global Positioning System
GRACE	Gravity Recovery And Climate Experiment
HRU	Hydrologic Response Unit
IGKV	Indira Gandhi Krishi Vishwavidyalaya
IITM	Indian Institute of Tropical Meteorology
IPCC	Intergovernmental Panel on Climate Change
LARS WG	Long Ashton Research Station Weather Generator
LULC	Land Use and Land Cover
MATLAB	Matrix Laboratory
MFC	Mahanadi Feeder Canal System
MODFLOW	Modular Three-Dimensional Finite-Difference Groundwater Flow Model
MSS	Multispectral Scanner
NASA	National Aeronautics and Space Administration
NCCR	North Central Chhattisgarh Region
NDVI	Normalized Difference Vegetation Index
NIH	National Institute of Hydrology
NOAA	National Oceanic and Atmospheric Administration
NRDA	Naya Raipur Development Authority
NRSC	National Remote Sensing Center
OGCM	Ocean General Circulation Model

OLS	Ordinary Least Squares
PEST	Parameter Estimation
PET	Potential Evapotranspiration
PRECIS	Providing Regional Climates for Impacts Studies
R^2	Coefficient of determination
RCM	Regional Climate Model
ROI	Region of Interest
SDSM	Statistical Downscaling Model
SOI	Survey of India
SRES	Special Report on Emissions Scenarios
SRTM	Shuttle Radar Topography Mission
SUFI 2	Sequential Uncertainty Fitting 2
SURQ	Surface Runoff
SWAT	Soil and Water Assessment Tool
TM	Thematic Mapper
UKC	Upper Kharun Catchment
UTM	Universal Transverse Mercator
USDA	United States Department of Agriculture
USGS	United States Geological Survey
ZEF	Center for Development Research

CHAPTER 1: INTRODUCTION

1.1 Background

Water is a precious resource for mankind. The world's increasing thirst for water is assumed to become one of the most pressing resource issues of the 21st century. Since water is limited, scarce and not spatially and temporally well distributed among the different regions and stakeholders, proper management and utilization is required to satisfy the current requirements as well as to meet the future demand in a sustainable way.

India accounts for more than 16% of the global population but has only 4% of the world's total freshwater resources. Water demand for the agricultural sector, households, and recreational and industrial use has been rapidly increasing during the past few decades and is expected to grow in days to come. Furthermore, water requirements (in terms of quantity and quality) to secure ecosystems and their functioning need to be considered more strongly than in the past. Indian's current population is around 1.18 billion with an annual growth rate of 1.6 % and is expected to rise to 1.6 billion by 2050. In addition, urbanization and industrialization are growing at a fast rate, and are energy and water intensive. To feed millions of people, India must increase its food production from about 208 million tons in the period 1999-2000 to around 350 million tons by 2050. Present statistics show that agriculture is the biggest consumer of water in the country. More than 85% of India's freshwater is utilized by agriculture alone and, according to the Ministry of Water Resources, it is expected that the irrigation needs will increase by 56% by the year 2050, while the demand for drinking water will double and the need for water for energy production will increase 16 fold (Asian Development Bank, 2003).

A path-breaking innovative study carried out by DLR's and NASA's twin satellite GRACE for the north-western Indian states (Rodell et al., 2009) has revealed that these regions are facing a serious, acute and alarming situation of declining groundwater tables. The report states that 109 km^3 of groundwater disappeared from the aquifers in Rajasthan, Punjab, Haryana and Delhi between 2002 and 2008. This amount of water is equivalent to double the capacity of India's largest reservoir and three times that of Lake Mead, the largest manmade reservoir in the USA. Rodell et al. (2009), a hydrologist team from NASA concluded that human activities may be the major cause for this drastic decline in groundwater. The study therefore not only reveals a loss of precious groundwater resources, but also indicates unsustainable water management practices in a densely populated (114 million) and highly vibrant agriculture belt in India. In case the alarming trend of groundwater depletion is not stopped or reversed by appropriate management of surface and groundwater resources, a serious and threatening problem is pointing towards a major food and water crisis in the near future.

For the last few decades, research regarding the impact of climate change and land-use / land cover change on water resource availability has been of great concern. According to the Intergovernmental Panel on Climate Change (IPCC, 2007), the global mean temperature may

increase between 1.8℃ and 4℃ by 2100 and will severely affect the availability of water resources and the water demand across the world.

India's freshwater resources are mainly generated by the southwest monsoon. As a consequence, fulfilling water requirements for agriculture, industries, domestic purposes, energy sectors and ecosystems depends on this climatic phenomenon. More than 80% of the annual rainfall occurs during the monsoon period. Therefore, any change in the climate especially, in the southwest monsoon, over India would have a significant impact particularly on agricultural production, which is already under stress due to the current population increase, problems related to water resources management, and the overall socioeconomic situation in the country.

Numerous studies have predicted changes in temperature and rainfall over the entire landscape of India. Throughout the 21st century, it is projected that India and Southeast Asian countries will face more warming than the global mean. There will be greater variation in temperature with more warming in winter than in summer in India (Christensen et al., 2007). The longevity of heat waves in India has increased in recent years, resulting in warmer nights and hotter days, and this trend is continuing (Cruz et al., 2007). These heat waves resulted in increased variability in summer monsoon precipitation, severely affecting water resources and causing drastic losses in the agricultural sector (Bhadwal, 2003).

Climate change is likely to severely affect the surface and groundwater resources due to changes in precipitation and evapotranspiration and their spatio-temporal distribution. Increased intensity of precipitation in short heavy spells in tendency leads to more surface runoff, an increase in flood risk in low lying areas and a decrease in the groundwater recharge. A rise in temperature causes higher evapotranspiration and a greater demand for water for irrigation. In addition, rising sea levels may lead to increased saline intrusion into coastal and island aquifers, while increased frequency and severity of floods may affect groundwater quality in alluvial aquifers (Mall et al., 2006).

Declining groundwater tables due to reduced recharge and increasing withdrawals (at least partly caused by climate change) not only impacts on water balances, but also exerts an adverse feedback to the atmosphere in terms of CO_2-emissions, thus leading to increasing climate change. As a consequence, improvements in water management are strategies towards climate change adaption as well as mitigation. "The most optimistic assumption suggests that an average drop in groundwater level by one meter would increase India's total carbon emissions by over 1%, because the deeper groundwater level is increasing the amount of groundwater to be lifted and this is raising the requirements on pump capacity (and in turn fuel demand). A more realistic assumption reflecting the area projected to be irrigated by groundwater suggests that the increase in carbon emission could be 4.8% for each meter drop in groundwater levels" (Mall et al., 2006).

The impact of climate change on the hydrological cycle has been reported from different parts of world (Dragoni, 1998; Buffoni et al., 2002; Labat et al., 2004; Huntington, 2006; IPCC,

2007). Benderev et al. (2008) observed that, due to climate change, the groundwater recharge to the aquifers in Bulgaria dropped significantly from 1982-1994. Groundwater recharge is an important issue, because it links surface and groundwater resources and can be used as a starting point to conceive options intervening in surface water management aiming at sustainable use of surface and groundwater resources. Rising sea levels due to climate change have resulted in the intrusion of saline water into the fresh groundwater in coastal aquifers of India and this is thus severely affecting groundwater resources (IPCC, 4^{th} assessment report, 2007). Groundwater resources in arid regions are especially endangered by the effects of climate change, and a minor change in precipitation has a significant impact on the groundwater resources in these regions (Delude, 2010). Gosain et al. (2006) reported that under the influence of climate change the freshwater availability is likely to decrease significantly in many river basins in India. The situation will deteriorate till 2050 due to the growing population, the increasing food, water and energy demand by different sectors, and the improving living standard.

The impact of future climate change will be felt more severely in developing countries such as India, whose economy is largely dependent on agriculture and is already under stress due to the current population increase and associated demands for energy, freshwater and food. In spite of the uncertainties about the precise magnitude of climate change and its possible impacts, particularly on regional scales, measures must be taken to anticipate, prevent or minimize the causes of climate change and mitigate and/or adapt to its adverse effects on surface and groundwater availability.

Land-use / land cover change has a direct and significant impact on the amount of evapotranspiration, surface runoff and groundwater recharge driven by infiltration during and after precipitation events. These factors regulate the water budget of surface streams and groundwater aquifers and hence the amount of water available for both ecosystem functions and human uses (Houghton and Hackler, 2003; Mustard and Fisher, 2004; Sakai et al., 2004; Jarosz et al., 2009).

According to a number of climate models, it has been concluded that land-use changes also affect temperature patterns and global precipitation, ultimately affecting the global hydrological cycle (Chase et al., 2000).

A number of studies worldwide have confirmed that land-use/ land cover changes such as conversion of forest to agriculture, industrial development, mining, etc., have a severe effect on the accelerated rate of surface runoff, and on groundwater recharge, erosion, sediment transport and land degradation. The worldwide annual river discharge has increased significantly since 1900, and research suggests that land-use change may be directly responsible for more than 50% of this increase (Piao et al., 2007).

One of the important factors responsible for increasing surface runoff and evapotranspiration is the amount and type of vegetative land cover. It has been found that the forests are responsible

for higher rates of evapotranspiration and interception as compared to grass and scrublands, which ultimately influences the amount of water available for direct drainage into streams or for aquifer recharge (Farley et al., 2005). Interception is an important process which directly affects the water balance. Leaves and litter of forest trees store a significant amount of water during precipitation and then facilitate the water infiltration into the soil. Without this interception, the excess precipitation immediately tends to run off and discharge into the stream flow. Hence, deforestation causes more surface runoff, higher stream yield and less groundwater recharge during the precipitation events and lower base flow between precipitation events (Costa et al., 2003).

Conversion of forest and agricultural land driven by urban development into settlements and infrastructures forms a sealed surface, which is adversely changing the partitioning of precipitation towards more surface runoff and reduced groundwater recharge (Mustard and Fisher, 2004; Shanahan and Jacobs, 2007; Jat et al., 2009). Additionally, the disposal of urban waste has a severe impact on groundwater quality (Shanahan and Jacobs, 2007).

Mustard and Fisher (2004) concluded that the change in land-use from native vegetation (e.g., forest area) to cropland has a significant impact on the evapotranspiration, infiltration and surface runoff of a watershed. Despite the type and area of a crop, there has always been some proportion of bare land even during the peak of the growing season, and cropland may be completely bare before the planting season. In both cases, most of the rainfall received on these bare soils is directly discharged to streams, which leads to increased peak discharge and decrease in groundwater recharge.

Bosch and Hewlett (1982) conducted an analysis of 94 paired watershed studies throughout the world, and concluded that there is a consistent relationship between the amount of forest cover and water yield (the net amount of water that leaves the sub-basin and contributes to streamflow). A decrease in forest cover leads to more surface runoff and hence increased stream flow and vice versa. It has been reported that on average, deforestation causes a 4-fold increase in water yield as compared to loss of grassland and by a factor of 1.6 as compared to loss of shrubland. It should be mentioned that even the type of forest might have an impact on the water balance. Young and Evans (1998) studied the impact of land-use change on groundwater quantity in the green triangle area of South Australia and Victoria. They found that deep-rooted forest trees such as pines are responsible for groundwater depletion, and that the replacement of pines with shallow-rooted trees or crops would be a solution for managing the declining groundwater tables in the area.

Since land-use change has a significant and profound impact on water quality and quantity, there is an urgent need to integrate land-use change, hydrology and water resources management in future research initiatives (DeFries and Eshleman, 2004).

Models are needed to estimate the impacts on water fluxes and balances caused by future trends of influential factors (e.g., impact of changing rainfall patterns under the influence of climate change on future water balances and effect of land-use change on water fluxes).

Groundwater recharge by percolation links surface and groundwater resources, and is the dominating input into the groundwater system. Therefore, by improving the precision of the recharge estimation, a considerable improvement for modelling and managing surface as well as groundwater resources can be expected.

The Soil and Water Assessment Tool (SWAT) is such a surface water model, which provides quite effective capabilities to model the spatio-temporal distribution of groundwater recharge and thus the integration of the spatio-temporal percolation as an input into groundwater models (e.g., MODFLOW). This is a promising step towards improving the results of groundwater modeling.

1.2 Problem definition

Surface water and groundwater are linked components of the hydrological cycle. They interact in nature and are hydraulically connected to each other. However, their interactions are difficult to observe and measure, so these interactions have often been ignored in modeling and water resource management (Winter et al., 1998). Surface water significantly contributes to the groundwater flow and chemical budget of groundwater and vice versa.

Surface and groundwater are linked mainly by percolation (groundwater recharge), and eventually (depending on water levels) by direct contact between surface water bodies (rivers, lakes, irrigation canals, drainage ditches) and the aquifer.

In order to provide the base for proper surface and groundwater management, determination of groundwater recharge needs to be conducted with an appropriate spatial (and temporal) resolution. Though there are approaches to determine the recharge (from water balancing), these are not appropriate for spatial and temporal estimation of groundwater recharge. Surface water models are efficient in spatio-temporal mapping of groundwater recharge, whereas groundwater models are efficient for groundwater flow modeling. Hence, a combined application of surface and groundwater modeling tools has the potential to provide the appropriate understanding of the hydrological processes and interaction of a system.

A number of studies have assessed the impact of climate-change scenarios on the hydrology of various regions throughout the world. However, so far little work has been done on the hydrological impacts of possible climate changes for basins in India (Mall et al., 2006). Based on existing literature review, it is clear that land-use change has a significant impact on water resources. However there appears to be a critical gap in research that considers the potential response of water resources to land-use change for sustainable management of water resources at the watershed scale (Sahin and Hall, 1996; MacMillan and Liniger, 2005).

1.3 Problems related to the study area (Upper Kharun Catchment)

Water resources in the Upper Kharun Catchment (UKC) are under pressure due to urbanization and intensification of irrigated agriculture and, as a consequence, improvements in water management are urgently needed. The following features and trends in the UKC illustrate this assessment:

(1) Groundwater resources are increasingly used in the study region mainly due to extension of groundwater irrigated areas in the dry season.
(2) Current and especially future trends will strongly influence the water fluxes and balances in a manifold and complex way. Urbanization in Raipur and the surrounding area due to the establishment of the capital city of Chhattisgarh creates a tendency towards increasing surface runoff and decreasing percolation and groundwater recharge. Expanding and intensifying irrigated agriculture may lead to higher percolation. The resulting trends in terms of water fluxes depend on the above-mentioned spatio-temporal drivers, and need to be answered by spatially explicit water management strategies. Thus, consideration of spatial distribution of the time-dependent hydrological processes is necessary.
(3) The impacts of land-use dynamics on water fluxes and balances are overlaid by the consequences of climate change influencing rainfall, which is a major input into hydrological systems, and also temperature, a relevant factor on the water demand side.
(4) Current analyses do not sufficiently consider the impacts of climate and land-use change and their interaction on the water resources in UKC.
(5) There is an urgent need for improving management in terms of joint consideration of surface and groundwater resources. Modelling spatio-temporal water fluxes in the catchment and deriving the percolation/groundwater recharge interlinking surface and groundwater resources is a promising starting point.
(6) Current analyses on the impact of climate change and land-use change on hydrology do not sufficiently consider the groundwater recharge. However, groundwater needs special consideration because it offers interesting features for usage, but on the other side needs careful protection. As climate change is expected to increase the variability especially of the surface water resources, the storage capacity of aquifers is an interesting feature to buffer short-term demand-supply gaps. On the other hand, groundwater is the main source for drinking water and irrigation, and changes in terms of depletion and quality are rather slow, but they are time consuming and costly to reverse. Furthermore, in periods of low discharge in the rivers, groundwater strongly contributes to discharge. As these are critical periods in terms of low water flow with a risk of demand-supply gaps, integration of groundwater management into overall water management at basin level is urgently needed.

Main objectives of the research

The overall aim of this research is to investigate the impact of climate change and land-use / land cover change on the water resources of the Upper Kharun Catchment, India.

Sub-objectives:

- Time series trend detection of rainfall and temperature.
- Bias correction and analysis of regional climate change scenarios (PRECIS).
- To estimate the water fluxes and the water budget with high spatio-temporal resolution using SWAT considering the features of irrigation and land-use dynamics in the study region.
- To derive the ground-water recharge and its spatio-temporal behaviour from the percolation estimated by SWAT.
- To provide a procedure to transfer percolation by SWAT referring to Hydrological Response Units (HRU) into grid-based recharge as input to groundwater model (MODFLOW).
- To analyse the impact of climate change on the water resources of the Upper Kharun Catchment.
- To analyse the impact of land-use / land cover changes on the water resources of the Upper Kharun Catchment using SWAT.

Research questions

- What is the impact of climate change on the water resources of the Upper Kharun Catchment?
- What is the effect of changing land-use/ land cover on the water resources of the Upper Kharun Catchment?
- What are the appropriate strategies for sustainable surface and groundwater management?

1.4 Structure of the thesis

This thesis consists of eight chapters, which are briefly outlined below. Each chapter tackles a major research theme of the thesis and provides a complete analysis including introduction, methodology, data used and results.

Chapter 1 and Chapter 2: Chapter 1 provides a general introduction, defines and describes the problem addressed by the research in the study area and presents the main and sub-objectives of the overall research and the research questions. Chapter 2 is devoted to the description of the study area and includes the physical features, climatic conditions and population dynamics. It also discusses the various data and their sources used in the current study.

Chapter 3: Climate change analysis
This chapter presents the historical time series trend detection analysis of rainfall and temperature. Results of both parametric and non-parametric methods of trend detection analysis are discussed in detail. The PRECIS regional climate model for future rainfall and temperature scenarios of the study area were downscaled or bias corrected to station level and compared with the baseline observed scenarios, and the results are discussed.

Chapter 4: Land-use
This chapter describes the approach to develop land-use maps of three decades (1991, 2001 and 2011). The future land-use map of 2021 was prepared based on information gained from the government development planning unit, past land-use change statistics and expert knowledge.
The land-use maps were prepared at two scales: broad (5 classes) and detailed (19 classes) classification and the land-use changes over the decades analyzed.

Chapter 5: Irrigation
This chapter contains the description of the canal networks, identifies the sources of irrigation water at different locations of the study area, differentiates the extent of surface and groundwater irrigated areas, and analyses the amount of irrigation water applied. Furthermore, statistics describing the change in irrigated areas over the decades are established.
Hot-spot locations/ villages utilizing extensive groundwater resources for irrigation were identified, and a trend detection analysis of groundwater levels was carried out for the study area.

Chapter 6: SWAT model set up, sensitivity analysis, calibration and validation
In this chapter, the input data for and the setup of the SWAT model are described. Analyses deal with sensitive hydrological parameters, model uncertainties and the calibration and validation.
An approach of linkage file preparation, which converts the HRU-based percolation as an output from SWAT model into grid format required for input into MODFLOW, is discussed.

Chapter 7: Analyses on the impact of climate change and land-use changes on water resources in the Upper Kharun Catchment
This chapter presents the impact analysis of PRECIS climate change scenarios (q0, q1 and q14) on water balance components of the study area. The past and potential future land-use changes are driven by the model to analyse the impact of land-use changes on the water resources. The land-use impact analysis is performed at the level of the entire catchment and at a refined resolution using the sub-catchment scale.

The impact of both climate change and land-use change on water balance components is also investigated.

Chapter 8: Conclusions and recommendations for further research
This chapter summarizes the results of all chapters and highlights the main contribution and findings of this research. Furthermore, the limitations of the model taking the situation of the study area into account are summarized and recommendations for future research are made.

CHAPTER 2: STUDY AREA

2.1 Introduction

The study area, Upper Kharun Catchment (UKC), is a part of the Seonath sub-basin (a tributary of Mahanadi river basin). In terms of administrative units, the UKC is located in parts of Raipur, Durg and Dhamtari districts of Chhattisgarh state, India. It is one of the most important, economically sound and highly populated catchments of this state. Raipur is the capital city and is the most developed district followed by Durg and Dhamtari districts. The UKC covers diverse land-use types, i.e., urban, rural, agricultural, forest and industrial areas.

2.1.1 Background

Chhattisgarh state is located in the central part of India. It is a newly formed state, carved out from Madhya Pradesh state in 2000. It covers an area of 135,100 km^2. With respect to hydrology, the state is divided into five major river basins, i.e., Mahanadi, Godavari, Ganga, Brahmani and Narmada. These basins drain out 75859, 38694, 18407, 1394 and 744 km^2 of the catchment area, respectively. Seonath sub-basin is a part of Mahanadi river basin, located between 20^0 16' N and 22^0 41' N latitude and 80^0 25' E and $82^0$35' E longitude and covers an area of 30,860 km^2. The sub-basin is further divided into 16 catchments, i.e., Kharun, Jamunia, Khorsi, Lilagal, Arpa, Maniyari, Sakari, Karua, Dotua, Surhi, Amner, Sukha Gamriya, Dalekasa, Kharkhara, Tandula and Seonath main (Figure 2.1).

2.1.2 Location

Kharun River is one of the main tributaries of the Seonath River. It is a non-perennial river, which gets dry during the mid-winter season. It originates from Petechua village of Balod block in the southeast of Durg district, and after flowing about 164 km joins Seonath River near Somnath in the north. The total catchment area of Kharun river is 4118 km^2 and is located between 20^0 33' 30" - 21^0 33' 38" N latitude and 81^0 17' 51" E - 81^0 55' 25" E longitude. The catchment upstream to the gauging and discharge measuring station of the central water commission situated at Patharidih comprises the study area and is denoted as the Upper Kharun Catchment (UKC) covering an area of 2486 km^2. The study area lies between 20^0 33' 30" N - 21^0 22' 05" N latitude and 81^0 17' 53" E - 81^0 45' 17" E longitude. From the origin to the gauging station Patharidih, the length of Kharun River is 120 km. The GPS location of Patharidih discharge measuring station is 21° 20' 23.9" N latitude and 81° 35' 59.9" E longitude.

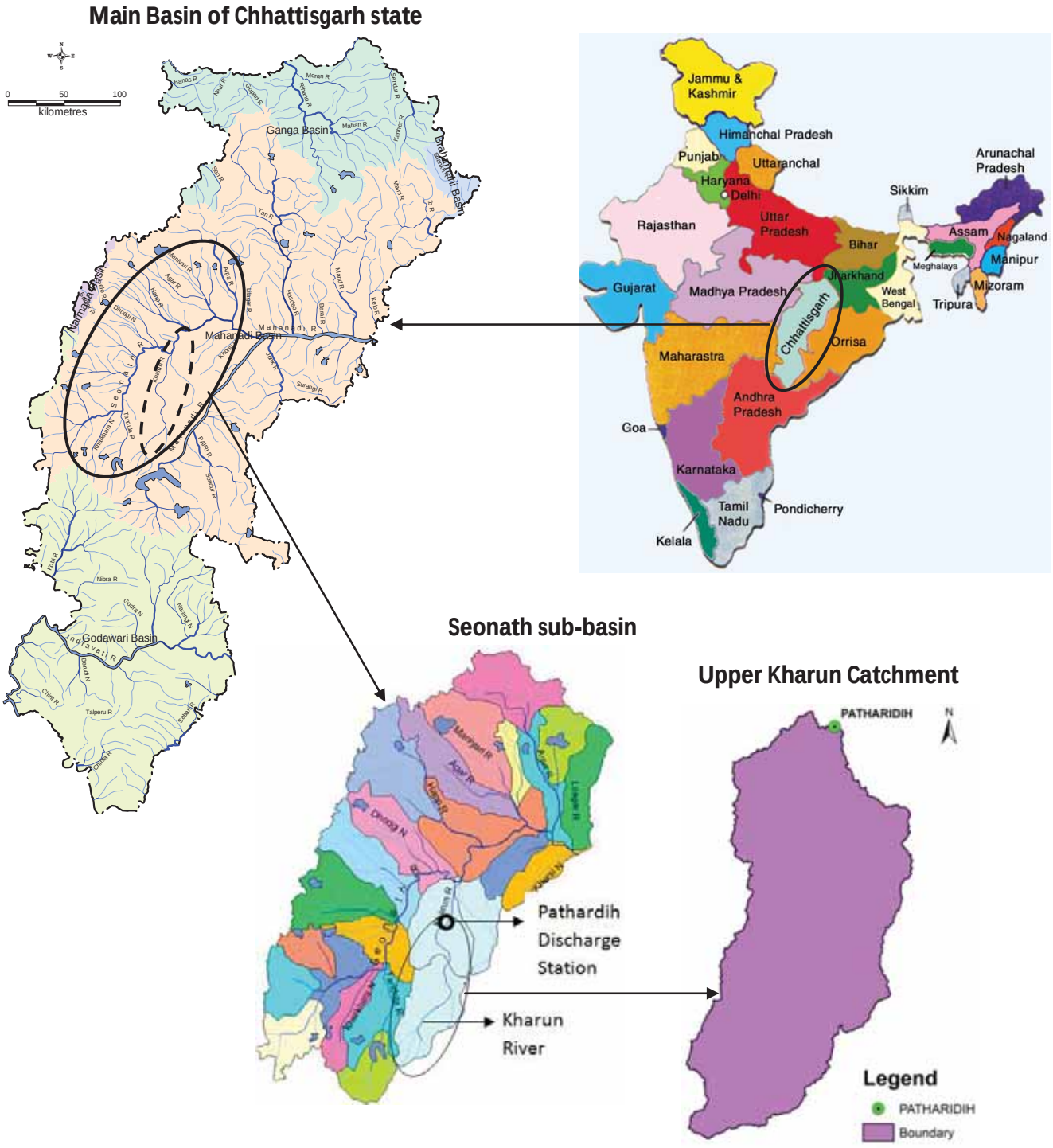

Figure 2.1: Location of the Upper Kharun Catchment

2.1.3 Upper Kharun Catchment

The boundary of the Upper Kharun Catchment (UKC) is delineated based on a digital elevation model and also on manual digitization based on the elevation contours and drainage network of

toposheets. Later, a comparison was made, and it was found that both delineated UKC boundaries matched well, which confirms the accuracy of the boundary for further study.

Administrative boundary maps and spatial shapefiles of Raipur, Durg and Dhamtari at village, block and district level were collected from the Council of Science and Technology, Raipur. The projection systems of these administrative units are in Universal Transverse Mercator (UTM). Later, the boundary shapefile of the UKC was overlaid on these administrative units one by one and the exact district, block and village areas located in the UKC were spatially clipped off and the area in hectares was calculated using ArcGIS 10.1.

The census book information was further used to differentiate between the urban and rural settlements. The rural settlements are the names of the villages and the urban settlements are Municipal Corporation, towns or cities.

On the border of the UKC, some villages and urban areas are only partly located in UKC. Only the areas inside the UKC were considered, clipped and used for further analysis.

The study area lies in three districts, i.e., Durg, Dhamtari and Raipur, covering 1511 km^2, 554 km^2 and 421 km^2 respectively. The UKC is situated in parts of 12 blocks of Chhattisgarh and consists of 541 villages and 62 towns/cities (Table 2.1 and Figure 2.2).

Patan block is the largest area in the UKC with 29.84 % of the total area, followed by Gurur Block with 18.89 %. Balod, Durg, Berla and Arang only cover small areas, i.e., 1.83, 1.24, 0.52 and 0.01 % of the UKC, respectively.

Detailed basic information about irrigated area, population, land-use etc., were gathered and processed at village and city/town level, and summed up to block level. Hence, a highly informative database was prepared for the study. The census book reports of 1991and 2001 were procured from the Population and Census office, Raipur. Regional agriculture offices in each block and irrigation departments in Raipur, Durg and Rudri provided the basic village information for 2011.

Table 2.1 Area of Upper Kharun Catchment

S.N	District Name	Area (km^2)	Block name	Area in UKC (km^2)	% of total area	Number of villages	Number of cities / urban areas
1	**Raipur**	420.5	Dharsiwa/Raipur	186.4	7.5	24	25
2		(16.9%)	Abhanpur	233.8	9.4	46	1
3			Arang	0.3	0.0	1	0
4	**Dhamtari**	554.2	Dhamtari	253.6	10.2	63	7

5		(22.3%)	Kurud	300.6	12.1	78	2
6	**Durg**	1511.2	Patan	741.9	29.8	142	15
7		(60.8%)	Berla	12.9	0.5	5	0
8			Balod	45.6	1.8	20	0
9			Durg	30.7	1.2	5	5
10			Dhamdha	129.8	5.2	26	5
11			Gunderdehi	80.8	3.3	25	0
12			Gurur	469.5	18.9	106	2
			TOTAL	**2485.9**		**541**	**62**

Districts in UKC=03	**Blocks in UKC=12**	**Rural and Urban areas in UKC=603**
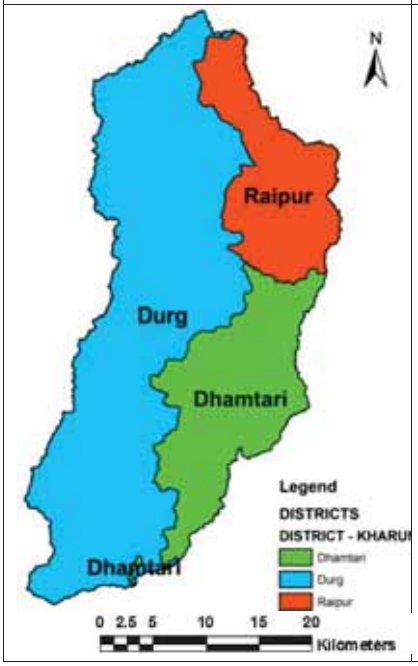		

Figure 2.2: Districts, blocks and rural and urban administrative boundaries in UKC

2.1.4 Transportation network

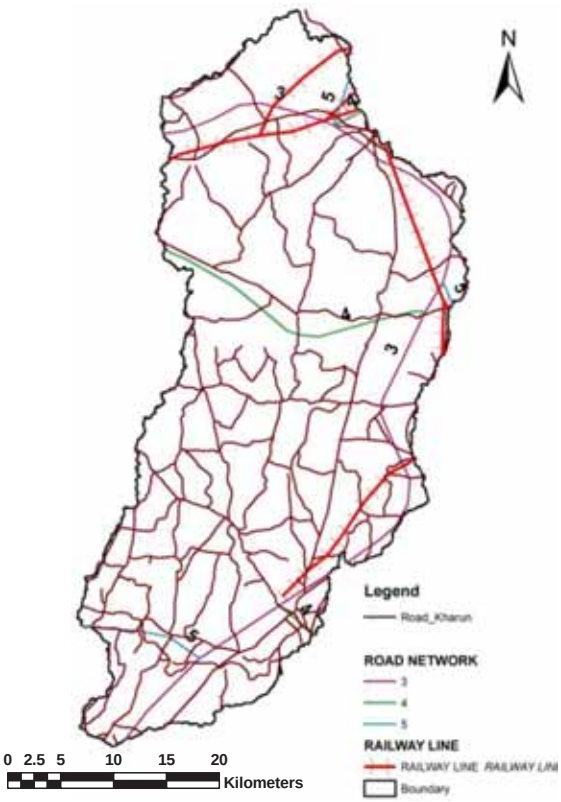

Figure 2.3: Transportation network

There are two national highways running parallel to the UKC boundary on the east and west side. There is also a railway line between Dhamtari, Abhanpur and Raipur that also connects Raipur to the Bhilai Steel Plant and Durg. The villages of the UKC are connected to each other by roads. Electricity is available to all the villages in the UKC.

2.1.5 Demography: population dynamics of UKC

The census book reports on population at village level for 1991, 2001 and 2011 were processed and the exact population of each village was derived based on the percentage of village area in the UKC. Later, the village population is summed up for each block (Table 2.2).

Only the village Ramchandi is in Arang block. The village has been deserted for over a decade.

Based on the increase in population over the decades, an annual growth rate between 1991 and 2001 and between 2001 and 2011 was estimated for each block. Overall, there was a rapid rise in the population. The total population in 2011 was 1936851, which increased at an annual growth rate of 2.62 % between 2001 and 2011.

Population annual growth rate is calculated as:

$$\text{Population future} = \text{Population present}\ (1 + \text{Population annual growth rate}/100)^{n} \quad (2.1)$$

where n= number of years

Assumption: In the present study, the population growth rate of 2011 (2.62%) is considered as constant for future decade and is applied to predict the population growth in 2021 for each block in the UKC. This assumption is just one scenario out of many probabilities; the future population growth rate is highly uncertain and depends on many factors.

Table 2.2 Population dynamics of Upper Kharun Catchment

S.N	Block Name	Population 1991	Population 2001	Population 2011	Present growth rate	Population projection 2021
1	Dharsiwa / Raipur	427293	614391	920488	4.12	1379086
2	Abhanpur	60250	77991	94920	1.98	115524
3	Arang	0	0	0	0	0
4	Dhamtari	141689	172084	202198	1.63	237582
5	Kurud	79172	98331	112457	1.35	128612
6	Patan	212666	279973	325702	1.52	378900
7	Berla	1400	3454	3873	1.15	4343
8	Balod	12316	15101	16595	0.95	18237
9	Durg	25168	35016	41331	1.67	48785
10	Dhamdha	31523	54741	59210	0.79	64044
11	Gunderdehi	16547	20786	22991	1.01	25430
12	Gurur	102307	125185	137086	0.91	150118
	TOTAL (UKC)	**1110331**	**1497053**	**1936851**	**2.62**	**2508512**

2.2 Topography

The topography of the study area was analysed using survey of India toposheets, satellite images and field observations. There were 8 survey of India toposheets representing the Upper Kharun Catchment at 1:50,000 scale. The toposheet numbers are G – 7, 8, 11 & 12 and H – 5, 6, 9 & 10. The toposheets were procured from office of the Director, Chhattisgarh Geo Spatial Data Centre,

survey of India. The toposheets were used for extracting the information on elevation contours, drainage networks and land-use type.

2.2.1. Drainage network

The surface water and base flow of the UKC drains out to Kharun River, which is a tributary of Seonath River. The hydrograph of Kharun River is driven by the monsoon and dry periods resulting in high intra-annual variation of the discharge with peaks in August, and the River is mostly dried out in mid-February. The rainfall-runoff relationship of the UKC is shown in Figure 2.11.

Kharun River flows mainly from south to north and north-east in the center of the catchment. It is considered as the lifeline of UKC and provides water to rural and urban areas, industries and small-scale irrigation.

As in many parts of India, many small water bodies (ponds) are a typical feature of the UKC. Ponds are a traditional option in regions with distinct dry and wet seasons for storing water in the monsoon for use in the periods with low water availability. Approximately 2-3 ponds are available in each village. These ponds are used for domestic purposes and small-scale irrigation in some places. The drainage network and ponds in the UKC are shown in Figure 2.4.

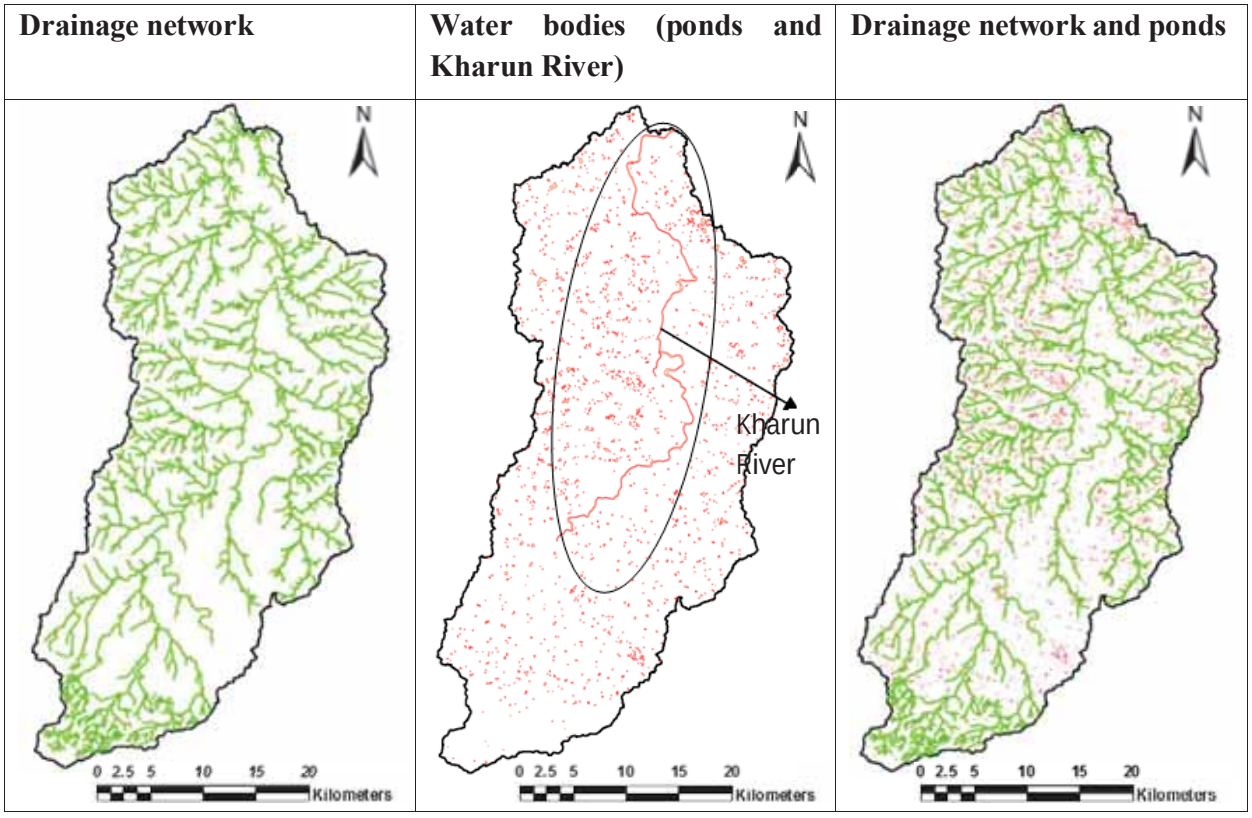

Figure 2.4: Drainage network and ponds in Upper Kharun Catchment

2.2.2 Digital Elevation Model

The study area has a gently undulating and predominantly flat topography. The elevation difference is only 192 m ranging from 258 – 450 m.a.s.l. The elevation decreases from south to north and slopes range from 0 – 8.09 degrees (Figure 2.5 and Figure 2.6).

Figure 2.5: Digital Elevation Model (DEM) in meters

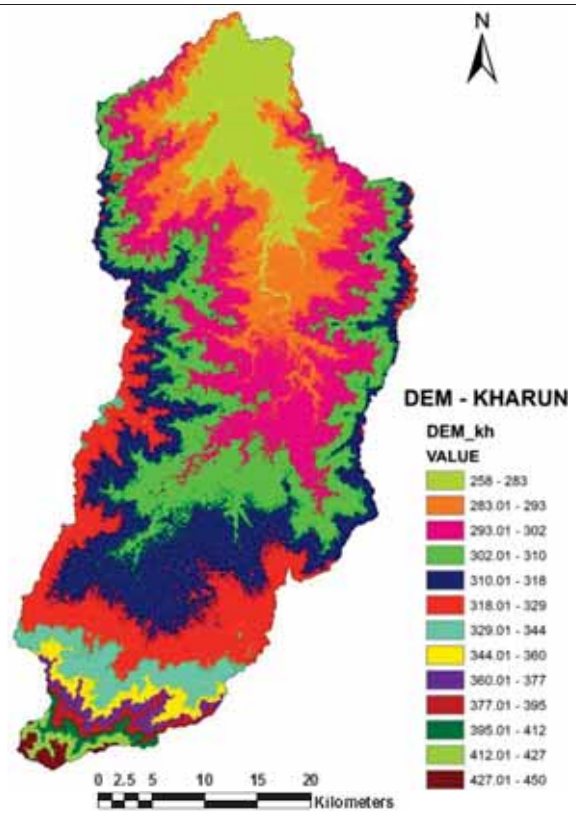

Figure 2.6: Slope in degrees

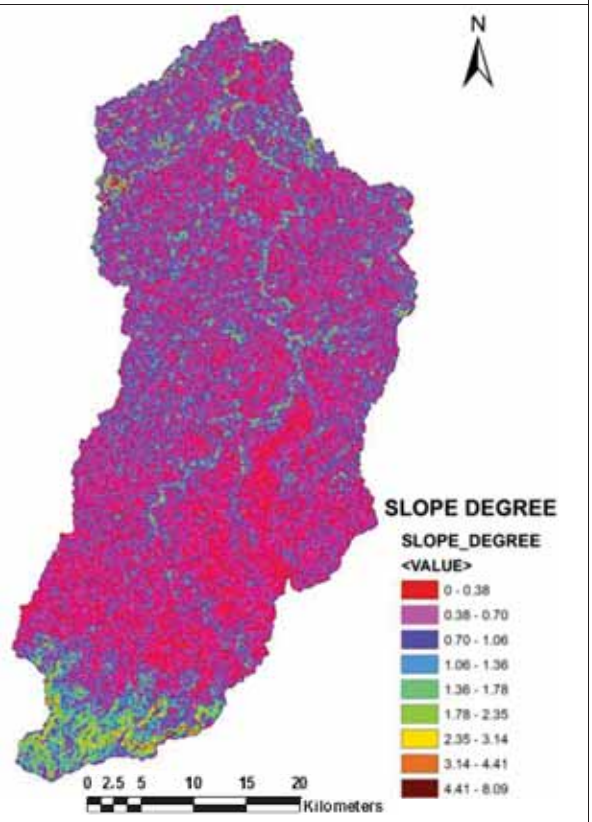

2.3 Soil

The soil map at 1:50,000 scale was procured from the State data centre. This soil map does not contain sufficient information to run the hydrological model SWAT. So the existing soil map was modified by collecting information from the soil survey office located at Nagpur and the soil science department, Raipur Agriculture University. In addition, field visits were carried out to test the major physical and chemical properties of the soil samples.

A detailed analysis of soil physical properties was conducted. In some places where no information was available for the soil hydrological properties, the software soil par version 2.0 (Acutis, 2003) was used to estimate soil bulk density and soil hydraulic conductivity based on various combinations of the available soil parameters such as soil texture, soil pH, organic carbon

and cation exchange capacity. Point and pedo-transfer function in soil par 2.0 were used to estimate the soil hydrological parameters.

A detailed database of soil properties with 64 different attribute types was prepared and attached to the modified shapefile of the soil map; further the shapefile was converted to a raster map and used as an input in the SWAT model.

General soil properties of UKC

Four major soil types are found in the UKC namely, Alfisols (loam also known as Dorsa), Vertisols (clay also known as Kanhar), Entisols (sandy loam also known as Bhata) and Inceptisols (sandy clay loam also known as Matasi).

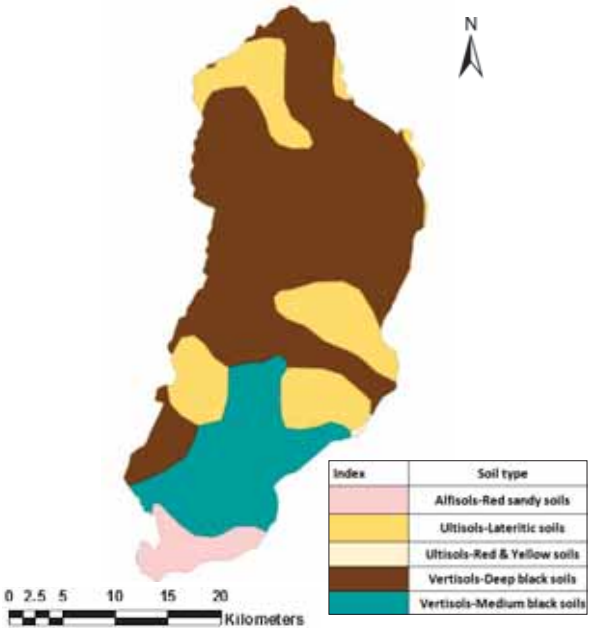

Figure 2.7: General soil map of Upper Kharun Catchment

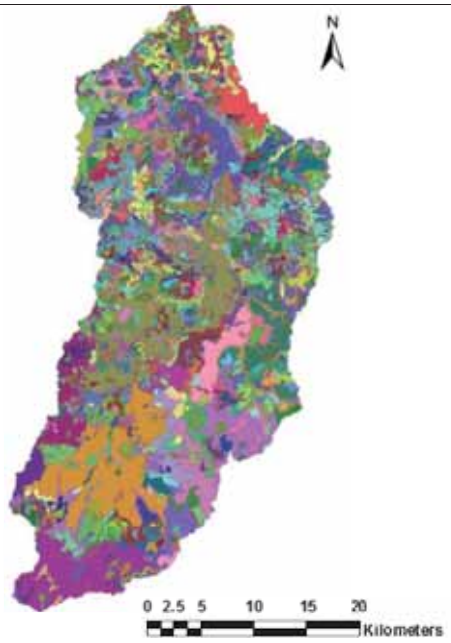

Figure 2.8: Detailed soil map of Upper Kharun Catchment

The soil along Kharun River is fertile, the groundwater table is shallow, and hence this area is used to cultivate all three-season crops with paddy as a summer crop (Figure 4.20; see Chapter 4).

Inceptisols are red and yellow loamy soil; they are poor in nitrogen and humus content and found in Durg and Raipur districts. Vertisols are black in colour and ideal for crop cultivation. Loam and sandy clam loam soil (midland soil) are suitable for rice production, whereas sandy loam soils (upland) are suitable for maize and kodo.

2.4 Land-use

The UKC is characterized by diverse land-use types. The area comprises agriculture land, rural settlements, urban areas, industrial areas and forest in the south.

The majority of the study area is agricultural land with 514 villages. The main crop grown in the area is paddy (rice). The study area is part of Chhattisgarh, which is known as the rice bowl of central India. There are many rice varieties grown in the study area and it is the leading region in the state for rice production.

Rice is grown as a single main crop in the monsoon season. Farmers stick to their traditional habit of cultivating rice in the area. However, in dry seasons (winter and summer) in the case of limited or no irrigation, the second crop is oilseeds, wheat, coarse grains, groundnut, maize and pulses. Yet, at locations with sufficient groundwater availability and irrigation facilities, the choice of a second and/or third crop is paddy only. Chapter 4 provides a comprehensive description and analyses on the crop rotation and spatial distribution of the cropping area over the decades.

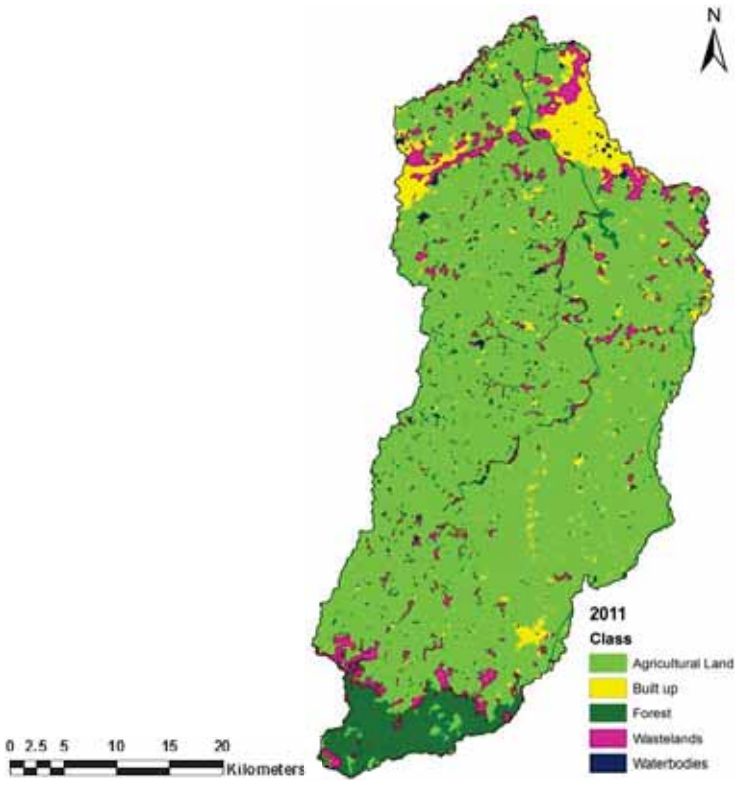

Figure 2.9: Land-use types in Upper Kharun Catchment

The proportion of a second and third crop has been increasing in the past decade because of improved irrigation and groundwater pumping facilities.

A detailed irrigation analysis (surface and groundwater) over the decades (1991, 2001 and 2011) is discussed in Chapter 5 (section 5.5). The pumping of groundwater for irrigation purposes has increased considerably recently, which is a threat to the availability of precious groundwater in the future.

Some portion of southernmost part of the study area is covered by moderately dense forest and open forest areas. On the north and northwest side of the study area, industries like Bhilai steel plant, etc., are located. There has been a rapid change in the extent of urban areas since 2000 when Chhattisgarh was formed as a new state. Recently, the government has been establishing a new Raipur area, which is an outgrowth of the capital city Raipur. This converts many villages to urban areas. A detailed description on the land-use is given in Chapter 4.

2.5 Geological characteristics

The UKC comprises eight different geological layers: alluvium, Deodonagar sandstone, Chandi limestone, Gunderdehi shale, Churmuria limestone and shale, Churmuria siltstone and Churmuria sandstone (Table 2.3). These geological layers have distinct hydrological features that govern groundwater occurrence, movement and availability.

2.5.1 Dongargarh group

The proterozoic Dongargarh supergroup is comprised of tholetic basalt-rhyolite in association with epizonal granite pluton and stocks.

2.5.2 Chhattisgarh super group

This represents the major geological group in the UKC. The rocks consist of two types of sub-groups, i.e., Chandrapur group and Raipur group.

The rocks of Chandrapur Group are the oldest in origin and can be further divided into three formations, i.e., Lohardih, Choparadih and Kansapathar arranged in the ascending order of superposition.

The rocks of Raipur group comprise a predominantly argillite-carbonate sequence. The group is further classified into six formations, viz Charmuria, Gunderdehi, Chandi, Tarenga, Hirri and Maniyari arranged in the ascending order of superposition. In the study area only the Charmuria, Gunderdehi and Chandi formations are well developed.

Table 2.3: Geology of Upper Kharun Catchment

Age	Group			Lithology
Quaternary	Alluvium/Colluvium			
	Laterite			
Middle Protorozoic	Chhattisgarh Supergroup	Raipur group	Tarenga	Shale & Dolomite
			Chandi / Bamandihi	Limestone & Shale

			Gunderdehi	Shale
			Charmuria	Limestone & Shale
		Chandrapur Group		Sandstone, Siltstone, Shale & Conglomerate
Lower protorozoic	Dongargarh group			Granite

Source: CGWB (2006), state report: Hydrogeology of Chhattisgarh, NCCR, Raipur

2.5.3 Laterites

Laterite occurs as a thin cover over sandstone, limestone and shale. Over the sandstone it is very hard and thick, while on limestone it is pisolitic with less clayey material. The lateritic capping on shale is soft, clayey and more ferruginous.

2.6 Climatic characteristics

The climate of Chhattisgarh state is mainly characterized as a tropical (hot and humid type). It covers three agro-climatic zones, viz. Chhattisgarh plains zone, northern hilly zone, and Bastar plateau zone. UKC is situated in Chhattisgarh plains zone. The study area experiences three typical Indian seasons, namely winter (mid October to mid February), summer (mid February to mid June) and monsoon (mid June to mid October).

2.6.1 Rainfall

The rainfall in the UKC is strongly controlled by the movement of the monsoon that dominates the rainfall of the entire Indian sub-continent. A high share of the annual rainfall (more than 90%) occurs during June – October. July and August are the rainiest months. The onset of the monsoon usually starts in mid June and lasts up to mid October.

The maximum daily rainfall recorded was 370.6 mm on 30 June 2007 at Raipur rainfall station. The rainfall gradually decreases from southeast to northwest.

Rainfall data are recorded on a daily time scale (mm/day) with non-recording rain gauges. Automated rainfall gauges were recently installed at the meteorological station in Raipur.

2.6.2 Temperature

May and January are the warmest and coldest month of the year, respectively.

The climatic characteristics of the UKC (past changes and expected future changes) are analysed and described in detail in Chapter 3.

2.7 Discharge data

The discharge from the UKC is measured at Patharidih gauge-discharge site and recorded on a daily basis (8:00 am) starting from June 1989 by Central Water Commission, Ministry of Water Resources, Govt. of India, New Delhi. The velocity of flow across the cross section of the Kharun River is measured by a current meter (m^3/s) and the discharge is estimated using the velocity-area method. Apart from discharge measurement, the Central Water Commission is also responsible for monitoring the Kharun River water quality. Water tests have been carried out twice a year (pre- and post-monsoon) since 1990. The daily gauge-discharge data from 1990 to 2010 were obtained from the Central Water Commission, Bhubaneswar, Orissa.

The discharge is very low from January onwards, and in the Indian summer season (mid February till mid June) the Kharun River generally dries up completely. Therefore discharge was not measured during January till mid June after 2000. The maximum discharge of 2000 m^3/s was recorded on 14th September 2005.

Discharge and Gauging site - Patharidih	**Field visit at Patharidih discharge measuring station**
	

Figure 2.10 Location of discharge and gauging site in Upper Kharun Catchment

2.8 Runoff-rainfall analysis

A detailed runoff-rainfall ratio analysis of the UKC was performed for the period between 1989 and 2008 (Table 2.4 and Figure 2.11). The observations were from June to May and that was considered as a calendar year for analysis. A runoff-rainfall ratio comparison between the monsoon periods (June to October) was also performed.

The results of the analysis follow a general trend. In years with higher rainfall, runoff also increased compared to other periods (Table 2.4 and Figure 2.11). Runoff over proportionally increased or decreased with the increase and decrease in the rainfall amount. Yet there are examples not matching this general pattern. For example, in 2005/06, runoff was higher compared to 2003/04 in spite of less rainfall.

Table 2.4: Runoff-rainfall ratio for Upper Kharun Catchment

Years	Rain (mm)	Runoff (mm)	Runoff/Rain	Monsoon (June – October)	Rain (mm)	Runoff (mm)	Runoff/Rain
1989-90	1052.3	175.3	0.167	1989	921.5	170.7	0.185
1990-91	1450.6	804.7	0.555	1990	1437.2	786.7	0.547
1991-92	1085.3	438.3	0.404	1991	1077.1	425.4	0.395
1992-93	1089.8	525.8	0.482	1992	1074.7	516.8	0.481
1993-94	1028.2	337.8	0.329	1993	1020.8	323.0	0.316
1994-95	1613.9	873.0	0.541	1994	1576.0	839.0	0.532
1995-96	1076.1	554.2	0.515	1995	1069.7	528.7	0.494
1996-97	1096.0	320.8	0.293	1996	1042.6	307.9	0.295
1997-98	1130.7	329.9	0.292	1997	1011.5	294.3	0.291
1998-99	927.9	212.2	0.229	1998	815.6	183.6	0.225
1999-00	1137.8	333.8	0.293	1999	1093.8	319.7	0.292
2000-01	726.2	149.0	0.205	2000	692.1	149.0	0.215
2001-02	1078.6	431.0	0.400	2001	1061.1	426.4	0.402
2002-03	771.6	130.1	0.169	2002	741.1	127.8	0.172

2003-04	1413.8	487.6	0.345	**2003**	1304.5	474.1	**0.363**
2004-05	1086.3	388.3	0.358	2004	947.2	374.4	0.395
2005-06	1347.3	697.0	0.517	**2005**	1220.8	684.1	**0.560**
2006-07	1045.3	482.0	0.461	2006	1016.8	474.1	0.466
2007-08	1282.8	453.5	0.354	2007	1248.6	443.1	0.355
				2008	837.5	225.0	0.269

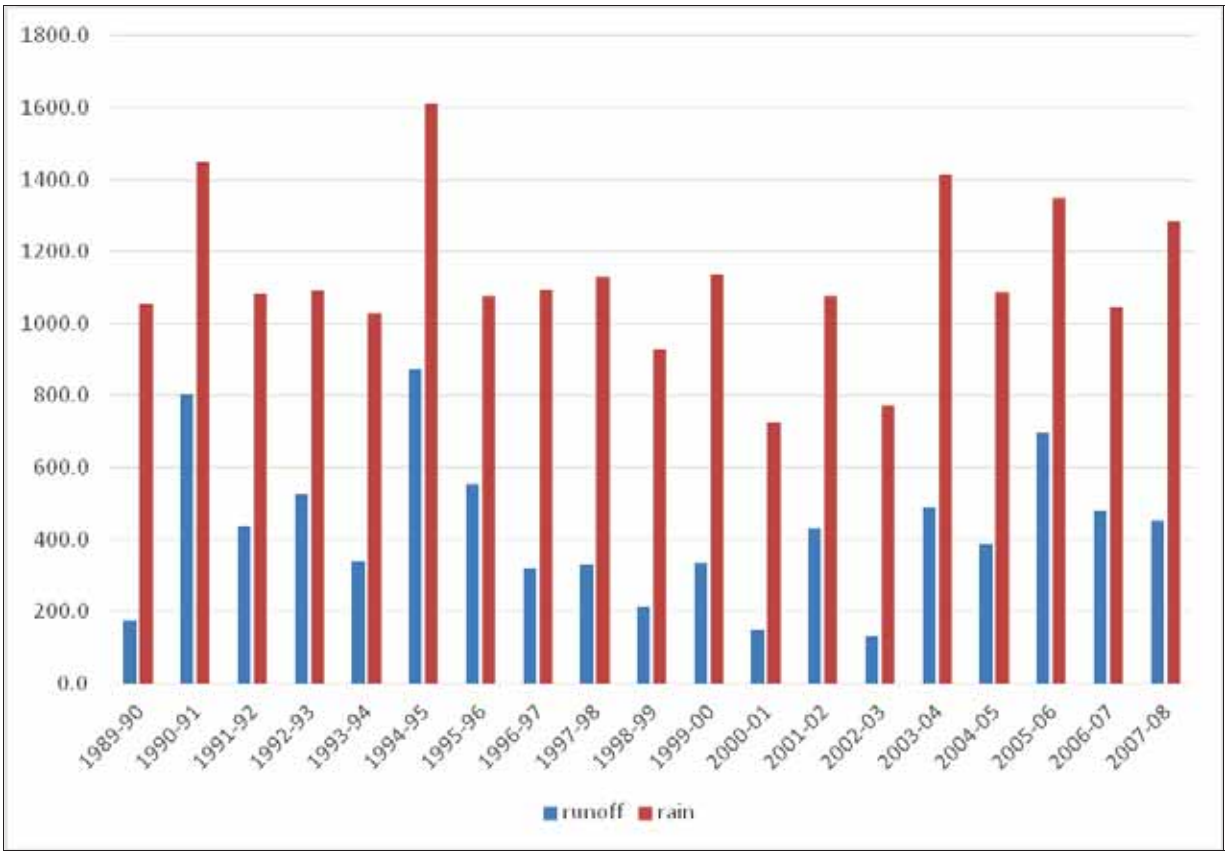

Figure 2.11: Runoff-rainfall relationship in Upper Kharun Catchment

To detect the reason behind this pattern, the number of rainfall events with more than 3 mm and 5 mm during the periods June 2003 to May 2004 and June 2005 to May 2006 for all 14 rainfall stations of the UKC were counted. Later, Thiessen weights were assigned to each rainfall station, and finally the weighted number of rainfall days (more than 3mm and 5mm) was calculated.

It was observed that the number of days with rainfall more than 3 mm in 2003-04 were 59 whereas the number of rainfall days more than 3 mm in year 2005-06 was 40. Also the number

of days with rainfall more than 5 mm in 2003-04 was 51 whereas the number of rainfall days more than 5 mm in 2005-06 was 35.

Conclusion: As the number of days with rainfall above 3 and 5 mm was much lower in 2005-06 compared to 2003-04, rainfall intensity in tendency was higher, which leads to a higher runoff-rainfall ratio in 2005-06. Additionally, for the period between 1989 and 2010, the maximum daily discharge of 2000 m^3/s was recorded on 14th September 2005, which was quite high compared to the maximum daily discharge of 1243 m^3/s in 2003-04.

CHAPTER 3: CLIMATE CHANGE ANALYSIS FOR THE UPPER KHARUN CATCHMENT

3.1. Introduction

Rainfall and temperature are the two most influential and critical variables of climate and hydrological studies. A change in any of these two components will severely affect the hydrological cycle, streamflow and the associated demand of water by different sectors. Thus, an analysis of the time series behavior of rainfall and temperature pattern is important for understanding the climate dynamics. This is useful for the prediction of future climate change scenarios and for framing strategies for current and future action plans in water resource management. There are numerous trend detection methods, each with its own pros and cons with certain underlying assumptions. The selection of a method depends on the data-sets and conditions prevailing for a particular case study.

Climate change has been confirmed by the Intergovernmental Panel on Climate Change (IPCC, 2007). It has been pointed out that the global mean temperature may increase between 1.8°C and 4°C by 2100, and this will severely affect the availability of water resources across the world.

India is mainly dependent on the southwest monsoon for its major freshwater supply for agriculture, industries, domestic purposes, and the energy sectors and for maintaining the functioning of ecosystems. More than 80% of the annual rainfall occurs during this period. So any changes in the climate over the regions of India would have a significant impact on agricultural production, which accounts for the biggest share of water withdrawals in India and is already under stress in several regions due to the current population increase, water resource management and the overall socio-economic situation in the country.

Gosain et al. (2006) reported that under the influence of climate change the freshwater availability is likely to decrease significantly for many river basins in India. In terms of water availability versus demand relations, the situation will become worse in India till the 2050s when accounting for the rising population, increasing food, water and energy demand by different sectors, and the improving living standard.

General Circulation Models (GCMs) are the tools to predict the future climate change scenarios and are often used in impact analysis in water resource management. However, they have a too coarse resolution (150-300 km x 150-300 km), which restricts their use for global studies. The management or action scale for water resource management usually applies at local or basin boundaries. In order to analyze the impacts of climate change at basin and catchment scale, downscaling of GCM scenarios at finer resolution is required. However the downscaling has its own biases problems that should be consider.

Most of the trend detection studies and downscaling or bias correction of future climate change scenarios on rainfall and temperature in India were confined to basin, state or national level. However, there are literature gaps in the analysis of these variables at local or watershed level, which are primarily natural boundaries for the management of water resources and will directly relate to the community and ecosystem prevailing there. So in this study, an attempt is made to detect the climate change signals at catchment level (UKC) by employing various methods of trend detection and downscaling techniques described in the following sections.

3.2 Literature review of trend analysis of rainfall for the India

Studies that reported no significant trend in annual rainfall at all India scale are those by Mooley and Parthasarathy (1984), Sarker and Thapliyal (1988), Thapliyal and Kulshrestha (1991), and Lal and Singh (2001). However, a significant trend was identified at different regional and local levels in India by Koteswaram and Alvi (1969), Jagannathan and Parthasarathy (1973), Raghavendra (1974), Chaudhary and Abhyankar (1979), Srivastava et al. (1998), Kumar et al. (2005), Dash et al. (2007) and Kumar and Jain (2010).

Rupa Kumar et al. (1992) used linear trend analysis for 306 rainfall stations and found both increasing and decreasing trends in different parts of India. They concluded that the northeast region and northeast and northwest peninsula show a decreasing trend in southwest monsoon rainfall. However, an increasing trend was reported for the west coast, central peninsula and northwest India. The decreasing trend ranges between 6 to 8% of the normal per 100 years while the increasing trend is about 10 to 12%.

Based on analysis of rainfall time series data from 1871-2002 of India, Dash et al. (2007) reported a decreasing trend in monsoon rainfall and an increasing trend in pre- and post-monsoon periods.

Guhathakurta and Rajeevan (2008) performed a linear trend analysis for monthly rainfall observations of 1476 rain gauge stations located in 36 meteorological sub-divisions (representing different parts of India) during the period 1901-2003, and found that there was a significant decrease in monsoon rainfall for Jharkhand, Chhattisgarh and Kerala sub-divisions whereas eight sub-divisions showed a significant increase.

Kumar et al. (2010), based on their research on 30 sub-divisions (representing different parts of India) and 135 years (1871-2005) time series data, found that 15 sub-divisions showed an increasing trend in annual rainfall while another 15 sub-divisions showed a decreasing trend. However, the increase in annual rainfall is statistically significant only for 3 sub-divisions (Haryana, Punjab and Coastal Karnataka), and the decrease only for one sub-division, i.e., Chhattisgarh.

The study area (UKC) is a part of Chhattisgarh state. Guhathakurta and Rajeevan (2008) and Kumar et al. (2010) found that the monsoon rainfall is decreasing in Chhattisgarh state.

3.3 Literature review on trend analysis of temperature for India

Hingane et al. (1985) worked on long-term time series temperature records starting from 1901 to 1982 and from 73 stations located all over India. They found an increasing trend of mean annual surface air temperature. A rise of 0.4 °C was noted during the time span of eight decades.

Pant and Kumar (1997) investigated the presence of a trend in annual and seasonal air temperatures during a period from 1881-1997, and found that there was a statistically significant increasing trend for mean annual temperature at the rate of 0.57°C per 100 years.

Singh and Sontakke (2002) performed a study on the Indo-Gangetic Plains of India and found that there was a significantly (1% level) increasing trend for mean annual temperature at the rate of 0.53°C/100 years during the period 1875–1958. However, during 1958–1997, there was a significantly (5% level) decreasing trend at the rate of 0.93°C per 100 years.

Kothawale and Rupa Kumar (2005) performed a trend detection test for surface temperature over India for the period 1901–2003, and found that there was a significantly increasing trend for mean annual temperature at the rate of 0.05°C per decade. However, considering the time period 1971–2003, they observed an accelerated increase in mean annual temperature by 0.22°C per decade. This rise in temperature is also applied to daytime and nighttime temperatures, which indicates an unprecedented warming during the last few decades.

Singh et al. (2008) detected an increasing trend in mean annual temperature for seven out of nine river basins in central and northwest India.

The Central Water Commission (CWC) and National Institute of Hydrology (NIH) (2008), based on a trend detection analysis of temperature data of 125 stations located all over India, observed an increase of 0.42°C, 0.92°C and 0.09°C in mean annual temperature, mean maximum temperature and mean minimum temperature, respectively, over the time span of the last 100 years.

3.4 Trend detection studies for Mahanadi river basin

The study area (UKC) lies in the Seonath sub-basin, which is a tributary of the Mahanadi river basin. Therefore a literature review on climate change analysis in Mahanadi river basin was performed.

Rao (1993) used a linear regression time series analysis for Mahanadi basin and found no significant trend in monsoon or annual rainfall during the period 1901–1980. However, a significant rise in temperature was observed during the same period. They concluded that the change in land-use and anthropogenic activities were responsible.

Chakraborty et al. (2013) performed Mann Kendall and Spearman correlation trend detection tests for rainfall analysis over the Seonath basin during a period from 1960 – 2008. Both tests

showed a decreasing trend in annual and seasonal rainfall series for the whole river basin. Cumulative sum and cumulative deviations tests were applied, and 1980 was detected as a change point. The time series is divided in two parts, i.e., before the change point (1980), 1960 to 1980, and after the change point i.e., 1980 to 2008. An increasing and decreasing rainfall trend before and after the change point, respectively, was observed.

In the 1970s, the trend detection techniques gained attention in climate change science and hydrology, and later a number of studies applying trend detection methods were performed. Some of the pioneer work includes: Sen's non parametric slope estimator (Sen, 1968), least squares linear regression for the detection of trends in time series of hydrological variables (Haan, 1977), Spearman rank correlation test (Lettenmaier, 1976) and Mann Kendall test (Kendall, 1975).

3.5 Time series analysis

Time series data is a chronologically ordered sequence of observations for a variable taken at regular intervals of time.

There are two kinds of time series data:

(1) Continuous data: Here continuous measurements are taken, e.g., electrocardiograms, etc.

(2) Discrete data – Here measurements are taken at usually regularly spaced time intervals, e.g., meteorological data (daily rainfall, temperature, wind speed, etc.).

3.5.1 Time series data components

(1) **Seasonal variations**, which repeat over a specific period of time such as a day, week, month, season, etc.

(2) **Trend variations, also known as secular movements,** are a general tendency of data to increase or decrease in a reasonably predictable pattern.

(3) **Cyclical variations**, which correspond to changes as a result of booms and depressions. These are non-periodic fluctuations.

(4) **Random variations, also known as irregular or erratic variations,** represent the residuals (error or noise) component of the time series after the other components have been removed.

Time series are best displayed in a scatter plot. The time series data are plotted on a vertical Y axis against the time (t) on a horizontal X axis.

3.5.2 Time series analysis

Time series analyses comprise methods that are used to describe and summarize time series data that account for the internal characteristics of the dataset such as autocorrelation, trend or seasonal variation, and statistical models that fit the data, and make forecasts.

3.5.3. Use of time series analysis

The analysis of time series is of great importance for the diverse group of scientific and research communities ranging from climatologists, hydrologists, hydro-geologists, astronomists, geologists, sociologists, biologists, etc., for the below-mentioned reasons.

- It supports an understanding of the underlying forces and structures that produced the observed data.

- It analyses the historical time series data and helps in understanding the behavior and characteristics of past events. The information gained from the past data analysis is extremely useful for predicting behavior in the future, and helps in planning strategies for future actions or monitoring or provides feedback and feed forward control.

3.5.4. Identification of patterns in time series data

Generally, time series data consist of systematic patterns and random noise often called error, which usually makes it difficult to identify a pattern. There are techniques to filter out noise in order to make patterns more visible.

3.5.5 Exploratory analysis of seasonality in time series data

Seasonality is a component of time series data which has a tendency to repeat itself over a regular interval of time. Autocorrelation correlogram and partial autocorrelation analysis are employed to examine the seasonal patterns of time series data.

Removal of serial dependency - Serial dependency for a particular lag of k can be removed by differencing the series, i.e., converting each i'th element of the series into its difference from the (i-k)'th element.

Removal of serial dependency is useful to identify the hidden nature of seasonal dependencies in the series and also makes the series stationary, which is necessary for autoregressive integrated moving average (ARIMA) and other techniques (Wang et al., 2013).

3.5.6. Smoothing

If the time series data contain considerable noise (errors), seasonal variations and cyclic variations then the first step in the process of trend identification is smoothing.

Smoothing is a technique for local averaging of data such that the non-systematic components of individual observations cancel out each other so that the remaining characteristics of the data are more visible.

Types of smoothing technique: Moving average smoothing, exponential smoothing, running median smoothing, etc.

3.6 Trend analysis

Trend analysis is a technique for detecting a pattern of rate of change of a variable in time series. It examines whether a variable of interest is increasing, decreasing or keeping constant over the years in a time series. The detection, estimation and future prediction of a trend are important aspects of climate change impact studies.

The simplest way of detecting trends in seasonal data is to take the mean of observations over a certain period of time. If the mean changes with time, it indicates that there is a trend in the time series. However, there are many formal tests to detect trend in time series.

If the trend component is linear, the level of the series increases by a constant amount each time, and if the trend component is exponential, the level of the series increases by a constant percentage each time.

Methods of trend detection

A trend may be linear or non-linear. So a best fit for modeling a trend can be straight lines, polynomials, etc. The selection of the model depends on the behavior of the dataset. Least-squares or regression methods are the most commonly used methods to estimate the slope of a trend. Linear trendlines are generally used for simple data, logarithmic trendlines are employed for data having sharp changes, moving average trendlines are commonly used to fit the random fluctuating dataset, the polynomial trendline fit is generally used for gradually fluctuating dataset having peaks and valleys, and the Gaussian fit is used for bell-shaped distributed datasets. The Prais-Winsten AR test is commonly used for serially correlated datasets (Mudelsee, 2010).

Correlation analysis is often employed for trend detection. Some common examples are the Mann Kendall test with Theil-Sen's slope estimate, Kendall τ test, Spearman test, Pearson test, etc.

Time series data may be auto-correlated and therefore the accounting for serial correlation is essential for time series analysis. There are many methods which handle the serial correlation. A popular example is the Prais-Winsten AR test (Mudelsee, 2010).

Parametric and non-parametric methods are generally used for trend detection and analyzing the statistical significance of a detected trend.

(1) Parametric methods are well known and widely used elementary statistical methods. The parametric formulae are simple to understand, faster to compute and considered to have more statistical power compared to non-parametric methods. However, parametric methods are based on more assumptions than non-parametric methods. If any of the assumptions is/are not fulfilled the results will be very misleading.

Examples: Student t test, f test, z test, linear regression, Prais-Winsten AR, Pearson product-moment correlation coefficient (r), etc.

(2) Non-parametric methods are also known as distribution-free inferential statistical methods. Unlike parametric tests, they are not based on the assumption that the data are drawn from a given probability distribution and normally distributed. Since most of the hydro-meteorological time series data are not normally distributed (Huth and Pokorna, 2004; Van Belle and Hughes, 1984; Helsel and Hirsch, 1988), non-parametric tests are commonly used. Non-parametric methods are based on fewer assumptions, and hence they are more robust and their applicability is much broader as compared to parametric methods. However, they are considered to have less statistical power compared to parametric methods.

Examples: Spearman rank correlation coefficient, Kendall τ test, chi square, Fisher extract test, Mann Kendall test with Theil-Sen's slope, etc.

The Mann Kendall test has been used for trend detection in hydro-meteorological time series world-wide. Examples for such work include: Steele et al. (1974), Hirsch et al. (1982), Crawford et al. (1983), Van Belle et al. (1984), Cailas et al. (1986), Hipel et al. (1998), Demaree and Nicolis (1990), Zetterqvist (1991), McLeod et al. (1991), Chiew and McMahon (1993), Yue et al. (1993), Lettenmaier et al. (1994), Burn (1994), Yulianti and Burn (1990), Lins and Slack (1999), Douglas et al. (2000), Zhang et al. (2001), Yue et al. (2002), Burn and Elnur (2002), Yue and Hashino (2003), Xu et al. (2003), Huth and Pokorna (2004), Kahya and Kalayci (2004), Partal and Kalya (2006), Sansigolo and Kayano (2010), Weng (2010), Streck et al. (2011), Blain and Pires (2011), Minuzzi et al. (2011), Tabari and Talaee (2011), Back et al. (2012) and Carvalho et al. (2013).

The Spearman correlation coefficient for trend detection in hydrological and hydro-meteorological time series data is less frequently applied compared to the Mann Kendall test. The Spearman correlation coefficient test was employed for trend detection in hydrological and hydro-meteorological time series data by Lettenmaier et al. (1976), El Shaarawi (1983), Pilon et al. (1985), McLeod et al. (1991) and Hipel and McLeod (1994). However, the results of the Spearman correlation test are mostly close to those of the Mann Kendall test (Yue et al., 2002).

The selection of a trend detection method and testing the statistical significance depend on the nature of the dataset and its distribution. A researcher must know the underlying assumption for estimates of a trend and statistical test employed.

(3) A straightforward approach for trend detection: Gaussian-linear trend detection

There might be the possibility of serial autocorrelation in time series data especially related to hydrological data which violates the rule of independency in datasets. Therefore, before using any parametric or non-parametric test, an autocorrelation test for the variables needs to be performed. To deal with autocorrelation in time series, various methods are available such as the moving average smoothing technique, pre-whitened method (Von Storch, 1995), etc. However, using such techniques does not necessarily fulfil the assumptions underlying the different trend detection techniques. Even removing some of the autocorrelation may introduce another form of autocorrelation which might have not existed earlier, or components of a trend may be removed, which leads to under- or over-estimation. Each method has its own pros and cons, and serious attention is required during their application.

Keeping in mind the challenges in time series trend analysis, a straightforward approach is introduce in this section, where the integrity of annual time series data is maintained and considered as a whole without any transformation or smoothing. The approach is termed as ''Gaussian-linear regression time series analysis.''

The annual rainfall time series data used in this study show a bell shaped curve, which suggests fitting of a Gaussian function (Figure 3.4). Annual rainfall data for each year were first fitted with the Gaussian function, and then a linear regression was applied on the fitted amplitude, position of the amplitude and standard deviation over the years to detect a trend. This method utilizes the natural distribution characteristics of the dataset and maintains integrity. Furthermore, it satisfies the assumption of a parametric test.

The next section deals with the future climate change scenarios and its applicability to the study area.

3.7 General Circulation Models (GCM)

General Circulation Models (GCMs) are mathematical models of the general circulation of a planetary atmosphere or ocean. Currently, they are the most credible tools designed to simulate time series of climate variables (e.g., air temperature, precipitation, wind speed, pressure, etc.) on a global scale with respect to increasing greenhouse gases concentration in the atmosphere. They are often used for understanding the climate dynamics and projecting future climate change (Thorpe, 2005), and provide a basic input for climate change impact studies on a very large scale (continental – global scale).

Types of GCM:

- Atmospheric GCMs (AGCMs) - model the atmosphere.

- Oceanic GCMs (OGCMs) model the ocean.

- Coupled atmosphere-ocean (AOGCMs) – combine both atmosphere and oceanic GCMs.

These models are the only tools that serve as a basis for sophisticated model predictions of future climate, and are used by the Intergovernmental Panel on Climate Change (IPCC).

Based on future emission scenarios that are used for driving the global circulation models, IPCC has developed several climate change scenarios. These scenarios are often used in impact analysis and water resource management.

The resolution at which GCM operates varies between ranges of 150-300 km x 150-300 km, which is too coarse for any climate change impact studies on regional to local scales.

Precipitation, which is the main component of any hydrological model, cannot be modelled by GCM for basin to sub-basin scale, and hence restricts its application to climate change impact studies on the hydrology at the regional and local level. To study the impact of climate change on the hydrology of basin to watershed scale, the local topographic features and climate fluctuations must be considered. For obtaining the climate variables at a regional scale, the projections of climate variables must be downscaled from the GCM results, utilizing either dynamical or statistical methods (IPCC, 2001).

The process of converting GCM outputs into local meteorological variables required for reliable hydrologic modeling are usually referred as downscaling techniques (Dibike and Coulibaly, 2005; Huntingford et al., 2003). There are two main methods of downscaling the GCM scenarios: dynamic downscaling techniques (e.g., Regional Climate Models (RCM) and statistical downscaling techniques (e.g., Long Ashton Research Station Weather Generator (LARS-WG), Statistical Down Scaling Model (SDSM), etc.). Both methods have their pros and cons.

3.8 Dynamic downscaling technique

The dynamic downscaling technique is generally referred to as the Regional Circulation Model (RCM). Compared to GCM, it produces high resolution climate variables in a range of 50 km or even less. It is driven by boundary conditions from a GCM to derive smaller-scale information. RCMs are usually in better agreement with observations compared to those of the GCMs. A number of researchers have found that the RCMs reproduce precipitation extremes well at scales not accessible to GCMs (e.g., Frei et al. (2003), Huntingford et al. (2003) and Christensen and Christensen (2003) and better than GCMs on their grid scale (Durman et al., 2001). The disadvantage of this technique is the use of GCM as the starting boundary condition, which may introduce certain biases in the results.

3.8.1 PRECIS RCM

The RCM model used in this study is Providing Regional Climates for Impact Studies (PRECIS).

PRECIS is a regional climate modeling system developed by the Hadley Centre for Climate Prediction and Research, UK. In collaboration with the Indian institute of Tropical Meteorology (IITM), Pune, India, PRECIS RCM scenarios were developed for India for impact studies. This is the reason behind the selection of PRECIS scenarios for the current study.

PRECIS is an atmospheric and land-surface model of a limited area and with high resolution which can be configured for any part of the globe. Dynamical flow, atmospheric sulfur cycle, clouds and precipitation, radiative processes, land surface and the deep soil are all formulated in the model, and boundary conditions are required to be specified at the limits of the model's domain. Information about every aspect can be diagnosed from the model. The basic aspects explicitly handled by the model are briefly outlined in Naguer et al. (2002).

Salient features of PRECIS

- PRECIS is a high-resolution, limited-area model driven at its lateral and sea-surface boundaries by output from HadAM and HadCM (GCM). The grid resolution is 0.44º latitude x 0.44º longitude grid point (equivalent to 50 km x 50 km).

- PRECIS was developed for the Indian climatic conditions, and simulates gross features of the Indian climate (monsoon) for studying potential impacts of climate change in different sectors of India.

- PRECIS has three different climate simulations (ensembles) of IPCC SRES A1B scenario, i.e., q0, q1 & q14.

- PRECIS represents three time periods: 2011 to 2040 (2020s), 2041 to 2070 (2050s) and 2071 to 2098 (2080s). The baseline period represents the period from 1961–1990 (1970s) and is often referred to as the control run. PRECIS does not have a downscaled re-analysis run.

- The calendar day for each month is fixed 30 days. The recent RCM scenario follows the actual calendar, and thus the modern methods of statistical downscaling techniques are developed keeping in mind the actual calendar. This leads to difficulties in bias correction (statistical downscaling) of PRECIS scenarios to station level. Simple mean averaging methods can be employed to bias-correct the PRECIS scenarios.

- PRECIS cannot deal with hourly rainfall. Surface temperature is measured at 1.5m from the ground, and wind speed is measured continuously.

- Each year has 360 days in PRECIS. All the simulations are for 138 years, i.e., 1961-2098. So the total number of days is 138*360= 49680.

The 360 days of each year in PRECIS are comparable to the actual calendar year, i.e., the average monthly values of PRECIS scenarios correspond to the actual calendar average monthly values, irrespective of the number of days in a month.

PRECIS has a nominal time scale. Therefore, comparing observed data with model output on a daily scale is not possible. To detect the climate change in different time periods, climatology (average of the climate variables over 20-30 years) should be considered and compared. For example: PRECIS scenarios representing 4 time steps: Baseline (1960-1990), 2020s (2011-2040), 2050s (2041-2070) and 2080s (2071-2098). For calibration and validation of PRECIS scenarios, the observed mean monthly rainfall values for 1990-2008 were taken and compared with the model simulation values of 1990-2008.

3.9 Statistical downscaling technique

Statistical downscaling establishes a relationship between the measured small-scale (station level) variables and large-scale (GCM) variables (Goodess et al., 2005) using regression analysis, analogue methods or a neural network method. Once the relationship is developed, the equations are further projected to future GCM scenarios to obtain finer details at the local level. Examples of statistical downscaling methods are weather generators (Wilby et al., 2004). The disadvantage of this technique is that it is based on the relationship of large historical datasets with GCM during the calibration period. The relationship in future will not hold well if the future weather and climate conditions change with respect to time compare to those used for calibration.

Special consideration for PRECIS RCM scenarios:

Since PRECIS is a regional climate model developed by dynamic downscaling of GCM scenarios, the lateral boundary condition of GCM might have introduced systematic biases in the scenarios, which leads to over- or under-estimation of future climate variables. Kumar et al. (2011) reported such biases in PRECIS scenarios.

Due to the boundary limitation of the dynamical downscaling approach, the generated downscale scenarios need to be further statistically post-processed before they can be used as an input for hydrological models.

3.10 Statistical downscaling (or bias correction) of PRECIS RCM scenarios at station level

Simple bias correction of RCM output using mean monthly scaling adjustment

A simple monthly scaling adjustment methodology was used and executed in MATLAB software for bias correction of future rainfall and temperature of PRECIS RCM scenarios at station level.

The bias correction can be considered as a type of statistical downscaling of RCM scenarios at station level.

The above-mentioned methodology was chosen for bias correction because of its simplicity and direct approach to solve the problem and also because PRECIS scenarios have a 360 day calendar and only limited techniques can be applied.

The variables used for bias correction are:

1. Daily rainfall values of 14 stations in and around the study area.

2. Daily maximum temperature of Raipur meteorological station.

3. Daily minimum temperature of Raipur meteorological station.

There are 14 rainfall stations and one temperature station in and around the study area. The data recorded for the rainfall stations vary from 1971-2011. Some stations have data for 1971-2011, while the majority of stations have data from 1990-2011. For a single available temperature station, the time series data are available from 1971 to 2011. Bias correction is performed in MATLAB. The detailed step-by-step methodology is discussed in section 3.12.2.

3.11 Climate characteristics of Upper Kharun Catchment

The climate of Chhattisgarh state is mainly a tropical climate (hot and humid type). The state comprises three agro-climatic zones viz. Chhattisgarh Plains Zone, Northern Hilly Zone and Bastar Plateau Zone. The study area (UKC) is situated in Chhattisgarh Plains Zone, and experiences three typical Indian seasons, namely winter (mid October to mid February), summer (mid February to mid June) and monsoon (mid June to mid October).

3.11.1 Location of rainfall stations and meteorological station

Of the 14 rainfall stations in and around the UKC, 12 stations were considered for trend detection analysis, and all 14 stations were used in bias correction of GCM scenarios and hydrological modeling. Rainfall is measured daily.

The few gaps in rainfall measurements were filled using different statistical techniques. However, these filled gaps were not used in trend detection analysis. Only the actual measurements were considered and, if there was gap it was left vacant. Thus, out of 14 rainfall stations, the 12 stations with few gaps were selected for trend detection analysis and 2 stations with a high number of gaps were not considered in the analysis.

Daily rainfall data for the 14 rainfall station covering the entire study area (Figure 3.1 and 3.2) were obtained from the State Data Centre, Department of Water Resources, Raipur, Council of science and Technology, Raipur and Indian Meteorological Department, Pune.

The Thiessen method is used for representative extrapolation from point to area, and is considered as appropriate because no clear relationship between rainfall amount and influencing

factors (e.g., topography) is expected. The study area has a flat terrain with an elevation difference of only 192 m.

Figure 3.1 Rainfall stations and Raipur meteorological station

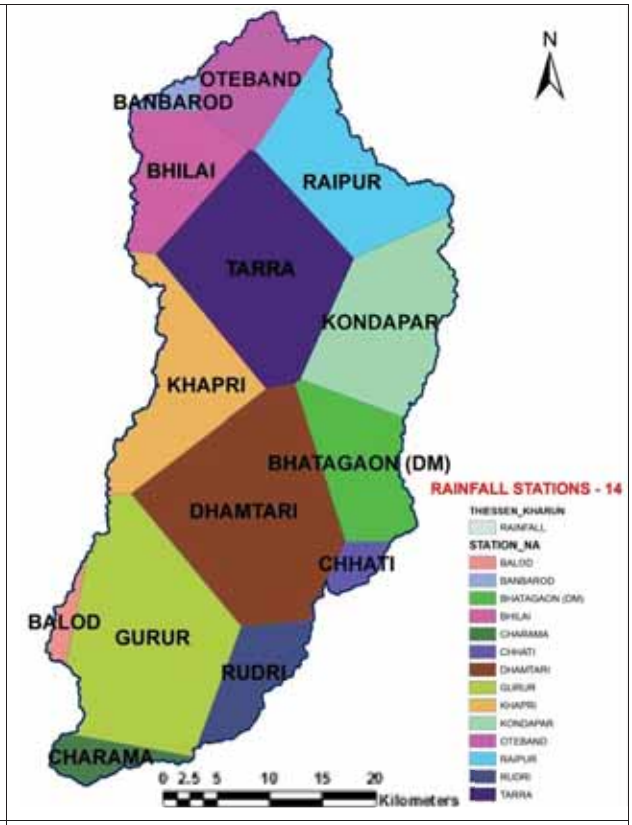

Figure 3.2 Rainfall Thiessen Polygons

Rainfall is recorded with the help of non-recording rain gauges (mm/day). Automated rainfall gauges were recently installed at the meteorological observation station, Raipur.

Meteorological daily observation data from 1971-2011 were collected from IGKV, Agriculture University, meteorological observation station, Raipur (Figure 3.3).

The parameters include daily rainfall (mm), maximum temperature (°C), minimum temperature (°C), relative air humidity (%), wind speed (km/h), evaporation (mm) and sunshine (hr).

Figure 3.3 Meteorological observation station located at IGKV Agriculture University, Raipur

3.11.2 Pre-analysis of rainfall data

Gaps occurred in the data of the rainfall stations. Missing values were filled using different statistical techniques. The statistical approaches included

- The averaging of nearby station values to fill the missing value. More weight was given to nearby stations compared to more distant ones.
- Pair-wise station comparison (section 3.13.4) was used as a basis for gap filling.

The stations were compared with each other for the mean annual rainfall values for 20 years with 95% confidence interval. The stations which were statistically similar were selected for filling the data gaps.

3.11.3 Analysis of meteorological variables

Only the Raipur meteorological station is in the UKC, and records daily maximum temperature, minimum temperature, relative humidity, wind speed and sunshine hours. Data were obtained for 1971–2011. After analysing the data, no missing values were found for the above meteorological variables.

3.11.4 Rainfall

The rainfall of the UKC is strongly controlled by the movement of the monsoon, which dominates the rainfall of the entire Indian sub-continent. Most of the annual rainfall (more than 90%) occurs during June – October. July and August are the rainiest months. Rainfall gradually decreases from

southeast to northwest. The onset of the monsoon in Chhattisgarh usually starts in mid June and extends up to mid October. Long-term time series data show recurrence of meteorological droughts on a lower scale every 3 to 4 years. Maximum daily rainfall recorded was 370.6 mm on 30 June 2007 at Raipur rainfall station.

The intra-annual representative rainfall pattern for the UKC based on the Thiessen approach is given in Table 3.1.

Table 3.1: Mean monthly rainfall for UKC from 1989 – 2010 based on weighted 14 rainfall stations

Jan	Feb	Mar	Apr	May	Jun	Jul	Aug	Sep	Oct	Nov	Dec	Annual	Max
7.5	5.6	5.8	5.6	14.2	190.2	321.0	320.4	163.9	46.0	3.9	2.2	1086.3	370.6

3.11.5 Temperature

The UKC generally has a moderate dry tropical climate. May and January are the warmest and coldest months of the year, respectively. The absolute maximum temperature in May reaches 47.6^{o}C and the absolute minimum temperature drops to 3.6^{o}C in January (Table 3.2, 3.3 and 3.4).

Table 3.2: Mean monthly average temperature for Upper Kharun Catchment from 1971 – 2010

Jan	Feb	Mar	Apr	May	Jun	Jul	Aug	Sep	Oct	Nov	Dec	Annual
19.4	22.1	26.5	31.2	34.1	31.7	27.6	27.0	27.5	26.0	22.2	19.2	26.2

Table 3.3: Mean monthly maximum temperature for Upper Kharun Catchment from 1971 – 2010

Jan	Feb	Mar	Apr	May	Jun	Jul	Aug	Sep	Oct	Nov	Dec	Annual	Max
27.4	30.2	35.2	39.8	42.0	37.2	31.2	29.9	31.0	31.0	29.3	27.3	32.6	47.6

Table 3.4: Mean monthly minimum temperature for Upper Kharun Catchment from 1971 – 2010

Jan	Feb	Mar	Apr	May	Jun	Jul	Aug	Sep	Oct	Nov	Dec	Annual	Max
11.3	13.8	17.7	22.6	26.3	26.0	24.1	24.1	23.9	20.8	15.0	11.1	19.7	3.6

3.11.6 Potential evapotranspiration

Data on daily wind speed (km/hr), maximum and minimum temperature (°C), relative humidity (%), sunshine hours and solar radiation (MJ/ m^2/ day) were used to estimate the potential evapotranspiration (mm/day) as reference evapotranspiration ET_0 according to FAO-concept

according to Allen et al. (1998) based on the Penman-Monteith method using Cropwat 8.0 software (Table 3.5).

Table 3.5: Mean monthly potential evapotranspiration (mm/day) for Upper Kharun Catchment from 1990 – 2010

Jan	Feb	Mar	Apr	May	Jun	Jul	Aug	Sep	Oct	Nov	Dec	Annual	Max
2.4	3.2	4.1	5.2	8.0	10.4	9.8	8.2	5.1	2.9	2.5	2.0	5.6	12.7

3.12 Materials and methods

The climate change analysis was performed in two phases:

1. Trend detection for historic time series data of rainfall and temperature.

2. Statistical downscaling or bias correction of future PRECIS RCM climate change scenarios to station level.

Stata SE 13.0 was used for trend detection analysis and MATLAB 2014a was used for bias correction of PRECIS RCM scenarios.

3.12.1 Trend detection analysis of observed rainfall and temperature

As discussed in the previous sections, each trend detection method has its pros and cons, and serious attention is required during their application. The accuracy of results depends entirely on the nature of the time series datasets, underlying assumptions and the prevailing conditions. Any method can be better than another if the underlying criteria meet.

In the present study, the most commonly trend detection methods were employed. Parametric (linear regression, Prais-Winsten AR method and Pearson correlation coefficient) and non-parametric (Spearman rank correlation coefficient, Kendall τ test and Mann Kendall test with Theil-Sen's slope estimate) methods were applied for 12 rainfall stations located in and around the study area. A straightforward approach, Gaussian - linear regression trend analysis is introduced, applied and discussed in section 3.6.

(A) Trend analysis of rainfall in Upper Kharun Catchment

The trend analysis for rainfall was conducted in 13 steps:

(I). Check for annual mean monthly rainfall pattern over the years (1961-2011) considering all stations together.

(II). Test for quality of input data in trend detection analysis.

(III). Investigation of the overall stations tendency for rainfall (mm) over the years (1961 -2011). Six rainfall variables were considered for analysis: mean annual rainfall, mean monthly rainfall in monsoon, maximum monthly rainfall in a year, maximum monthly rainfall in monsoon, minimum monthly rainfall in a year and minimum monthly rainfall in monsoon.

(IV). Analysis of: (1) Time effect of rainfall over the years for all stations, (2) difference between rainfall patterns between the stations, (3) test for any modification of rainfall for all the stations (together) with time.

(V). Pair-wise station comparison of rainfall: for all six above listed variables.

(VI). Trend detection test for each station for the six rainfall variables was performed (parametric and non-parametric tests).

(VII). Trend detection-correlation test for each month and for each station was performed.

(VIII). Trend detection test for all stations taken together for all six rainfall variables was performed (parametric and non-parametric tests).

(IX). Trend detection-correlation test for each month and for all stations taken together was performed.

(X). Analysis of mean monthly annual rainfall for each year (1961 to 2011) considering all stations together. A Gaussian function was fit to the data.

(XI). Trend detection test for all stations taken together for all six rainfall variables was performed (parametric and non-parametric tests) on Gaussian fit data.

(XII). Gaussian-linear regression trend analysis - linear regression were applied for fitted amplitude, position of amplitude and standard deviation of monthly rainfall of each year.

(XIII). Trend detection-correlation test for each month and for all stations considered together on the Gaussian fit data were performed.

(B) Trend analysis of temperature in Upper Kharun Catchment

The trend analysis for temperature was conducted in 2 phases: (1) mean annual temperature and (2) mean monthly temperature.

Only Raipur meteorological station records the temperatures in the UKC. The temperature parameters considered for trend detection were maximum, minimum and average temperature.

Parametric methods (linear regression, Prais-Winsten AR (1) and auto-segmented linear regression) and non-parametric methods (Spearman rank correlation coefficient, Kendall τ test and Mann Kendall test with Theil-Sen's slope estimate) were used.

3.12.2. Bias correction (statistical downscaling) of future PRECIS RCM climate scenarios

Simple bias correction of PRECIS future RCM scenarios (rainfall, maximum and minimum temperature) at station level using mean monthly scaling (multiplicative for rainfall and additive for temperature) adjustment was performed.

The bias correction for rainfall was carried out for all 14 stations, and the bias correction of temperature was performed for the Raipur station.

Bias correction of PRECIS RCM scenarios were performed in 4 steps:

Step 1: Analysis of observed time series data

The observed rainfall and temperature values were divided into calibration and validation periods. Here the Raipur meteorological station is taken as an example, where both rainfall and temperature data were recorded from 1971–2010.

The time series observed data from 1971-2010 were divided into calibration period (1971–2005) and validation period (2006–2010).

The mean monthly rainfall and temperature values for calibration and validation periods were calculated.

Step 2: Analysis of original PRECIS RCM data

The PRECIS RCM data for the period 1971 to 2010 were extracted from each scenario (q0, q1 and q14) and divided into calibration (1971-2005) and validation (2006-2010) period as for the observed time series, and the mean monthly rainfall and temperature values were estimated for the calibration and validation period.

Step 3: Monthly scaling factor (multiplicative and additive monthly adjustment approach)

Mean monthly observed and mean monthly RCM calibration period data were compared and, based on the comparison, a monthly scaling factor for each month was estimated. The mean monthly scaling factor indicates the difference or ratio between the mean monthly observed and RCM data during a period from 1971–2005 (calibration).

There are two forms of scaling factors:

1. Multiplicative adjustment approach for rainfall values. Here the monthly scaling factor is determined as:

Scale rainfall = Mean monthly observed value / Mean monthly RCM scenario value

2. Additive adjustment approach for temperature values. Here the monthly scaling factor is determined as:

Scale temperature = Mean monthly observed value – Mean monthly RCM scenario value

Step 4: Validation and application to future climate change scenarios

The above scaling factors were later applied to the validation period (2006–2010) of the RCM scenarios and then compared with the observed data for the same period. Coefficient of correlation was used to judge the results of the validation period.

If the validation results were satisfactory, the scaling factors were applied for the future scenarios (2011–2098).

This application of a scaling factor on RCM scenarios to make them comparable to the actual observed values is known as bias correction. Here, the biases in RCM scenarios occur due to the lateral boundary condition of GCM scenarios, which is systematic in nature and can be corrected satisfactorily based on the simple monthly scale technique of bias correction discussed in this section.

3.13 Trend detection analysis for rainfall

3.13.1 Monthly rainfall pattern (1961-2011) for the observation stations

The monthly rainfall pattern for selected twelve observation stations of the UKC during the period between 1961 and 2011 was plotted (Figure 3.4).

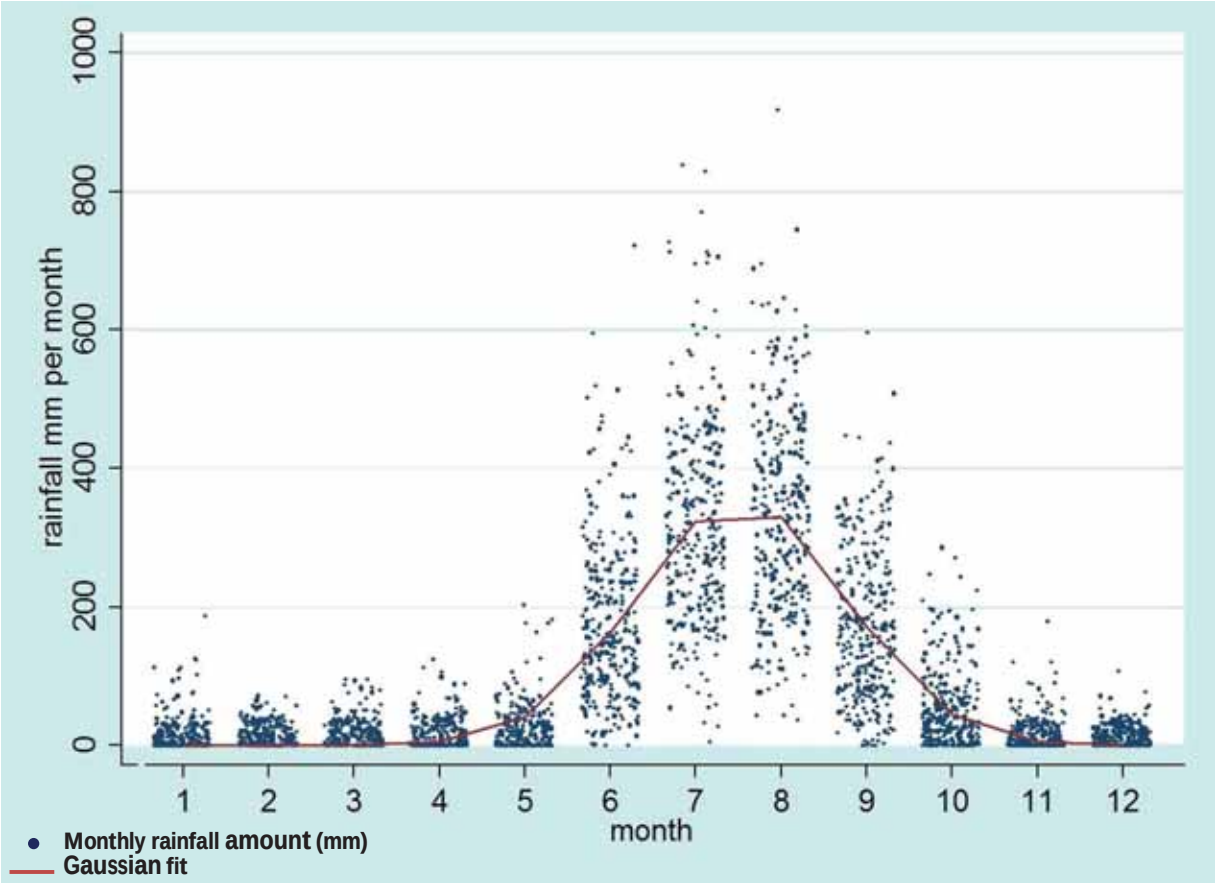

Figure 3.4: Monthly rainfall (mm) pattern (1961-2011) of 12 observation stations

The monthly rainfall pattern (1961-2011) of all the stations shows a bell-shaped curve with a peak in mid July. The Gaussian fit is used to represent the curve (Figure 3.4).

Table 3.6: Goodness of best-fitted bell-shaped curve

Source	SS	df	MS		
				Number of obs =	3398
Model	81955122.4	3	27318374.1	R-squared =	0.7940
Residual	21258217.7	3395	6261.62523	Adj R-squared =	0.7939
				Root MSE =	79.13043
Total	103213340	3398	30374.7322	Res. dev. =	39346.08

Note: r^2 shows that 79.4 % of the rainfall variation is explained by this model and this fit

Table 3.7: Estimates of the best-fitted bell-shaped curve

mm	Coef.	Std. Err.	t	P>|t|	[95% Conf.	Interval]
/a	355.6863	3.813743	93.26	0.000	348.2088	363.1637
/b	7.529885	.0151606	496.68	0.000	7.50016	7.559609
/c	1.219603	.0153149	79.63	0.000	1.189575	1.24963

Parameter a: Height of the curve peak: 355.7 mm (maximum monthly rainfall)

Parameter b: Position of center of peak: 7.53 (mid July: maximum rainfall)

Parameter c: Inflection point distance to b. The two inflection point positions are b + c and b - c (controls the width of the bell)

3.13.2 Measured rainfall data of each station: quality aspects

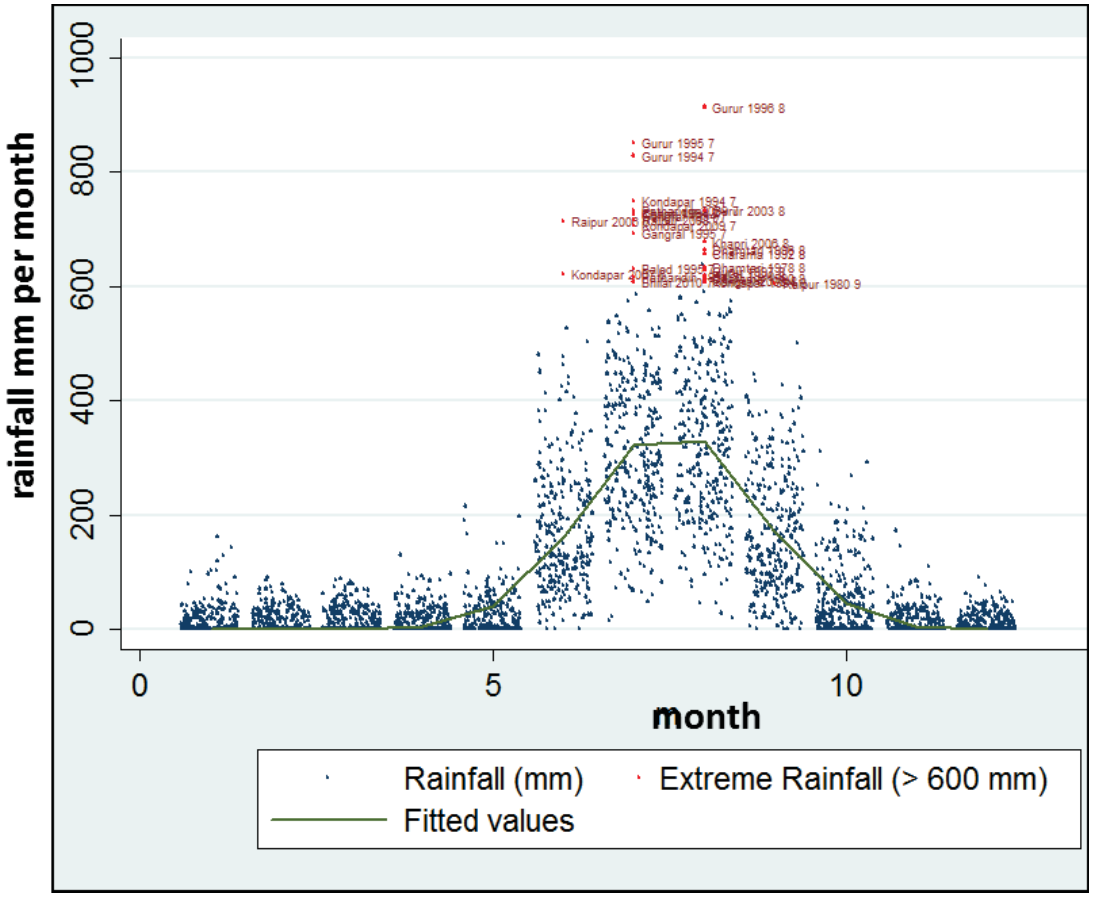

Figure 3.5 Monthly rainfall amounts exceeding 600 mm

1. The monthly rainfall values more than 600 mm were observed for certain rainfall stations (Figure 3.5). 600 mm is high monthly rainfall amount compared to the other years. However, it is quite possible that in a few months in the time series rainfall may be much higher than usual. The measurements of stations with more than 600 mm monthly rainfall were tested for quality. The monthly values were compared to the nearby stations, where the measurements were available for the same period and the results show that their monthly rainfall values were close to the investigated stations. This gives confidence to include the data in the calculation, and the reliability of the data was trusted for trend detection analysis.

2. No changes in the surrounding of rainfall stations (established in rural areas) except Bhilai.

3. All 14 rainfall stations show the same rainfall pattern over the years.

4. Same type of rain gauge was installed by the government department at all stations.

5. Rain gauge is used for rainfall measurement. Precision of the measurement varies from 5-8%

3.13.3 Overall station tendency for rainfall (mm) over the years

Six rainfall variables were considered for analysis between 1961 and 2011. Definition of the rainfall variables:

(1) Mean annual rainfall of each station was determined by dividing the total annual rainfall value by 12.

(2) Maximum monthly rainfall in a year is the maximum monthly rainfall amount within a year.

(3) Minimum monthly rainfall in a year is the minimum monthly rainfall amount within a year.

(4) Mean monthly rainfall in monsoon is the mean monthly rainfall amount for monsoon months (June to September).

(5) Maximum monthly rainfall in monsoon is the maximum monthly rainfall amount for monsoon months (June to September). This is basically the same as maximum monthly rainfall in a year because the month receiving the maximum rainfall is in the monsoon season only.

(6) Minimum monthly rainfall in monsoon is the minimum monthly rainfall amount between the months June to September.

The random effect Generalized Least Square regression method was applied to all six variables and the analysis is done for the below listed questions:

A) Is there any time effect for rainfall over the years for all 12 stations?

B) Is there any difference between rainfall patterns between the stations?

C) Is there any modification of rainfall for all 12 stations together with time?

The p test was used to check the level of significance. If p is significant, then the time series of the stations are not parallel, the time effect is modified by the stations and called interaction.

Table 3.8: Results of overall station tendency for rainfall

Variable	Time effect	Between stations	Station and time
Mean annual rainfall	p value = 0.683 (NS)	1st test P>chi = 0.660 (NS)	2nd test P>chi = 0.655 (NS)
Mean monthly rainfall in monsoon	p value = 0.990 (NS)	1st test P>chi = 0.4215 (NS)	2nd test P>chi = 0.4246 (NS)
Maximum monthly rainfall in a year	p value = 0.384 (NS)	1st test P>chi = 0.0789 (S)	2nd test P>chi = 0.0798 (S)
Maximum monthly rainfall in monsoon	p value = 0.374 (NS)	1st test P>chi = 0.0553 (S)	2nd test P>chi = 0.0560 (S)
Minimum monthly rainfall in a year	p value = 1.0 (NS)	1st test P>chi = 0.0230 (S)	2nd test P>chi = 0.0224 (S)
Minimum monthly rainfall in monsoon	p value = 0.518 (NS)	1st test P>chi = 0.8175 (NS)	2nd test P>chi = 0.8170 (NS)

****NS: Non-significant at p>0.1 and S: Significant at p≤0.1**

The analysis results suggest that the time series of the stations are parallel, and that there was no significant change in rainfall with time for six variables (Table 3.8). The time effect is not modified by the stations, and there is no station interaction for mean annual rainfall, mean monsoon rainfall and minimum monsoon rainfall over the years from 1991-2011.

The time effect is modified by the stations, and there is station interaction for maximum monthly rainfall in monsoon (p=0.05 level of significance), maximum monthly rainfall in a year (p=0.08) and minimum monthly rainfall in a year (p=0.02) over the years from 1991–2011.

3.13.4 Pair-wise station comparison for rainfall

For the 12 rainfall observation stations, the mean of the selected six rainfall variables from 1991-2011 with 95% confidence interval were analyzed and plotted (Figures 3.6 to 3.11).

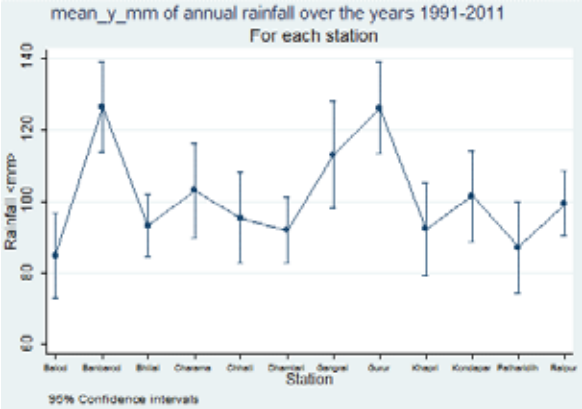

Figure 3.6: Mean annual rainfall

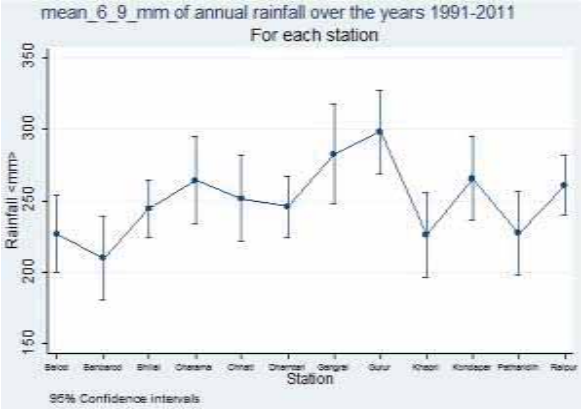

Figure 3.7: Mean monthly rainfall in monsoon

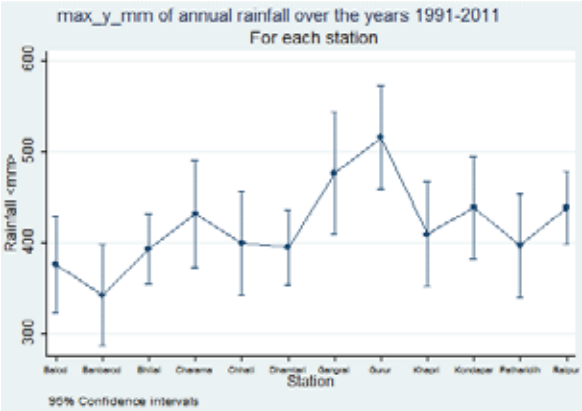

Figure 3.8: Maximum monthly rainfall in a year

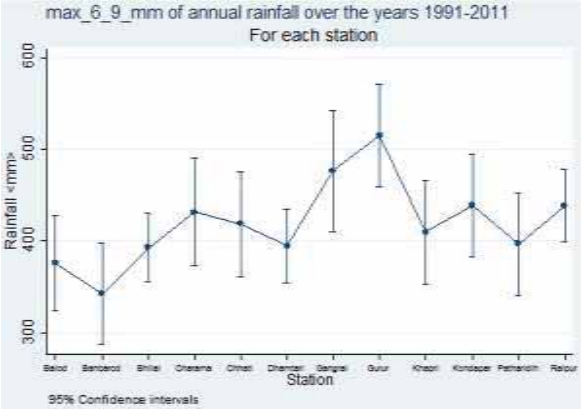

Figure 3.9: Maximum monthly rainfall in monsoon

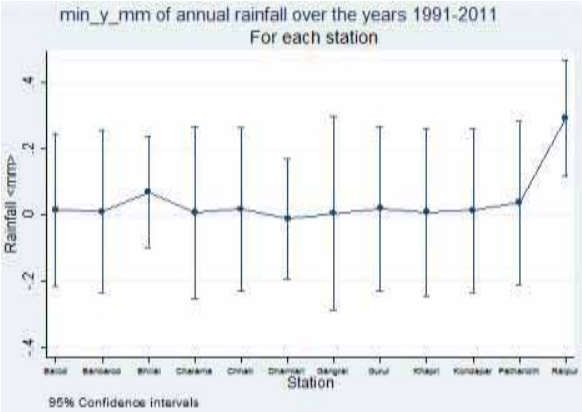

Figure 3.10: Minimum monthly rainfall in a year

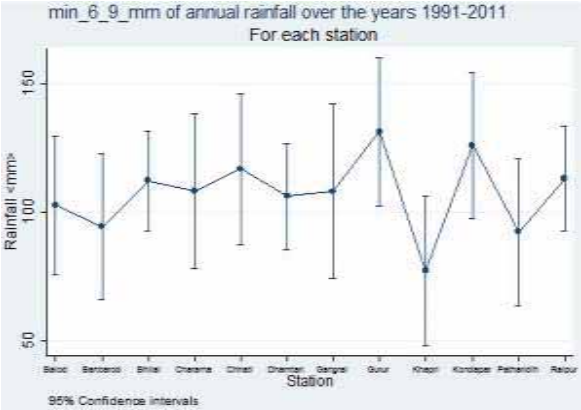

Figure 3.11: Minimum monthly rainfall in monsoon

(1) Mean annual rainfall: Certain stations behaved similarly over the 20 years (1991–2011) at 95 % confidence interval. For example: mean annual rainfall for Bhilai and Dhamtari is significantly similar. However, for these 2 stations the mean annual rainfall is significantly different compared to other 10 stations with 95 % confidence interval (Figure 3.6). This means that in case of gaps in rainfall data for a particular time, the values of Bhilai can be considered for filling gaps for Dhamtari and vice versa.

Banbarod and Gurur stations seem to show similar behavior. But this is not the case. The missing values of Banbarod were not filled. There are no measurements for specific periods between 1991 and 2011. Banbarod is the only station where the missing value is not available for the same period over the last 20 years. This leads to misleading results with respect to the mean over the year, and hence the similarity between the rainfall pattern between Gurur and Banbarod should not be considered.

(2) Maximum monthly rainfall in a year: maximum monthly rainfall in a year for Chhati and Khapri and Bhilai and Dhamtari rainfall stations were similar over the period of 20 years with 95% confidence interval (Figure 3.8). However, these stations were close to each other with slightly lower than 95% confidence interval. Charama and Kondapar show a similar pattern over the years at 95% confidence interval.

(3) Minimum monthly rainfall in a year: minimum monthly rainfall in a year is similar for all stations over the 20 year period with 95% confidence interval except for Raipur station (Figure 3.10).

(4) Mean monthly rainfall in monsoon: Bhilai and Dhamtari rainfall stations and Khapri and Patharidih rainfall stations show a similar pattern for mean monthly rainfall in the monsoon period (Figure 3.7).

(5) Maximum monthly rainfall in the monsoon period: Bhilai and Dhamtari rainfall stations show a similar rainfall pattern. However, the rainfall pattern of Patharidih is similar to that of Bhilai and Dhamtari but with a slightly higher confidence interval (Figure 3.9).

(6) Minimum monthly rainfall in the monsoon period: Khapri rainfall station received the lowest minimum monthly rainfall in the monsoon period. Charama and Gangral show a similar pattern with 95% confidence interval (Figure 3.11). However, all other stations received different amounts of rainfall (though they receive close rainfall amounts but not similar with 95% confidence interval).

3.13.5: Trend detection test for each station with six variables

(1) Mean annual rainfall (mm): regression analysis for each station

Both linear regression with ordinary least square (OLS) and Prais–Winsten AR (1) method were employed for trend detection (Table 3.9). Prais–Winsten AR (1) deals with the serial

autocorrelation in the time series dataset. The time variable y varies from 1961 to 2011 depending on station data availability, b estimates the tendency for the parameter over the years for each station, and p is used to test the level of statistical significance.

Table 3.9: Regression analysis test for each station for mean annual rainfall (1961-2011)

STATION	**OLS REG** **m=μ+ß*y**	**PRAIS – WINSTEN AR (1): m=μ+ß*y** **corrected for serial correlation**	**RESULT**
BALOD	b = -0.634 in [-2.3; 1.0] p=0.43160	b = -0.608 in [-2.6; 1.4] p=0.5329	No significant time effect.
BANBAROD	b = 1.405 in [-1.24; 4.05] p=0.27927	b = 1.542 in [-0.52; 3.60] p=0.13316	No significant time effect.
BHILAI	b = 0.50 in [0.08; 0.9] p=0.02128	b = 0.507 in [0.14; 0.87] p=0.00736	**There is a slightly significant time effect**
CHARAMA	b = -1.047 in [-3.98; 1.88] p=0.45942	b = -1.110 in [-2.9; 0.68] p=0.20773	No significant time effect.
CHHATI	b = -1.596 in [-4.02; 0.83] p=0.18382	b = -1.911 in [-5.162; 1.339] p=0.23263	No significant time effect.
DHAMTARI	b = 0.170 in [-0.4; 0.740] p=0.54918	b = 0.168 in [-0.420; 0.756] p=0.56571	No significant time effect.
GANGRAL	b = -1.407 in [-4.45; 1.64] p=0.33355	b = -1.420 in [-4.185; 1.344] p=0.28477	No significant time effect.
GURUR	b = 1.387 in [-1.38; 4.15] p=0.30585	b = 1.380 in [-1.340; 4.100] p=0.30058	No significant time effect.
KHAPRI	b = -3.204 in [-6.66; 0.25] p=0.06713	b = -3.198 in [-6.748; 0.353] p=0.07453	No significant time effect.
KONDAPAR	b = 0.246 in [-2.33; 2.82] p=0.84339	b = 0.288 in [-2.670; 3.246] p=0.84002	No significant time effect.
PATHARIDIH	b = 1.074 in [-1.11; 3.26] p=0.31591	b = 1.078 in [-1.137; 3.293] p=0.32011	No significant time effect.
RAIPUR	b = 0.101 in [-0.52; 0.72] p=0.74168	b = 0.102 in [-0.489; 0.692] p=0.72918	No significant time effect.

Conclusion: Based on both linear regression and Prais–Winsten AR (1) test, it can be concluded that there is a statistically significant increase in mean annual rainfall for Bhilai rainfall station.

The increase in mean annual rainfall is 0.5 mm per year at p=0.02 level of significance for the linear regression test, and p=0.007 (high) level of significance for the Prais–Winsten AR (1) test.

Yet, in the case of the Bonferroni criterion (p=0.05/12 ~ 0.004), the test should be judged at p=0.004 as the level of significance. Since both tests applied in this study have p < 0.004 level of significance, the increase in mean annual rainfall for Bhilai station is considered non-significant. However, the level of significance in the Prais–Winsten AR (1) test is p=0.007, which is quite close to the Bonferroni criterion of p=0.004 level of significance.

(2) Mean annual rainfall (mm): correlation analysis for each station

Here correlation analysis tests were performed to test the statistical significance of the observed trend. i.e., Pearson correlation coefficient test (parametric test), Spearman test (non-parametric test) and Kendall τ test (non-parametric test) (Table 3.10). However, these tests cannot estimate the strength of trend. Therefore to determine a trend through a correlation method, the modified non-parametric test i.e., Mann Kendall test using Theil-Sen's slope estimate was used. This test was applied only for those stations showing statistically significant result from those of the earlier tests.

Table 3.10: Correlation analysis test for each station for mean annual rainfall (1961-2011)

STATION	Kendall τ test:	Spearman test	Pearson test	Result
BALOD	tau a = -0.075 tau b = -0.075 p =0.6345	c.f. = -0.081 p = 0.7132	c.f. = -0.172 p = 0.4450	No significant time effect.
BANBAROD	tau a = 0.200 tau b = 0.200 p = 0.2300	c.f. = 0.268 p = 0.2539	c.f. = 0.254 p = 0.2793	No significant time effect.
BHILAI	tau a = 0.207 tau b = 0.207 p = 0.0350	c.f. = 0.304 p = 0.0316	c.f. = 0.325 p = 0.0213	**There is a slightly significant time effect.**
CHARAMA	tau a = -0.059 tau b = -0.059 p = 0.7619	c.f. = -0.123 p = 0.6273	c.f. = -0.186 p = 0.4746	No significant time effect.
CHHATI	tau a = -0.158 tau b = -0.158 p = 0.3468	c.f. = -0.235 p = 0.3195	c.f. = -0.310 p = 0.2254	No significant time effect.

DHAMTARI	tau a = 0.044 tau b = 0.044 p = 0.7061	c.f. = 0.053 p = 0.7537	c.f. = 0.100 p = 0.5492	No significant time effect.
GANGRAL	tau a = -0.165 tau b = -0.165 p = 0.4434	c.f. = -0.244 p = 0.4006	c.f. = -0.279 p = 0.3698	No significant time effect.
GURUR	tau a = 0.168 tau b = 0.168 p = 0.3145	c.f. = 0.245 p = 0.2976	c.f. = 0.241 p = 0.3059	No significant time effect.
KHAPRI	tau a = -0.158 tau b = -0.158 p = 0.3630	c.f. = -0.332 p = 0.1655	c.f. = -0.429 p = 0.1227	No significant time effect.
KONDAPAR	tau a = -0.053 tau b = -0.053 p = 0.7703	c.f. = -0.056 p = 0.8158	c.f. = 0.047 p = 0.8434	No significant time effect.
PATHARIDIH	tau a = 0.137 tau b = 0.137 p = 0.4173	c.f. = 0.191 p = 0.4199	c.f. = 0.236 p = 0.3159	No significant time effect.
RAIPUR	tau a = 0.005 tau b = 0.005 p = 0.9721	c.f. = 0.044 p = 0.7888	c.f. = 0.054 p = 0.7417	No significant time effect.

Conclusion: Based on the Kendall τ, Spearman and Pearson test, it is concluded that there is a statistically significant increase in mean annual rainfall for Bhilai rainfall station, which supports the results of the regression analysis.

The trend is significant at p=0.035 level of significance for Kendall τ test, p=0.03 level of significance for Spearman correlation test, and p=0.02 level of significance for Pearson correlation test.

Yet, according to the Bonferroni criterion (=0.05/12 ~ 0.004), the test should be judged at p=0.004 level of significance. None of the above-mentioned correlation tests fulfill the Bonferroni criterion for level of statistical significance.

The Mann Kendall test with Theil-Sen's slope was applied for Bhilai rainfall station, and also confirms the trend in mean annual rainfall. The rise of mean annual rainfall is detected as 0.4 mm per year at p=0.035 level of significance.

(3) Maximum monthly rainfall in a year (mm): regression analysis for each station

Linear regression with ordinary least square and Prais–Winsten AR (1) was employed for trend detection (Table 3.11).

Table 3.11: Regression analysis test for each station for maximum monthly rainfall in a year (1961-2011)

STATION	OLS regression	PRAIS–WINSTEN AR(1)	RESULT
BALOD	b = -4.135 in [-12.01; 3.74] p=0.28731	b = -4.013 in [-12.196; 4.170] p=0.31935	No significant time effect.
BANBAROD	b = 0.105 in [-6.150; 6.36] p=0.97232	b = 0.146 in [-5.760; 6.052] p=0.95920	No significant time effect.
BHILAI	b = 3.480 in [1.607; 5.352] p=0.00050	b = 3.472 in [1.768; 5.176] p=0.00016	**There is a significant time effect.**
CHARAMA	b = -5.666 in [-17.05; 5.72] p=0.30721	b = -7.081 in [-14.244; 0.083] p=0.05239	No significant time effect.
CHHATI	b = -6.136 in [-15.83; 3.56] p=0.20037	b = -5.478 in [-18.793; 7.84] p=0.39881	No significant time effect.
DHAMTARI	b = 0.282 in [-3.226; 3.79] p=0.87142	b = 0.236 in [-3.852; 4.325] p=0.90727	No significant time effect.
GANGRAL	b = -2.281 in [-17.7; 13.17] p=0.75333	b = -1.942 in [-18.466; 14.58] p=0.80219	No significant time effect.
GURUR	b = -10.59 in [-25.33; 4.25] p=0.15178	b = -9.978 in [-26.55; 6.599] p=0.22216	No significant time effect.
KHAPRI	b = -4.784 in [-17.67; 8.10] p=0.44408	b = -4.971 in [-15.708; 5.765] p=0.34233	No significant time effect.
KONDAPAR	b = 0.213 in [-9.446; 9.87] p=0.96357	b = 0.234 in [-9.611; 10.078] p=0.96080	No significant time effect.

PATHARIDIH	b = 7.957 in [-2.74; 18.65] p=0.13534	b = 8.064 in [-3.639; 19.77] p=0.16492	No significant time effect.
RAIPUR	b = 0.414 in [-2.895; 3.72] p=0.80150	b = 0.442 in [-2.160; 3.044] p=0.73271	No significant time effect.

Conclusion: Based on both linear regression and Prais–Winsten AR (1) test, it is concluded that there is a statistically significant increase in maximum monthly rainfall in a year for Bhilai rainfall station.

The increase in maximum monthly rainfall in a year is 3.48 mm per year at p=0.0005 (very high) level of significance for linear regression test and p=0.00016 (very high) level of significance for Prais–Winsten AR (1) test

If we consider the Bonferroni criterion (p=0.004 level of significance), both the tests found p > 0.004 level of significance, thus the increase in maximum monthly rainfall in a year for Bhilai station is considered statistically highly significant.

(4) Maximum monthly rainfall in a year (mm): correlation analysis for each station

The results of the correlation analysis of maximum monthly rainfall in a year are presented in Table 3.12.

Table 3.12: Correlation analysis test for each station for maximum monthly rainfall in a year (1961-2011)

STATION	Kendall's test	Spearman test	Pearson test	Result
BALOD	tau a = -0.083 tau b = -0.083 p = 0.5974	c.f. = -0.154 p = 0.4825	c.f. = -0.232 p = 0.3126	No significant time effect.
BANBAROD	tau a = -0.032 tau b = -0.032 p = 0.8711	c.f. = -0.024 p = 0.9198	c.f. = 0.008 p = 0.9723	No significant time effect.
BHILAI	tau a = 0.332 tau b = 0.332 p = 0.0007	c.f. = 0.471 p = 0.0006	c.f. = 0.475 p = 0.0005	**There is significant time effect.**
CHARAMA	tau a = -0.190 tau b = -0.190 p = 0.2889	c.f. = -0.238 p = 0.3408	c.f. = -0.255 p = 0.3377	No significant time effect.
CHHATI	tau a = -0.158	c.f. = -0.328	c.f. = -0.299	No significant time

	tau b = -0.158 p = 0.3468	p = 0.1582	p = 0.2400	effect.
DHAMTARI	tau a = 0.030 tau b = 0.030 p = 0.8015	c.f. = 0.019 p = 0.9112	c.f. = 0.027 p = 0.8714	No significant time effect.
GANGRAL	tau a = 0.033 tau b = 0.033 p = 0.9128	c.f. = 0.042 p = 0.8873	c.f. = -0.092 p = 0.7553	No significant time effect.
GURUR	tau a = -0.168 tau b = -0.168 p = 0.3145	c.f. = -0.224 p = 0.3423	c.f. = -0.333 p = 0.1971	No significant time effect.
KHAPRI	tau a = -0.193 tau b = -0.193 p = 0.2629	c.f. = -0.272 p = 0.2601	c.f. = -0.187 p = 0.4596	No significant time effect.
KONDAPAR	tau a = -0.021 tau b = -0.021 p = 0.9225	c.f. = -0.056 p = 0.8158	c.f. = 0.011 p = 0.9636	No significant time effect.
PATHARIDIH	tau a = 0.284 tau b = 0.284 p = 0.0855	c.f. = 0.305 p = 0.1906	c.f. = 0.346 p = 0.1353	No significant time effect.
RAIPUR	tau a = -0.036 tau b = -0.036 p = 0.7531	c.f. = -0.043 p = 0.7933	c.f. = 0.041 p = 0.8015	No significant time effect.

Conclusion: Based on Kendall τ, Spearman and Pearson test, it is concluded that there is a statistically significant increase in maximum monthly rainfall in a year for Bhilai rainfall station.

The trend is highly significant at p=0.007 level of significance for Kendall τ test, p=0.0006 level of significance for Spearman correlation test, and p=0.0005 level of significance for the Pearson correlation test.

All of the above-mentioned correlation tests also satisfy the Bonferroni criteria at p=0.004 level of significance for Bhilai station.

The Mann Kendall test with Theil-Sen's slope was applied for Bhilai rainfall station. The test confirms an increase in maximum monthly rainfall in a year at the rate of 3.7 mm per annum (p=0.0007 level of significance).

The Mann Kendall test with Theil-Sen's slope also detects an increase in maximum monthly rainfall in a year for Patharidih rainfall station. The increase is 8.75 mm per year at p=0.08 level of significance. However, both Spearman and Pearson correlation tests and also both regression tests found no significant trend. Thus it can be concluded that there is no significant change in Patharidith rainfall station.

(5) Mean monthly rainfall in monsoon: regression analysis for each station

The results of the regression analysis for mean monthly rainfall in the monsoon are presented in Table 3.13.

Table 3.13: Regression analysis test for each station for mean monthly rainfall in monsoon (1961-2011)

STATIONS	OLS regression	PRAIS–WINSTEN AR(1)	RESULT
BALOD	b = -0.967 in [-5.566; 3.63] p = 0.66622	b = -0.631 in [-6.144; 4.882] p=0.81411	No significant time effect.
BANBAROD	b = 2.503 in [-1.533; 6.540] p=0.20901	b = 2.710 in [-0.587; 6.008] p=0.10127	No significant time effect.
BHILAI	b = 1.270 in [0.136; 2.404] p=0.02896	b = 1.285 in [0.306; 2.264] p=0.01120	There is a slight significant time effect.
CHARAMA	b = -2.141 in [-9.723; 5.441] p=0.55779	b = -2.311 in [-6.685; 2.063] p=0.27925	No significant time effect.
CHHATI	b = -1.846 in [-6.232; 2.54] p=0.38684	b = -1.845 in [-6.237; 2.547] p=0.38783	No significant time effect.
DHAMTARI	b = 0.156 in [-1.452; 1.764] p=0.84519	b = 0.149 in [-1.609; 1.907] p=0.86455	No significant time effect.
GANGRAL	b = -0.869 in [-8.199; 6.46] p=0.80061	b = -1.063 in [-7.404; 5.277] p=0.72122	No significant time effect.
GURUR	b = -1.743 in [-7.954; 4.467] p=0.56273	b = -2.101 in [-7.174; 2.972] p=0.39577	No significant time effect.
KHAPRI	b = -4.067 in [-10.976; 2.84] p=0.23108	b = -3.716 in [-11.774; 4.34] p=0.34418	No significant time effect.
KONDAPAR	b = 0.545 in [-5.035; 6.125] p=0.83960	b = 0.599 in [-5.164; 6.363] p=0.82952	No significant time effect.
PATHARIDIH	b = 2.999 in [-2.586; 8.584]	b = 2.999 in [-2.587; 8.585]	No significant time

	p=0.27409	p=0.27416	effect.
RAIPUR	b = 0.316 in [-1.398; 2.031] p=0.71067	b = 0.309 in [-1.292; 1.909] p=0.69829	No significant time effect.

Conclusion: Based on linear regression, the test is statistically non-significant at p=0.01 level of significance for all stations. However, the Prais–Winsten AR (1) test shows that for Bhilai rainfall station the mean monthly rainfall in the monsoon is increasing @ 1.285 mm per year at p=0.01 level of significance. Considering the Bonferroni criterion (p=0.05/12 ~ 0.004 level of significance), both tests show p < 0.004, thus the increase in mean monthly rainfall in monsoon for Bhilai station is considered non-significant.

(6) Mean monthly rainfall in monsoon: correlation analysis for each station

Table 3.14: Correlation analysis test for each station for mean monsoon rainfall (1961-2011)

STATION	Kendall τ test	Spearman test	Pearson test	Result
BALOD	tau a = -0.043 tau b = -0.043 p = 0.7917	c.f. = -0.019 p = 0.9322	c.f. = -0.095 p = 0.6690	No significant time effect.
BANBAROD	tau a = 0.189 tau b = 0.189 p = 0.2561	c.f. = 0.269 p = 0.2511	c.f. = 0.294 p = 0.2090	No significant time effect.
BHILAI	tau a = 0.200 tau b = 0.200 p = 0.0412	c.f. = 0.266 p = 0.0617	c.f. = 0.309 p = 0.0290	There is a slight significant time effect.
CHARAMA	tau a = -0.046 tau b = -0.046 p = 0.8202	c.f. = -0.088 p = 0.7293	c.f. = -0.148 p = 0.5663	No significant time effect.
CHHATI	tau a = -0.135 tau b = -0.135 p = 0.4415	c.f. = -0.184 p = 0.4503	c.f. = -0.211 p = 0.4073	No significant time effect.
DHAMTARI	tau a = 0.018 tau b = 0.018 p = 0.8801	c.f. = 0.008 p = 0.9641	c.f. = 0.033 p = 0.8452	No significant time effect.
GANGRAL	tau a = -0.121 tau b = -0.121	c.f. = -0.152	c.f. = -0.074	No significant time

	p = 0.5841	p = 0.6048	p = 0.8017	effect.
GURUR	tau a = -0.111 tau b = -0.111 p = 0.5162	c.f. = -0.110 p = 0.6449	c.f. = -0.138 p = 0.5700	No significant time effect.
KHAPRI	tau a = 0.088 tau b = 0.088 p = 0.6243	c.f. = -0.221 p = 0.3631	c.f. = -0.288 p = 0.2690	No significant time effect.
KONDAPAR	tau a = 0.021 tau b = 0.021 p = 0.9225	c.f. = 0.044 p = 0.8551	c.f. = 0.048 p = 0.8396	No significant time effect.
PATHARIDIH	tau a = 0.126 tau b = 0.126 p = 0.4555	c.f. = 0.188 p = 0.4274	c.f. = 0.257 p = 0.2741	No significant time effect.
RAIPUR	tau a = 0.041 tau b = 0.041 p = 0.7180	c.f. = 0.046 p = 0.7791	c.f. = 0.061 p = 0.7107	No significant time effect.

Conclusion: Based on Kendall τ, Spearman and Pearson test (Table 3.14), it is concluded that there is a statistically significant increase in mean monthly rainfall in monsoon for Bhilai rainfall station.

The trend is significant at p=0.04 level of significance for Kendall τ test, p=0.06 level of significance for Spearman correlation test, and p=0.03 level of significance for Pearson correlation test. However, for the Bonferroni criterion (p=0.05/12 ~ 0.004 level of significance), none of the above-mentioned correlation tests satisfies.

The Mann Kendall test with Theil-Sen's slope was applied for Bhilai rainfall station. The test confirms an increase in mean monthly rainfall in monsoon at the rate of 1.064 mm per annum (p=0.04 level of significance).

(7) Maximum monthly rainfall in monsoon: regression and correlation analysis for each station:

Here the results are the same as those for maximum monthly rainfall in a year.

Both the regression and correlation test state that the maximum monsoon rainfall for Bhilai station is increasing at the rate of 3.5 mm per year at p = 0.00016 (very high level) level of statistical significance.

(8) Minimum monthly rainfall in monsoon: regression analysis for each station

Table 3.15: Regression analysis test for each station for minimum monthly rainfall in monsoon (1961-2011)

STATION	OLS regression	PRAIS–WINSTEN AR(1)	RESULT
BALOD	b = -0.092 in [-4.696; 4.512] p=0.96725	b = 0.065 in [-5.333; 5.462] p=0.98030	No significant time effect.
BANBAROD	b = 3.137 in [-2.133; 8.407] p=0.22715	b = 3.513 in [-0.305; 7.330] p=0.06909	No significant time effect.
BHILAI	b = -0.618 in [-1.780; 0.544] p=0.29016	b = -0.616 in [-1.628; 0.397] p=0.22735	No significant time effect.
CHARAMA	b = -3.226 in [-9.783; 3.332] p=0.31256	b = -3.072 in [-7.366; 1.223] p=0.14895	No significant time effect.
CHHATI	b = 2.699 in [-1.756; 7.153] p=0.21833	b = 2.738 in [-1.102; 6.577] p=0.15087	No significant time effect.
DHAMTARI	b = -0.345 in [-2.089; 1.398] p=0.69021	b = -0.345 in [-2.087; 1.396] p=0.68998	No significant time effect.
GANGRAL	b = -0.228 in [-5.682; 5.225] p=0.92878	b = -0.022 in [-4.877; 4.834] p=0.99238	No significant time effect.
GURUR	b = -0.316 in [-7.679; 7.047] p=0.92910	b = -0.125 in [-8.043; 7.794] p=0.97401	No significant time effect.
KHAPRI	b = -4.256 in [-9.846; 1.334] p=0.12662	b = -3.897 in [-10.376; 2.581] p=0.22143	No significant time effect.
KONDAPAR	b = 1.204 in [-4.945; 7.352] p=0.68573	b = 1.080 in [-4.372; 6.533] p=0.68213	No significant time effect.
PATHARIDIH	b = 1.166 in [-2.792; 5.123] p=0.54378	b = 0.724 in [-2.061; 3.508] p=0.59178	No significant time effect.
RAIPUR	b = 0.416 in [-1.022; 1.853] p=0.56185	b = 0.410 in [-0.997; 1.816] p=0.55901	No significant time effect.

Conclusion: Based on both linear regression and Prais–Winsten AR (1) test (Table 3.15), it is concluded that the test for all the station for minimum monthly rainfall in monsoon is statistically non-significant at any level of significance.

(9) Minimum monthly rainfall in monsoon: correlation analysis for each station

Table 3.16: Correlation analysis test for each station for minimum monthly rainfall in monsoon (1961-2011)

STATION	Kendall τ test	Spearman test	Pearson test	Result
BALOD	tau a = -0.051 tau b = -0.051 p = 0.7513	c.f. = -0.021 p = 0.9251	c.f. = -0.009 p = 0.9673	No significant time effect.
BANBAROD	tau a = 0.200 tau b = 0.200 p = 0.2300	c.f. = 0.257 p = 0.2738	c.f. = 0.283 p = 0.2272	No significant time effect.
BHILAI	tau a = -0.161 tau b = -0.161 p = 0.1011	c.f. = -0.224 p = 0.1180	c.f. = -0.153 p = 0.3013	No significant time effect.
CHARAMA	tau a = -0.176 tau b = -0.176 p = 0.3247	c.f. = -0.243 p = 0.3322	c.f. = -0.252 p = 0.3424	No significant time effect.
CHHATI	tau a = 0.240 tau b = 0.240 p = 0.1617	c.f. = 0.305 p = 0.2038	c.f. = 0.296 p = 0.2183	No significant time effect.
DHAMTARI	tau a = -0.001 tau b = -0.001 p = 1.0000	c.f. = -0.016 p = 0.9252	c.f. = -0.067 p = 0.6915	No significant time effect.
GANGRAL	tau a = -0.011 tau b = -0.011 p = 1.0000	c.f. = -0.077 p = 0.7938	c.f. = -0.026 p = 0.9288	No significant time effect.
GURUR	tau a = 0.042 tau b = 0.042 p = 0.8203	c.f. = 0.048 p = 0.8403	c.f. = -0.021 p = 0.9291	No significant time effect.
KHAPRI	tau a = -0.211 tau b = -0.211 p = 0.2199	c.f. = -0.340 p = 0.1545	c.f. = -0.363 p = 0.1775	No significant time effect.
KONDAPAR	tau a = -0.032 tau b = -0.032 p = 0.8711	c.f. = -0.036 p = 0.8799	c.f. = 0.096 p = 0.6857	No significant time effect.

PATHARIDIH	tau a = 0.053 tau b = 0.053 p = 0.7701	c.f. = 0.127 p = 0.5932	c.f. = 0.144 p = 0.5438	No significant time effect.
RAIPUR	tau a = 0.104 tau b = 0.104 p = 0.3513	c.f. = 0.151 p = 0.3519	c.f. = 0.095 p = 0.5618	No significant time effect.

Conclusion: Based on Kendall τ, Spearman and Pearson test (Table 3.16), it is concluded that there is no statistically significant trend in minimum monthly rainfall in monsoon for any of the rainfall stations.

3.13.6: Correlation analysis for rainfall of each station and month over the years

A correlation analysis for each station was performed to detect the trend at each month over the years (1961-2011).

Pearson, Spearman, Kendall tau and Mann Kendal test with Theil-Sen's slope correlation tests were employed to detect the trend at $p \leq 0.1$ level of statistical significance (Table 3.17).

Table 3.17: Correlation test: overview of significant change at each station for specific months

Months	Balod	Bhilai	Charama	Chhati	Dhamtari	Khapri	Patharidih	Raipur	Gangral, Banbarod, Gurur and Kondapar
Jan			**+ (S)**						Non-significant
Feb									
Mar					**+ (S)**				
Apr				**+ (S)**					
May	**+ (S)**			**+ (S)**					
June									
July						**- (S)**			
Aug		**+ (S)**							
Sep							**+ (S)**	**+ (S)**	

Oct	**- (S)**								
Nov									
Dec									

**** + (S) represents increasing significant trend and - (S) represents decreasing significant trend at p≤0.1 level of statistical significance**

A detailed description of the magnitude of change per station in each month (if statistically significant) is provided below:

(1) Balod rainfall station

A monthly rainfall trend is detected for May (p=0.035 for Kendall τ test, p=0.03 for Spearman test and non-significant for Pearson test) and October (p=0.09 for Kendall τ test, p=0.05 for Spearman test and non-significant for Pearson test).

The Mann Kendall test with Theil-Sen's slope shows a very small increase in monthly rainfall at the rate of 0.0001 mm per annum for May at p=0.05 level of significance and a decreasing trend for October at the rate of 0.5 mm per annum; however the significance level is less than p=0.1.

(2) Bhilai rainfall station

A monthly rainfall trend is detected for August at p=0.07 for Kendall τ test, p=0.08 for Spearman test and p=0.08 for Pearson test.

The Mann Kendall test with Theil-Sen's slope shows an increase in mean monthly rainfall at the rate of 2.43 mm per annum (p=0.1) for August.

(3) Charama rainfall station

A monthly rainfall trend is detected for January at p=0.1 for Kendall τ test, and p=0.092 for Spearman test. However, it is not statistically significant for the Pearson test (p=0.38). However, the Mann Kendall test with Theil-Sen's slope does not show any significant change for January. The reason might be the very low magnitude of rainfall in that month.

(4) Chhati rainfall station

A monthly rainfall trend is detected for April at p=0.1 for Kendall τ test, p=0.08 for Spearman test and p=0.1 for Pearson test.

The Mann Kendall test with Theil-Sen's slope shows an increase in monthly rainfall at the rate of 0.22 mm per annum (p=0.1) for April.

A monthly rainfall trend is detected for May at p=0.09 for Kendall τ test, and p=0.05 for Spearman test. However it is not statistically significant for the Pearson test (p=0.26).

The Mann Kendall test with Theil-Sen's slope shows a very small increase in monthly rainfall at a rate of 000.1 mm per annum (p=0.1) for May. Thus it is concluded that there is no significant change in rainfall for May.

A monthly rainfall trend is detected for August at p=0.03 for Kendall τ test, and p=0.02 for Spearman test. However, it is not statistically significant for the Pearson test (p=0.07).

(5) Dhamtari rainfall station

A monthly rainfall trend is detected for March at p=0.02 for Kendall τ test, p=0.01 for Spearman test and p=0.03 for Pearson test.

The Mann Kendall test with Theil-Sen's slope shows a slight increase in monthly rainfall at the rate of 0.0001 mm per annum (p=0.05) for March.

A monthly rainfall trend is detected for December at p=0.05 for Kendall τ test, p=0.04 for Spearman test and p=0.1 for Pearson test.

The Mann Kendall test with Theil-Sen's slope does not show an increase in monthly rainfall for December.

(6) Khapri rainfall station

A monthly rainfall trend is detected for July at p=0.08 for the Kendall τ test, and p=0.06 for the Spearman test. However, it is not statistically significant for the Pearson test (p=0.15). The Mann Kendall test with Theil-Sen's slope shows a decrease in monthly rainfall at (p=0.11, non-significant) for July.

(7) Patharidih rainfall station

A monthly rainfall trend is detected for September at p=0.08 for Kendall τ test, p=0.08 for Spearman test, and p=0.05 for Pearson test.

The Mann Kendall test with Theil-Sen's slope shows an increase in monthly rainfall at the rate of 5.56 mm per annum (p=0.12, non-significant) for September.

(8) Raipur rainfall station

A monthly rainfall trend is detected for September at p=0.08 for Kendall τ test, and p=0.1 for Spearman test. However, it is not statistically significant for the Pearson test (p=0.43).

The Mann Kendall test with Theil-Sen's slope shows an increase in monthly rainfall at the rate of 2.32 mm per annum for September at p=0.08 level of significance.

(9) Gangral, Banbarod, Gurur and Kondapar rainfall stations

No significant trend is detected for monthly rainfall for Gangral, Banbarod, Gurur and Kondapar rainfall stations.

3.13.7 Discussion on Bhilai rainfall station

In the trend analysis, out of the 12 rainfall stations only Bhilai rainfall station shows a significant increase in rainfall. The probable reasons are:

Bhilai rainfall station is located in an industrial area (Figure 3.12). There has been an expansion of the area over the years. The resulting increase in pollution and dust particles, which favor condensation, might be a reason for the significant increase in rainfall. The increase in urbanization in Bhilai might be another reason.

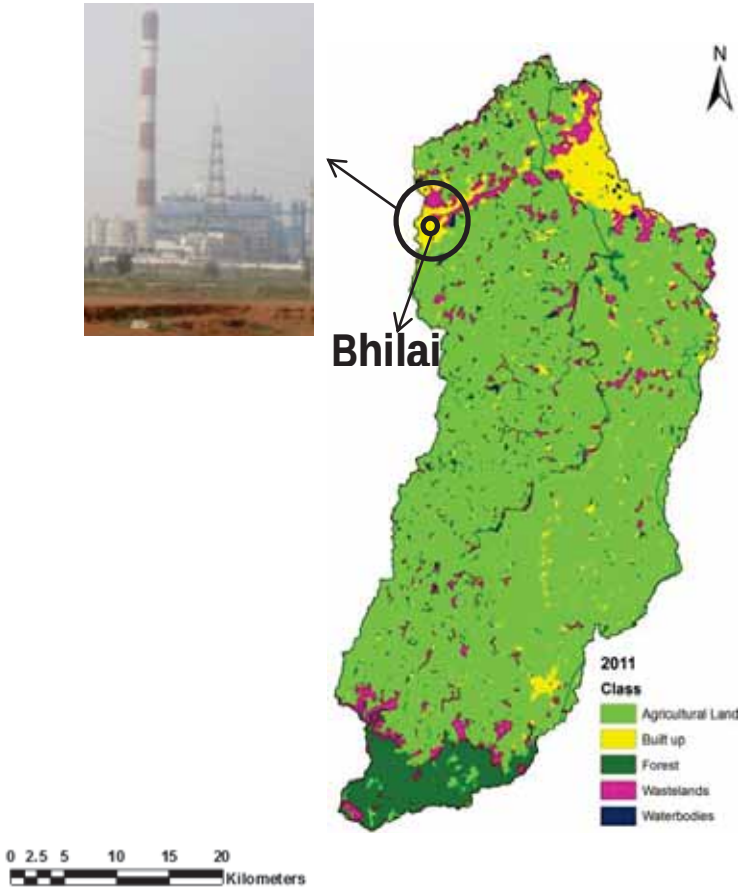

Figure 3.12: Location of Bhilai rainfall station

3.13.8 Trend detection analysis of rainfall (considering all stations together)

Considering the observations of all 12 rainfall stations together, the trend detection analysis of rainfall (all six variables) is described in the current section.

The rainfall observations (irrespective of the different time interval) of each station were used together for regression and correlation tests of trend detection.

(1) Mean annual rainfall: regression analysis

Linear regression with ordinary least square and Prais–Winsten AR (1) method was used for trend detection analysis. The time variable (1961 to 2011) depending on stations observation was considered.

The linear regression model was fitted in the time series data, and it can be seen that mean annual rainfall is increasing at the rate of 0.33 mm per year at p=0.04 level of statistical significance. The results of the Prais–Winsten AR (1) confirm that the mean annual rainfall is increasing at the rate of 0.32 mm per year at p=0.1 level of statistical significance (Figure 3.13).

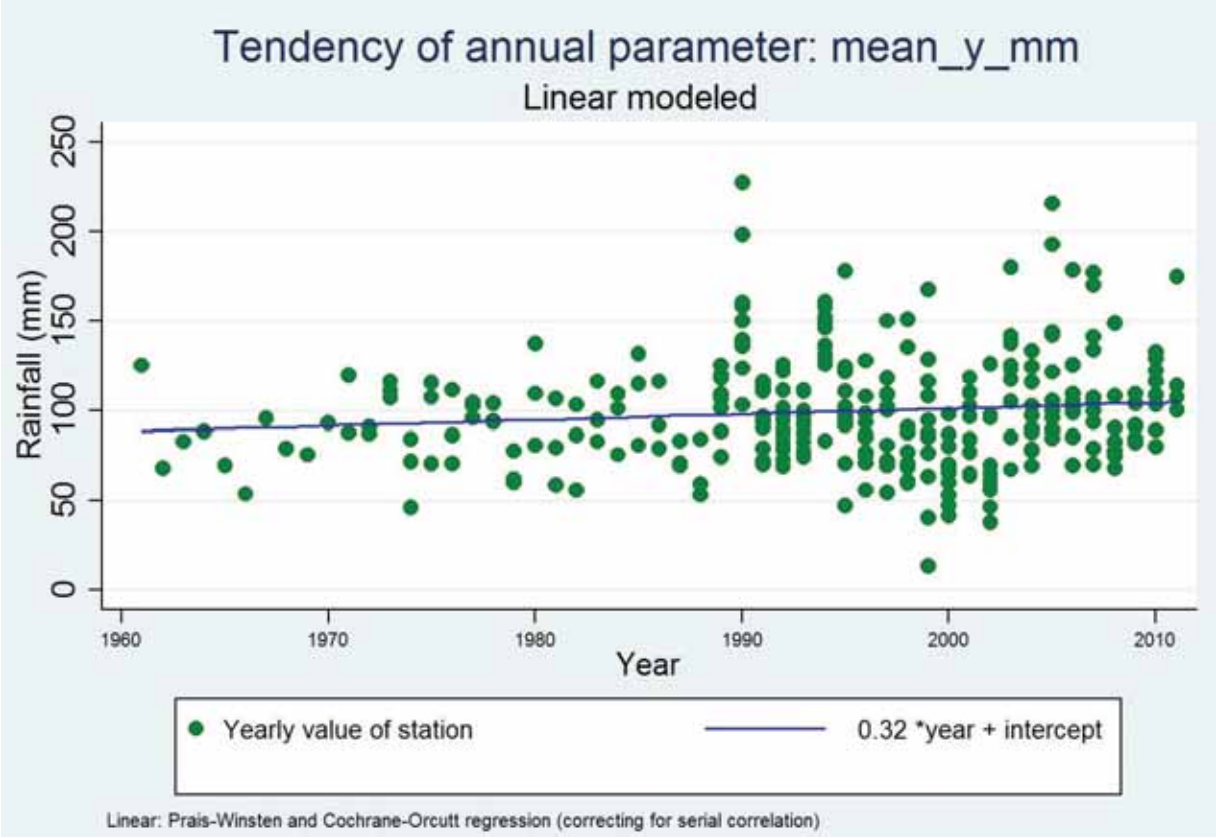

Figure 3.13: Mean annual rainfall (all stations together)

(2) Maximum monthly rainfall in a year: regression analysis

The linear regression model was fitted in the time series data and the results reveal that the maximum monthly rainfall in a year is increasing at the rate of 1.18 mm per year at p=0.09 level of statistical significance. However, according to the Prais–Winsten AR (1) test, the increase in maximum monthly rainfall in a year (at the rate of 1.17 mm per annum) was found to be non-significant (p=0.14) (Figure 3.14).

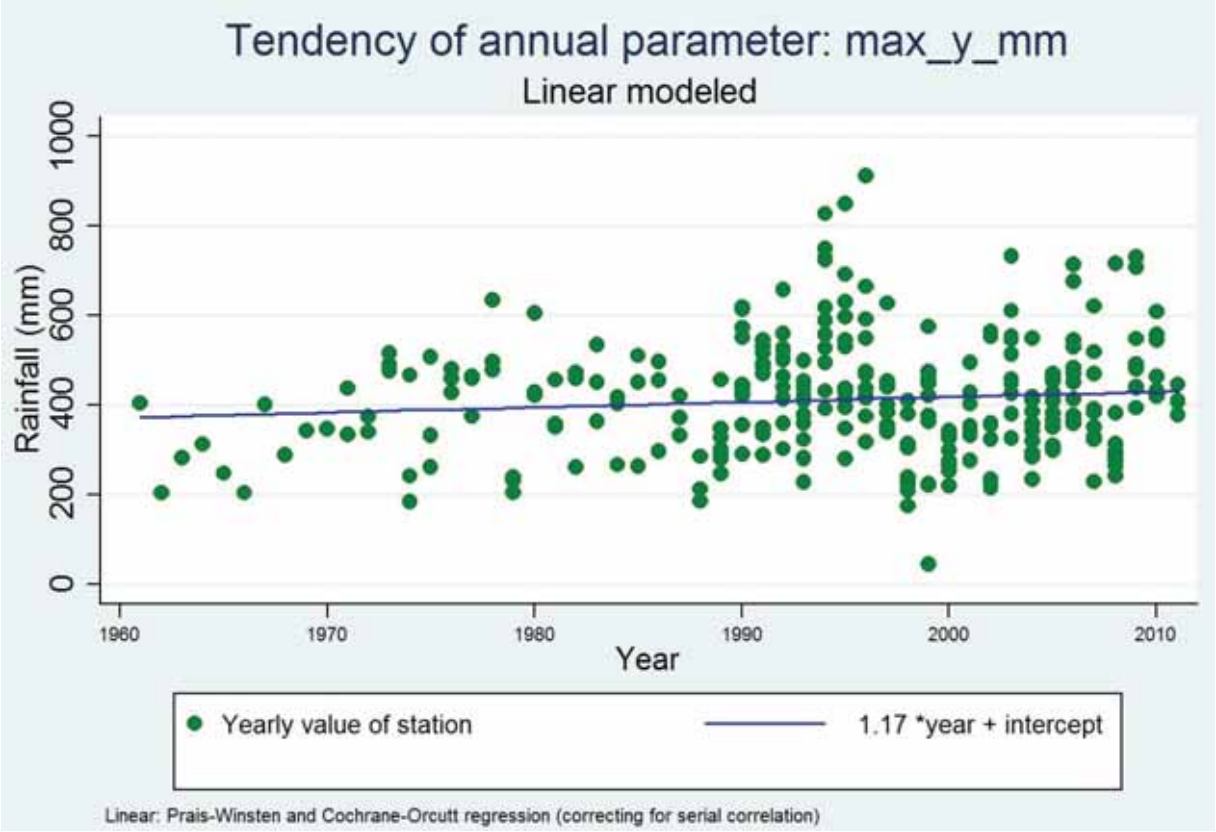

Figure 3.14: Maximum monthly rainfall in a year (all stations together)

(3) Mean monthly rainfall in monsoon: regression analysis

Linear regression model and Prais–Winsten AR (1) were fitted in the time series data, and both the models suggest that there is an increase in mean monthly rainfall in monsoon at the rate of 0.5 mm. However, both tests are non-significant (p=0.18 & p =0.20 respectively) (Figure 3.15).

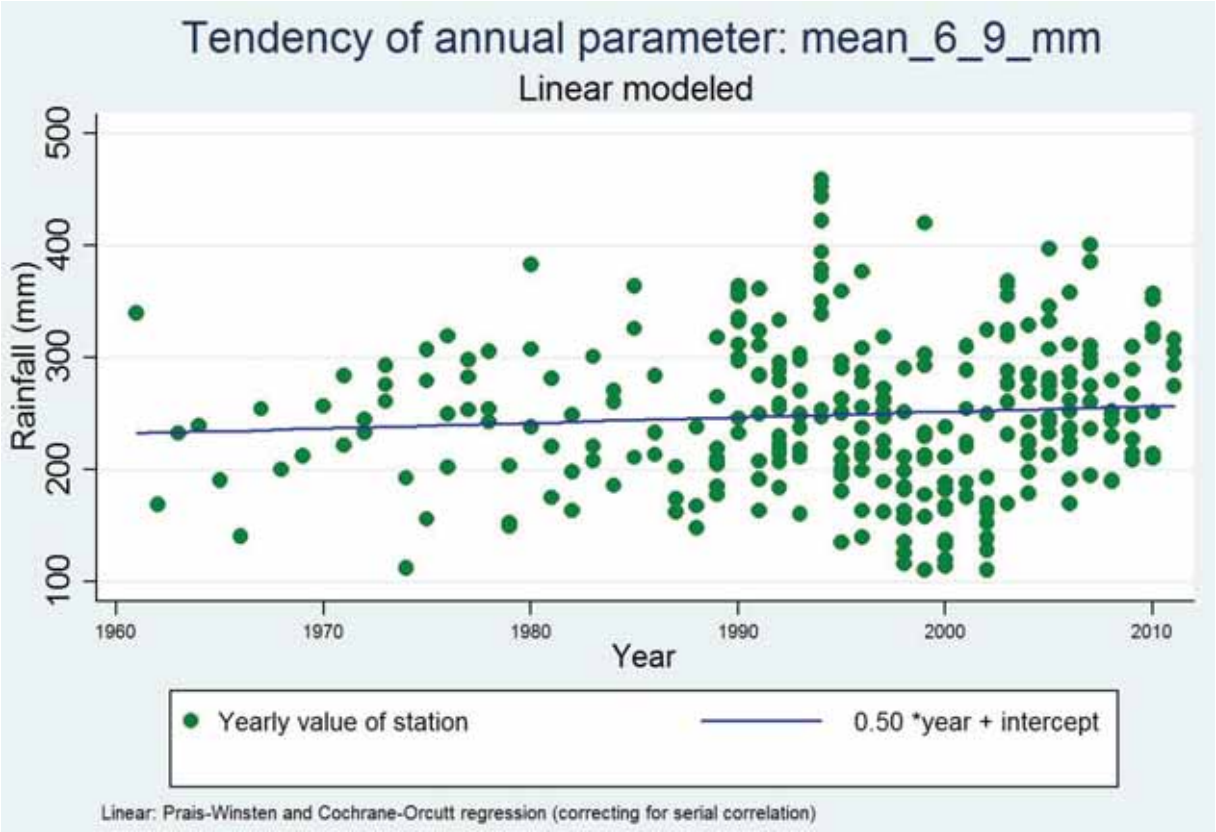

Figure 3.15: Mean monthly rainfall in monsoon (all stations together)

(4) Maximum monthly rainfall in monsoon: regression analysis

The linear regression model results reveal that the maximum monsoon rainfall is increasing at the rate of 1.22 mm per year at p=0.07 level of significance. The Prais–Winsten AR (1) test also confirms an increasing rate of 1.22 mm per year, but the test was found to be non-significant (p=0.12) Figure (3.16).

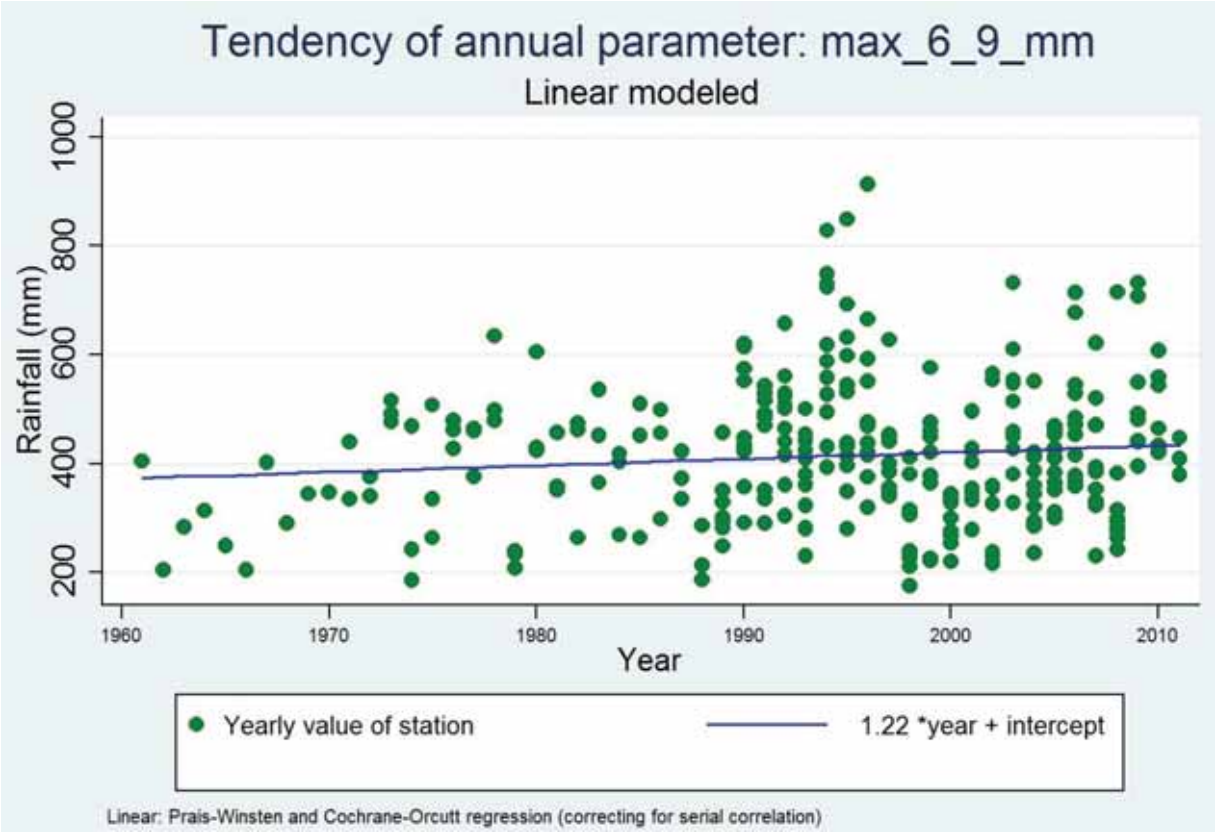

Figure 3.16: Maximum monthly rainfall in monsoon (all stations together)

(5) Minimum monthly rainfall in monsoon: regression analysis

Linear regression and Prais–Winsten AR (1) tests reveal that the minimum monthly rainfall in the monsoon is decreasing at the rate of 0.2 mm per annum, but both tests were non-significant (p=0.55 & p=0.55) (Figure 3.17).

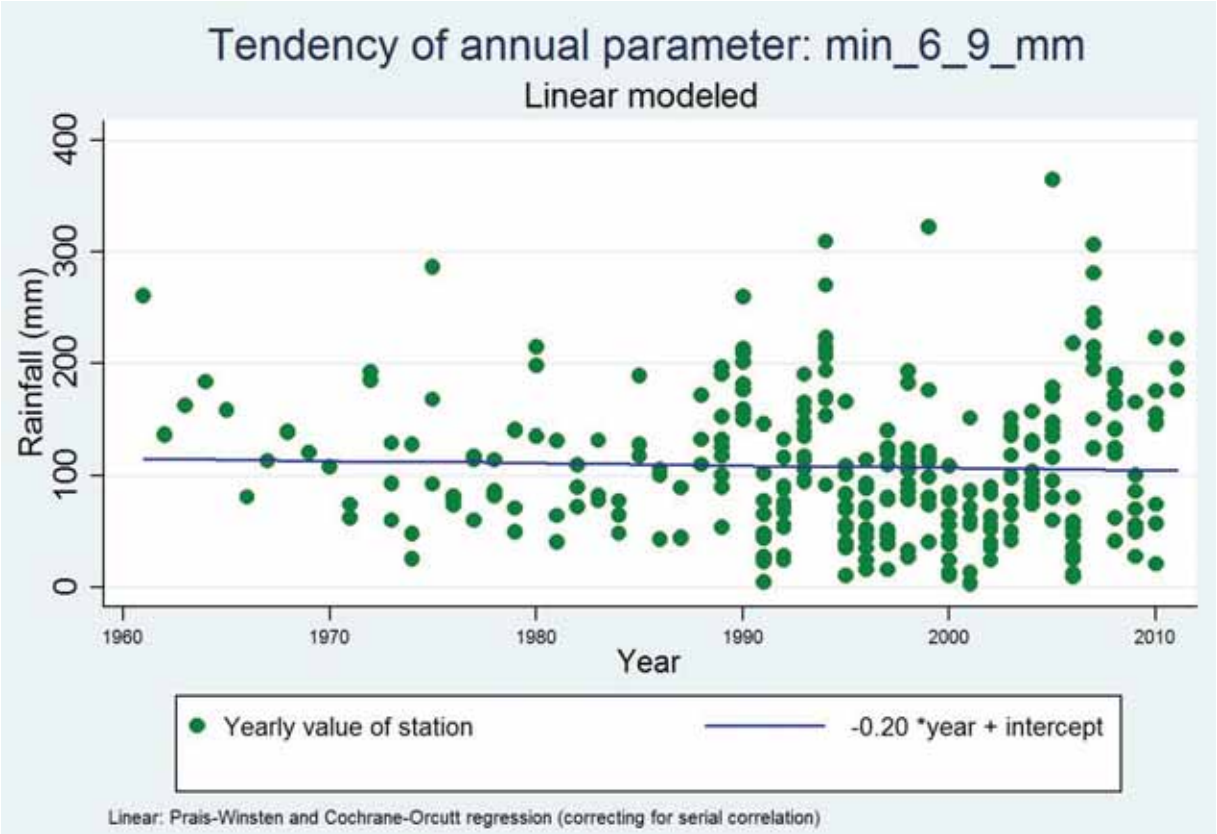

Figure 3.17: Minimum monthly rainfall in monsoon (all stations together)

(6) Correlation analysis of rainfall trend detection for all six variables considering all stations together from 1961 – 2011

The non-parametric tests – Kendall τ and Spearman correlation coefficient tests (see Table 3.18) - suggest that there is no statistically significant change in rainfall for all six variables over 1961-2011 considering all 12 stations together.

However, the Pearson correlation test (parametric test) found that the rainfall is statistically significantly increasing for mean annual rainfall (p=0.04), maximum annual rainfall (p=0.09), maximum monsoon rainfall (p=0.07) and statistical significantly decreasing for minimum annual rainfall (p=0.09).

Parametric and non-parametric tests show different results with respect to statistical significance. Hence, a third test termed as the Gaussian-linear trend detection analysis was used for trend detection.

(7) Month-wise correlation analysis of rainfall trend detection considering all stations together from 1961 – 2011

Table 3.18 : Correlation analysis of mean monthly rainfall values

```
********** Month = 1
 tau a tau b: -0.039-0.049     p:0.2880
 spearman   : -0.071           p:0.2550
 pearson    :  0.073           p:0.2387
********** Month = 2
 tau a tau b: -0.023-0.028     p:0.5418
 spearman   : -0.036           p:0.5591
 pearson    : -0.002           p:0.9773
********** Month = 3
 tau a tau b: -0.021-0.025     p:0.5843
 spearman   : -0.029           p:0.6395
 pearson    : -0.068           p:0.2757
********** Month = 4
 tau a tau b: -0.026-0.030     p:0.5071
 spearman   : -0.039           p:0.5300
 pearson    :  0.076           p:0.2190
********** Month = 5
 tau a tau b: -0.020-0.022     p:0.6208
 spearman   : -0.027           p:0.6695
 pearson    : -0.023           p:0.7091
********** Month = 6
 tau a tau b: -0.029-0.029     p:0.4603
 spearman   : -0.037           p:0.5206
 pearson    :  0.005           p:0.9337
********** Month = 7
 tau a tau b:  0.068 0.069     p:0.0789
 spearman   :  0.100           p:0.0842
 pearson    :  0.108           p:0.0612
********** Month = 8
 tau a tau b: -0.034-0.035     p:0.3742
 spearman   : -0.059           p:0.3084
 pearson    : -0.012           p:0.8341
********** Month = 9
 tau a tau b:  0.092 0.093     p:0.0180
 spearman   :  0.132           p:0.0233
 pearson    :  0.069           p:0.2370
********** Month = 10
 tau a tau b: -0.058-0.060     p:0.1341
 spearman   : -0.090           p:0.1191
 pearson    : -0.086           p:0.1409
********** Month = 11
 tau a tau b: -0.015-0.022     p:0.6236
 spearman   : -0.029           p:0.6125
 pearson    :  0.035           p:0.5478
********** Month = 12
 tau a tau b: -0.016-0.027     p:0.5534
 spearman   : -0.033           p:0.5706
 pearson    :  0.019           p:0.7478
```

Conclusion:

Based on the correlation test results (Table 3.18), it is found that:

- A monthly increase in rainfall trend is detected for July at p=0.08 level of significance for Kendall τ test, p=0.08 level of significance for Spearman test and p=0.06 level of significance for Pearson test.

- Kendall τ and Spearman correlation tests reveal an increase in the monthly rainfall trend for September at p=0.02 level of statistical significance. However, the Pearson correlation test (parametric) test was non-significant (p=0.24).

- Apart from July and September, the trend does not show statistically significant changes in monthly rainfall over the years (1961–2011).

3.13.9 Trend detection analysis of Gaussian-fitted rainfall observations (12 stations together)

As discussed earlier (section 3.13.1), a bell-shaped Gaussian fit was found suitable for the monthly rainfall pattern of all 12 stations. Thus, a bell-shaped curve was also fitted for the annual monthly rainfall pattern of 12 stations for each year between 1961 and 2011. The parameters of the fitted curve, i.e., annual amplitude, peak position of amplitude and standard deviation, were used for linear regression for trend analysis.

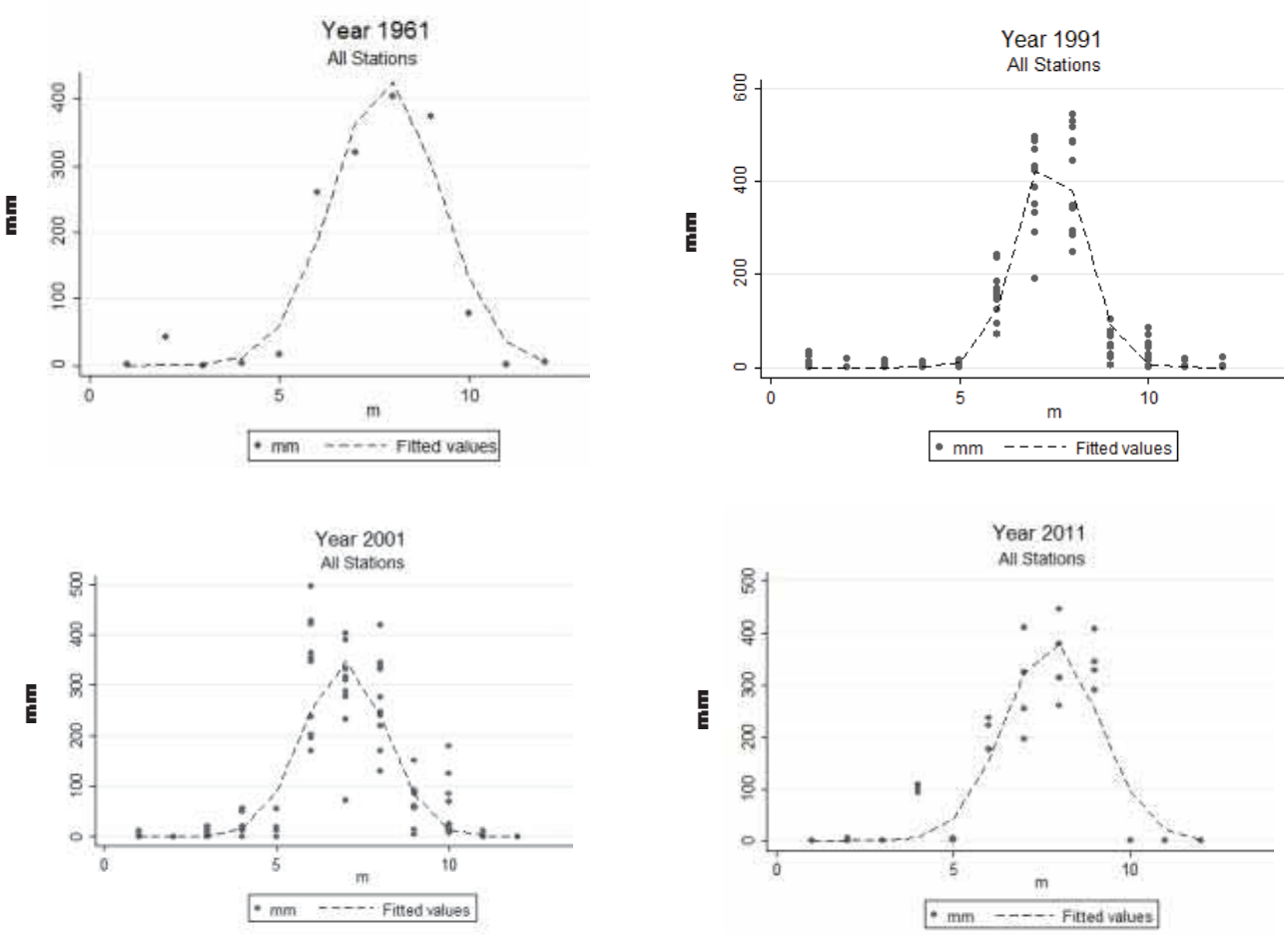

Figure 3.18: Examples of Gaussian-fitted monthly rainfall pattern of 12 stations (together)

(1) Trend detection for amplitude of fitted monthly rainfall patterns (1961-2011)

A straightforward approach termed as Gaussian – linear regression time series analysis was used. Here, the linear regression model was applied on each year's amplitude of the bell-shaped fitted monthly rainfall patterns (1961-2011).

Table 3.19: Linear regression analysis for amplitudes of annual rainfall (1961-2011) for all stations

```
reg amp year
```

Source	SS	df	MS		
Model	41779.2468	1	41779.2468	Prob > F	0.0325
Residual	422839.197	49	8629.37137	R-squared	0.0899
				Adj R-squared	0.0713
Total	464618.444	50	9292.36888	Root MSE	92.894

Number of obs	51
F(1, 49)	4.84

amp	Coef.	Std. Err.	t	P>|t|	[95% Conf.	Interval]
year	1.944461	.8837073	2.20	0.033	.1685844	3.720337
_cons	-3495.699	1755.091	-1.99	0.052	-7022.686	31.2883

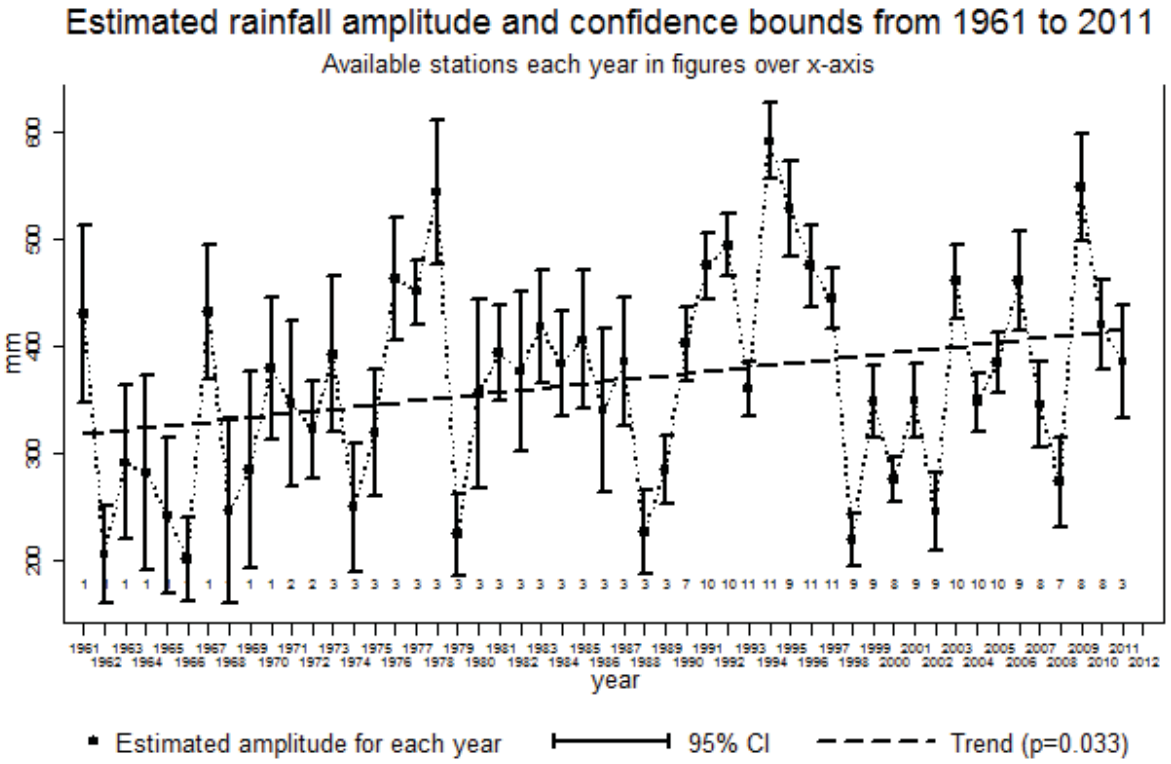

Figure 3.19: Estimated annual rainfall amplitude and confidence bound (95%) for all stations from 1961-2011

Conclusion: Based on the Gaussian-fitted linear regression (Table 3.19 and Figure 3.19), it is concluded that the annual rainfall amplitude (i.e., maximum monthly rainfall in a year) is significantly increasing at a rate of 1.94 mm per annum at p=0.033.

(2) Linear regression analysis for position of peak rainfall months

Linear regression analysis was applied on the positions of the peak rainfall month (1961 -2011)

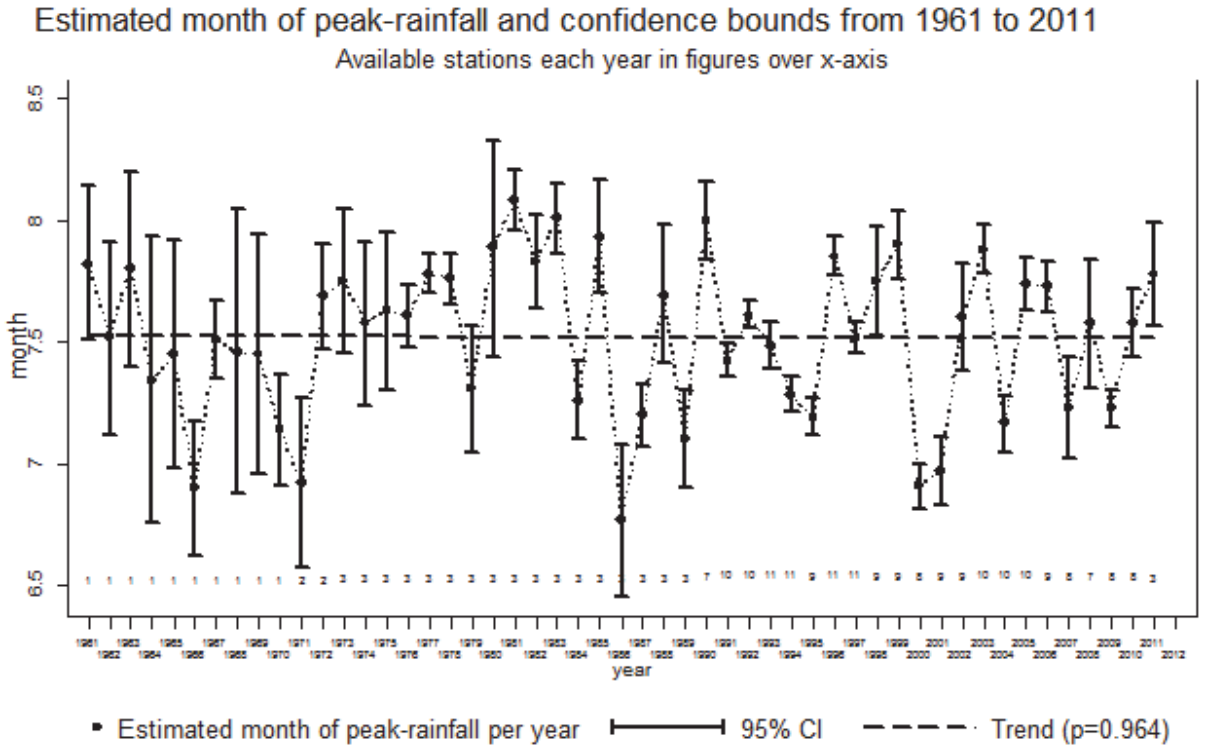

Figure 3.20: Estimated month of peak rainfall and confidence bound (95%) considering all stations together from 1961-2011

Conclusion: Based on the regression results (Figure 3.20), it is concluded that there is no statistically significant change in the month of peak annual rainfall. Mid July is the period of peak rainfall over the years (1961 – 2011). This also suggests that there is no shift in the peak monsoon rainfall month in the study area.

(3) Linear regression analysis for standard deviation of Gaussian fitted monthly rainfall (1961-2011)

A linear regression analysis was applied on each year's standard deviation of Gaussian-fitted monthly rainfall (1961 -2011).

Conclusion: The regression result reveals that there is no significant change in the standard deviation of annual rainfall (1961 to 2011).

The trend analysis of temperature is discussed in the next section.

3.14 Trend detection analysis for temperature in the study area

The trend analysis of temperature was performed in 2 phases:

(1) For mean annual, and (2) for mean monthly temperature values for Raipur station between 1971 and 2011.

Temperature parameters (°C): Maximum, minimum and average temperatures were analyzed separately. Parametric (linear regression, Prais-Winsten AR (1) and auto-segmented regression) and non-parametric tests (Spearman correlation and Mann Kendall test with Theil-Sen's slope were used for trend detection.

3.14.1 Mean annual maximum temperature

The moving average smoothing technique was used to remove the intra-annual seasonal fluctuation from the observed mean monthly maximum temperature (1971-2011) (Figure 3.21 and 3.22). A simple linear regression analysis was applied on mean monthly maximum temperature (without annual seasonal fluctuation) from 1971–2011 (Table 3.20 and Figure 3.23).

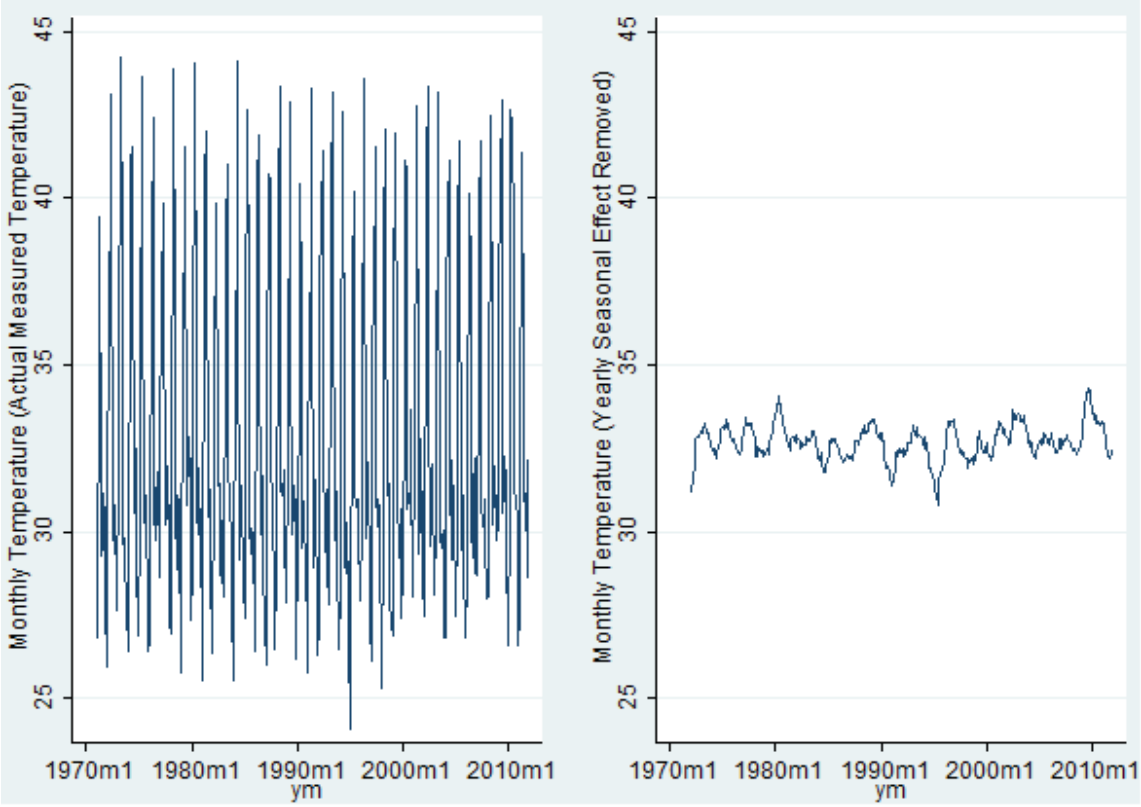

Figure 3.21: Observed mean monthly maximum temperature (L) and mean monthly maximum temperature after removed annual seasonal fluctuation (R)

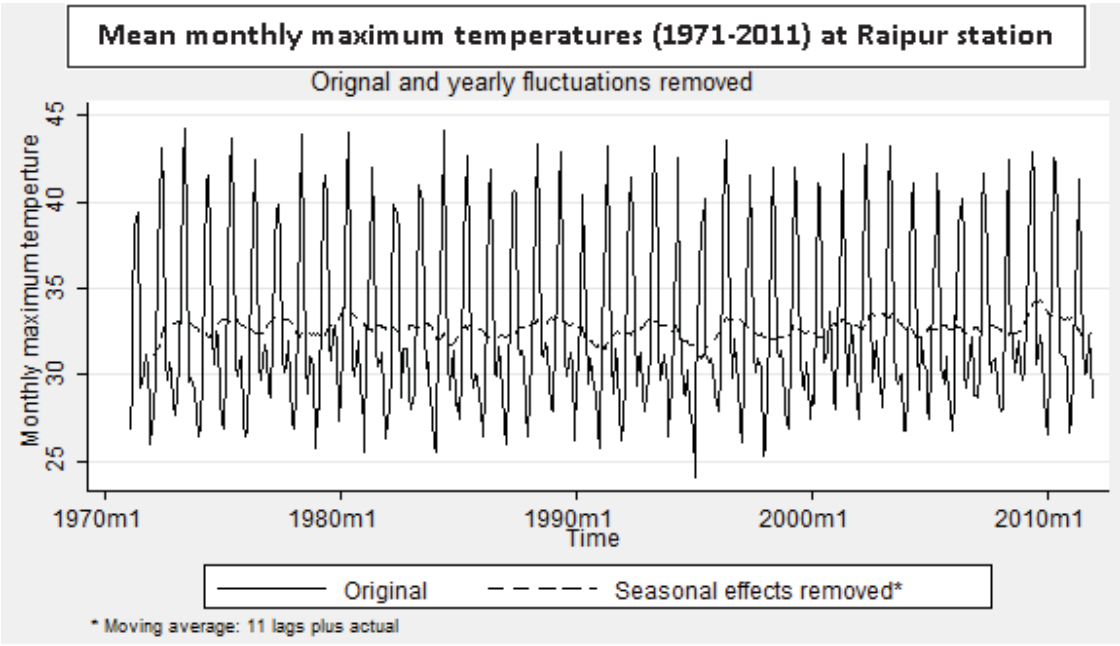

Figure 3.22: Mean monthly maximum temperature (original and annual seasonal effect removed) at Raipur station

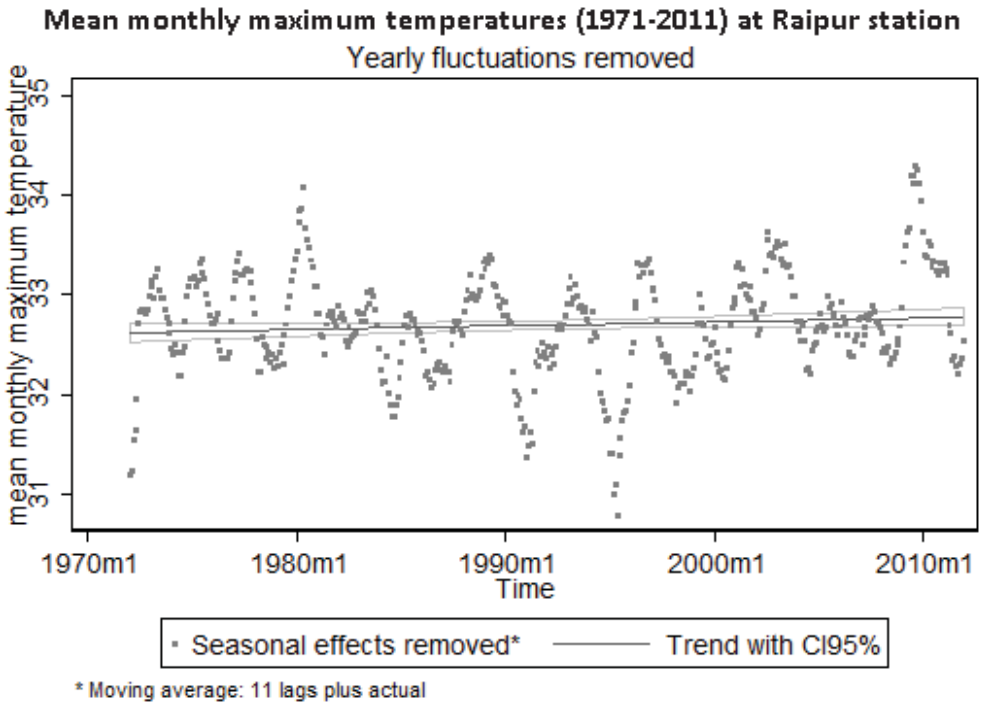

Figure 3.23: Fitted trend - mean monthly maximum temperature (annual seasonal effect removed) at Raipur station.

Table 3.20: Simple linear regression between mean monthly maximum temperatures (without seasonal fluctuation)

```
. reg t1 ym
```

Source	SS	df	MS		
Model	1.02938964	1	1.02938964	Number of obs =	480
Residual	127.469572	478	.266672745	F(1, 478) =	3.86
				Prob > F =	0.0500
Total	128.498962	479	.268265056	R-squared =	0.0080
				Adj R-squared =	0.0059
				Root MSE =	.5164

t1	Coef.	Std. Err.	t	P>|t|	[95% Conf.	Interval]
ym	.0003342	.0001701	1.96	0.050	-3.74e-08	.0006685
_cons	32.57053	.0693631	469.57	0.000	32.43423	32.70682

Conclusion: The simple linear regression shows a significant increase in mean annual maximum temperature by 0.0003342°C per annum, which is small and thus not relevant. The level of significance is p=0.05.

Table 3.21: Prais-Winsten AR (1) test

```
Prais-Winsten AR(1) regression -- iterated estimates

      Source |       SS       df       MS              Number of obs =     480
-------------+------------------------------           F(  1,   478) = 2709.44
       Model |  65.3736574     1  65.3736574            Prob > F      =  0.0000
    Residual |  11.5332454   478  .024128129           R-squared     =  0.8500
-------------+------------------------------           Adj R-squared =  0.8497
       Total |  76.9069028   479  .160557208           Root MSE      =  .15533

------------------------------------------------------------------------------
          t1 |      Coef.   Std. Err.      t    P>|t|     [95% Conf. Interval]
-------------+----------------------------------------------------------------
          ym |   .0008347   .0009121     0.92   0.361    -.0009574    .0026268
       _cons |   32.31727   .3754049    86.09   0.000     31.57962    33.05492
-------------+----------------------------------------------------------------
         rho |   .9499398
------------------------------------------------------------------------------
Durbin-Watson statistic (original)    0.091887
Durbin-Watson statistic (transformed) 1.593202
```

Conclusion: The Prais-Winsten AR (1) test (Table 3.21) was applied to correct the serial autocorrelation, and the result confirms that there is no significant difference over the years for the mean annual maximum temperature for Raipur station.

3.14.2 Trend detection analysis of mean monthly maximum temperature observations (1971-2011)

(1) Mean monthly maximum temperature (1971-2011) annual pattern for Raipur station

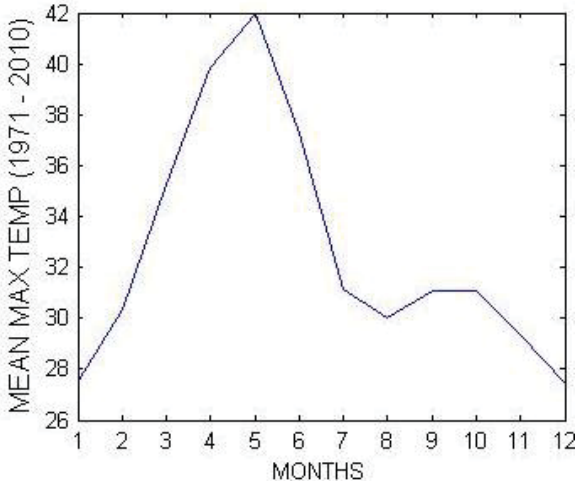

Figure 3.24: Mean monthly maximum temperature (1971-2011) annual pattern for Raipur station

The mean monthly maximum temperature for Raipur station over the years 1971–2011 is not normally distributed (Figure 3.24). So, the Gaussian function cannot be applied. To analyze the data in original form (maintaining the integrity of 12 months), i.e., without removing the seasonal effect, an auto-segmented linear function was used to fit the mean monthly temperature data. For trend detection, regression and correlation tests were applied on the fitted parameters (observed amplitude and predicted amplitude).

The mean monthly measured temperature was well fitted by auto-segmented linear functions for each year with R^2 square between 0.92 to more than 0.98 for most of the years from 1971-2011. The graphs of fitted data are shown for a few years as examples in Figures 3.25 and 3.26.

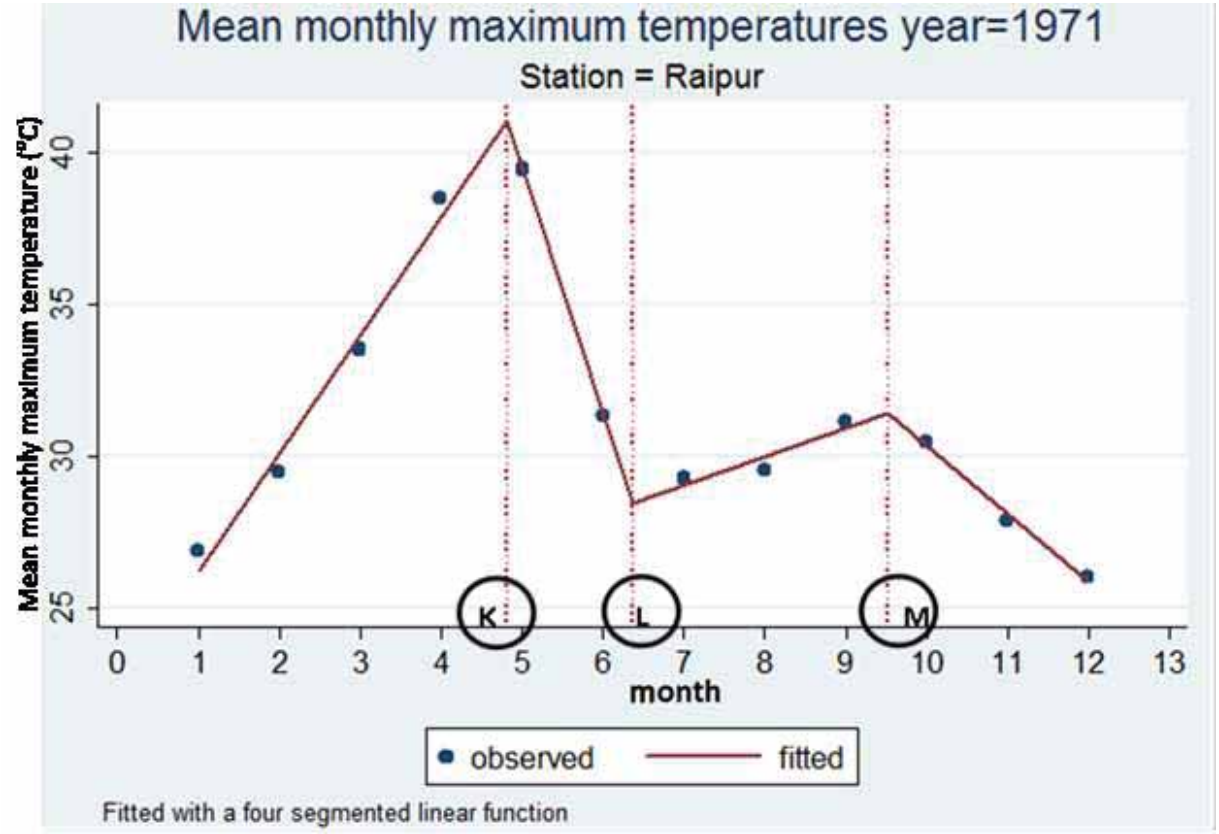

Figure 3.25: Auto-segmented fitted mean monthly maximum temperature for 1971

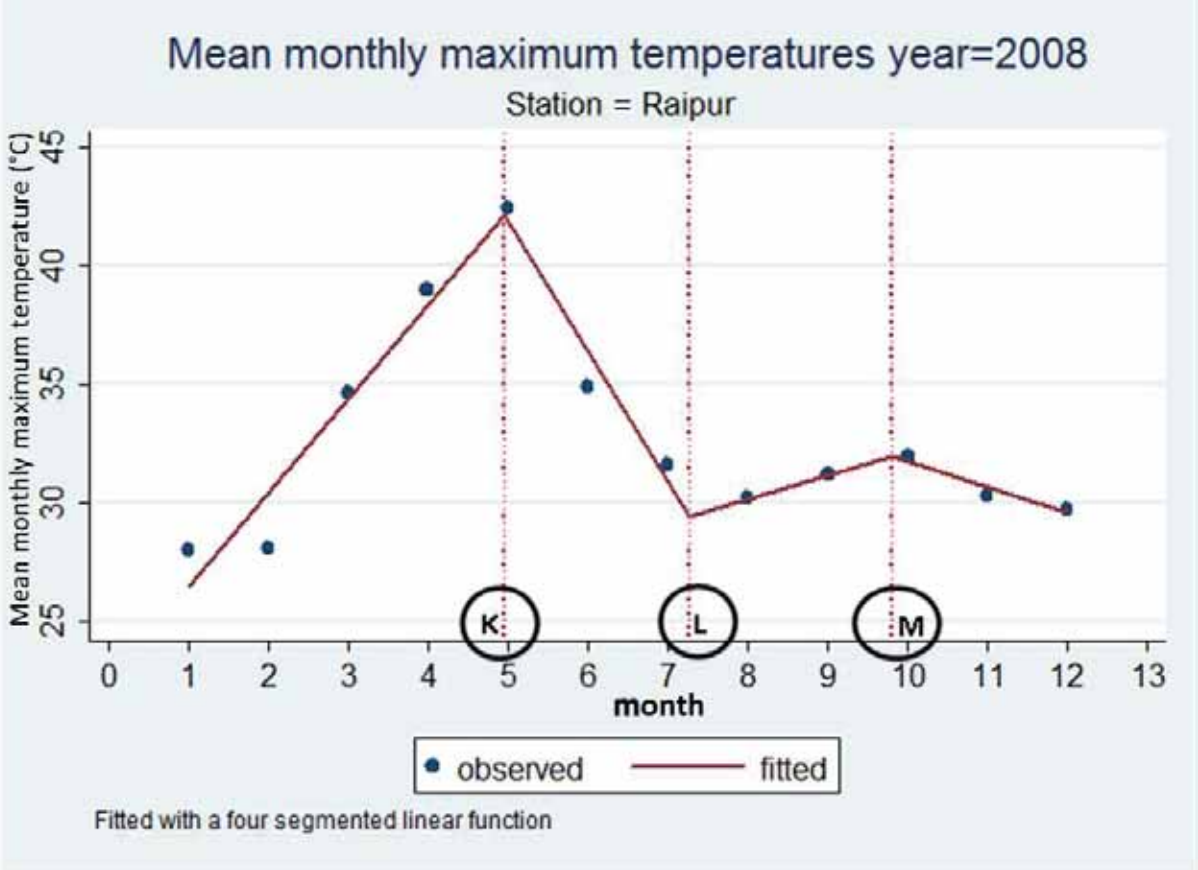

Figure 3.26: Auto-segmented fitted mean monthly temperature for 2008

Conclusion: Both the regression and correlation test for fitted parameters (observed amplitude and predicted amplitude) were found to be non-significant. This confirms the results of the linear regression and Prais-Winsten AR (1), which state that the mean annual maximum temperature shows no significant changes between 1971 and 2011.

3.14.3 Mean annual minimum temperature

Similar to mean annual maximum temperature, linear regression, Prais-Winsten AR (1) and auto-segmentation methods were applied for trend analysis of mean annual minimum temperature.

The simple linear regression analysis for annual mean minimum temperature (seasonal effect removed) shows a significant increase in temperature by 0.0010202°C per annum, which is quite small and thus not relevant. However, it might be significant because of the large number of observations. The Prais-Winsten AR (1) test confirms that there is no significant difference (p=0.486) over the years for the annual mean minimum temperature for Raipur station.

Also, for auto-segmented test, the regression and correlation test for fitted parameters (observed amplitude and predicted amplitude) for mean annual minimum temperature were found to be non-significant.

3.14.4 Mean annual average temperature

Similar to mean annual maximum temperature, linear regression, Prais-Winsten AR (1) and auto-segmentation methods were applied for trend analysis of mean annual average temperature. All tests show non-significant change in annual average temperature for Raipur station between 1971 and 2011.

In the next sections, the results of the trend detection analysis are provided for mean monthly temperature (maximum, minimum and average) for Raipur station (1971-2011).

3.14.5 Month-wise correlation and regression analysis of mean monthly maximum temperature

Month-wise regression and correlation tests were conducted to identify the temperature change over the years from 1971-2011. The correlation equations were applied on two datasets: (1) on actual measured time series of mean monthly maximum temperature, and (2) mean monthly maximum temperature time series data with seasonal effect removed.

(1) Trend analysis of mean monthly maximum temperature (observed data)

The correlation tests based on Kendall τ, Mann Kendall with Theil-Sen's slope, Spearman and Pearson tests confirm that there is a significant increase in the mean monthly maximum temperature for November and December. In order to confirm the correlation tests for significance and also to estimate the magnitude of change, regression analysis was employed only for those months.

The Mann Kendall test with Theil-Sen's slope estimate, which is functionally similar to Kendall τ test, suggests that the temperature in the month of November is increasing by 0.04°C at p=0.01 level of significance.

Regression analysis confirms that the temperature at Raipur station in the month of November is increasing by 0.0349°C per year at p=0.017 level of significance. However, the increase in mean monthly maximum temperature is also observed at the significance level p=0.007 and 0.008 in the Kendall τ and Spearman tests, respectively.

Regression analysis confirms that the mean monthly maximum temperature of Raipur station in December is increasing by 0.03°C per year at p=0.037 level of significance. However, the increase in temperature can also be observed at significance level p=0.049 and 0.037 in the Kendall τ and Spearman tests, respectively.

The Mann Kendall test, which is similar to the Kendall τ test, suggests that the temperature in December is increasing annually at the rate of 0.03℃ at p=0.05 level of significance.

(2) Trend analysis for mean monthly maximum temperature (seasonal effect removed)

Based on regression and correlation analysis, it is concluded that there is no significant change in any month for mean monthly maximum temperature for Raipur station.

3.14.6 Month-wise correlation analysis for mean monthly minimum temperature

(1) Trend analysis for mean monthly minimum temperature (observed data)

The correlation tests based on the Kendall τ, Mann Kendall with Theil-Sen's Slope, Spearman and Pearson tests confirm that there was a significant change in the mean monthly minimum temperature for March, July and August. To confirm the correlation tests for significance and also to estimate the magnitude of change, a regression analysis was also employed for those months.

The regression analysis confirms that the mean monthly minimum temperature at Raipur station in March is increasing by 0.01℃ per year at p=0.088 level of significance. An increase in temperature was also detected at significance level p=0.088 and 0.07 in Kendall τ and Spearman tests, respectively. The Mann Kendall test with Theil-Sen's slope estimate reveals that the mean monthly minimum temperature of March is increasing by 0.028℃ at p=0.1 level of significance.

The regression analysis confirms that the mean monthly minimum temperature at Raipur station in July is increasing by 0.02℃ per annum at p=0.026 level of significance. An increase in temperature was also identified at significance level p=0.014 and 0.009 by the Kendal τ and Spearman tests, respectively. The Mann Kendall test with Theil-Sen's slope estimate, suggests that the mean monthly minimum temperature in July is increasing by 0.026°C at p=0.05 level of significance.

The regression analysis confirms that the mean monthly minimum temperature of Raipur station in August is increasing by 0.02℃ per year at p=0.019 level of significance. An increase in temperature was also identified at significance level p=0.0075 and 0.0051 in Kendall tau and Spearman tests, respectively. The Mann Kendall test with Theil-Sen's slope estimate, suggests that the mean monthly minimum temperature in August is increasing by 0.027 ℃ at p=0.01 level of significance.

(2) Trend analysis for mean monthly minimum temperature (seasonal effect removed)

Based on the results of the regression and correlation tests, it can be concluded that there is no significant change in any month for mean monthly minimum temperature for Raipur station.

3.14.7 Month-wise correlation analysis for mean monthly average temperature

(1) Trend analysis for mean monthly average temperature (observed data)

The correlation tests based on Kendall τ, Mann Kendall with Theil-Sen's slope estimate, Spearman and Pearson tests confirm that there is a significant change in mean monthly average temperature for July, August, November and December. In order to confirm the correlation tests for significance and also to estimate the magnitude of change, regression analysis was employed for those months.

The regression analysis confirms that the temperature at Raipur station in July is increasing by 0.016°C per annum at p=0.1 level of significance. An increase in temperature was also observed at significance level p=0.06 and 0.045 in Kendal τ and Spearman tests respectively. The Mann Kendall test with Theil-Sen's slope estimate, suggests that the temperature in July is increasing by 0.015°C at p = 0.1 level of significance.

The regression analysis confirms that the temperature of Raipur station in the month of August is increasing by 0.016°C per annum at p=0.043 level of significance. The increase in temperature was also observed at significance level p=0.043 and 0.032 in Kendall τ and Spearman tests, respectively. The Mann Kendall with Theil-Sen's slope estimate reveals that the mean monthly average temperature in July is increasing by 0.016°C at p=0.05 level of significance.

The regression analysis confirms that the mean monthly average temperature of Raipur station in November is increasing by 0.027°C per year at p=0.14 level of significance, which is non-significant. However, test is significant at the significance level p=0.034 and 0.055 in Kendall τ and Spearman tests, respectively. The Mann Kendall with Theil-Sen's slope estimate reveals that the mean monthly average temperature in November is increasing by 0.041°C at p=0.05 level of significance.

The regression analysis confirms that the mean monthly average temperature of Raipur station in December is increasing by 0.023°C per year at p=0.1 level of significance. The increase in temperature was also observed at significance level p=0.08 and 0.06 in Kendall tau and Spearman tests, respectively. The Mann Kendall test with Theil-Sen's slope estimate suggests that the mean monthly average temperature in December is increasing by 0.026°C at p=0.1 level of significance.

(2) Trend analysis for mean monthly average temperature (seasonal effect removed)

The correlation tests based on Kendall τ test indicate a significant change in mean monthly average temperature for March. However, no significant change was found in the Spearman and Pearson tests. To test the result of Kendall τ correlation test, regression analysis was applied. Here no significant change in mean monthly average temperature for March was detected (p=0.19). However, the Mann Kendall with Theil-Sen's slope estimate reveals that the mean monthly average temperature in March is increasing by 0.011°C at p=0.1 level of significance.

3.15 Summary of trend detection analysis

Three types of statistical analysis were performed for trend detection of rainfall and maximum, minimum and average temperature. Twelve rainfall stations and one temperature station observations were used in the analysis.

1. Parametric tests (linear regression (OLS), Prais-Winsten AR (1) and Pearson product-moment correlation coefficient (r))

2. Non-parametric tests (Spearman's rank correlation coefficient (ρ) Kendall τ rank correlation coefficient and Mann Kendall test with Theil-Sen's slope estimate)

3. Gaussian-linear trend detection analysis

The statistical tests were judged at $p \leq 0.1$ level of statistical significance

3.15.1 Trend detection analysis of rainfall

The trend detection analysis for rainfall was performed in 2 phases (1) for all stations together and (2) for each station.

12 rainfall stations in and around the UKC were selected for trend detection analysis.

(1) Trend detection analysis using all stations together for 6 rainfall variables

S.N.	Rainfall variable	Parametric test	Non-parametric tests
1	Mean annual rainfall	Linear regression (OLS): increasing @ 0.33 per annum (p=0.04) Prais–Winsten AR (1): increasing @ 0.33 per annum (p=0.04)	Non-significant
2	Maximum monthly rainfall in a year	Linear regression (OLS): increasing @ 1.18 per annum (p=0.09) Prais–Winsten AR (1): increasing @ 1.17 per annum (p=0.14) – non-significant	Non-significant
3	Mean monthly rainfall in monsoon	Non-significant	Non-significant
4	Maximum monthly rainfall in monsoon	Non-significant	Non-significant
5	Minimum monthly rainfall in monsoon	Non-significant	Non-significant

6	Minimum monthly rainfall in a year	Non-significant	Non-significant

The Gaussian-linear trend detection analysis shows an increasing maximum monthly rainfall at a year at a rate of 1.94 mm per annum at p=0.033. However, there is no significant change in the month of peak annual rainfall. Mid July remains the period of peak rainfall over the years (1961 – 2011). There is also no significant change in the standard deviation of annual rainfall (1961 to 2011).

(2) Trend detection analysis using all stations together: for each month

S.N.	Month	Parametric test	Non-parametric test
1	July	Non-significant	Kendall τ test increasing trend (p=0.08) Spearman ρ test increasing trend (p=0.06)
2	September	Non-significant	Kendall τ test increasing trend (p=0.02) Spearman ρ test increasing trend (p=0.02)
3	Rest months (except July and September)	Non-significant	Non-significant

(3) Trend detection analysis for each station: six rainfall variables

Out of 12 rainfall stations only Bhilai rainfall station shows a significant trend for rainfall.

S.N.	Rainfall variable Bhilai station	Parametric test	Non-parametric test
1	Mean annual rainfall	Linear regression (OLS): increasing trend @ 0.5 mm per annum at p = 0.02 and p= 0.007 for Prais–Winsten AR (1)	Mann Kendall test: increasing trend @ 0.4 mm per annum at p = 0.03 and Spearman ρ test (p = 0.02)
2	Maximum monthly rainfall in a year	Linear regression (OLS): increasing trend @ 3.48 mm per annum at p = 0.0005 and p= 0.00016 for Prais–Winsten AR (1)	Mann Kendall test: increasing trend @ 3.7 mm per annum at p = 0.0007 and Spearman ρ test (p = 0.0006)
3	Mean monthly rainfall in monsoon	Linear regression (OLS): increasing trend @ 1.27 mm per annum at p = 0.02 and p= 0.01 for Prais–Winsten AR (1)	Mann Kendall test: increasing trend @ 1.06 mm per annum at p = 0.04 and Spearman ρ test (p = 0.06)
4	Maximum monthly rainfall in monsoon	Same as maximum monthly rainfall in a year	Same as maximum monthly rainfall in a year
5	Minimum monthly rainfall in monsoon	Non-significant	Non-significant
6	Minimum monthly rainfall in a year	Non-significant	Non-significant

(4) Trend detection analysis for each station for each month

Out of 12 rainfall stations only Bhilai and Raipur rainfall station shows a significant trend for rainfall.

S.N.	Station	Month	Parametric test	Non-parametric test
1	Bhilai	August	Pearson test: increasing trend at p = 0.08	Mann Kendall test: Increasing @ 2.43 mm per annum (p=0.1) and p = 0.08 for Spearman test
2	Raipur	September	Non-significant	Mann Kendall test: Increasing @ 2.32 mm per annum (p=0.08) and p = 0.1 for Spearman test
3	Rest 10 rainfall stations	All 12 months	Non-significant	Non-significant

(5) Discussion on Bhilai rainfall station

In the trend analysis, out of the 12 rainfall stations only Bhilai rainfall station shows a significant increase in rainfall. The probable reasons are that Bhilai rainfall station is located in an industrial area, which has expanded over the years. Therefore, an increase in pollution and dust particles, which favor condensation, might be one reason for the significant increase in rainfall. The increase in urbanization in Bhilai might be another.

3.15.2 Trend detection analysis of temperature

Mean annual maximum, minimum and average temperature and mean monthly maximum, minimum and average temperature for Raipur meteorological station were considered for time series trend detection analysis.

(1) Trend detection analysis: annual trend

Mean annual maximum temperature, mean annual minimum temperature and mean annual average temperature show no significant trend between 1971 and 2011.

(2) Trend detection analysis for each month

Maximum temperature	Month	Parametric test	Non-parametric test
Mean monthly maximum temperature	November	Linear regression (OLS): increasing @ by 0.035 °C per annum (p=0.02)	Mann Kendall test: increasing @ 0.04°C per annum (p=0.01) and p = 0.008 for Spearman test

Minimum temperature	Month	Parametric test	Non-parametric test
Mean monthly minimum temperature	March	Linear regression (OLS): increasing @ by 0.01°C per annum (p=0.09)	Mann Kendall test: increasing @ 0.028°C per annum (p=0.1) and p = 0.07 for Spearman test
	July	Linear regression (OLS): increasing @ by 0.02°C per annum (p=0.03)	Mann Kendall test: increasing @ 0.026°C per annum (p=0.05) and p = 0.009 for Spearman test
	August	Linear regression (OLS): increasing @ by 0.02 °C per annum (p=0.02)	Mann Kendall test: increasing @ 0.027 °C per annum (p = 0.01) and p = 0.01 for Spearman test

Average temperature	Month	Parametric test	Non-parametric test
Mean monthly average temperature	July	Linear regression (OLS): increasing @ 0.016 °C per annum (p=0.1)	Mann Kendall test: increasing @ 0.015 °C per annum (p=0.1) and p = 0.05 for Spearman test
	August	Linear regression (OLS): increasing @ 0.016 °C per annum (p=0.043)	Mann Kendall test: increasing @ 0.016 °C per annum (p=0.05) and p = 0.03 for Spearman test
	November	Non-significant	Mann Kendall test: increasing @ 0.041 °C per annum (p=0.05) and p = 0.06 for Spearman test
	December	Linear regression (OLS): increasing @ 0.023 °C per annum (p=0.1)	Mann Kendall test: increasing @ 0.026 °C per annum (p=0.1) and p = 0.06 for Spearman test

3.16 Downscaling of PRECIS climate change scenarios

As both dynamic and statistical downscaling techniques have their characteristic pros and cons in transferring the GCM scenarios to a higher resolution, a combination of the advantages of both techniques was used to yield the best possible future scenarios for the study area.

The PRECIS RCM scenarios (result of dynamic downscaling technique) produced for India and that especially consider the characteristics of the Indian southwest monsoon are used for this study. The PRECIS scenarios show better resolution and characteristics of Indian conditions compared to GCM scenarios. Kumar et al. (2011) reported that PRECIS scenarios show reasonable skill in simulating the Indian monsoon climate. As documented in literature, PRECIS scenarios have been used for climate change impact analysis in agriculture and water resource management in India; such work includes that of Gosain et al. (2011), Geethalakshmi et al. (2011) and Roy and Mazumdar (2013).

However, PRECIS is a product of a dynamic downscaling technique, so there might be the possibility of systematic biases in the results due to the lateral boundary condition of the GCM scenarios. Such biases in PRECIS are confirmed by Kumar et al. (2011), who found substantial wet biases in model simulation over the west coast and east central India (location of study area) in the baseline simulation of ensembles q0 and q14.

In order to obtain the best possible climate change scenarios for the area of interest, it is necessary to apply the statistical downscaling technique for bias correction of PRECIS scenarios at station level. Keeping the above facts in mind, a simple bias correction technique named ‘mean monthly scaling method’ was introduced (see section 3.12.2).

3.16.1 Simple bias correction of RCM using mean monthly scaling adjustment

Multiplicative scaling adjustment is applied for rainfall and additive scaling adjustment for temperature. For details of the method and results of bias correction of PRECIS RCM scenarios (q0, q1 & q14) of Raipur station see sections 3.12.2, 3.16.2, 3.16.3 and 3.16.4. For the other 13 rainfall stations, only a summary of the results is provided in section 3.16.5. In section 3.16.6, rainfall for the entire UKC is discussed for the q0, q1 and q14 scenarios and compared with the observed baseline scenario (1990-2008).

3.16.2 PRECIS RCM q0 rainfall scenario of Raipur station

Table 3.22: Mean monthly observed rainfall and q0 PRECIS RCM rainfall scenario of baseline (1971-2005) for Raipur rainfall station

Months		Jan	Feb	Mar	Apr	May	Jun	July	Aug	Sep	Oct	Nov	Dec
Observed rainfall	1971 to	0.49	0.49	0.44	0.46	0.77	6.05	10.12	10.9	6.03	1.64	0.46	0.17

(mm/day)	2005												
PRECIS rainfall (mm/day)	1971 to 2005	0.48	0.41	0.54	0.61	2.92	10.3	14.78	12.0	8.39	2.28	1.22	0.65
Scaling factor		1.03	1.20	0.82	0.75	0.26	0.59	0.68	0.91	0.72	0.72	0.38	0.26

A comparison was made between the mean monthly observed rainfall and PRECIS RCM q0 rainfall scenario for the period 1971 to 2005. The PRECIS RCM q0 scenarios show a significant wet biasness in the rainfall observations. There is always a tendency of PRECIS to significantly over-estimate high rainfall values especially for the monsoon months from June to September. However, for January and February it slightly under-underestimates the rainfall values (Table 3.22).

The wet biasness behavior of PRECIS RCM scenarios is due to the lateral boundary conditions of the GCM scenarios from which they were derived. Since this biasness is systematic in nature, it was corrected using the simple mean monthly scaling adjustment technique (multiplicative approach) as discussed in detail in section 3.12.2.

The derived bias correction scaling factor was applied to the observed rainfall values for the period between 2006 and 2010. The validation of observed values and bias-corrected q0 RCM scenario rainfall values from 2006 to 2010 was compared and it was found that the correlation coefficient is 0.8315. This confirms that the applied method and scaling factor are quite acceptable, and later the same scaling factor was applied for bias correction of the future scenarios from 2011 to 2098.

Figure 3.27 to 3.30 shows the different phases of the multiplicative approach of bias correction of the q0 PRECIS RCM rainfall scenario for Raipur station.

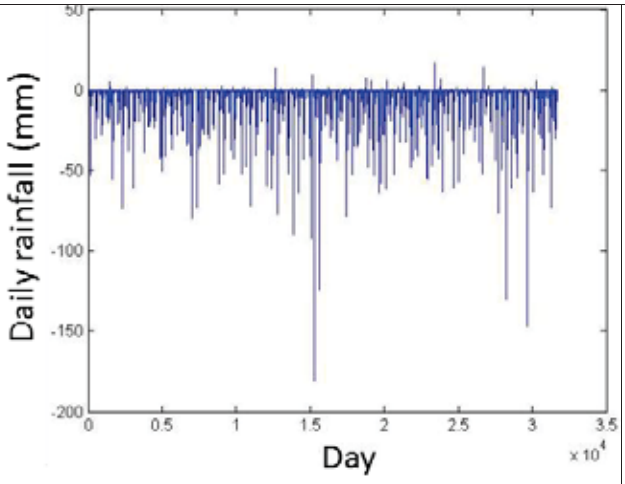

Figure 3.27: Wet biases of q0 PRECIS rainfall scenario for Raipur station

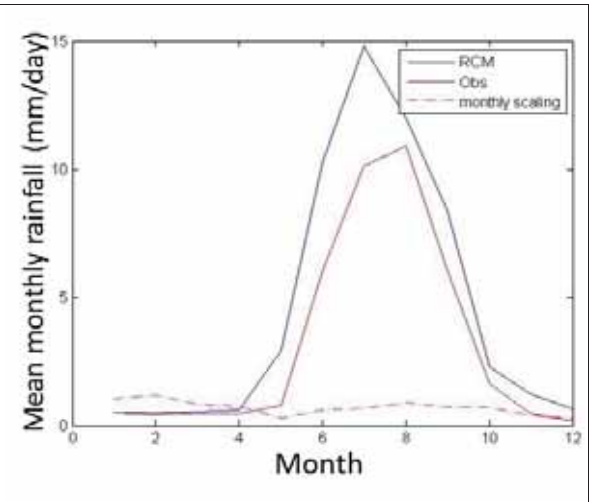

Figure 3.28: Mean monthly observed & q0 PRECIS rainfall scenario for 1971-2005 and scaling factor

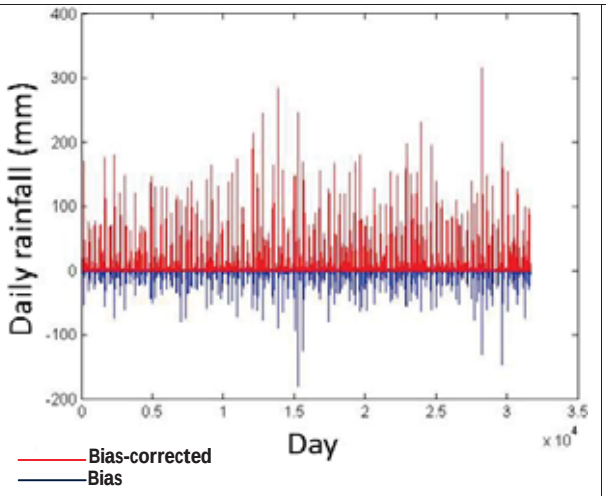

Figure 3.29: Bias-corrected q0 PRECIS scenario vs. original PRECIS

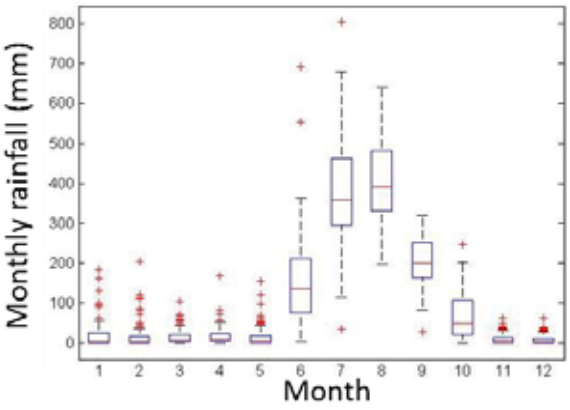

Figure 3.30: Box plot of q0 PRECIS 2011 - 2098

Analysis of bias-corrected q0 PRECIS RCM rainfall scenarios for Raipur station

The PRECIS RCM periods are represented as 2011 – 2040 (2020s), 2041 – 2070 (2050s) and 2071 – 2098 (2080s)

Table 3.23: Monthly rainfall statistics for PRECIS bias-corrected future q0 rainfall scenarios and observed rainfall (baseline scenario) for Raipur station

Months		Jan	Feb	Mar	Apr	May	Jun	July	Aug	Sep	Oct	Nov	Dec	Total
Observed rainfall in mm (baseline)	1971 to 2005	15.2	13.7	13.6	13.8	23.9	181.5	313.7	337.3	180.9	50.8	13.8	5.3	1163.5
PRECIS RCM – bias-corrected q0 rainfall in mm	2011 to 2040	15.5	8.7	13.3	20.1	15.0	138.9	306.0	335.7	202.8	71.7	8.2	3.6	1139.3
	2041 to 2070	22.3	24.5	18.0	14.7	22.1	168.1	397.9	409.3	187.6	51.2	9.9	11.6	1337.1
	2071 to 2098	19.7	19.9	11.8	17.9	13.1	133.9	444.6	480.5	218.9	74.6	11.5	10.2	1456.7

Conclusion: According to the q0 rainfall scenarios, the mean annual rainfall for Raipur station for the 2020s will slightly decrease by 2.12% compare to the baseline, whereas it will increase by 14.92% for the 2050s and by 25.2% for the 2080s.

3.16.3. PRECIS RCM q1 rainfall scenario of Raipur station

Table 3.24: Mean monthly observed rainfall and q1 PRECIS RCM rainfall scenarios of baseline (1971-2005) for Raipur rainfall station:

Months		Jan	Feb	Mar	Apr	May	Jun	Jul	Aug	Sep	Oct	Nov	Dec
Observed rainfall (mm/day)	1971 to 2005	0.49	0.49	0.44	0.46	0.77	6.05	10.12	10.9	6.03	1.64	0.46	0.17
PRECIS rainfall (mm/day)	1971 to 2005	0.14	0.20	0.17	0.44	0.61	3.26	10.39	11.1	6.04	1.52	0.42	0.30
Scaling factor		3.55	2.48	2.51	1.04	1.26	1.85	0.97	0.98	1.00	1.08	1.09	0.57

A comparison was made between the mean monthly observed rainfall and PRECIS RCM q1 scenarios for the period 1971 to 2005. The PRECIS RCM q1 scenario shows a slight wet biasness in the rainfall observations. There is always a tendency of PRECIS to over-estimate significantly high rainfall values especially for the monsoon months from July to September.

However, for June there is a significant under-estimation of rainfall. For January, February, March, April, May, October and November, rainfall values were slightly under-estimated (Table 3.24).

The derived bias correction scaling factor was applied to the observed rainfall values for the period between 2006 and 2010. The validation of observed values and bias-corrected q1 RCM scenario rainfall values from 2006 to 2010 was compared and it was found that the correlation coefficient is 0.79.

This confirms that the applied method and scaling factor are quite acceptable in down-scaling the PRECIS rainfall scenarios. Later the same scaling factor was applied for bias correction of the future scenarios from 2011 – 2098.

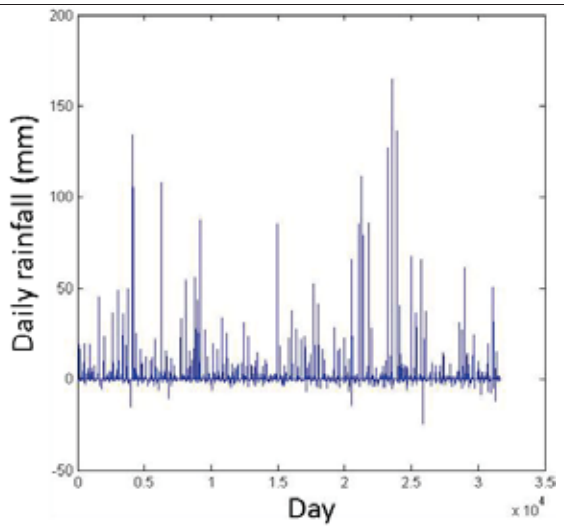

Figure 3.31: Wet biases of q1 PRECIS rainfall scenario for Raipur station

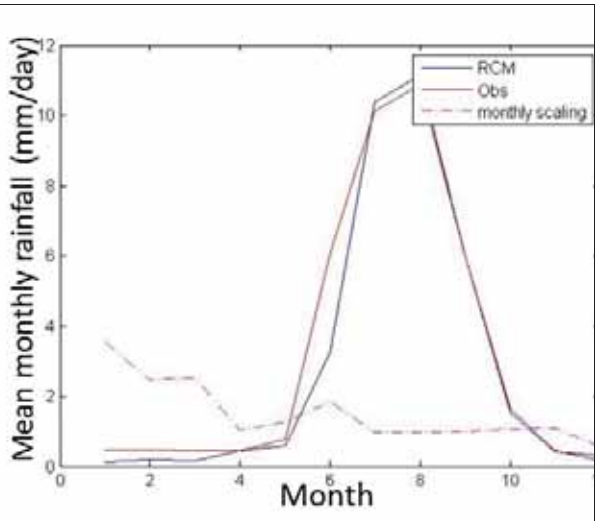

Figure 3.32: Mean monthly observed & q1 PRECIS rainfall scenario for 1971-2005 and scaling factor

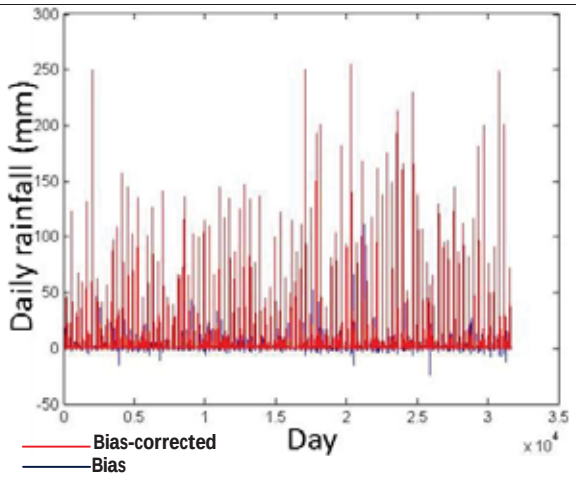

Figure 3.33: Bias-corrected q1 PRECIS scenario vs. original PRECIS

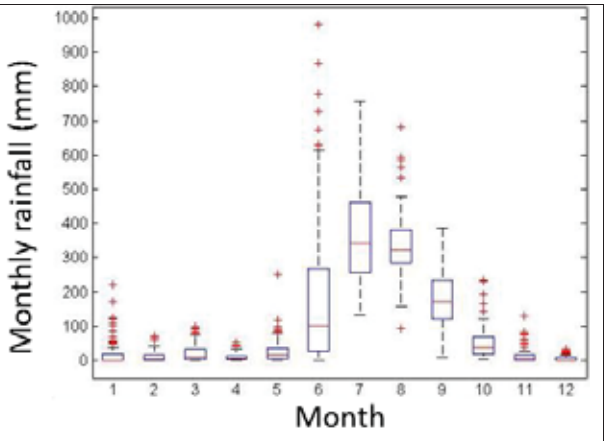

Figure 3.34: Box plot of q1 PRECIS 2011-2098

Figures 3.31 to 3.34 show the different phases of multiplicative approach of bias correcting the q1 PRECIS rainfall scenario for Raipur station.

Analysis of bias-corrected PRECIS RCM q1 rainfall scenarios for Raipur station

Table 3.25: Monthly rainfall statistics for PRECIS bias-corrected future q1 rainfall scenarios and observed rainfall (1971-2005) for Raipur station

Months		Jan	Feb	Mar	Apr	May	Jun	Jul	Aug	Sep	Oct	Nov	Dec	Total
Observed rainfall (mm)	1971 to 2005	15.2	13.7	13.6	13.8	23.9	181.5	313.7	337.3	180.9	50.8	13.8	5.3	1163.5
PRECIS RCM – bias-corrected q1 rainfall (mm)	2011 to 2040	12.8	9.60	29.5	11.1	32.4	196.6	309.7	289.1	164.2	49.6	15.5	3.7	1123.7
	2041 to 2070	26.0	10.9	19.3	11.4	22.1	146.2	354.4	357.8	190.4	53.4	16.0	4.5	1212.6
	2071 to 2098	19.8	12.6	16.0	7.8	29.3	223.1	453.7	351.1	182.6	52.9	9.8	7.7	1366.6

Conclusion: According to results of the q1 rainfall scenarios (Table 3.25), the mean annual rainfall for Raipur station for the 2020s will slightly decrease by 3.14% compared to the baseline, whereas it will increase by 4.21% for the 2050s and by 17.46% for the 2080s.

3.16.4. PRECIS RCM q14 rainfall scenario of Raipur station

Table 3.26: Mean monthly observed rainfall and q14 RCM rainfall scenarios of baseline (1971-2005) for Raipur rainfall station:

Months		Jan	Feb	Mar	Apr	May	Jun	Jul	Aug	Sep	Oct	Nov	Dec
Observed rainfall (mm/day)	1971 to 2005	0.49	0.49	0.44	0.46	0.77	6.05	10.12	10.9	6.03	1.64	0.46	0.17
RCM rainfall scenario (mm/day)	1971 to 2005	1.24	0.68	0.86	0.89	1.55	10.6	15.44	11.6	6.98	1.75	0.60	1.47
Scaling factor		0.39	0.72	0.51	0.52	0.50	0.57	0.66	0.93	0.86	0.94	0.76	0.12

A comparison was made between the mean monthly observed rainfall and PRECIS RCM q14 rainfall scenario for the period 1971 to 2005. The PRECIS RCM q14 rainfall scenario shows a significant wet biasness in the rainfall observations. There is always a tendency of PRECIS to over-estimate significantly high rainfall values especially for the monsoon months from June to September and slightly over-estimate for rest of the months (Table 3.26).

The derived bias-correction scaling factor was applied to the observed rainfall values for the period between 2006 and 2010. The validation of observed values and bias corrected q14 RCM scenario rainfall values from 2006 to 2010 was compared and it was found that the correlation coefficient is 0.62 (less as compared to q0 and q1 scenarios). However, the applied method and scaling factor were considered satisfactory in downscaling. Later the same scaling factor was applied for bias correction of the future scenarios from 2011 to 2098.

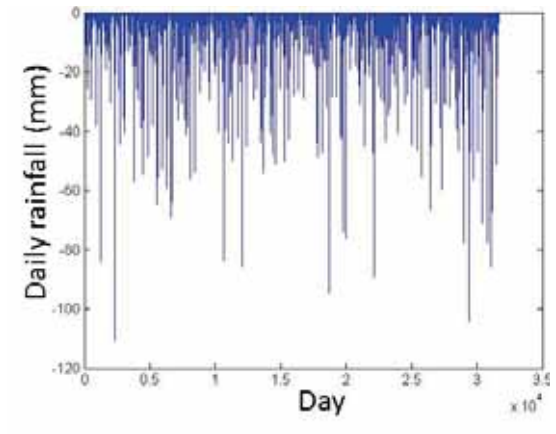

Figure 3.35: Wet biases of q14 PRECIS rainfall scenario for Raipur Station

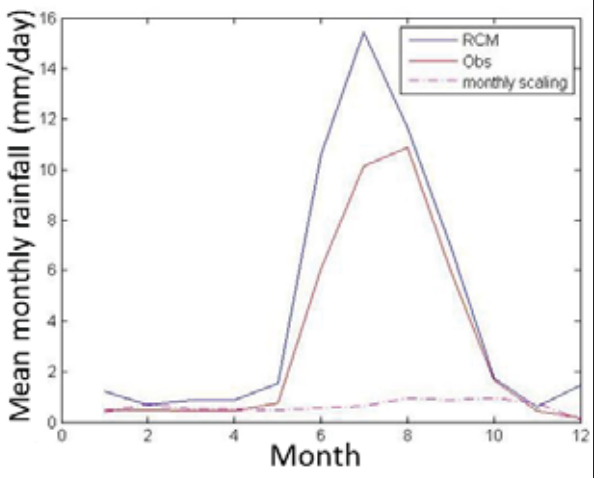

Figure 3.36: Mean monthly observed and q14 PRECIS rainfall scenario for 1971-2005 and scaling factor

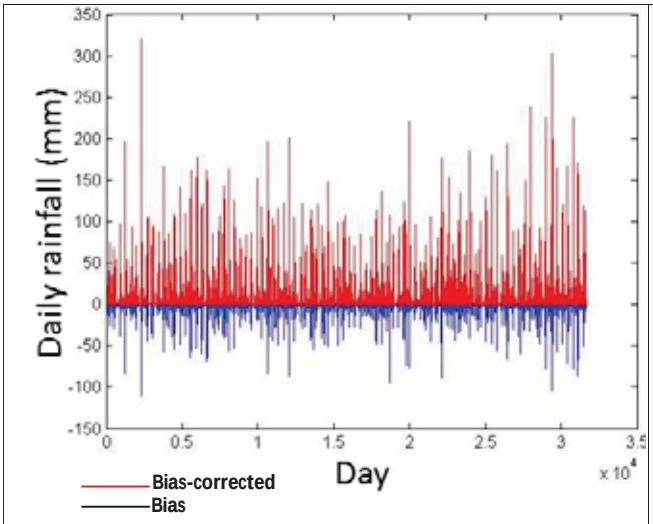

Figure 3.37: Bias-corrected q14 PRECIS RCM scenario vs. original PRECIS

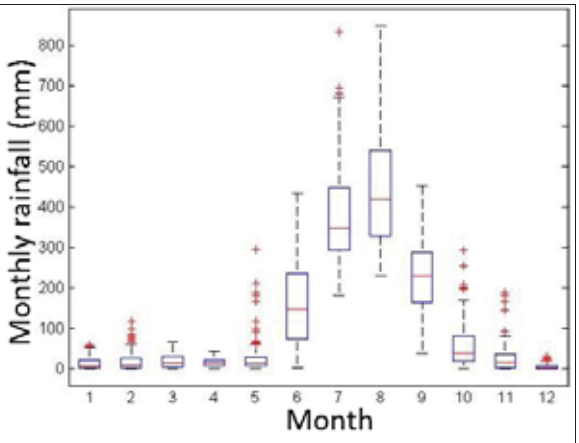

Figure 3.38: Box plot of q14 PRECIS RCM 2011 - 2098

Figure 3.35 to 3.38 shows the different phases of multiplicative approach of bias-correction of the q14 PRECIS rainfall scenario of Raipur station.

Analysis of bias-corrected PRECIS RCM q14 rainfall scenarios for Raipur station

Table 3.27: Monthly rainfall statistics for PRECIS bias-corrected future q14 rainfall scenarios and observed rainfall (baseline scenario) for Raipur station

Months		Jan	Feb	Mar	Apr	May	Jun	Jul	Aug	Sep	Oct	Nov	Dec	Total
Observed rainfall (mm) (baseline)	1971 to 2005	15.2	13.7	13.6	13.8	23.9	181.5	313.7	337.3	180.9	50.8	13.8	5.3	1163.5
PRECIS RCM – bias-corrected q14 rainfall scenarios (mm)	2011 to 2040	9.2	17.6	16.9	16.4	35.0	177.0	362.6	370.9	223.0	53.6	13.9	4.3	1300.5
	2041 to 2070	13.7	16.1	15.8	12.9	20.1	156.8	344.9	419.4	212.8	46.8	22.4	5.4	1287.1
	2071 to 2098	14.8	29.7	20.4	16.2	40.9	143.7	420.2	540.9	248.9	74.9	44.1	6.7	1601.2

Conclusion: According to the q14 rainfall scenarios (Table 3.27), the mean annual rainfall at Raipur station for the 2020s will increase by 11.77% compared to the baseline, while it will increase by 10.62% for the 2050s and by 37.61% for the 2080s.

3.16.5 Bias correction of PRECIS RCM rainfall scenarios (q0, q1 and q14) for other 13 rainfall stations

The PRECIS RCM scenarios (q0, q1 and q14) of the other 13 rainfall stations in the UKC were bias corrected using the same procedure as discussed above for the Raipur rainfall station.

(1) Summary of results for bias-corrected q0 scenarios for each rainfall station

The correlation coefficient during the validation period was found satisfactory (correlation coefficient varies in the range 0.75 to 0.95) for bias correction of q0 rainfall scenarios for all stations other than Raipur.

It is observed that there is wet and dry biasness in the rainfall q0 scenarios for all 13 stations. Mean annual rainfall is slightly decreasing from the baseline period for all the stations by the 2020s. However, a significant increase in rainfall is predicted for the 2050s and 2080s.

(2) Summary of results for bias-corrected q1 scenarios for each rainfall station

The same procedure as mentioned in section 3.16.2 is applied, and the q1 rainfall scenarios of all the rainfall stations in the UKC were bias corrected.

The correlation coefficient during the validation period was satisfactory (correlation coefficient varies between 0.75 – 0.95) for bias correction of q1 rainfall scenarios for all stations. Wet and dry biasness occurs in these q1 scenarios for all 13 stations. Mean annual rainfall is slightly decreasing compared to the baseline period for all stations by 2020s. However, a significant increase in rainfall is predicted for the 2050s and 2080s.

(3) Summary of results for bias-corrected q14 scenarios for each rainfall station

The correlation coefficient during the validation period was satisfactory (correlation coefficient varies between 0.75 – 0.95) for bias correction of q14 rainfall scenarios for all 13 stations. Wet and dry biasness in rainfall occurs for all stations. Mean annual rainfall is increasing significantly compared to the baseline period for all stations in the 2020s, 2050s and 2080s.

3.16.6 PRECIS rainfall statistics for Upper Kharun Catchment

In order to derive a rainfall value representative for the UKC, observations from the 14 rainfall stations were weighted using the SWAT model approach. Each delineated sub-catchment in the model receives the rainfall values from the gauge that is nearest to its centroid. The weighted average rainfall for bias-corrected q0, q1 and q14 PRECIS scenarios were analysed against the measured baseline monthly values (Table 3.28).

Conclusions:

For q0 rainfall scenarios: Based on the results (Table 3.28), it is concluded that the mean annual rainfall for the UKC compared to the baseline (mean annual observed values, 1990-2008) will slightly decrease by 10 mm (0.9%) in the 2020s, increase by 202 mm (18.2%) in the 2050s, and further increase by 323.4 mm (29.1)% in the 2080s.

For q1 rainfall scenarios: Compared to the baseline period, there is a significant decrease of 136.4 mm (12.3%) rainfall for the 2020s, a decrease of 74.5 mm (6.7%) for the 2050s and an increase of 128.2 mm (11.5%) for the 2080s (Table 3.28).

For q14 rainfall scenarios: Compare to the baseline period, there is a significant increase of 126.9 mm (11.4%) rainfall for the 2020s, an increase of 80.2 mm (7.2%) for the 2050s and an increase of 227.2 mm (20.5%) for the 2080s (Table 3.28).

Table 3.28: Percentage change in rainfall in different PRECIS scenarios and time compared to baseline

PRECIPITATION (mm)										
UKC	BASELINE	Q0	Q1	Q14	Q0	Q1	Q14	Q0	Q1	Q14
Month	1990-2008	% 2020s			% 2050s			% 2080s		
Jan	3.29	-22.49	5.78	-23.40	13.07	110.03	3.95	6.38	91.79	22.49
Feb	0	0.00	0.00	0.00	0.00	0.00	0.00	0.00	0.00	0.00
Mar	9.4	-18.51	59.79	-10.43	6.70	7.34	-13.62	-24.68	-0.96	11.38
Apr	11.61	8.70	-8.70	28.77	-10.51	-4.91	1.29	1.46	-32.90	17.92
May	8.03	-22.67	6.85	17.93	15.44	-18.43	-35.87	-30.01	-2.49	19.05
Jun	360.12	-27.91	-20.62	-3.67	-3.80	-38.79	-13.26	-29.17	-7.01	-29.41
Jul	352.48	6.25	-12.24	29.43	35.67	4.46	19.00	63.88	36.48	42.49
Aug	244.82	17.24	-6.17	-2.07	34.54	15.15	18.20	69.39	10.43	38.95
Sep	61.97	-1.55	-22.83	10.41	-9.68	-6.89	3.84	7.12	-7.63	26.77
Oct	56.14	55.84	7.77	57.46	18.63	23.82	30.21	59.90	9.98	109.94
Nov	2.39	-35.56	22.59	-13.81	-9.62	43.10	37.66	-12.97	-19.67	179.50
Dec	0	0.00	0.00	0.00	0.00	0.00	0.00	0.00	0.00	0.00
Annual	1110.24	-0.90	-12.29	11.4	18.19	-6.71	7.2	29.13	11.54	20.5

The PRECIS future climate scenarios show wide variations in rainfall predictions. The q1 scenario shows a decreasing trend for rainfall in the 2020s and 2050s, while q0 and q14 shows an increasing trend for the same period. The reason might be that q0 and q14 show good skill in their ability to simulate the quantum of seasonal monsoon rainfall, whereas q1 shows a dry bias, which might be the reason for the decreasing trend for rainfall (Kumar et al., 2011).

3.16.7 PRECIS RCM maximum temperature scenarios for Upper Kharun Catchment (Raipur station)

(1) PRECIS RCM q0 scenarios for maximum temperature

Table 3.29: Mean monthly maximum temperature for observed and q0 PRECIS RCM scenarios of baseline (1971-2005) for Raipur station:

Months		Jan	Feb	Mar	Apr	May	Jun	Jul	Aug	Sep	Oct	Nov	Dec
Observed maximum temperature (°C)	1971 to 2005	27.37	30.23	35.23	39.83	41.97	37.18	31.18	29.94	31.02	31.01	29.29	27.29
PRECIS-q0 maximum temperature scenario (°C)	1971 to 2005	26.88	32.80	38.48	43.20	44.29	36.86	29.04	29.37	29.99	29.94	27.47	25.67

Scaling factor	0.49	-2.57	-3.25	-3.38	-2.33	0.32	2.14	0.57	1.03	1.08	1.81	1.62

A comparison was made between the observed mean monthly maximum temperature and PRECIS RCM q0 maximum temperature scenarios from 1971 to 2005. It is concluded that the PRECIS RCM q0 scenarios have significant warm and cold biases in the maximum temperature observations (Table 3.29). There is always a tendency of PRECIS to significantly over-estimate maximum temperature values from February to May. However, in the months from June to January, it under-estimates the temperature values.

The biases in the behavior of the PRECIS RCM scenarios were due to the lateral boundary conditions of the GCM scenarios from which they were derived. Since these biases are systematic in nature, they were corrected using the simple mean monthly scaling – additive approach (section 3.12.2).

The derived bias-correction scaling factor was applied to the observed maximum temperature values for the period between 2006 and 2010. For validation, the observed maximum temperature values and bias corrected q0 scenario values from 2006 to 2010 was compared, and it was found that the correlation coefficient is 0.8937. This confirms that the applied method and scaling factor are quite acceptable and later the same scaling factor was applied for bias correction of the future PRECIS q0 scenarios from 2011–2098.

Figure 3.39 to 3.42 shows the different phases of additive approach of bias correcting the q0 PRECIS maximum temperature scenario of Raipur station.

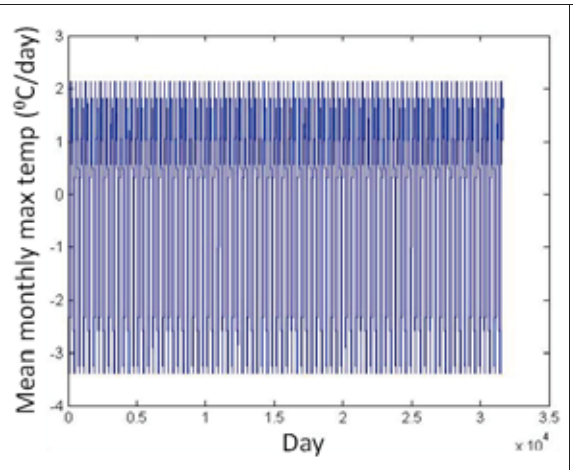

Figure 3.39: Biases of PRECIS q0 maximum temperature scenario for Raipur station

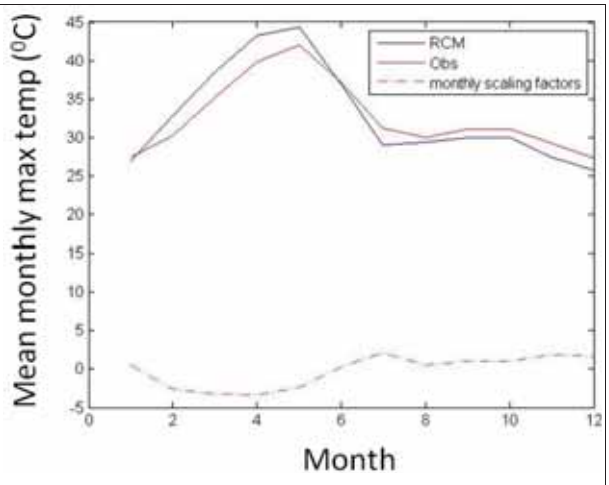

Figure 3.40: Mean monthly maximum temperature for observed and PRECIS q0 scenario and scaling factor for baseline (1971-2005)

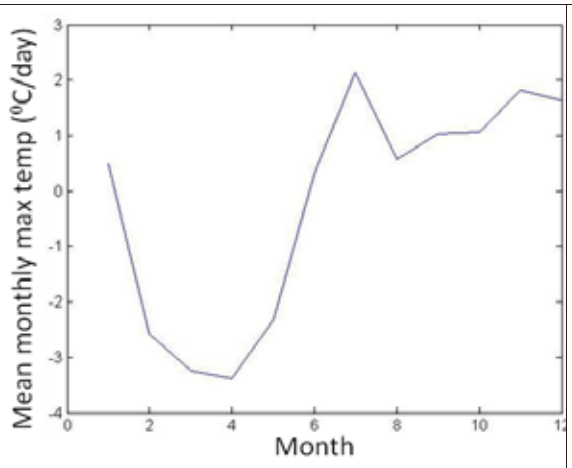

Figure 3.41: Scaling factor (observed – RCM)

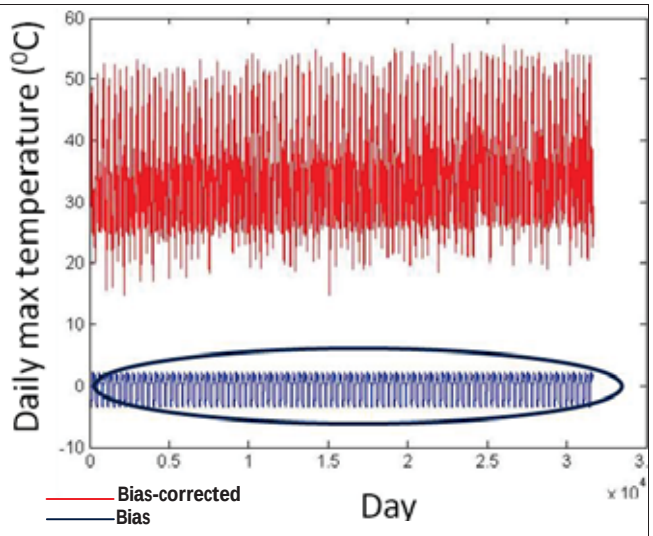

Figure 3.42: Bias-corrected PRECIS q0 scenario vs. biases

Analyses of bias-corrected PRECIS q0 mean monthly maximum temperature scenarios for Raipur station

Table 3.30: Mean monthly maximum temperature statistics for bias-corrected PRECIS future q0 scenarios and observed (baseline scenario) for Raipur station

Months		Jan	Feb	Mar	Apr	May	Jun	Jul	Aug	Sep	Oct	Nov	Dec	Avg.
Observed temperature (°C) (Baseline)	1971 to 2005	27.4	30.2	35.2	39.8	42.0	37.2	31.2	29.9	31.0	31.0	29.3	27.3	32.6
Bias-corrected PRECIS q0 scenarios (°C)	2011 to 2040	29.4	31.6	36.3	40.5	43.6	40.1	32.6	30.5	32.0	32.4	30.8	29.0	34.1
	2041 to 2070	29.9	32.4	37.3	42.2	44.7	40.2	32.4	31.1	33.4	34.4	32.8	30.0	35.1
	2071 to 2098	31.2	33.8	39.7	43.3	46.7	42.8	33.0	31.4	34.0	35.7	33.4	31.0	36.3

Conclusions: For the q0 maximum temperature scenarios, the results (Table 3.30) show that the mean annual maximum temperature for the UKC compared to the baseline (observed values,

1971-2005) will increase by 1.5 ℃ for the 2020s, by 2.5 ℃ for the 2050s and by 3.7 ℃ for the 2080s.

It is found that the mean monthly maximum temperature of all months in q0 scenarios will increase compared to the baseline scenarios.

(2) PRECIS RCM q1 scenarios for maximum temperature

Table 3.31: Mean monthly maximum temperature for observed and q1 PRECIS RCM scenarios of baseline (1971-2005) for Raipur station:

Months		Jan	Feb	Mar	Apr	May	Jun	Jul	Aug	Sep	Oct	Nov	Dec
Observed maximum temperature (℃)	1971 to 2005	27.37	30.23	35.23	39.83	41.97	37.18	31.18	29.94	31.02	31.01	29.29	27.29
PRECIS q1 maximum temperature scenario (℃)	1971 to 2005	29.18	34.05	39.50	43.38	45.76	43.49	32.24	29.63	30.93	31.33	29.40	28.04
Scaling factor		-1.81	-3.82	-4.27	-3.55	-3.79	-6.31	-1.06	0.32	0.10	-0.32	-0.12	-0.75

A comparison was made between the mean monthly observed maximum temperature and PRECIS RCM q1 scenarios between the years 1971 to 2005, and it can be concluded that these scenarios have significant warm and cold biases in the maximum temperature observations. There is always a tendency of PRECIS to significantly over-estimate maximum temperature values from January to July and October to December. However, for August and September it under-estimates the values (Table 3.31).

The derived bias-correction scaling factor was applied to the observed maximum temperature values for the period between 2006 and 2010. For validation, the observed maximum temperature values and bias-corrected q1 scenario values from 2006 to 2010 were compared and it was found that the correlation coefficient is 0.91. This confirms that the applied method and scaling factor are quite acceptable, and later the same scaling factor was applied for bias correction of the future PRECIS q1 scenarios from 2011 – 2098.

Analyses of bias-corrected PRECIS q1 mean monthly maximum temperature scenarios for Raipur station

Table 3.32: Mean monthly maximum temperature statistics for bias-corrected PRECIS future q1 scenarios and observed (baseline scenario) for Raipur station

Months		Jan	Feb	Mar	Apr	May	Jun	Jul	Aug	Sep	Oct	Nov	Dec	Avg.
Observed temperature (°C) (baseline)	1971 to 2005	27.4	30.2	35.2	39.8	42.0	37.2	31.2	29.9	31.0	31.0	29.3	27.3	32.6
Bias-corrected q1 scenarios (°C)	2011 to 2040	28.9	31.9	36.4	41.2	43.0	38.0	31.9	30.8	32.3	31.9	30.1	28.0	33.7
	2041 to 2070	30.4	32.8	37.5	42.3	44.1	39.4	32.6	31.7	33.8	34.9	32.1	30.0	35.1
	2071 to 2098	31.8	33.9	38.9	43.5	45.0	39.3	32.4	32.4	35.7	36.6	34.2	30.9	36.2

Conclusions: For the q1 maximum temperature scenarios, the mean annual maximum temperature for the UKC compared to the baseline (observed values, 1971-2005) will increase by 1.1 °C for the 2020s, by 2.5 °C for the 2050s and by 3.6 °C for the 2080s (Table 3.32).

It is found that the mean monthly maximum temperature of all months in q1 scenarios will increase compared to the baseline.

(3) PRECIS RCM q14 scenarios for maximum temperature

Mean monthly observed maximum temperature and PRECIS RCM q14 scenarios between the years 1971 and 2005 were compared. The comparison leads to the conclusion (Table 3.33) that the PRECIS RCM q14 scenarios have significant warm and cold biases in the maximum temperature observations. There is always a tendency of PRECIS to significantly over-estimate maximum temperature values for the months from February to June and October and November. However, from July to September and December and January it under-estimates the temperature values.

Table 3.33: Mean monthly maximum temperature for observed and q14 PRECIS RCM scenarios of baseline (1971-2005) for Raipur station

Months		Jan	Feb	Mar	Apr	May	Jun	Jul	Aug	Sep	Oct	Nov	Dec
Observed maximum temperature (°C)	1971 to 2005	27.37	30.23	35.23	39.83	41.97	37.18	31.18	29.94	31.02	31.01	29.29	27.29

Bias-corrected PRECIS q14 scenario (°C)	1971 to 2005	25.79	31.96	38.21	43.29	46.13	37.85	28.86	29.24	30.89	32.18	29.37	26.34
Scaling factor		1.58	-1.73	-2.98	-3.47	-4.16	-0.66	2.32	0.70	0.13	-1.17	-0.08	0.95

The derived bias-correction scaling factor was applied to the observed maximum temperature values for the period between 2006 and 2010. For validation, the observed maximum temperature values and bias-corrected q14 scenario values from 2006 to 2010 were compared and it was found that the correlation coefficient is 0.911. This confirms that the applied method and scaling factor are quite acceptable and later the same scaling factor was applied for bias correction of the future PRECIS q14 scenarios from 2011–2098.

Analyses of bias-corrected PRECIS q14 mean monthly maximum temperature scenarios for Raipur station

Table 3.34: Mean monthly maximum temperature statistics for bias-corrected PRECIS future q14 scenarios and observed (baseline scenario) for Raipur station

Months		Jan	Feb	Mar	Apr	May	Jun	Jul	Aug	Sep	Oct	Nov	Dec	Avg.
Observed temperature (°C) (Baseline)	1971 to 2005	27.4	30.2	35.2	39.8	42.0	37.2	31.2	29.9	31.0	31.0	29.3	27.3	32.6
Bias-corrected PRECIS q14 scenarios (°C)	2011 to 2040	29.8	31.8	36.4	40.6	43.2	37.9	31.6	30.8	32.0	31.3	30.5	29.0	33.7
	2041 to 2070	31.0	32.8	38.5	42.9	45.5	40.6	32.6	31.7	33.3	34.9	33.1	30.6	35.6
	2071 to 2098	30.9	33.3	38.4	44.0	45.4	41.9	33.5	31.9	34.2	36.6	33.2	29.9	36.1

Conclusion: For the q14 maximum temperature scenarios, the results (Table 3.34) show that the mean annual maximum temperature for the UKC compared to the baseline (observed mean annual maximum temperature values, 1971-2005) will increase by 1.1 °C for the 2020s, by 3.0 °C for the 2050s and by 3.5 °C for the 2080s.

It is found that the mean monthly maximum temperature of all months in q14 scenarios will increase compared to the baseline scenario.

3.16.8 PRECIS RCM minimum temperature scenarios for Upper Kharun Catchment (Raipur station)

Here the bias correction of q0, q1 and q14 scenarios of minimum temperature is done as described above.

(1) Analyses of bias-corrected PRECIS q0 mean monthly minimum temperature scenarios for Raipur station

Table 3.35: Mean monthly minimum temperature statistics for bias-corrected PRECIS future q0 scenarios and observed (baseline scenario) for Raipur station

Months		Jan	Feb	Mar	Apr	May	Jun	Jul	Aug	Sep	Oct	Nov	Dec	Avg.
Observed temperature (°C) (baseline)	1971 to 2005	11.2	13.7	17.6	22.5	26.2	25.9	24.0	23.9	23.9	20.8	14.8	10.9	19.6
Bias-corrected PRECIS q0 scenarios (°C)	2011 to 2040	13.5	16.0	18.5	24.2	27.9	27.8	25.7	25.1	25.5	23.1	17.8	14.0	21.6
	2041 to 2070	14.5	16.9	20.8	26.2	30.7	30.8	26.1	25.8	26.4	25.1	20.2	15.2	23.2
	2071 to 2098	18.4	22.5	25.2	30.1	32.8	31.4	27.4	26.6	27.8	27.0	26.1	20.5	26.3

Conclusion: For q0 minimum temperature scenarios

The mean annual minimum temperature for the UKC based on q0 compared to baseline will increase by 2.0 °C for the 2020s, by 3.6 °C for the 2050s and by 6.7 °C for the 2080s (Table 3.35).

It is found that the mean monthly minimum temperatures of all months in q0 scenarios are increasing compared to the baseline, and that the mean annual minimum temperature is increasing more than the mean annual maximum temperature.

(2) Analyses of bias-corrected PRECIS q1 mean monthly minimum temperature scenarios for Raipur station

Table 3.36: Mean monthly minimum temperature statistics for bias-corrected PRECIS future q1 scenarios and observed (baseline scenario) for Raipur station

Months		Jan	Feb	Mar	Apr	May	Jun	Jul	Aug	Sep	Oct	Nov	Dec	Avg.
Observed temperature (°C) (baseline)	1971 to 2005	11.2	13.7	17.6	22.5	26.2	25.9	24.0	23.9	23.9	20.8	14.8	10.9	19.6
Bias-corrected PRECIS q1 scenarios (°C)	2011 to 2040	13.3	15.5	19.7	24.0	27.9	26.8	24.7	24.8	24.8	22.3	16.3	12.1	21.0
	2041 to 2070	14.8	16.5	20.2	25.3	29.1	28.4	25.7	25.6	25.9	24.3	18.4	14.4	22.4
	2071 to 2098	16.6	17.4	22.1	26.5	30.4	28.8	26.1	26.3	27.3	25.8	20.1	15.9	23.6

Conclusion: For the q1 minimum temperature scenarios (Table 3.36), it can be concluded that the mean annual minimum temperature for the UKC compared to the baseline will increase by 1.4 ℃ for the 2020s, 2.8 ℃ for the 2050s and 4.0 ℃ for the 2080s. It is found that the mean monthly minimum temperatures of all the months in q1 scenarios are increasing compared to the baseline.

(3) Analyses of bias-corrected PRECIS q14 mean monthly minimum temperature scenarios for Raipur station

Table 3.37: Mean monthly minimum temperature statistics for bias-corrected PRECIS future q14 scenarios and observed (baseline scenario) for Raipur station

Months		Jan	Feb	Mar	Apr	May	Jun	Jul	Aug	Sep	Oct	Nov	Dec	Avg.
Observed temperature (°C) (baseline)	1971 to 2005	11.2	13.7	17.6	22.5	26.2	25.9	24.0	23.9	23.9	20.8	14.8	10.9	19.6
Bias-corrected PRECIS q14	2011 to 2040	13.6	15.8	18.9	24.0	27.8	26.7	24.8	24.8	24.8	21.8	16.3	12.5	21.0

scenarios (°C)	2041 to 2070	15.3	16.9	21.3	26.2	30.5	29.2	25.7	25.7	26.2	24.4	19.3	14.0	22.9
	2071 to 2098	16.3	18.8	22.3	27.9	30.8	30.1	26.8	26.5	27.2	26.6	20.8	14.9	24.1

Conclusion: For the q14 minimum temperature scenarios, it can be concluded that the mean annual minimum temperature for the UKC compared to the baseline will increase by 1.4 °C for the 2020s, 3.3 °C for the 2050s and 4.5 °C for the 2080s (Table 3.37).

It is found that the mean monthly minimum temperatures of all the months in q14 scenarios are increasing compared to the baseline.

CHAPTER 4: LAND-USE MAPPING

4.1 Introduction

Land-use maps provide information which can be utilized to draw valuable conclusions through interpretation and analyses. Land-use is dynamic in nature, and an understanding of underlying processes requires regular monitoring to detect areas of rapid change and to ascertain reasons and drivers of the change. The change in land-use is the result of many interacting processes caused by a mix of reasons ranging from variations of natural resources (e.g., climate change) to socio-economic dynamics (e.g., population growth, changes in cropping patterns). Due to the increasing rate of environmental degradation adversely impacting human health mainly in urban and sub-urban environments, natural and human-induced environmental changes have become matters of great concern. Insufficient information on the rates of land-use change is a great hindrance to appropriate land-use management and planning.

In order to understand processes driving land-use changes/dynamics, a combination of remote sensing and traditional methods of collecting field information is needed. Remote sensing satellite images provide tremendous capability to observe and capture the different processes occurring on the earth surface at regular intervals of time, and consider many time steps.

Land-use classification is a method of delineation or differentiation between the different land-use forms. Several land-use classification and change detection techniques have been developed over the time, providing the important information contained in land-use maps for different stakeholders. Land-use maps enable planners and administrators to initiate the appropriate measures for preventing the degradation of natural resources and for identification of sites suitable for specific purposes.

Originally, land-use mapping was restricted to aerospace technology, but currently due to advancement in space technology, routine mapping over large areas is now prevalent in various fields of technology. At present, various remote sensing satellite images are available with different spatial, temporal and spectral resolution. The selection of satellite images for land-use mapping entirely depends on the specific task or purpose of the question to be answered, availability, and cost of acquiring the images.

Some of the commonly used satellite images for land-use mapping studies are: LANDSAT - 30 m (Still and Shih, 1985; Yuan et al., 2005; Huang et al., 2007; Villarreal et al., 2011), ASTER - 30 m (Zhu and Blumberg, 2001; Jianwen et al., 2005; Yüksel et al. 2008), LISS III - 23.5 m (Saha et. al, 2005; Kanungo and Sarkar, 2011), MODIS - 250 m (Jonathan et al. 2005; Song et al., 2011), Rapid eye - 5.0 m (Schulthess et al., 2006; Stefanski et al. 2013), etc.

For mapping, LANDSAT satellite images are the most commonly and widely used data. Most of the LANDSAT scenes are available free of charge with quite reasonable spatial and temporal resolution for several environmental impact analysis studies. Moreover, LANDSAT is the

satellite product which provides historical data going back to 1972 (Xie et al. 2008). Hence, in comparison with other satellite products, LANDSAT provides the only opportunity for land-use change detection studies covering decades.

Chhattisgarh is a newly formed state, which was carved out from Madhya Pradesh state in 2000. After the formation, the growth and development of the area has been rapid. Considerable population growth, the expansion of urban areas, industrialization, and increase in irrigation areas and facilities for meeting the increasing food demand, etc., are typical trends in Chhattisgarh. The Government of Chhattisgarh has planned the formation of a new capital city near Raipur. The suburbs of Raipur city will further merge with this new capital city. This planning unit is partly in the study area, and hence it will be interesting and important to know the impact of future land-use change on the water resources of the UKC. Furthermore, the decadal governmental developmental plans for the year 2021 for Raipur, Durg and Dhamtari urban areas in the UKC were considered for the preparation of future land-use scenarios.

Generally, land-use classification can be carried out by different computer-assisted programs, from basic supervised and unsupervised classification to advanced object-oriented classification, and fuzzy logic sub pixel-based classification. Each of these methods has specific pros and cons that need to be considered when selecting the method, which mainly depends on the purpose and the type of research question to be answered.

In the present study, an on-screen visual digitization technique using the various satellite image derivatives was employed for time series land-use mapping. The selection of this method is based on the following reasons:

1. On-screen visual digitization provides high flexibility and operational feasibility to capture most of the variability existing in nature depending on the satellite imagery resolution and information gathered from various sources. The digitizer has full control to perform mapping based on his/her experience, domain knowledge, ground control points, and visual interpretation of satellite images.

2. In the case of multi-seasonal land-use changes within a year, this method provides an easy integration of annual seasonal information in a single map. The UKC features distinct dry and wet periods within a year, and therefore intra-annual changes of cropping patterns and use of irrigation are especially relevant in this region.

3. Image interpretation keys, i.e., Texture, Pattern, Association or Context, Colour, Tone, Shape and Size, can be used for feature identification, interpretation and digitization.

4. Multiband and multi-season satellite image information can be extracted using various image enhancement techniques and image derivative indices.

5. Apart from other advanced land-use classification methods, this technique is not affected by satellite sensor radiometry and date of pass. It is rarely possible to have the historical time series images of same radiometry and exact date of pass, which may lead to significant errors during the land-use classification. The on-screen digitization approach allows editing and modifying the polygons of past land-use maps after detecting the areas of current changes. Hence, it maintains spatial consistency and the same conditions during the preparation of different time series land-use maps.

On-screen visual digitization techniques have been used by several national agencies to prepare land-use maps and change detection studies at regional to country scale. Some examples are National Land Use Land Cover Mapping using multi-temporal satellite data – India (NRSC, 2012) and CORINE Land Cover project – Germany (Kiel, 2005). Other work includes Anttila (2002), Asner et al. (2002) and Franklin et al. (2000).

4.2. Materials and methods

Time series land-use / land cover classification of the UKC was performed through computer-assisted analysis of digital satellite imageries data using on-screen visual digitization. Land-cover information was extracted from multi-seasonal LANDSAT Thematic Mapper (TM) and LANDSAT ETM+ for 19 land-use types. The land-use maps were prepared for 3 years which were 10 years apart i.e., 1991, 2001 and 2011, in order to investigate the land-use changes and their impact on water resources. A land-use scenario for 2021 was prepared based on findings extracted from analyses of dynamics in the past, and from governmental plans and expert interviews.

The selection of decadal year (1991, 2001 and 2011) for land-use mapping, change detection and impact analysis on water resources is based on the following facts:

- Satellite images of the study area before the 1990s for all the three seasons were not available in the archive and also not in the agencies providing the satellite images. The discharge data necessary for calibration and validation of the hydrological model are available from 1990 onwards.

- The information about the land-use and irrigated areas at village level is available as census book report for the decadal year (1991, 2001 and 2011) but not for each year. This information was used as ancillary and ground-truth data for the preparation of past land-use maps.

- Chhattisgarh state was formed as a new state in 2000. Since then, there has been rapid growth and development in and around the capital city Raipur and in Durg and Dhamtari districts. The study area is in parts of these districts and might have witnessed significant changes in land-use. Hence, it is interesting to investigate the land-use change and its impact on water resources for the periods 1991, 2001, 2011 and 2021.

4.2.1 Satellite data

Time series LANDSAT TM, LANDSAT ETM+ and LANDSAT 8 (Table 4.1) were acquired from USGS and Glovis website and Geo-informatics and Space technology Development Agency, Ministry of Science and Technology, Bangkok, Thailand.

Table 4.1: Satellite data used in the study

Data used	Path/row	Date of pass (Format: dd-mm-yyyy)	Spatial resolution (m)
LANDSAT TM	142/45,46	11-02-1990, 12-10-1991, 15-03-1996, 09-10-1996, 10-10-1999, 11-11-1999, 28-10-2000, 15-12-2000, 30-01-2001, 03-04-2001, 22-04-2001, 04-02-2002, 25-04-2002, 16-09-2002 and 03-11-2002	07 Bands 30 m (1-4 bands) Range: 30–120 m
LANDSAT ETM+	142/45,46	15-10-2001, 19-12-2010, 27-10-2011 01-15-2012, 16-02-2012, 03-03-2012, 06-05-2012 and 13-10-2012	08 Bands 30 m (1-4 bands) Range: 15–90 m
LANDSAT - 8 ETM	142/45,46	15-04-2013, 01-05-2013, 09-11-2013, 25-11-2013, 27-12-2013, 12-01-2014, 28-01-2014 and 13-02-2014	11 Bands 30 m (1-5 bands) Range: 15–100 m

4.2.2 Ancillary data

Eight Survey of India (SOI) topographic maps (64G – 07, 08, 11 & 12 and 64H – 05, 06, 09 and 10) at 1:50,000 scale covering the entire UKC were procured from the office of the Director, Chhattisgarh Geo Spatial Data Centre, Survey of India, Chhattisgarh. These maps were used for preparing base map layers, e.g., drainage, contours and delineation of watershed, etc., geo-referencing of satellite data, ground truth and mapping.

4.2.3 Software and equipment

ArcGIS 10.1 was used for geo-referencing of the satellite images and on-screen digitization. ERDAS 9.2 was applied for image enhancement and derivation of vegetation indices (NDVI, tasseled cap indices, etc.). A Global Positioning System (GPS) – (Garmin – 76CSx) with a horizontal accuracy of +/- 3 m was employed to collect the ground control points.

4.2.4 Digital image processing

Pre-processing of satellite images: radiometric and geometric correction was applied on the raw LANDSAT images. This approach produces the adjusted satellite imageries, which are radiometrically and geometrically quite similar to the characteristics of the radiant energy of the original scene (Jensen, 1996).

During the acquisition of satellite imageries, several geometric distortions may occur because of factors like earth curvature, radial symmetric distortion, relief displacement in the sensor's field of view, and atmospheric refraction. Geometric corrections are required for maintaining a good spatial correspondence between the multi-date satellite images.

Radiometric corrections are generally used to normalize the multi-temporal satellite imageries for time series comparisons (Schott et al., 1988). Local enhancement (data scaling and histogram equalization) was carried out on the temporal scenes for better interpretation.

Satellite-derived indices

The information about a specific feature can be derived by analyzing the different band combinations and rationing of satellite images. Different indices have been developed and are used in land-use mapping. NDVI and tasseled cap indices (brightness, greenness and wetness) were derived from satellite imageries for the study area. A brief description of these indices is given below:

4.2.4.1 Normalized Differential Vegetation Index (NDVI)

The Normalized Differential Vegetation Index is an indicator of vegetation growth. It shows high values with vegetation parameters such as leaf area index, green leaf biomass and green leaf area. Hence, it is used for vegetation discrimination in land-use mapping. NDVI typically ranges from -0.1 to 0.6. However, the possible range lies between -1.0 and 1.0 (NOAA coastal services centre, 2007).

$$NDVI = (Infrared - Red) / (Infrared + Red) \quad (4.1)$$

Seasonal NDVI maps (three seasons per year) were prepared for the decadal years 1991, 2001 and 2011 using the LANDSAT images. The 2001 NDVI map for the monsoon season is depicted in Figure 4.1.

The NDVI has been used in several studies related to vegetation dynamics and land-use change detection, e.g., Justice (1986), Verhoef et al. (1996), Lyon et al. (1998), Hayes and Sader (2001), Volcani et al. (2005), and Morawitz et al. (2006).

4.2.4.2 Tasseled cap indices

The "tasseled cap" transformation concept was invented by Kauth and Thomas (1976). The first three components of tasseled cap transformation (brightness, greenness and wetness indices) are directly related to biophysical characteristics of land (Crist and Cicone 1984, Crist and Kauth 1986), and hence provide an indication for the identification of different specific land-use features. Tasseled cap indices have been widely used in vegetation mapping and monitoring time series for land-use change detection (Cohen et al. 1995; Dymond et al. 2002; Franklin et al. 2002; Lunetta et al. 2004; Healey et al. 2005; Zhang and Ban 2010).

Brightness index is a measure of overall reflectance. Open barren land shows more reflectance compared to open scrublands, and also differentiates between dark soil and light soil.

Greenness index measures the presence and density of green vegetation.

Wetness index provides a measure of soil moisture content.

The tasseled cap indices map was prepared for all the three seasons of the decadal years 1991, 2001 and 2011 using the LANDSAT images. The maps for the monsoon season 2001 are shown in Figures 4.2, 4.3 and 4.4.

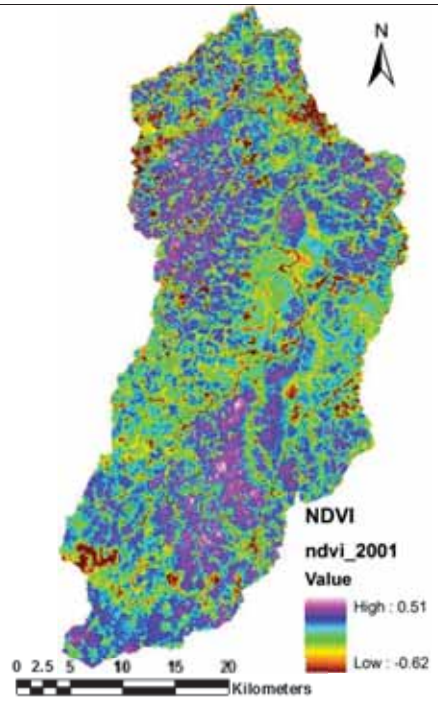

Figure 4.1: NDVI

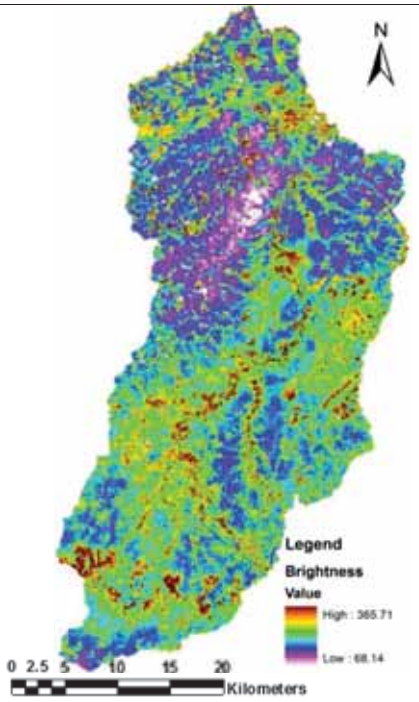

Figure 4.2: Brightness Index

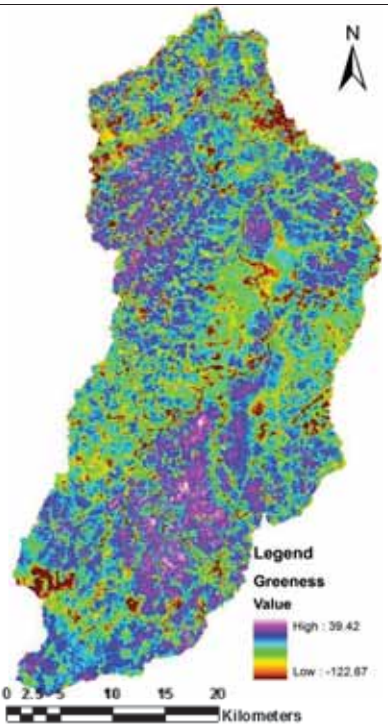

Figure 4.3: Greenness Index

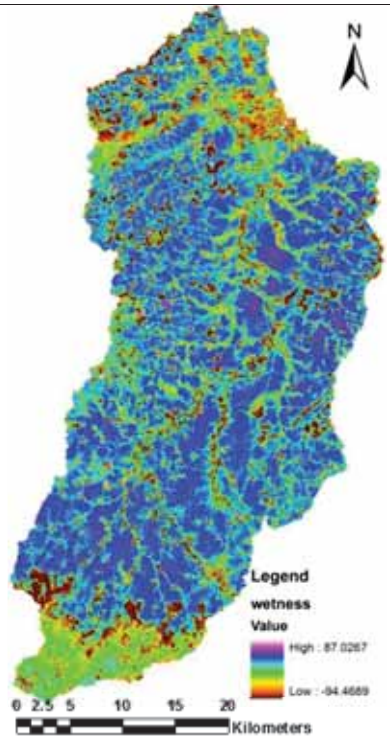

Figure 4.4: Wetness Index

4.2.5 Field visits and ground truth collection

Ground truthing refers to the acquisition of knowledge about the study areas from fieldwork, analysis of the field data sets, secondary data (statistics, maps, plans) and personal/expert knowledge. Ground-truth data are considered to be the most accurate (true) data available. Data for ground truthing should be collected at the same time as the remotely sensed data, so that the data correspond as much as possible to ground realities.

Extensive fieldwork was carried out in all the three seasons, i.e., summer (May-June 2011), spring/ monsoon (Oct-Nov 2011) and winter (January – February 2011) using a handheld GPS (Garmin–76CSx) with accuracy +/- 3 m. Around 650 well distributed points describing the land-use of the study area were collected. Other relevant information was gathered locally (informal talks with local experts, officials and other stakeholders).

Ground-truth information collected from a 1:50,000 scale toposheet and census book information at decadal time steps (1991, 2001 and 2011) on types of crop, irrigation and the area under each crop at village level was additional information useful in land-use mapping for the respective time steps.

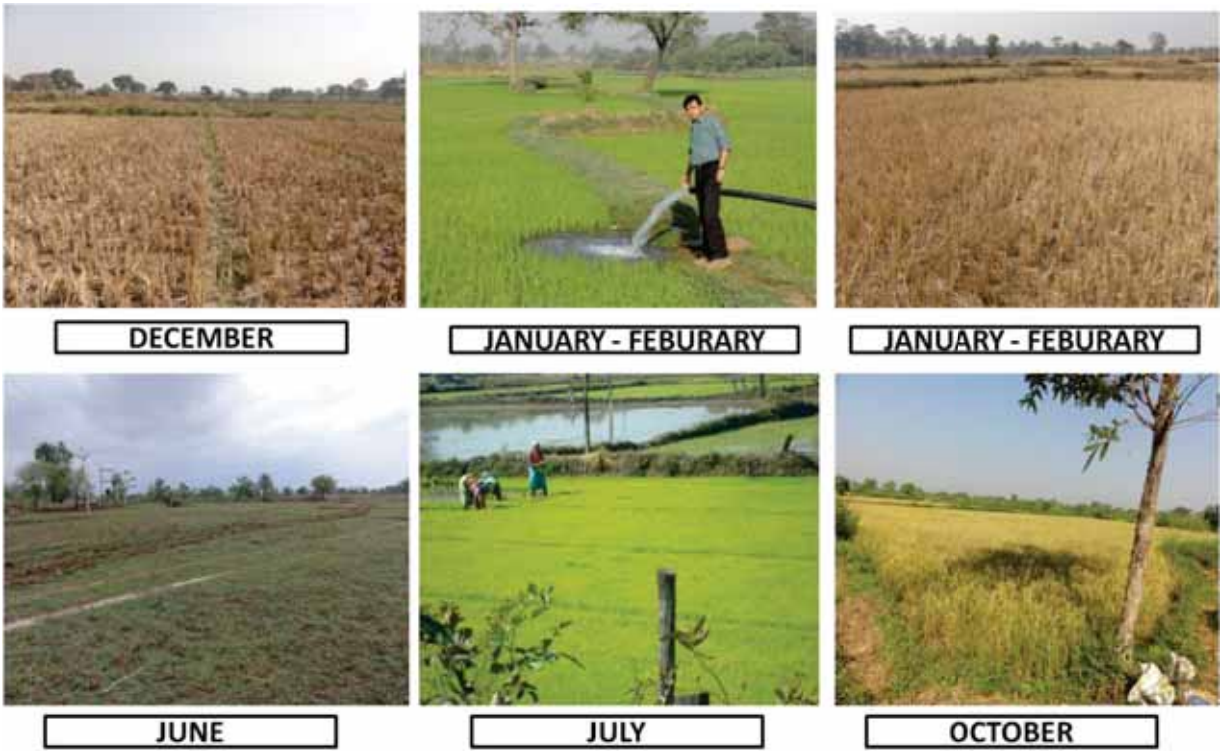

Figure 4.5: Land-use (different months)

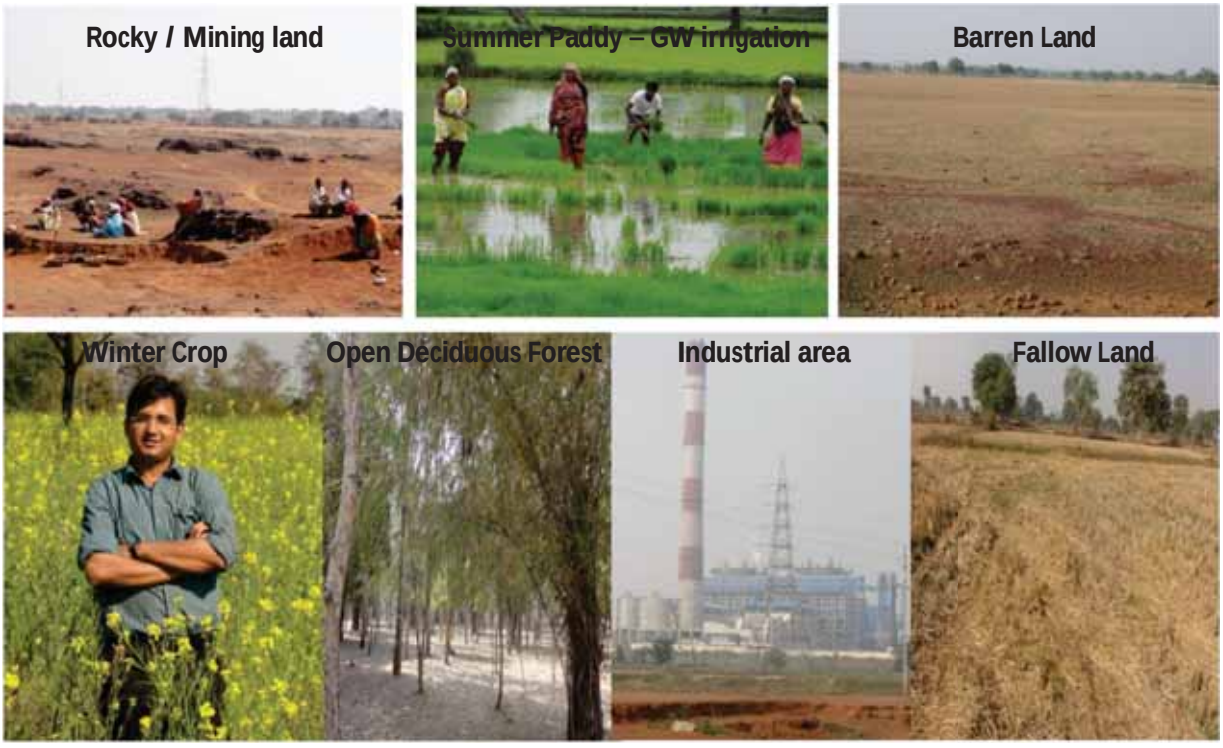

Figure 4.6: Different land-use types

4.2.6 Land-use classification

A two-step procedure in land-use classification was applied.

Firstly a broad land-use classification with 5 broad land-use classes (Agriculture, Built up, Forest, Wasteland and Water-bodies) was used.

Secondly a detailed land-use classification with 19 detailed classes was performed. The definition of different land-use classes were adopted from the technical manual on "National Land Use Land Cover Mapping using multi-temporal satellite data" (2012) prepared by the Land Use and Cover Monitoring Division Land Resources, Land Use Mapping and Monitoring Group, RSA National Remote Sensing Centre, Indian Space Research Organization, India.

Introducing detailed categories and shaping/defining the detailed categories were performed and guided by paying attention to hydrological relevant factors (cropping pattern, with/without irrigation) because this improves the input for the hydrological model (SWAT). The detailed land-use classes are:

Deciduous Forest – Open: Canopy cover/ density is 10% - 40%

Deciduous Forest – Dense: Canopy cover/ density is more than 40%

Scrub Forest: Area at the fringe of dense forest cover and settlements.

Agricultural land: Khariff/spring crop only (cultivated June-July to September-October), Rabi/winter crop only (cultivated November-December to February-October), Zaid/summer crop only (cultivated March-May), two-season crops and all the three-seasons cropped area.

Fallow land: Agricultural land that is not used for cultivation throughout the year during the satellite overpass.

Water bodies: Ponds, rivers, tanks, canals.

Waste land: Dense scrubland (land cover dominated by scrubs), open scrubland (sparse scrub cover and barren land), rocky, quarry and riverine area.

Settlement: Urban continuous (more than 80% of the total surface is impermeable), urban discontinuous (30 to 80 % of the total surface is impermeable), industrial area, transpiration, rural area (village settlement).

The geometrically and radiometrically corrected satellite images supported by the derived indices were applied to prepare a thematic land-use map employing on-screen visual interpretation in Arc GIS 10.1. To maintain consistency, the visual interpretation was carried out at 1:50,000 scale. The identification and classification of different features were conducted based on fundamental image characteristics like tone, texture, association shape, size, pattern, shadow and location. Different satellite-derived indices (section 4.2.4 and Figure 4.1 to 4.4) were also

employed to identify, verify and digitize the specific features. The topologies of prepared polygons were cleaned and finally the attributes are given to polygons to define the different land-use classes.

A brief methodology for satellite data pre-processing and preparation of land-use maps is depicted in Figure 4.8. The satellite imageries of 1990/1991, 2000/2001 and 2010/2011 were classified into 19 land-use classes. A scenario on the future land-use map for year 2021 was also prepared based on government plans, past land-use change patterns and expert interviews.

Land-use maps prepared at different time steps within a year can be combined to produce a single multi-temporal land-use classification (e.g., Villarreal et al. (2011), Yuan et al. (2005)). This approach captures and integrates all major variations within a year in a single map and hence better represents an area with multiple crop rotations. Therefore, the approach provides a better input in hydrological models and as a result enables more appropriate impact analysis, because time-depending hydrological processes are under the influence of intra-annual changes of the cropping patterns. This issue is relevant in the study region due to distinct dry and wet seasons with different cropping patterns with and without supplemental irrigation.

In the current study, multi-seasonal variations and crop rotations within a year were considered. Three different season satellite imageries and their derivatives were analyzed and finally the inter-seasonal information was integrated to produce a single representative land-use map of the year (considered as representative for the respective decade).

In the first step, a detailed land-use map of 2011 was prepared using the satellite derivatives and ground-control points by on-screen visual digitization. All three season satellite images were acquired, and an analysis of different land-use types during the different seasons within the single year was performed. First, the satellite image of the monsoon season (September), which is characterized by maximum crop stand on the agricultural land, was used to digitize the different land-use classes. Then, for the single year (2011), different-season satellite images and their derivatives were overlaid on the land-use map prepared for the monsoon season of the same year to detect any changes in the land-use class. Generally, the agricultural area and crop types change within the different seasons, whereas other land-use classes remain constant during the respective year. Therefore, additional information, i.e., one-season crops (either monsoon or winter or summer crop only), two-season crops, and three-season crops (summer paddy or other crop), etc., was incorporated within a single land-use map. Furthermore, additional information was available from different-season satellite images, as some land-use classes could be thus better identified and verified.

This land-use map of 2011 served as a basis for preparing land-use maps of 2001 and 1991. In the second step, a copy of the map of 2011 was overlaid onto the satellite images and derivatives of 2001. Then, a visual interpretation was conducted and wherever changes in land-use classes were observed on the satellite imagery, those polygons were edited further in different change-

class types. Those polygons where no changes were detected remained constant boundaries. Likewise, in step three, a copy of the 2001 land-use map served as a basis for further on-screen digitization. The satellite data and its derivatives of 1991 were overlaid, and change polygons were identified and edited in different land-use classes to finally generate the land-use map of 1991. The methodology to identify the change classes over the decades is presented in Figure 4.7 and the detailed methodology of the complete land-use mapping is described schematically in Figure 4.8.

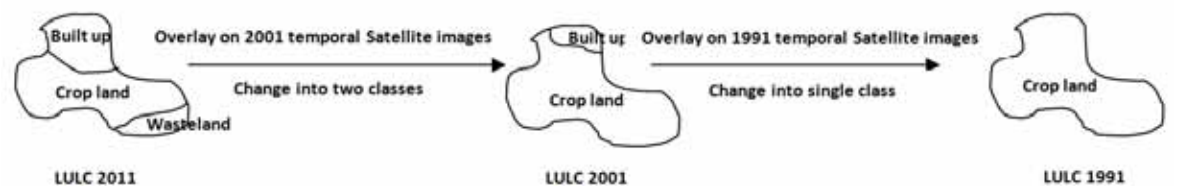

Figure 4.7: Methodology for interpretation and digitization of change classes in different decades

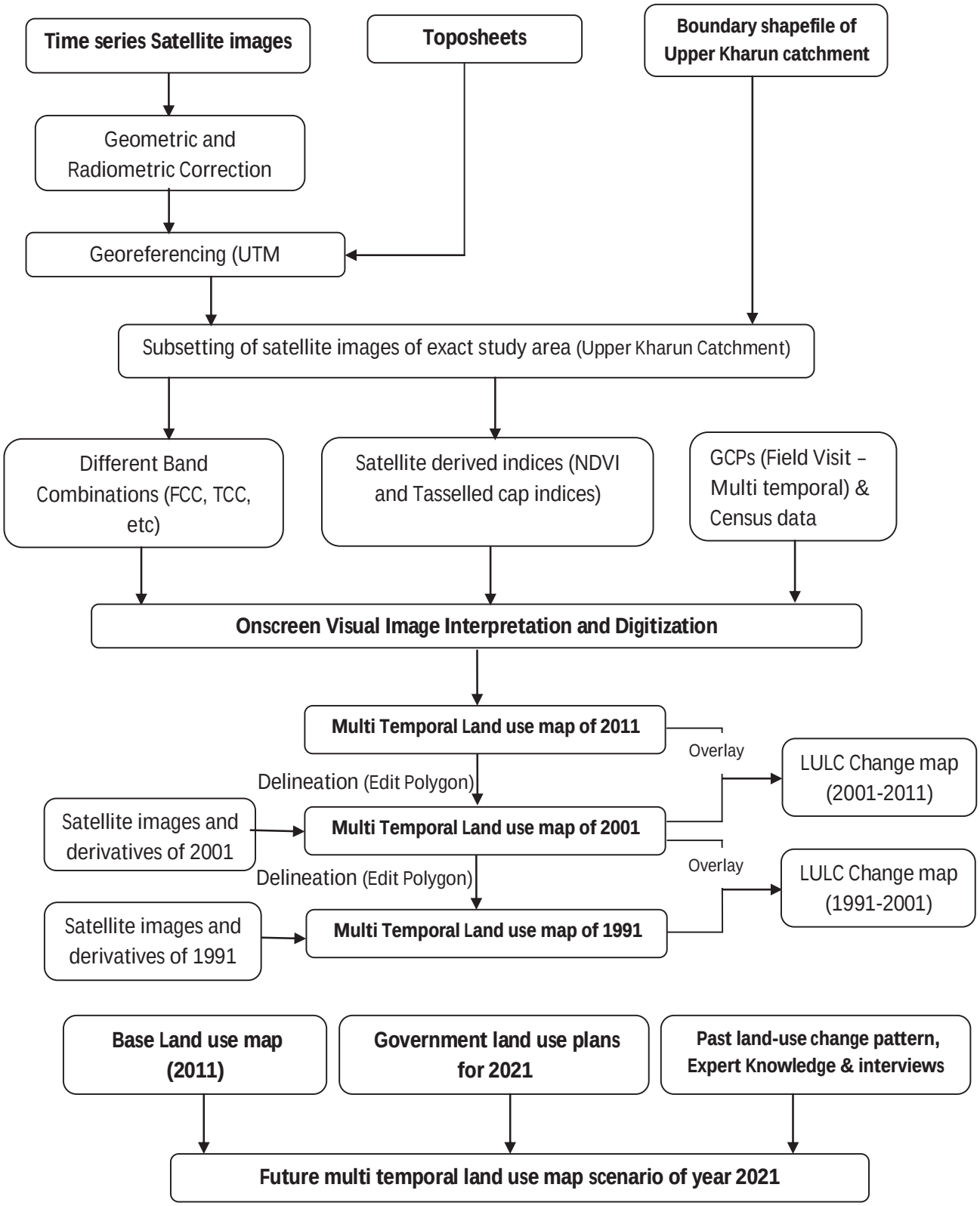

Figure 4.8: Methodology flow diagram for land-use mapping of different decadal years

4.2.7: Identification of groundwater-irrigated areas

The UKC receives irrigation water via four main canal systems from Tandula and Gangral reservoirs during the monsoon season. The canals are running only 2-3 months (September – October/November). Generally, there is no canal water supply during the winter and summer season. Detailed information on irrigation in the UKC is dealt with in Chapter 5.

The main crop (90-95%) grown during the monsoon season is paddy. After harvest of the paddy crop in mid November generally short-duration crops are grown, which utilize the moisture of the harvested paddy field without any additional irrigation. A major portion of the agricultural land follows this pattern. However, there are areas used for two- or three-season crop cultivation (winter and /or summer). The only source of irrigation water during the winter and summer periods are groundwater. Satellite images capture the crop area in these periods and hence provide an indirect indication of groundwater-irrigated areas. Figure 4.9 shows the groundwater irrigated area, the blue patches show the groundwater applied during field preparation prior to paddy cultivation. Figures 4.10 and 4.11 show the summer paddy and Figure 4.12 harvested paddy fields.

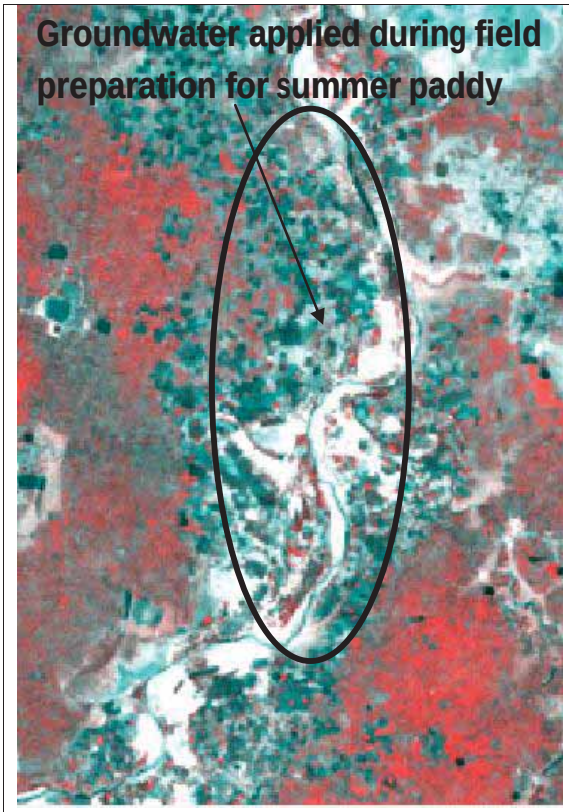

Figure 4.9: Satellite image 30 January 2000

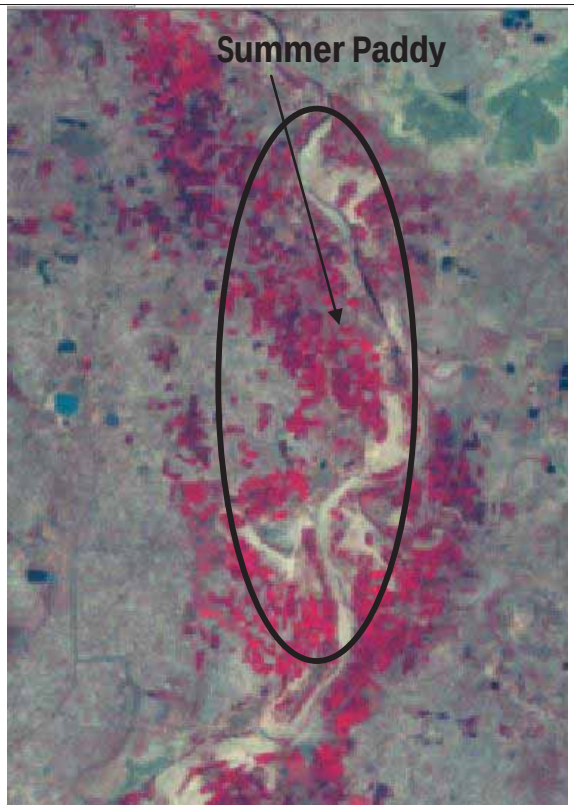

Figure 4.10: Satellite image 11 March 2003

Figure 4.11: Satellite image 22 April 2001

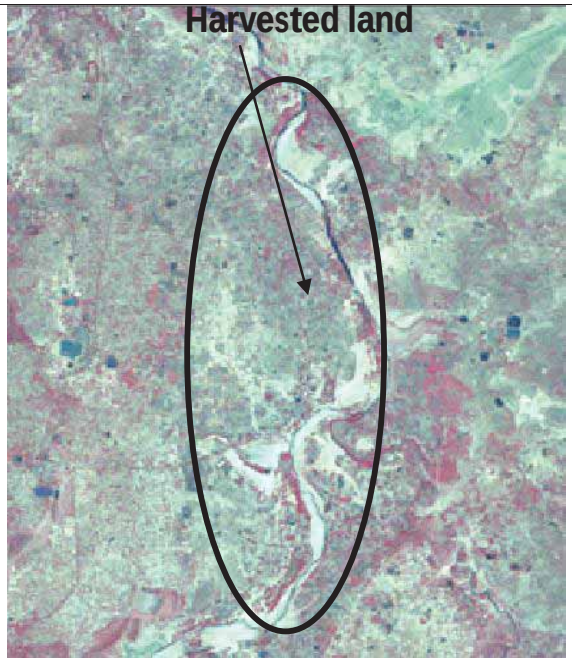

Figure 4.12: Satellite image 15 December 2000

4.2.8: Change detection and validation of land-use change maps

A detailed land-use map of 2011 was prepared and verified using a number of ground control checks distributed throughout the study area.

The land-use map of 2001 was compiled by modifying the polygons of the 2011 land-use change map, and likewise the land-use map of 1991 was generated by modifying the polygons of 2001. Areas of major changes were cross-verified by either visiting the area or interviewing the local people, or by referring to the census book (1991 and 2001) and other governmental records. The land-use change detection maps for three time periods (1991-2001, 2001-2011 and 1991-2011) were prepared and the areas of the classes were calculated. Two attributes, namely change and no change, were assigned to the maps. Overlay, union and frequency functions in Arc GIS 10.1 were used to estimate the change class statistics for the specified time periods.

4.2.9: Future land-use map: realistic land-use change scenario for 2021

The detailed and ground-verified land-use map of 2011 was used as a base map for preparing the scenario of 2021. The on-screen visual digitization technique as discussed above was employed. Necessary information to establish the maps on future land-use change was gathered from government land-use planning units, analysis of past land-use change dynamics and interviews with experts and local people.

The government land-use planning units for the year 2021 were used. These units cover urban and surrounding areas. The three urban and industrial development planning units in the study area are Raipur urban and new Raipur extension area, Dhamtari urban area, and Durg and Bhilai urban and industrial area (Figure 4.13).

Raipur urban area and new Raipur extension land-use planning unit: After the formation of the new state in 2000, Raipur became the capital of Chhattisgarh state. Due to ample opportunities for employment and development, there is a migration of people from other regions to Raipur, and hence the city is now overcrowded. With respect to future population growth and development, the government of Chhattisgarh has proposed a land-use planning unit (new capital city area around Raipur and present Raipur urban planning) till year 2021; the outgrowth of the present Raipur area will further expand and merge with the proposed capital city. The work is in progress. Several villages and their cropland will be changed to urban settlement.

Dhamtari land-use planning unit: 15 cities/towns and villages are located in this planning unit. The change of cropland area into urban area will increase the proportion of area with sealed surfaces (or at least low-infiltration), which may lead to lower groundwater recharge and more surface runoff in the near future.

Bhilai and Durg planning unit: A small segment of Durg urban area and Bhilai industrial area is situated on the upper northwest side of the study area. It serves and creates employment for thousands of people. This area has witnessed a significant increase in population and built-up area over the decades and therefore the government has prepared a land-use planning unit for this area for 2021 to foster the industrial development.

Irrigation: Advancement in technology and development of infrastructure may lead to further increase in the utilization of groundwater and canal water for irrigation purposes and thus, it is likely that two-season crops might be replaced by three-season crops in the near future.

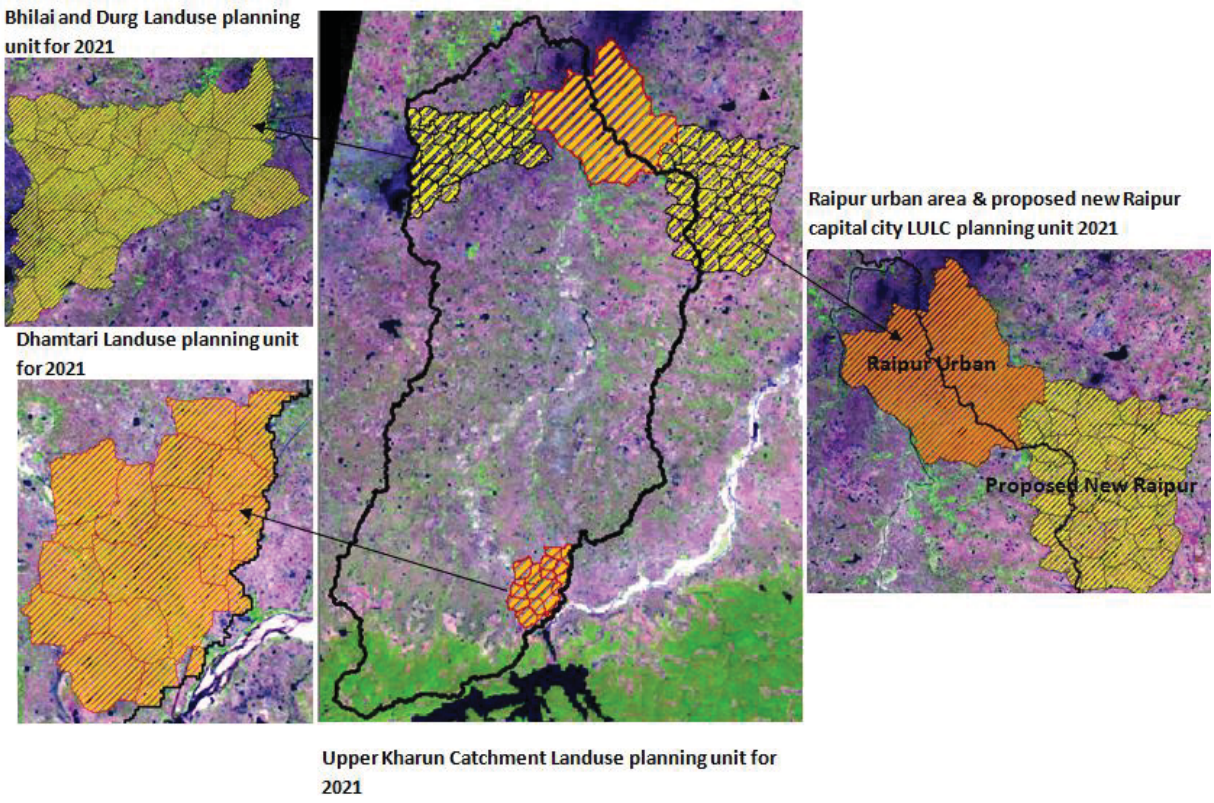

Figure 4.13: Land-use planning unit for Upper Kharun Catchment for 2021

Past land-use change detection maps: Apart from government land-use plans and expert interviews, the land-use change analysis for the period 1991-2011 was utilized as additional information. The detected dynamics of changing land-use class from one to another and the proportion over the decades helped in identifying the hot-spot areas, which were used in the generation of a realistic future land-use scenario for 2021 (Figure 4.21). Only those polygons were considered and modified for future change where land-use change occurred in the past (with exception of the above-mentioned land-use planning units). The detailed land-use change statistics and maps are presented in Section 4.3.

4.3 Results and discussion

4.3.1 Broad land-use classification

The decadal year land-use maps were broadly classified into five classes (Agricultural land, Built Up, Forest, Wastelands and Water bodies). The area under each class over the decades is listed in Table 4.2 and depicted in Figures 4.14, 4.15, 4.16 and 4.17.

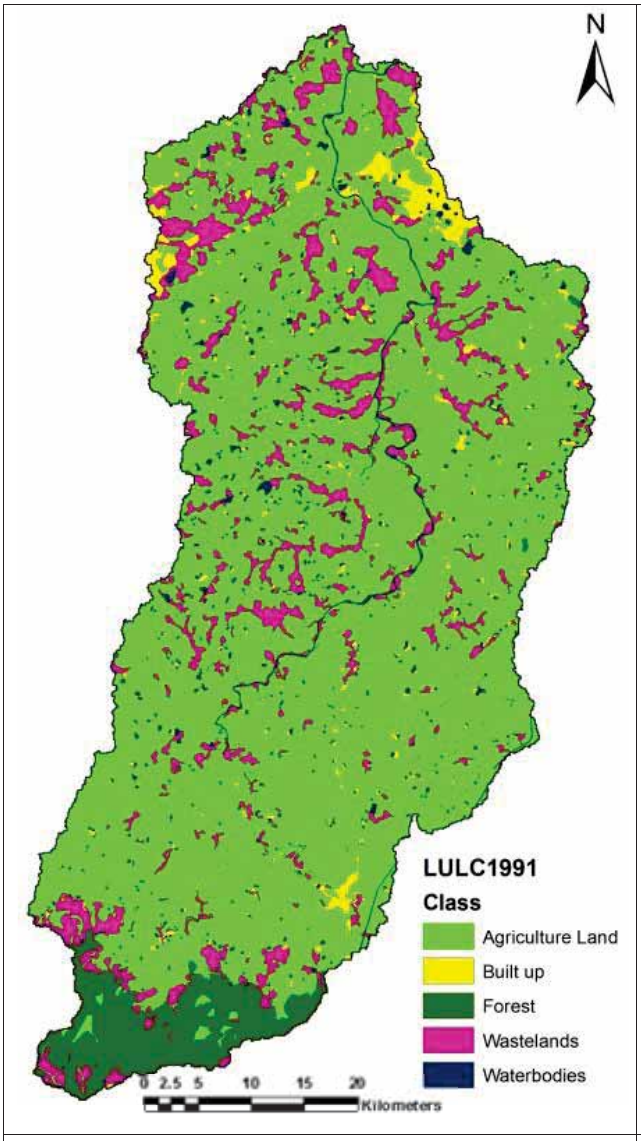

Figure 4.14: Land-use map 1991

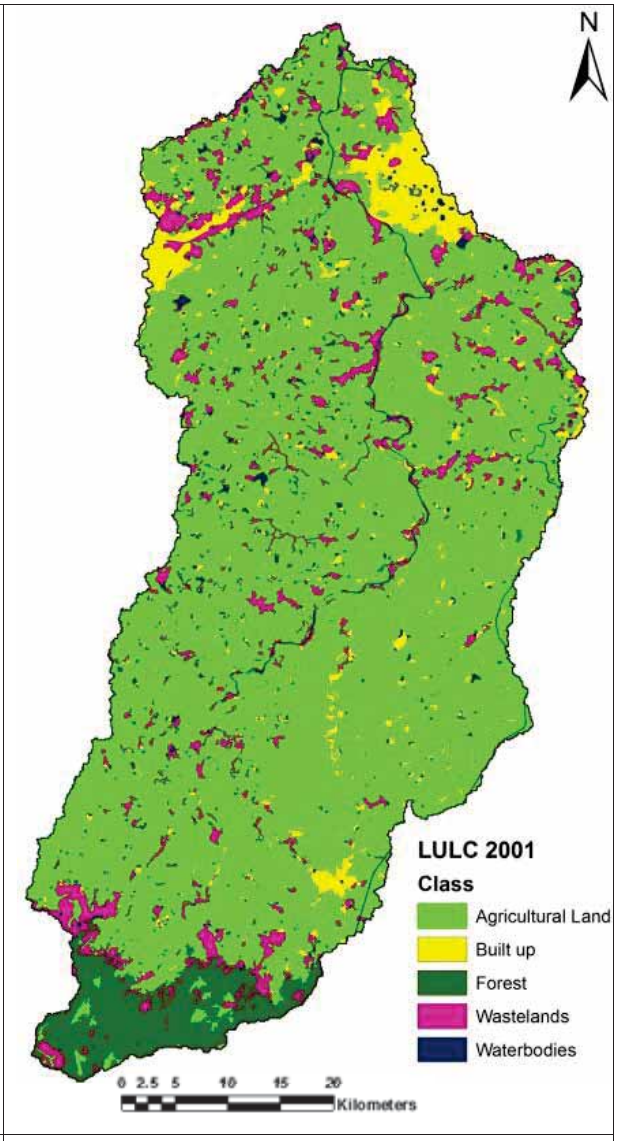

Figure 4.15: Land-use map 2001

Table 4.2: Area of land-use classes (km^2) 1991, 2001, 2011 and 2021

S.No.	Land-use class	1991	2001	2011	2021	% in 1991	% in 2001	% in 2011	% in 2021
1	Agricultural Land	1941.6	1936.4	1919.9	1881.1	78.0	77.8	77.2	75.6
2	Built up	105.3	194.3	221.5	287.1	4.2	7.8	8.9	11.5
3	Forest	127.3	119.9	132.1	131.8	5.1	4.8	5.3	5.3
4	Wastelands	264.7	193.3	171.1	144.6	10.6	7.8	6.9	5.8
5	Waterbodies	49.0	43.9	43.3	43.2	2.0	1.8	1.7	1.7

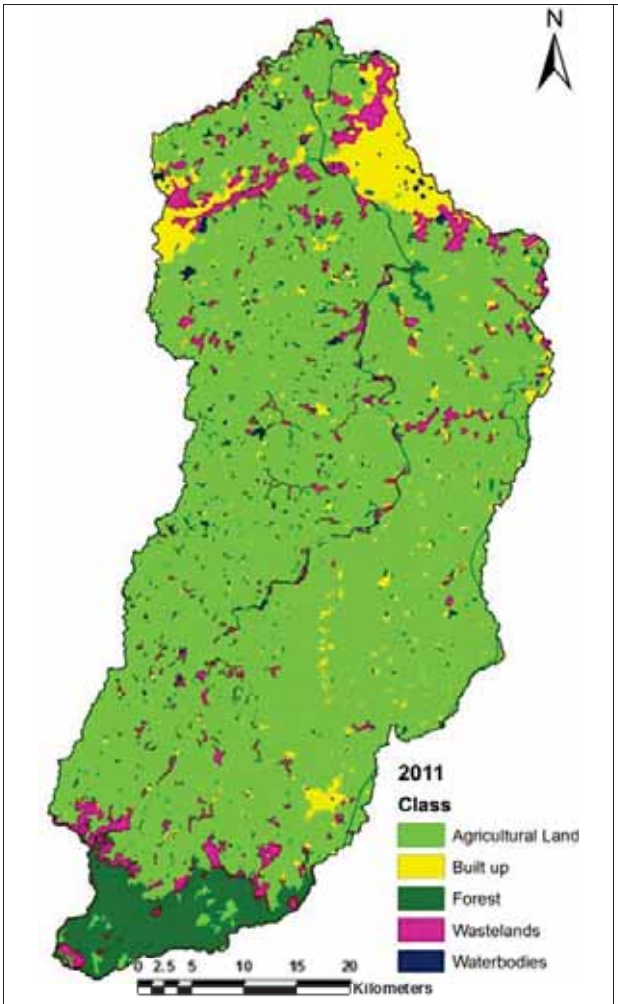

Figure 4.16: Land-use map 2011

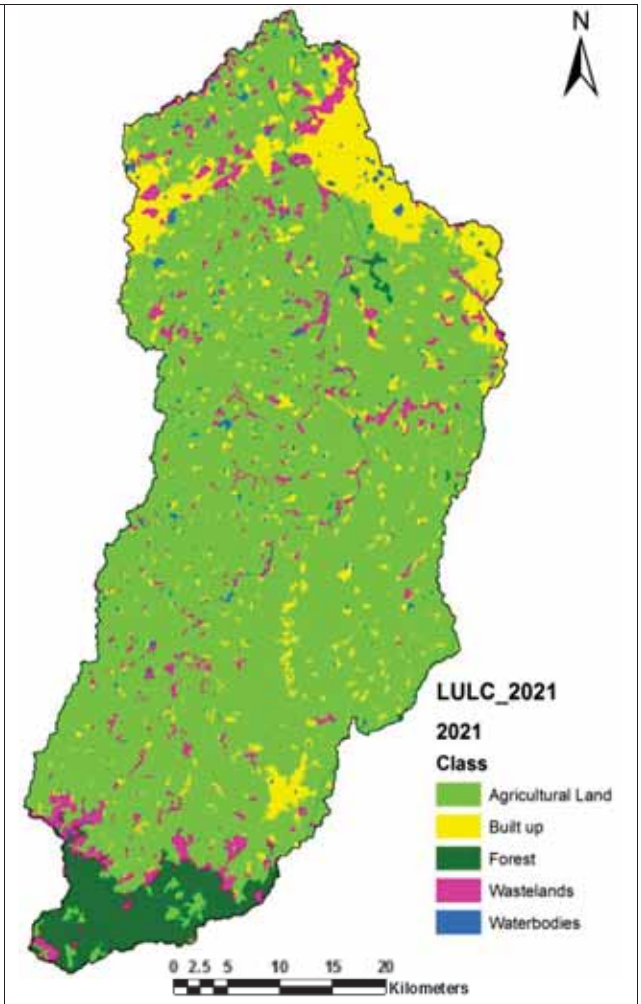

Figure 4.17: Land-use map 2021

Agricultural land: This class covers the land used for agriculture (crop production) with either one, two or three crops per year. It also contains fallow land currently not used for agriculture throughout the year, but having a potential for agricultural crop production. The decadal year land-use statistics reveal a slightly declining trend in the land used for agriculture.

Built-up area: This class captures the industrial areas, rural settlements (villages), urban compact continuous areas (towns and cities), urban discontinuous areas (medium density settlement and transportation areas covered by roads and railway lines), and urban vegetation areas. Decadal year land-use statistics (Table 4.2) show a significant almost 2-fold increase in the proportion of built-up areas in the UKC between 1991 (4.2%) and 2011 (8.9%). This indicates a significant rise in population and rapid development of the study area. This further leads to an increase in sealed areas generating surface runoff and lowering groundwater recharge in the respective areas. It is expected that there will be an increase in built-up areas by 2.6% of the UKC between 2011 and 2021.

Forest area: This class of land contains deciduous dense forest, deciduous open forest, scrub forest and evergreen open forest. The share of land under forest declined between 1991 and 2001 by 0.3%, but showed an increasing trend between 2001 and 2011 by 0.49%.

Wastelands: This class includes the barren land (rocky, quarry and riverine), scrubland (dense/ closed) and scrub land (open). The proportion of wasteland in the UKC is declining consistently. During 1991-2001, it declined by 2.87% and during 2001-2011 by 0.89%. The decrease in wasteland by 3.76% between 1991 and 2011 can be interpreted as an indication for high pressure on land resources (to use even an increasing area of waste land for other purposes). It is further expected to decrease by 1.1% between 2011 and 2021.

Water bodies: This class covers all the surface water bodies (ponds /river /tanks /canals). Ponds represent the main share of water bodies and are the characteristic feature of Chhattisgarh, where generally 2-3 ponds can be found in each village. The water bodies are either seasonal or perennial. Decadal year land-use statistics reveal a slight decline in the area during 1991 to 2001 by 0.2% and during 2001 to 2011 a further very slight decline of 0.02% area. It is expected that the area of water bodies will remain constant between 2011 and 2021 in spite of increasing demand by different sectors.

4.3.2 Detailed land-use classification

The land-use maps were further classified into more detail 19 land-use classes. (Tables 4.3 and 4.4; Figures 4.18, 4.19, 4.20 and 4.21).

A detailed description of different land-use types is given below. Management aspects especially referring to agricultural land including irrigation activities are incorporated in the description. Agricultural aspects influence evapotranspiration and irrigation activities, and strongly influence water fluxes and balances. Spatio-temporal features of these management activities will be considered as important input variables in the hydrological modeling.

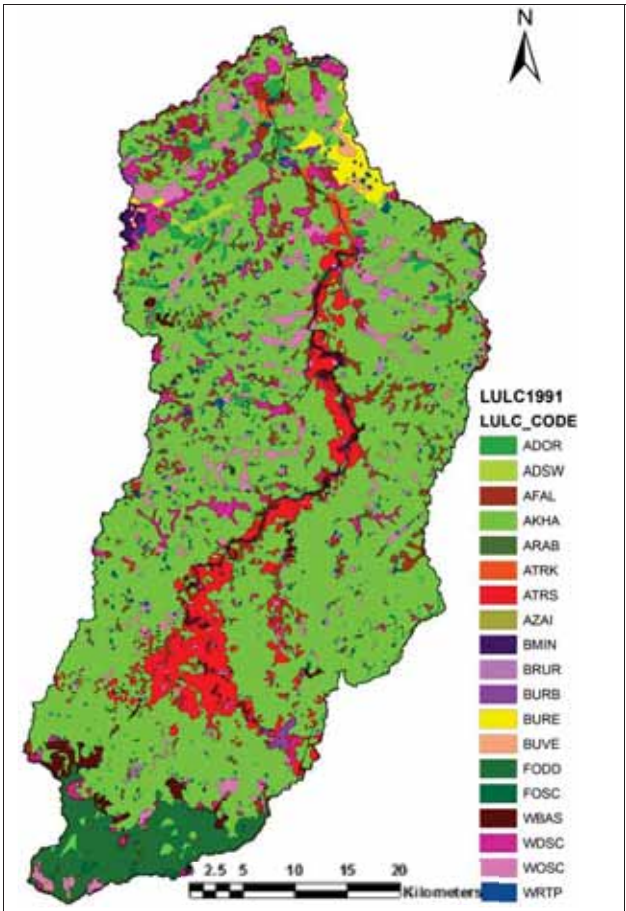

Figure 4.18: Detailed land-use map 1991

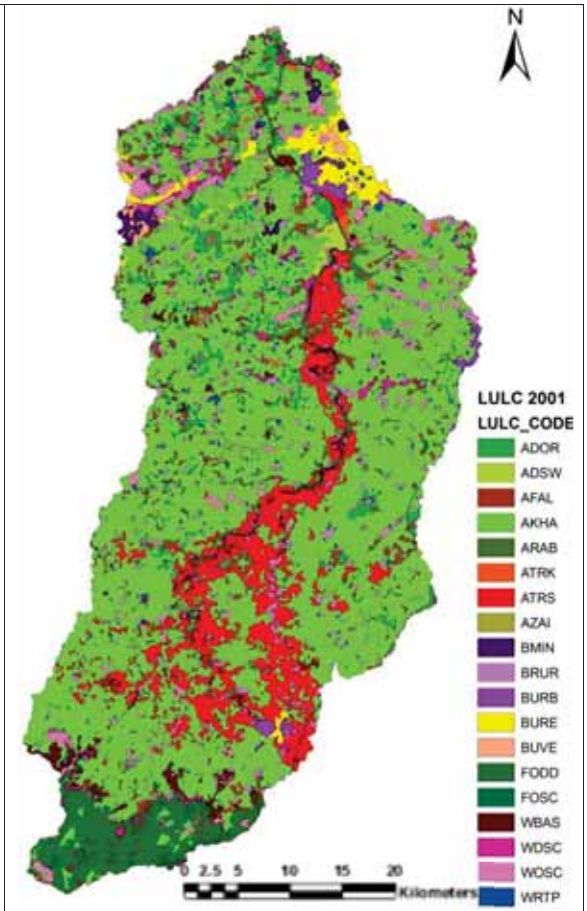

Figure 4.19: Detailed land-use map 2001

Spring/monsoon crop only (Kharif) - AKHA: This class consists of the area only used for a one-season crop, which is sown and grown during the monsoon period (mid July to mid November). During the rest of the year, the land is left fallow with harvested straw left in the fields. The only crop grown during the monsoon season is rice (paddy). The monsoon rain supplemented by canal irrigation during September and October is used for rice cultivation. Pumped groundwater is also applied in certain parts as an additional source for irrigation during the water-stress periods.

Generally after the harvest of the paddy crop, a second crop may be sown (mustard, lentils, etc.). These crops do not require additional irrigation water, because they use the soil moisture available in the harvested paddy field. This class is considered as a single season crop area in the mapping.

AKHA represents the main class covering more than 50% of the study area. The land-use statistics show a decrease in area under this category from 62.71% in 1991 to 53.68% in 2011 (Table 4.4). It is further predicted that the area under this class will significantly reduce from 53.68% to 21.82% of study area till 2021.

Table 4.3: Detailed land-use classes (1991, 2001, 2011 and 2021) in the UKC (km^2)

S.No.	Landuse Classes	Land-use code	1991	2001	2011	2021
1	Spring/Monsoon crop only (Kharif)	AKHA	1560.1	1470.6	1335.5	542.8
2	Winter crop only (Rabi)	ARAB	7.7	10.5	6.4	6.5
3	Summer crop only (Zaid)	AZAI	2.2	7.6	4.5	4.5
4	Cropped in two seasons (Kharif + Rabi)	ADOR	35.9	89.6	170.8	603.3
5	Cropped in two seasons - Summer Wheat (Others)	ADSW	9.0	16.7	24.5	36.1
6	Cropped in more than two seasons	ATRK	9.6	10.3	15.1	16.2
7	Cropped in more than two seasons (Summer Paddy)	ATRS	161.9	262.8	297.7	610.8
8	Fallow land (Permanently)	AFAL	149.4	68.4	65.4	60.9
9	Built Up - Industrial Area	BMIN	5.4	15.7	16.8	19.6
10	Built Up - Rural (Village)	BRUR	62.7	96.4	104.8	107.5
11	Built Up - Urban Sparse (Discontinuous)	BURB	10.0	23.0	33.0	47.9
12	Built Up - Urban Compact (Continuous)	BURE	27.2	47.2	57.5	106.4
13	Vegetated/ Open Area (Vegetables - 3 seasons)	BUVE	5.8	12.0	9.3	5.8
14	Deciduous Forest (Dry/ Moist/ Thorn)	FODD	124.7	111.2	125.0	124.7
15	Scrub Forest	FOSC	2.6	8.7	7.1	7.1
16	Barren Land (Rocky, Quarry & Riverine)	WBAS	44.4	42.6	27.8	27.6
17	Scrub Land - Dense/ Closed	WDSC	98.9	40.3	40.2	36.3
18	Scrub Land - Open	WOSC	121.3	110.5	103.1	80.7
19	Water body- Reservoir/Pond/River/Tank/Canal	WRTP	49.0	43.9	43.3	43.2
	Grand Total		2487.8	2487.8	2487.8	2487.8

Winter crop only (Rabi) – ARAB: This class stands for only one season crop (mustard, green gram, lentils, vegetables, etc.) grown during the winter season (mid November to mid February); during the rest of the year the land is kept fallow. The crop is irrigated by groundwater resources only and represents a very small fraction of the study area. It showed almost no change over the decades.

Summer crop only (Zaid) – AZAI: This class consists of only one season crops (wheat, mustard, etc.) grown during the summer season (mid February to mid May); the rest of the year the land is left fallow. The crop is irrigated by groundwater resources only and represents the smallest class of the study area. This class showed almost no change over the decades.

Cropped in two seasons (Kharif + Rabi) – ADOR: This class represents the two-season crops grown during the monsoon season (mid July to mid November) and winter season (mid November to mid-March). The rest of the period the land lies fallow. The crop is irrigated by canal water during the monsoon and by groundwater in winter.

There is a significant increase of 5.43 % area under this class from 1991 to 2011. Due to the development of irrigation infrastructure and the increasing demand for food, it is expected that there will be significant conversion of one-season crops (AKHA) to two-season crops (ADOR). Between 2011 and 2021, the increase in area for ADOR is 24.25% of the total study area, which is high compared to the other classes.

Table 4.4: Percentage of different land-use classes in the UKC: 1991, 2001, 2011 and 2021

S.No.	Landuse Classes	Land-use code	% in 1991	% in 2001	% in 2011	% in 2021
1	Spring/Monsoon crop only (Kharif)	AKHA	62.71	59.11	53.68	21.82
2	Winter crop only (Rabi)	ARAB	0.31	0.42	0.26	0.26
3	Summer crop only (Zaid)	AZAI	0.09	0.31	0.18	0.18
4	Cropped in two seasons (Kharif + Rabi)	ADOR	1.44	3.60	6.87	24.25
5	Cropped in two seasons - Summer Wheat (Others)	ADSW	0.36	0.67	0.98	1.45
6	Cropped in more than two seasons	ATRK	0.39	0.41	0.61	0.65
7	Cropped in more than two seasons (Summer Paddy)	ATRS	6.51	10.56	11.97	24.55
8	Fallow land (Permanently)	AFAL	6.01	2.75	2.63	2.45
9	Built Up - Industrial Area	BMIN	0.22	0.63	0.68	0.79
10	Built Up - Rural (Village)	BRUR	2.52	3.88	4.21	4.32
11	Built Up - Urban Sparse (Discontinuous)	BURB	0.40	0.93	1.33	1.93
12	Built Up - Urban Compact (Continuous)	BURE	1.09	1.90	2.31	4.28
13	Vegetated/ Open Area (Vegetables - 3 seasons)	BUVE	0.23	0.48	0.37	0.23
14	Deciduous Forest (Dry/ Moist/ Thorn)	FODD	5.01	4.47	5.02	5.01
15	Scrub Forest	FOSC	0.10	0.35	0.29	0.29
16	Barren Land (Rocky, Quarry & Riverine)	WBAS	1.79	1.71	1.12	1.11
17	Scrub Land - Dense/ Closed	WDSC	3.98	1.62	1.62	1.46
18	Scrub Land - Open	WOSC	4.88	4.44	4.14	3.24
19	Water body- Reservoir/Pond/River/Tank/Canal	WRTP	1.97	1.76	1.74	1.74

Cropped in two seasons (Kharif + summer wheat) – ADSW: This class represents the two-season (monsoon and summer) crop area. The second crop is summer wheat followed by monsoon paddy. Over the decades, there was a slight increase in the area under this class.

Cropped in more than two seasons – ATRK: This class represents the three-season (monsoon, winter and summer) crop area. The crops grown during the summer season are wheat and vegetables, etc., other than the paddy crop. Over the decades there was a slight increase in this class.

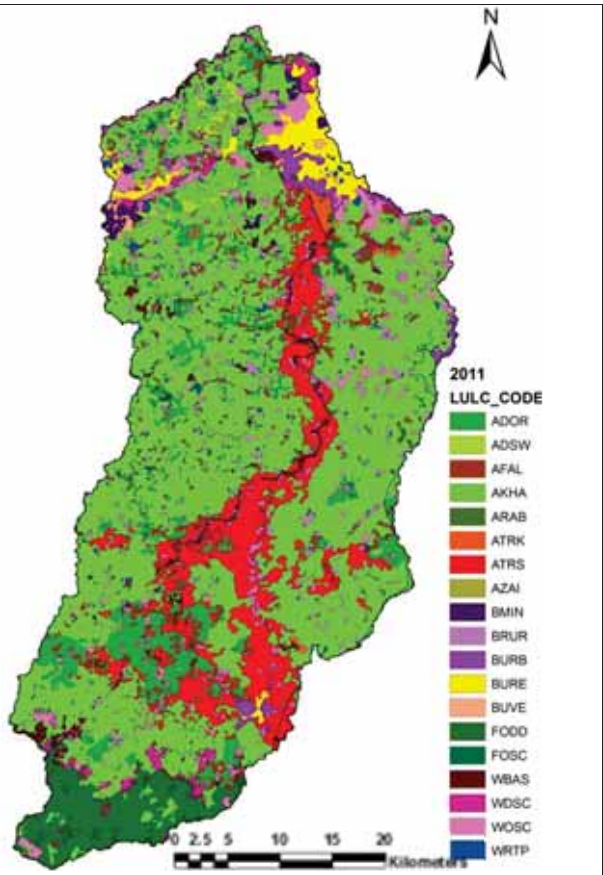

Figure 4.20: Detailed land-use map 2011

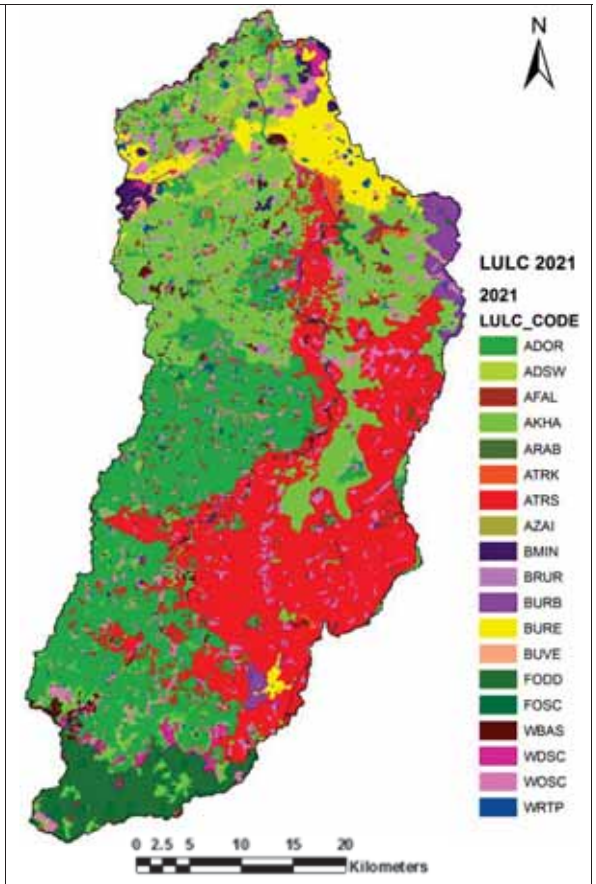

Figure 4.21: Detailed land-use map 2021

Cropped in more than two seasons (Summer Paddy) - ATRS: This class represents the three-season (monsoon, winter and summer) crop area. The crops grown during the summer season are only paddy. There was a significant increase in area of 5.67% under this class from 1991 to 2011. A significantly high increase of 12.57% area is expected between 2011 and 2021. This indicates an excessive increase in groundwater irrigation for some villages in the UKC and points to the limits of sustainable use of the precious groundwater resources.

The decrease in area with only one crop (AKHA) and increase in areas with two (ADOR) or three crops (ATRS) is considered as an indication for pressure on land and water resources, i.e., towards intensification driven by population growth.

Fallow land (permanent) – AFAL: This class covers those lands which are currently not used for agriculture throughout the year and left unused. Yet these lands are potentially fertile and have potential for crop production. The decadal year land-use statistics reveal a significant decrease of 3.38% area under this class from 1991 to 2011, which supports the above-mentioned pressure on land resources.

Built-up - Industrial area – BMIN: This class represents industrial areas, ashes /cooling pond/ effluent/ other waste and mining active area. The decadal year land-use statistics show an increase in area of 0.46% under this class from 1991 to 2011.

Built-up - Rural (Village) – BRUR: This class comprises the rural villages with low-density settlement areas. The decadal year land-use statistics document a significant increase in area of 1.69% under this class from 1991 to 2011.

Built-up - Urban Sparse (Discontinuous) – BURB: This class represents the medium density urban settlement areas and transport areas. The decadal year land-use statistics show that there was a significant increase in area of 0.93% under this class from 1991 to 2011, and the area is expected to increase by 0.6% between 2011 and 2021.

Built-up - Urban Compact (Continuous) – BURE: This class stands for the high-density urban settlement areas. The decadal year land-use statistics reveal a significant increase in area of 1.22% under this class from 1991 to 2011, and a further increase by 1.97% is expected between 2011 and 2021.

Vegetated/ Open area (Vegetables - 3 seasons) – BUVE: This class covers the vegetation area near and around the urban settlements. According to decadal year land-use statistics, there was a slight increase in area between 1991 and 2001 followed by a slight decrease between 2001 and 2011.

Deciduous Forest (Dry/ Moist/ Thorn) – FODD: This class represents the open and dense deciduous forest area. There was a decrease in area of 0.54% under this class from 1991 to 2001 and an increase of 0.55% was detected from 2001 to 2011.

Scrub Forest – FOSC: This class consists of the degraded open deciduous forest areas. Land-use mapping revealed an increase in area of 0.25% under this class from 1991 to 2001. However, the area was decreased by 0.06% during the period 2001 to 2011.

Barren Land (Rocky, Quarry and Riverine) – WBAS: This class represents the open waste land area without vegetation. It includes the exposed rocky areas, quarries and riverine sandy areas. These lands are degraded and infertile. The decadal year land-use statistics show that there was a significant decrease in the area of 0.67% from 1991 to 2011.

Scrubland - Dense/ Closed – WDSC: This class comprises wasteland with dense scrubland. The decadal year land-use statistics reveal a significant decrease in area of 2.36% under this class from 1991 to 2011. It is predicted that there will be slight decrease of 0.16% between 2011 and 2021.

Scrubland – Open – WOSC: This class represents the wasteland with open scrubland. The decadal year land-use statistics reveal a slight decrease in area of 0.74% under this class from 1991 to 2011, which is expected to further decrease by 0.9% between 2011 and 2021.

Water bodies - WRTP: This class covers all surface water bodies (ponds /rivers /tanks /canals). The water bodies can be either seasonal or perennial. Decadal year land-use statistics detect a slight decline in area during 1991 to 2001 by 0.2%, and during 2001 to 2011 the class experienced a further slight decline of 0.02%.

4.3.3 Land-use change maps and area statistics

Land-use change detection analysis was performed for three time steps from 1991 – 2011, 1991 – 2001, and 2001-2011. (Table 4.5, Figure 4.22, 4.23 and 4.24). Overlay and frequency functions of Arc GIS 10.1 were used to detect the change areas.

Land-use class change between 1991 and 2011

Table 4.5 shows the changes (km^2) from one land-use class to another during the period 1991-2011. Moving (horizontally) in the rows gives the change from the class mentioned at the left side into the other classes named in the top row. Moving (vertically) in the column gives the gains of the class mentioned in the top row from the classes named on the left side. The major changes are pointed out in following section.

(i) The total forest area, which is located in the southern part of the UKC, shows no significant change between 1991 and 2011. However, there was a change from dense deciduous forest (FODD) to open deciduous forest (FODO).

(ii) The three-season crop area with summer paddy (ATRS) shows a significant increase in coverage, probably due to development and advancement in the groundwater irrigation infrastructure. An area of 171.1 km^2 changed from one season crop (AKHA) to ATRS; however 99.1 km^2 under this class remained constant.

(iii) Rapid population growth and development of infrastructure facilities led to a significantly high increase in the built-up areas. Analysis results show that 24.3 km^2 areas was converted from single crop areas (AKHA) to rural built-up areas (BRUR); 15.8 km^2 area was converted from AKHA to urban discontinuous built-up areas (BURB) and 11.9 km^2 area was converted from AKHA to urban continuous built-up areas (BURE).

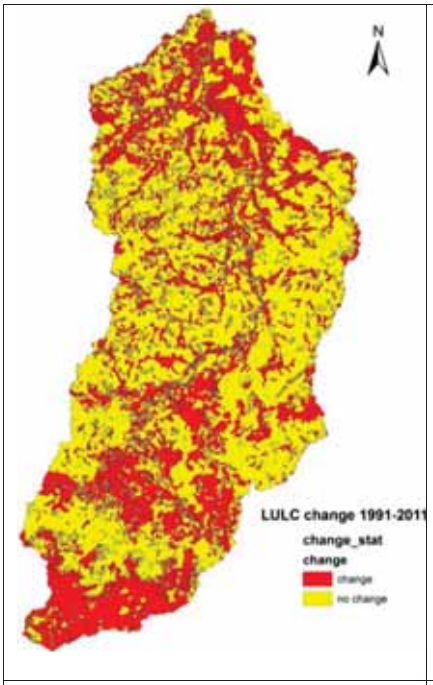

Figure 4.22: Land-use change map 1991-2011

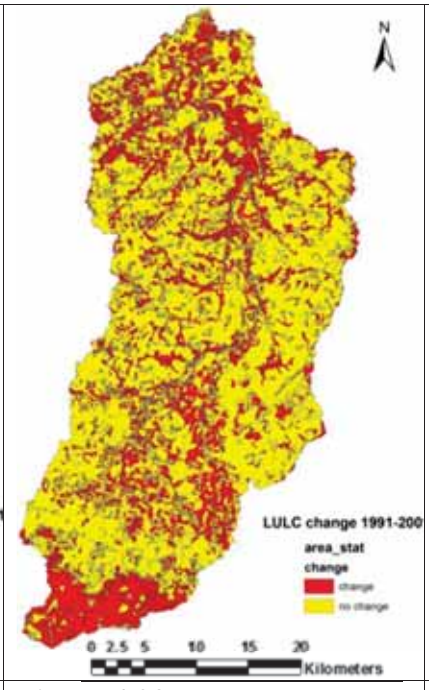

Figure 4.23: Land-use change map 1991-2001

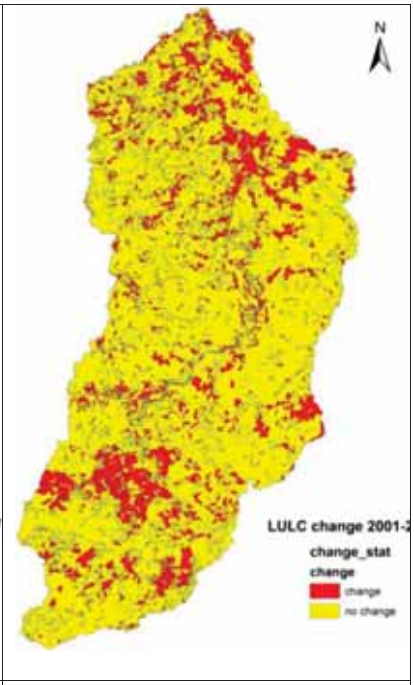

Figure 4.24: Land-use change map 2001-2011

Table 4.5: Change in land-use classes between 1991 and 2011 (km^2)

land use classes in 1991 (horizontal: rows) →

↓ land use classes in 2011 (vertical: columns)

LULC CODE	ADOR	ADSW	AFAL	AKHA	ARAB	ATRK	ATRS	AZAI	BMIN	BRUR	BURB	BURE	BUVE	FODD	FODO	FOSC	WBAS	WDSC	WOSC	WRTP	Grand Total
ADOR	6.40	2.69	0.67	20.70	0.11	1.98	0.08	0.80	0.04	0.36	0.06	0.69			0.17		0.04	0.09	0.93	0.05	35.85
ADSW	0.49	3.37	0.47	3.96		0.28				0.14		0.02	0.03		0.03				0.11	0.07	8.96
AFAL	6.46	1.53	20.04	43.27	1.45	0.34	7.37	0.51	3.51	14.97	4.02	1.70	0.27	0.05	0.64	0.39	4.21	8.22	27.93	2.54	149.42
AKHA	97.82	8.69	21.11	1143.30	0.87	7.28	171.11	0.64	2.41	24.26	15.83	11.88	1.73	0.07	3.32	0.72	2.93	7.54	29.87	8.72	1560.10
ARAB	0.61	0.01	0.43	1.94	0.38	0.54	1.66	0.03		0.24		0.41	0.03		1.06		0.00		0.36	0.01	7.70
ATRK	0.04	0.69	0.08	1.02		3.30	2.36	0.59	0.00	0.50	0.57		0.31				0.02			0.18	9.65
ATRS	41.69	0.03	0.67	11.82	0.40	0.08	99.11			3.42	1.08	0.08			0.10		1.04	0.27	1.38	0.72	161.87
AZAI		0.75		0.87				0.61										0.01			2.23
BMIN									4.13			0.03	1.13					0.14			5.43
BRUR	0.57	0.00	0.52	6.40	0.00	0.00	0.65		0.00	49.99	1.69	1.33	0.03		0.08	0.01	0.18	0.26	0.54	0.42	62.68
BURB	0.01		0.21	0.10			0.22	0.00		0.38	2.24	5.42	0.33			0.02	0.78		0.07	0.24	10.02
BURE				0.11		0.00			0.03		1.22	25.17	0.27					0.02	0.11	0.26	27.19
BUVE									0.25		0.01	2.82	2.22					0.39		0.08	5.78
FODD	0.13		0.26	3.77		0.04	0.04			0.04				5.81	105.69	4.22	0.71	1.80	1.87	0.19	124.57
FODO															0.12						0.12
FOSC															1.10	1.44			0.05		2.59
WBAS	1.22		2.10	5.63	0.49	0.03	5.93	0.05		1.83	0.16	0.03			0.77	0.05	12.85	6.30	6.20	0.77	44.41
WDSC	8.54	3.49	5.74	37.95	1.27	0.74	1.82	0.40	4.93	1.43	3.46	4.19	2.60		2.05	0.03	1.64	8.03	8.29	2.35	98.93
WOSC	5.70	3.05	12.51	43.15	1.36	0.36	4.64	0.83	0.70	4.61	2.22	3.06	0.21	0.02	3.77	0.07	1.69	6.88	24.33	2.15	121.31
WRTP	1.15	0.20	0.56	11.51	0.08	0.13	2.75	0.04	0.83	2.99	0.44	0.36	0.19		0.11	0.16	1.73	0.29	1.01	24.51	49.03
Grand Total	170.84	24.49	65.38	1335.48	6.40	15.10	297.73	4.51	16.83	105.14	32.99	57.21	9.32	5.94	119.01	7.11	27.81	40.23	103.05	43.26	2487.84

CHAPTER 5: IRRIGATION

5.1 Introduction

Chhattisgarh state is known as the rice bowl of India. Rice is grown as a single main monsoon crop and can be taken up as a winter and /or summer crop where sufficient groundwater is available to meet the water demand.

Rice is grown in basins which are permanently or at least for a high share of the vegetation period flooded with a water layer. As a consequence, crop-water requirements and percolation and seepage have to be matched by irrigation water input. Therefore, rice is one of the most water demanding crops requiring a large amount of water either by canals or from groundwater sources.

The UKC has a well distributed canal network system, which supplies water mainly for irrigation during the late and post monsoon months only (September to November). During the summer and winter season, there is no supply of water from the canal system for irrigation purposes. The canal water supply in monsoon comes from the Gangaral reservoir southeast and the Tandula reservoir southwest of the UKC, i.e., outside the study area (Figure 5.1). A detailed description of the canal network system is presented in section 5.3.

During the summer and winter seasons, the irrigation water demand of crops is met by groundwater resources only. According to the Central Ground Water Board (CGWB) report 2012, the demand to groundwater irrigation in Chhattisgarh has increased 6-fold from 2001-2010, mainly driven by rapid population growth and increase in food demand. As a result, groundwater resources are at the risk of being over-exploited for irrigation purposes at least in parts of the UKC.

The trends detected by CGWB referring to Chhattisgarh are in line with the findings of the land-use mapping for the UKC (Chapter 4). This confirmed an increase in groundwater-irrigated paddy areas from 161.8 km^2 in 1991 to 297.7 km^2 in 2011. The local people stick to their traditional practice of paddy cultivation, which is highly water demanding. Moreover, the government of Chhattisgarh is promoting and providing subsidies for electricity to pump groundwater for paddy cultivation. The practice of over-exploitation of precious groundwater resources may lead to a major water crisis in the near future, and therefore careful management is essential and as a prerequisite, reliable information on trends regarding withdrawals and recharge by percolation and seepage is needed.

The main share of groundwater exploitation is from the shallow aquifer only. The development of shallow aquifers plays an important role. Therefore, correct assessment of dynamic groundwater resources is significant for sustainable agricultural growth (CGWB, 2012).

In order to understand the surface and groundwater dynamics in the UKC, an in-depth study on the irrigation system and its functioning in the UKC was performed. To that end, data from (i) the census book collected from the Department of Population and Dynamics, Raipur, (ii) irrigation reports collected from the irrigation departments at Raipur, Rudri and Durg, (iii)

satellite data information, (iv) field visits, and (v) expert interviews were collected, analyzed and integrated.

Surface water modeling should consider the irrigation, crop rotation and management practices that might influence the water budget significantly. However, generally due to lack of detailed information, these components are often ignored during a modeling process.

The study area has a well developed canal network system, but there are literature gaps related to the irrigation and management practices in surface water modeling. The current study aims at a detailed analysis of irrigation data and amount of irrigation water applied in the UKC. The data is used as an input in the surface water modeling using SWAT.

The detailed land-use map provides information about the agricultural land and also identifies the area irrigated by surface and groundwater separately. The detected irrigated areas were further assigned with the irrigation amount (based on different factors for surface and groundwater as assessed by the CGWB report, 2012) in the management file of SWAT model.

The other aspect (or reason for dealing with irrigation issues) was to detect changes in the irrigated areas and water withdrawals in the UKC in decadal year time steps (1991, 2001 and 2011).

5.2 Materials and methods

The detailed irrigation analysis at village level was done for three time periods: 1991, 2001 and 2011. Further the village level information is summed at block level and the irrigation statistics presented in the later sections.

5.2.1 Detailed analysis of canal network system

- Canal networks inside the UKC were identified and digitized.
- Amount of seepage losses from the canal network system were estimated based on

(i) Differentiation of canal hierarchy (main, distributaries and minors)
(ii) Estimation of wetted area from canal dimension and length (canal irrigation report, 2011)
(iii) Use of empirical and site- (and canal hierarchy) specific losses (per million m^3 and day)
(iv) Estimation of losses by combining information from (ii) and (iii)

5.2.2 Estimation of irrigated areas for time periods 1991, 2001 and 2011

The irrigated areas were estimated with differentiation between canal and groundwater (monsoon, non-monsoon) irrigation using remote sensing satellite data, census book reports, irrigation department reports and field surveys.

5.2.3 Irrigation amount and losses

Spatial measurements on discharge/inflow to the irrigation systems in the UKC are not available. and therefore the irrigation amounts and irrigation losses (percolation) were estimated in this study.

(A) Estimation of irrigation amount

(i): Differentiation of canal and groundwater irrigated areas (done in previous step)
(ii): Derived irrigation amount per unit area (and season) (based on the factors mentioned in GEC 97, CGWB, and irrigation department reports, Table 5.1)
(iii): Estimation of irrigation amounts based on (i) and (ii)

(B) Estimation of irrigation losses (percolation) from irrigated fields

The surface water model SWAT estimates the irrigation losses (percolation from irrigated fields) during the model run.

The pothole function in the SWAT model was tested for the irrigation in the paddy fields. However, there were certain constraints in using this functionality and was not used. No surface runoff generation from the irrigated paddy field in dry periods was assigned to the model, as the paddy fields are bounded by dykes to store water for paddy cultivation. This allows considering the irrigation water in the paddy field for percolation estimation in the SWAT model.

5.3 Canal network

The UKC has a well-developed system of irrigation canal networks with main canals along the western, eastern and southern borders of the catchment. A detailed analysis of the canal system at main canal, distributory and minor level was performed to derive the information on the amount of water released for irrigation and the amount of seepage losses. This information is useful for recharge estimation in the study area.

The canal network index maps were procured from the irrigation department at Raipur, Rudri and Durg. They were scanned, digitized and georeferenced in Arc GIS 10.1. Detailed information on the canal system (hydraulic capacity, dimensions, material and losses) were prepared in spread sheets from the hard copies of the irrigation reports.

The digitized canal network was overlaid on the UKC boundary, and only those parts of main canals, distributaries and minors were selected that were exactly inside the boundary and irrigated areas in the UKC.

The irrigation canal system in the UKC consists of following main canal systems (Figure 5.1)
(1) Tandula Canal System,
(2) Mahanadi Main Canal System,
(3) Mandhar Branch System, and
(4) Mahanadi Feeder Canal System.

This section aims at deriving the characteristics of the canal network located in the UKC and the size of the irrigated areas. This enables estimating the amount of applied irrigation water and the seepage loss from the canal system.

Features of the canal system in UKC:

- The canal system supplies water primarily for irrigation. It also meets the requirements of industries and urban areas.

- During each year, the canal systems are only operated in late monsoon and post monsoon season (September-November) for 2-3 months depending on the water demand. Based on information collected from irrigation reports, expert interviews and field visits, 60 days are considered as a plausible operational period in this study.

- In summer (May), the Mahanadi main canal is operated for 12-15 days only to supply water to Kharun River, ponds and tanks to meet the requirements of the Raipur urban area.

- The Mahanadi feeder canal and Tandula main canal are operated throughout the year to supply water to the Bhilai steel plant (Maroda tank).

- Seepage loss from the canal system is calculated based on the average wetted area (m^2) of the main canal, distributaries and minors, and empirical data on the losses per square unit of wetted area and tie unit (for daily basis) provided by CGWB, 2012. Later, the total seepage loss is summed up for the total number of canal operation days (here 60 days).

5.3.1 Tandula canal system

The Tandula reservoir complex has an overall command area of nearly 3000 km^2. It is a part of the Mahanadi basin and embodies three reservoirs, i.e., Tandula, Gudhli and Kharkhara. Tandula command area is mostly located in Durg district and bounded by Kharun river in the east. It also gets water from Pt. Ravishankar Reservoir (Gangral) through the Mahanadi Feeder Canal (Figure 5.1).

A part of the Tandula main canal is in the UKC. It runs parallel to the west boundary of the UKC and has a length of approximately 74 km from south to north direction in the UKC. Only the right side of the system feeds the UKC.

5.3.2. Mahanadi main canal system

The Mahanadi main canal system originates from the Pandit Ravi Shankar Reservoir (Gangrel) at Rudri (Dhamtari block). Part of the canal is in the UKC. It runs parallel to the east boundary and has a length of approximately 49 km from south to north. Only the left side of the canal system feeds the UKC. The blocks under this irrigation system are Dhamtari and Kurud.

5.3.3. Mandhar branch system

The Mandhar branch originates from the Mahanadi main canal system at 49.26 km cutoff, and feeds Abhanpur and Dharsiwa block. Raipur is supplied by this branch system. It has a length of approximately 49 km from south to north. Only distributaries on the left side of the Mandhar branch provide water to the UKC.

The length of some distributaries and minors in this system has been reduced over the years because of the expansion and outgrowth of urban aggrolomates around Raipur.

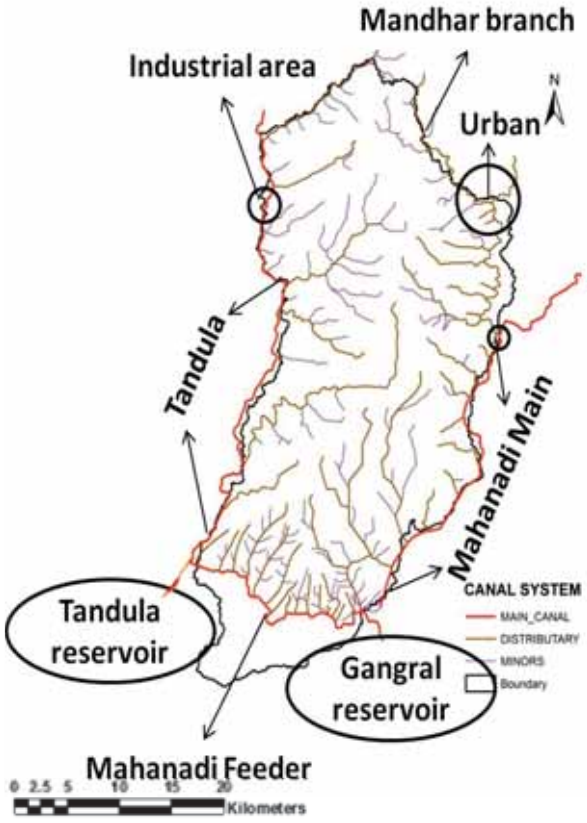

Figure 5.1: Canal network in the UKC

Figure 5.2: Canal infrastructure in the UKC

5.3.4 Mahanadi feeder canal system (MFC)

Mahanadi feeder canal connects Pt. Ravi shankar reservoir (Gangral) to the Tandula main canal. It is running throughout the year, and has a length of approximately 42 km from east to west direction in the southern part of the UKC. It feeds the whole block of Gurur and parts of Dhamtari and Balod blocks.

5.4 Seepage loss from canal network

Seepage losses refer to the amount of water that percolates through the wetted area of the canal (canal bottom and embankment) and recharges the groundwater. Seepage losses from irrigation

canal networks may result in a significant amount of recharge to the groundwater system. Hence, for groundwater recharge assessment studies, it is important to estimate these seepage losses.

In command areas, the recharge from canal network seepage losses depends on the size and cross-section of the canal, vertical depth of flow, soil properties in the bottom and embankment, location and level of drains on both sides of the canal, and canal material and lining.

A number of empirical formulae and methods have been developed to estimate the seepage losses from the canals; examples are inflow-outflow method, ponding method, seepage meter method, etc.

In Chhattisgarh, as recommended by GEC 97, groundwater recharge is estimated separately for the monsoon and non-monsoon season by the Central Ground Water Board (CGWB), Raipur, Government of India. The canals in Chhattisgarh are operated only during the late monsoon and post monsoon season to supplement the rain-fed irrigation to paddy crops. Surface water irrigation during the winter or summer season is practically non-existing.

The terrain of Chhattisgarh state is characterized by hard rock with high transmissivity and low storativity, which results in instantaneous recharge and a high amount of rejected recharge during the monsoon period. Hence, in the period of high rainfall (monsoon), the aquifer remains fully saturated, and thus the additional recharge from other sources is negligible (CGWB, 2012). A recharge factor is estimated for Chhattisgarh region and presented in Table 5.1.

Table 5.1: Recharge computation factors (GEC 97 and CGWB report 2012, Chhattisgarh)

Sl. No	Source of recharge	Range of recharge computation factors
1	Seepage from canals: ha m/day/10^6m^2 of wetted area (=10 litres/ m^2/day)	1-3
2	Return flow from surface water irrigation (as a fraction)	0.167-0.5
3	Return flow from groundwater irrigation (as a fraction)	0.15-0.45
4	Seepage from tanks and ponds (m/day)	0.00048-0.00144

Based on GEC 97, the groundwater estimation report of CGWB, Chhattisgarh (2004), states that for Durg and Dhamtari district (parts of study area), out of the total recharge (other than rainfall), 56% return flow comes from groundwater irrigation, 32% return flow is contributed by surface water irrigation, tanks and ponds accounts for 10% of total recharge, and only 2% seepage loss as recharge is contributed by the canal network.

Further, specifically for the UKC, the groundwater recharge estimation reports of CGWB consider the seepage loss factor as 1.0 ha m /day/10^6m^2 of wetted area, which is equivalent to 10 litres/ m^2/day. This factor is used in this study for estimating the canal seepage losses.

The information about the length of the canal network (main canal, distributaries and minors) and their wetted perimeter were collected from the irrigation departments in Raipur, Durg and

Rudri. Further, the exact length of canal network in the UKC was calculated by ARC GIS 10.1. The seepage loss by different canal systems was calculated separately, considering 60 days as the operation period of the canals per annum. Main canals, distributaries and several minors in the UKC are lined.

Seepage loss (m^3) = wetter perimeter of canal (m) * length of the canal (m) * recharge computation factor for UKC (10 l/ m^2/day) * 60/1000 (5.1)

5.4.1. Tandula canal system

The seepage loss from the Tandula canal system in Patan block is calculated to be 353040 m^3 in 60 days (Sept–Oct). This amount of water is the surface water recharge of the area of the Tandula canal system in Patan district. The seepage loss from Gorhi Dy, Armari Dy and Partial Supkona Dy is 432000 m^3 in 60 days. Thus, the total annual seepage loss from Tandula canal system in the UKC is calculated to be 785040 m^3 per annum (60 days operational period).

5.4.2. Mahanadi main canal system

The seepage loss from Mahanadi main canal is calculated to be 14750 m^3 per day (distributaries + minors = 4900 m^3 / day and main canal system = 9850 m^3 / day). Thus, the total seepage loss is estimated to be 885000 m^3 per annum (60 days operational period).

5.4.3 Mandhar branch system

The total seepage loss from Mandhar branch in the UKC is calculated to be: 23600 m^3 per day (distributaries + minors = 15700 m^3 / day and main Mandhar branch = 7900 m^3 / day). Thus, a total seepage loss is estimated to be 1416000 m^3 per annum (60 days operational period).

5.4.4. Mahanadi feeder canal system

The total seepage loss from Mahanadi feeder canal in the UKC is calculated to be 10440 m^3 per day (distributaries = 3200 m^3 / day, minors = 1130 m^3 / day and Mahanadi feeder canal main branch = 6110 m^3 / day). Thus, a total seepage loss is estimated to be 626400 m^3 per annum (60 days operational period).

5.4.5. Total seepage loss from the whole canal network in Upper Kharun Catchment

Considering the above seepage losses, the total seepage loss in the UKC is estimated to be 3712440 m^3 per annum (60 days operational period).

Only the main feeder canal and Tandula main canal is operational over the whole year to supply water to the Bhilai steel plant. However, the seepage loss is comparatively low as compared to the whole canal system; hence this is not considered in the present study.

5.5 Decadal year time series analysis of canal and groundwater supply for irrigation in UKC

A detailed analysis of irrigation water supply from canal and groundwater at village level for the UKC was performed. Only those villages or the parts of villages inside the UKC were digitized in ArcGIS 10.1 and considered for irrigation water supply. Later, the village-wise irrigated areas were summed up to block level for all the three decadal years (1991, 2001 and 2011) (Tables 5.3, 5.4, 5.5, 5.6 and 5.7).

The decadal years 1991, 2001 and 2011 were selected because of data availability for these years. The census book report records the annual land-use and irrigated area at village level. For 2011, the report was under preparation, so the information was collected from the different regional agricultural offices in the UKC (see also section 4.2).

Time series remote sensing satellite images and decadal census book reports (1991, 2001 and 2011) were used to extract the information on irrigated areas (Section 4.2.7).

At the UKC boundary, the part of village areas that lies in the UKC is considered during the data analysis and report preparation. Village boundaries were digitized in ARC GIS 10.1.

Table 5.2 Total area of UKC at block and district level

S.N.	District	Block/Taluk	Area in UKC (km^2)	Area in UKC (km^2) at district level
1	Raipur	Abhanpur	233.8	420.2
2	Raipur	Dharsiwa	186.4	
3	Durg	Balod	45.6	1511.2
4	Durg	Berla	12.9	
5	Durg	Dhamdha	129.8	
6	Durg	Durg	30.7	
7	Durg	Gunderdehi	80.8	
8	Durg	Gurur	469.5	
9	Durg	Patan	741.9	
10	Dhamtari	Dhamtari	253.6	554.2
11	Dhamtari	Kurud	300.6	
Total area of UKC			**2485.6**	**2485.6**

5.5.1. Analysis of irrigation water supply from surface water in the UKC in decadal years 1991, 2001 and 2011

Village-wise irrigation statistics for the decadal years 1991, 2001 and 2011 were analyzed. The number of villages irrigated from canal and groundwater irrigation was reported separately per block. A threshold criterion of 35 ha for irrigation was set. Those villages which utilize more

than 35 ha for irrigation by canal water were considered as surface-water-irrigated areas (Table 5.3).

In all blocks except the Dharsiwa block, the number of villages in the command area (irrigation by canal network) increased over the years from 1991 to 2011. The largest increase is observed for Patan and Gurur blocks, where the number of villages benefitting from the canal network increased to 25 and 19, respectively (Table 5.3).

Dharsiwa/Raipur is a single block where the extent of irrigated area and canal infrastructure decreased over the years. The reason is the rapid development of urban outgrowth. Most of the irrigated area changed to urban area; Raipur the capital city of Chhattisgarh is in this block. One distributor (no. 8) from the Mandhar branch decreased considerably due to industrial and settlement growth in and around Raipur city.

Table 5.3: Number of villages in non-command area in 1991, 2001 and 2011

Block/Taluk	**Total number of villages**	**In non-command area (1991)**	**In non-command area (2001)**	**In non-command area (2011)**	**In non-command area (1991 – 2001)**	**In non-command area (2001 – 2011)**	**In non-command area (1991 – 2011)**
Abhanpur	46	4	4	3	0	1	1
Dharsiwa/Raipur	49	23	27	33	**-4**	**-6**	**-10**
Balod	20	6	1	1	5	0	5
Berla	5	5	1	0	4	1	5
Dhamdha	31	14	1	1	13	0	13
Durg	10	4	4	4	0	0	0
Gunderdehi	25	9	7	6	2	1	3
Gurur	106	36	30	17	6	13	19
Patan	157	49	33	24	16	9	25
Dhamtari	70	18	18	12	0	6	6
Kurud	80	5	2	2	3	0	3
Total	**599**	**173**	**128**	**103**	**45**	**25**	**70**

The canal irrigation infrastructure has developed over the years. However, at present 103 villages (17.2%) in the UKC have no canal infrastructure. This needs serious consideration by the policy makers to find a plausible solution to provide irrigation facilities to those villages. Figure 5.3, 5.4 and 5.5 shows the development of canal infrastructure in 1991, 2001 and 2011 respectively.

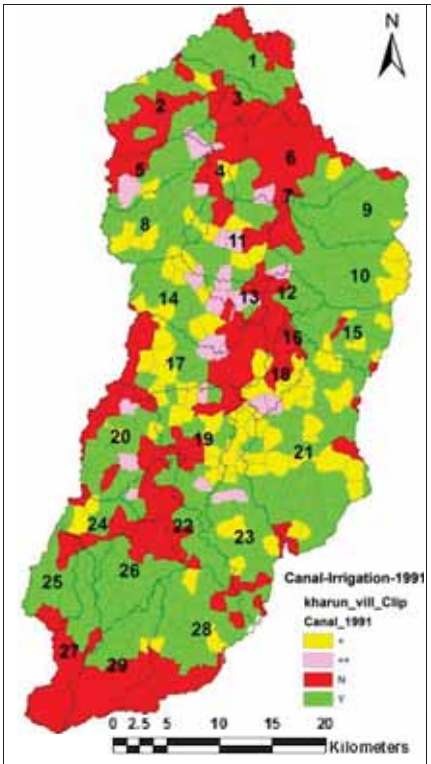

Figure 5.3: Canal-network irrigated areas in 1991

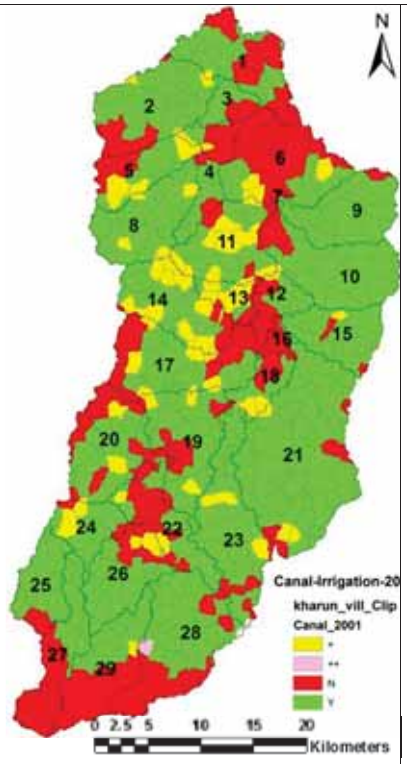

Figure 5.4: Canal-network irrigated areas in 2001

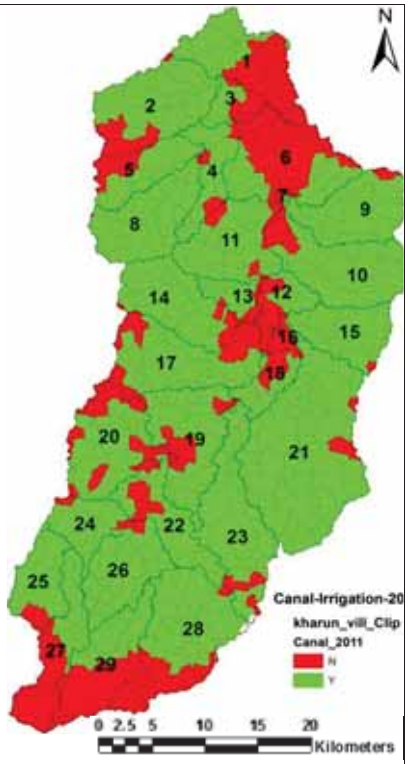

Figure 5.5: Canal-network irrigated areas in 2011

Legend:
Y: areas irrigated by canal networks
N: areas not irrigated by canal networks
+: areas under canal network construction between 2001 and 2011
++: areas under canal network construction between 1991 and 2011

5.5.2 Analysis of irrigation water supply from groundwater in the UKC in decadal years 1991, 2001 and 2011

Here again, a threshold criterion of 35 ha for irrigation was set. Those villages which utilize more than 35 ha for irrigation by groundwater resources were considered (Table 5.4).

Table 5.4: Number of villages utilizing groundwater irrigation (GWI) 1991, 2001 and 2011

Block/Taluk	Total number of villages	Villages using GWI 1991	Villages using GWI 2001	Villages using GWI 2011	Villages using GWI 1991 - 2001	Villages using GWI 2001 - 2011	Villages using GWI 1991 - 2011
Abhanpur	46	3	9	12	6	3	9
Dharsiwa/ Raipur	49	2	8	14	6	6	12
Balod	20	2	2	6	0	4	4
Berla	5	0	0	1	0	1	1
Dhamdha	31	1	12	24	11	12	23
Durg	10	0	0	2	0	2	2
Gunderdehi	25	1	4	6	3	2	5
Gurur	106	25	37	53	12	16	28
Patan	157	12	26	56	14	30	44
Dhamtari	70	11	29	36	18	7	25
Kurud	80	15	32	42	17	10	27
Total	**599**	**72**	**159**	**252**	**87**	**93**	**180**

In all blocks, the number of villages utilizing groundwater sources for irrigation increased significantly. The reason might be better electricity facilities, subsidies on electricity, and the improved pumping devices to withdraw groundwater. A strong increase in the number of villages utilizing groundwater can be observed for Patan block, followed by Gurur, Kurud, Dhamtari and Dhamdha.

During the past two decades (1991-2011), there was an increase of 180 villages (30% of study area) withdrawing groundwater resources for irrigation in the UKC. This indicates an alarming situation, and careful management of groundwater resources is advocated to ensure sustainability of this resource. Developing future strategies on groundwater management requires information to be gained from simulation with groundwater modeling. The major input into groundwater systems and consequently into groundwater modeling is the recharge. In a later section of the study, a detailed approach using the SWAT model will provide information on spatio-temporal percolation, which is the major input to the groundwater system via recharge.

5.5.3 Cropping pattern in Upper Kharun Catchment

There are three seasons in the UKC, i.e., monsoon/spring, winter and summer. Each season is characterized by typical crops.

Monsoon season crops: The main crop grown during this period is paddy (rice). More than 90% of agricultural land during the monsoon period has been allocated to paddy cultivation over the decades. Paddy is a water-demanding crop, and the demand is met by rainfall (July – September) and supplemented by irrigation from canal networks. According to the reports of CGWB (2012) the amount of canal water applied to paddy fields during the monsoon season (September – October/November) is 300 mm.

In the UKC, the areas having sufficient groundwater availability also utilize groundwater irrigation during the monsoon period for paddy field preparation. 100-150 mm of groundwater is utilized during this period (based on field survey and interviews with local farmers). The supply of canal water is restricted to the monsoon and late monsoon season (September to November) depending on water demand and availability.

Winter season or post-monsoon season crops: Depending on the groundwater depth, a second crop may be produce in different parts of the study area. Generally, groundwater availability is better in the southern part of the UKC compared to the northern. Therefore, two or three crops are generally more common in the south of the study area.

Some parts of study area where the groundwater table is shallow and black soils are prevailing are considered for a second crop without groundwater irrigation. The less-water demanding crops (lentils, etc.) use the moisture available after the harvest of the paddy crop.

The winter crops grown are mustard, lentils, pulses, vegetables, etc. The amount of groundwater required for these crops is between 200-300 mm (based on field surveys and interviews with local farmers).

Summer crops: In the case of sufficient groundwater availability, only paddy crops are cultivated. The amount of groundwater utilized for paddy cultivation during the summer season is estimated to be 640 mm (CGWB report, 2012). Short-duration paddy crops (90 days) are generally cultivated from mid February to mid May (Figures 4.18, 4.19 and 4.20).

5.5.4. Decadal year analysis of the amount of irrigation water released for crop production in the UKC in 1991, 2001 and 2011

The amount of surface water supplied by the canal network system in the monsoon season for paddy production is 300 mm, and the amount of groundwater utilized during the summer paddy cultivation is 640 mm (CGWB, 2012).

The amount of irrigation water applied per village is calculated as hectares meters (ha m) by multiplying the irrigated area (ha per village) and the above-mentioned amount of irrigation water applied in meters. This information is summed up to block level, and the amount of surface and groundwater released/withdrawn for irrigation purposes for the year 1991, 2001 and 2011 is calculated in million cubic meters (Table 5.5 and 5.6 and 5.7).

Table 5.5: Irrigation water amounts at block level for 1991
SW = surface water; GW = groundwater and 1 ha m = 0.01 million m^3

Block/Taluk	Total annual irrigated area by SW & GW – 1991 (ha)	Irrigation by SW (Total) 1991 (ha)	Irrigation by GW (Total) 1991 (ha)	Irrigation by GW (Monsoon) 1991 (ha)	Irrigation by GW (non monsoon) 1991 (ha)	Amount of SW released in 1991 (million m^3)	Amount of GW withdrawn in 1991 (million m3)
Abhanpur	14163.1	12653.9	1509.2	781.1	728.1	38.0	6.7
Dharsiwa	4976.9	4027.2	949.6	630.3	319.3	12.1	3.8
Balod	1995.8	1638.8	357.0	178.1	179.0	4.9	1.6
Berla	29.7	16.5	13.2	6.6	6.6	0.0	0.1
Dhamdha	2608.1	2145.4	462.7	208.1	254.6	6.4	2.2
Durg	514.2	504.0	10.2	5.1	5.1	1.5	0.0
Gunderdehi	2069.7	1993.2	76.5	68.5	8.0	6.0	0.3
Gurur	24054.0	15293.9	8760.1	3823.4	4936.7	45.9	41.1
Patan	25708.1	22634.2	3073.9	1602.1	1471.8	67.9	13.6
Dhamtari	14478.6	12691.0	1787.7	423.8	1363.8	38.1	9.5
Kurud	16540.2	13952.8	2587.4	790.9	1796.5	41.9	13.2
248557.0	**107138.4**	**87550.9**	**19587.5**	**8518.0**	**11069.5**	**262.7**	**92.1**

In 1991, 43.1% of the area of the UKC was irrigated by both surface and groundwater, out of which 35.2% was irrigated by surface water whereas only 7.9% area was irrigated by groundwater. However, the percentage of area irrigated by groundwater during the monsoon was 3.4% and during the non-monsoon period it was 4.5% (Table 5.5).

Table 5.6: Irrigation water amounts at block level for 2001 (SW = surface water; GW = groundwater)

Block/Taluk	Total annual irrigated area by SW & GW – 2001 (ha)	Irrigation by SW (Total) 2001 (ha)	Irrigation by GW (Total) 2001 (ha)	Irrigation by GW (Monsoon) 2001 (ha)	Irrigation by GW (Non-Monsoon) 2001 (ha)	Amount of SW released in 2001 (million m3)	Amount of GW released in 2001 (million m3)
Abhanpur	17210.1	13793.3	3416.8	1750.5	1666.3	41.4	15.2
Dharsiwa	5690.5	3692.5	1998.0	1146.0	852.0	11.1	8.6
Balod	3273.2	2506.8	766.4	381.3	385.1	7.5	3.5
Berla	94.7	60.9	33.8	16.9	16.9	0.2	0.2
Dhamdha	5740.4	4233.0	1507.4	673.9	833.5	12.7	7.0
Durg	577.1	540.5	36.6	28.0	8.6	1.6	0.1
Gunderdehi	3189.1	2461.2	727.9	404.3	323.6	7.4	3.2
Gurur	29224.7	16431.7	12793.0	5229.0	7564.0	49.3	61.1
Patan	37465.6	29862.4	7603.2	3693.6	3909.6	89.6	34.5
Dhamtari	22590.4	15247.8	7342.6	1216.4	6126.2	45.7	40.4
Kurud	26941.8	20079.7	6862.1	1721.8	5140.3	60.2	36.0
248557.0	**151997.6**	**108909.8**	**43087.8**	**16261.7**	**26826.1**	**326.7**	**209.7**

In 2001, 61.1% of the UKC was irrigated by both surface and groundwater sources; 43.8% of area was irrigated by surface water whereas 17.3% area was irrigated by groundwater. The percentage of area irrigated by groundwater during the monsoon was 6.5%, whereas the share of area irrigated by groundwater in the non-monsoon period amounted to 10.8% (Table 5.6).

Table 5.7: Irrigation water amounts at block level for 2011 (SW = surface water; GW = groundwater)

Block/Taluk	Total annual irrigated area by (SW & GW) – 2011 (ha)	Irrigation by SW (Total) 2011 (ha)	Irrigation by GW (Total) 2011 (ha)	Irrigation by GW (Monsoon) 2011 (ha)	Irrigation by GW (Non Monsoon) 2011	Amount of SW released in 2011 (million m3)	Amount of GW released in 2011 (million m3)
Abhanpur	19841	14656	5184	2668	2516	44	23.1
Dharsiwa	5911.1	3185.2	2726	1538.3	1187.7	9.6	11.7
Balod	3833.5	2528.4	1305.1	574.3	730.8	7.6	6.1
Berla	461.3	420.3	41	18.5	22.5	1.3	0.2
Dhamdha	8105.9	4609.5	3496.4	1608	1888.4	13.8	16.2
Durg	766.1	654.1	112	56	56	2	0.5
Gunderdehi	4293.1	2968.9	1324.2	675.9	648.3	8.9	5.9
Gurur	38346.5	19855.7	18490.8	6991	11499.8	59.6	90
Patan	50338.3	36420	13918.3	6789	7129.4	109.3	63.1
Dhamtari	31395.5	17263.8	14131.7	2283.1	11848.7	51.8	77.9
Kurud	34398.5	20977	13421.6	2656.1	10765.5	62.9	72.6
248557.0	**197690.4**	**123539.1**	**74151.5**	**25858.5**	**48293.3**	**370.8**	**367.3**

In 2011, 79.5% of total geographical area of the UKC was irrigated by both surface and groundwater sources; 49.7% of area was fed by surface water whereas 29.8% was irrigated by groundwater. The share of area irrigated by groundwater in the monsoon was 10.4% whereas 19.4% of the area was irrigated by groundwater in the non-monsoon period (Table 5.7).

Table 5.8: Surface water irrigation at block level and comparison between the years 1991, 2001 and 2011 (SW = surface water)

Block/Taluk	Total Area (ha)	% of area irrigated by SW (Total) 1991	% of area irrigated by SW (Total) 2001	% of area irrigated by SW (Total) 2011	% Increase in SW irrigation (1991-2001)	% Increase in SW irrigation (2001-2011)	% Increase in SW irrigation (1991-2011)
Abhanpur	23378.0	54.1	59.0	62.7	4.9	3.7	8.6
Dharsiwa	18638.0	21.6	19.8	17.1	-1.8	-2.7	-4.5
Balod	4557.0	36.0	55.0	55.5	19.0	0.5	19.5
Berla	1290.0	1.3	4.7	32.6	3.4	27.9	31.3
Dhamdha	12977.0	16.5	32.6	35.5	16.1	2.9	19.0
Durg	3074.0	16.4	17.6	21.3	1.2	3.7	4.9
Gunderdehi	8084.0	24.7	30.4	36.7	5.8	6.3	12.1
Gurur	46950.0	32.6	35.0	42.3	2.4	7.3	9.7
Patan	74191.0	30.5	40.3	49.1	9.7	8.8	18.6
Dhamtari	25359.0	50.0	60.1	68.1	10.1	7.9	18.0
Kurud	30059.0	46.4	66.8	69.8	20.4	3.0	23.4
	248557.0	**35.2**	**43.8**	**49.7**	**8.6**	**5.9**	**14.5**

The analysis results show that the surface water irrigation area in the UKC increased over the years (Table 5.8). The canal infrastructure has been developed, and of the area under surface irrigation increased by 8.6% from 1991 to 2001 and by 5.9% from 2001 to 2011. The total increase from 1991 to 2011 was 14.5%.

At present, almost 50 % of the area of the UKC benefits from canal irrigation. There might be potential for further expansion of canal infrastructure in the region.

Table 5.9: Groundwater irrigation at block level and comparison between the years 1991, 2001 and 2011 (GW = groundwater)

Block/Taluk	Total area (hectares)	% of area irrigated by GW (Total) 1991	% of area irrigated by GW (Total) 2001	% of area irrigated by GW (Total) 2011	% Increase in GW irrigation (1991-2001)	% Increase in GW irrigation (2001-2011)	% Increase in GW irrigation (1991-2011)
Abhanpur	23378.0	6.5	14.6	22.2	8.2	7.6	15.7
Dharsiwa	18638.0	5.1	10.7	14.6	5.6	3.9	9.5
Balod	4557.0	7.8	16.8	28.6	9.0	11.8	20.8
Berla	1290.0	1.0	2.6	3.2	1.6	0.6	2.2
Dhamdha	12977.0	3.6	11.6	26.9	8.1	15.3	23.4
Durg	3074.0	0.3	1.2	3.6	0.9	2.5	3.3
Gunderdehi	8084.0	0.9	9.0	16.4	8.1	7.4	15.4
Gurur	46950.0	18.7	27.2	39.4	8.6	12.1	20.7
Patan	74191.0	4.1	10.2	18.8	6.1	8.5	14.6
Dhamtari	25359.0	7.0	29.0	55.7	21.9	26.8	48.7
Kurud	30059.0	8.6	22.8	44.7	14.2	21.8	36.0
	248557.0	**7.9**	**17.3**	**29.8**	**9.5**	**12.5**	**22.0**

Groundwater irrigation area in the UKC is increased over the years. Besides pressure towards higher agricultural production driven by population growth, the improved irrigation and electricity facilities and the modern pumping devices might be reasons for such expansion. It can be observed that the area under groundwater irrigation increased by 9.5% from 1991 to 2001 and by 12.5% from 2001 to 2011, while it increased by 22.0% between 1991 and 2011 (Table 5.9).

There was a major increase in the groundwater irrigation area for Dhamtari block, followed by Kurud, Dhamdha and Gurur. At present, almost 30% of the area of the UKC relies on groundwater irrigation. Especially the increasing trend of groundwater use creates the need to study the sustainable management of the groundwater resources in the area.

Table 5.10: Total irrigation statistics of surface and groundwater at block level and comparison between the decadal years 1991, 2001 and 2011 (SW = surface water; GW = groundwater)

Block/Taluk	Total area (ha)	% irrigated area by SW + GW (Total) 1991	% irrigated area by SW + GW (Total) 2001	% irrigated area by SW + GW (Total) 2011	% increase in SW + GW irrigated area (1991-2001)	% increase in SW + GW irrigated area (2001-2011)	% increase in SW + GW irrigated area (1991-2011)
Abhanpur	23378.0	60.6	73.6	84.9	13.0	11.3	24.3
Dharsiwa	18638.0	26.7	30.5	31.7	3.8	1.2	5.0
Balod	4557.0	43.8	71.8	84.1	28.0	12.3	40.3
Berla	1290.0	2.3	7.3	35.8	5.0	28.4	33.5
Dhamdha	12977.0	20.1	44.2	62.5	24.1	18.2	42.4
Durg	3074.0	16.7	18.8	24.9	2.0	6.1	8.2
Gunderdehi	8084.0	25.6	39.4	53.1	13.8	13.7	27.5
Gurur	46950.0	51.2	62.2	81.7	11.0	19.4	30.4
Patan	74191.0	34.7	50.5	67.8	15.8	17.4	33.2
Dhamtari	25359.0	57.1	89.1	123.8	32.0	34.7	66.7
Kurud	30059.0	55.0	89.6	114.4	34.6	24.8	59.4
	248557.0	**43.1**	**61.2**	**79.5**	**18.0**	**18.4**	**36.4**

The analysis results reveal an increasing trend of the total irrigated area in the UKC from 1991 to 2011 (Table 5.10). The area under both surface and groundwater irrigation increased by 18.0% from 1991 to 2001, by 18.4% from 2001 to 2011 and by 36.4% from 1991 to 2011(Figure 5.7). There was a major increase in the total irrigation area (both surface and groundwater) for Dhamtari block, followed by Kurud, Dhamdha, Patan and Gurur.

5.5.5. Analysis of extensive groundwater irrigating villages in the UKC

In 2011, the villages withdrawing extensive groundwater resources for irrigation were determined, i.e., those villages irrigating more than 75 ha with groundwater (Figure 5.6). A total of 216 villages were determined. This information is useful to locate the 'hotspot' areas of excessive groundwater extraction. A water balance analysis of groundwater recharge and withdrawal needs to be done spatially for the hotspot areas. Such information would be useful for decision makers and government officials to frame strategies for sustainable management of water resources in the UKC.

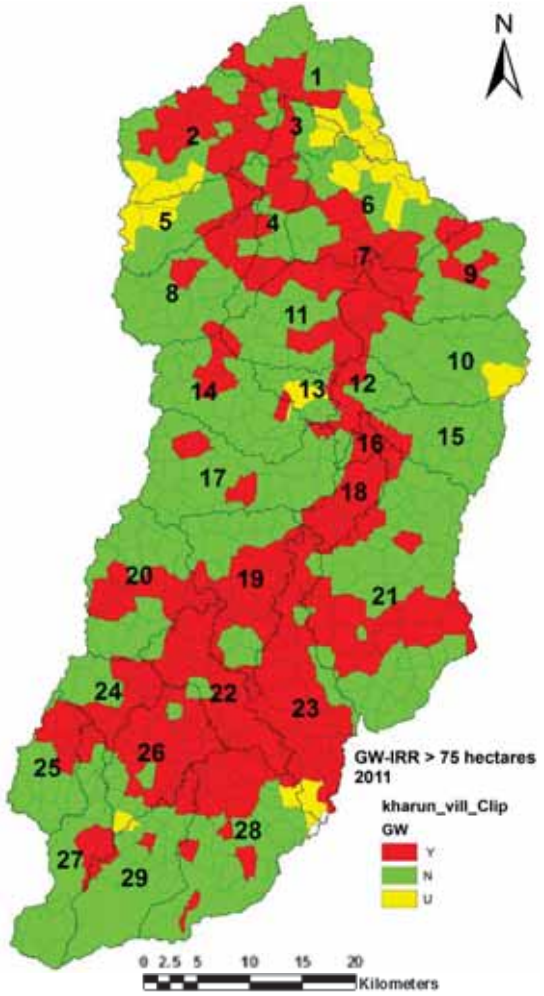

Figure 5.6: Villages irrigating more than 75 ha with groundwater in 2011

Legend:
Y: Villages with more than 75 ha irrigation by groundwater
N: Villages with less than 75 ha irrigation by groundwater
U: Urban areas with no groundwater irrigation

5.5.6. Irrigated and non-irrigated areas in the UKC in 2011

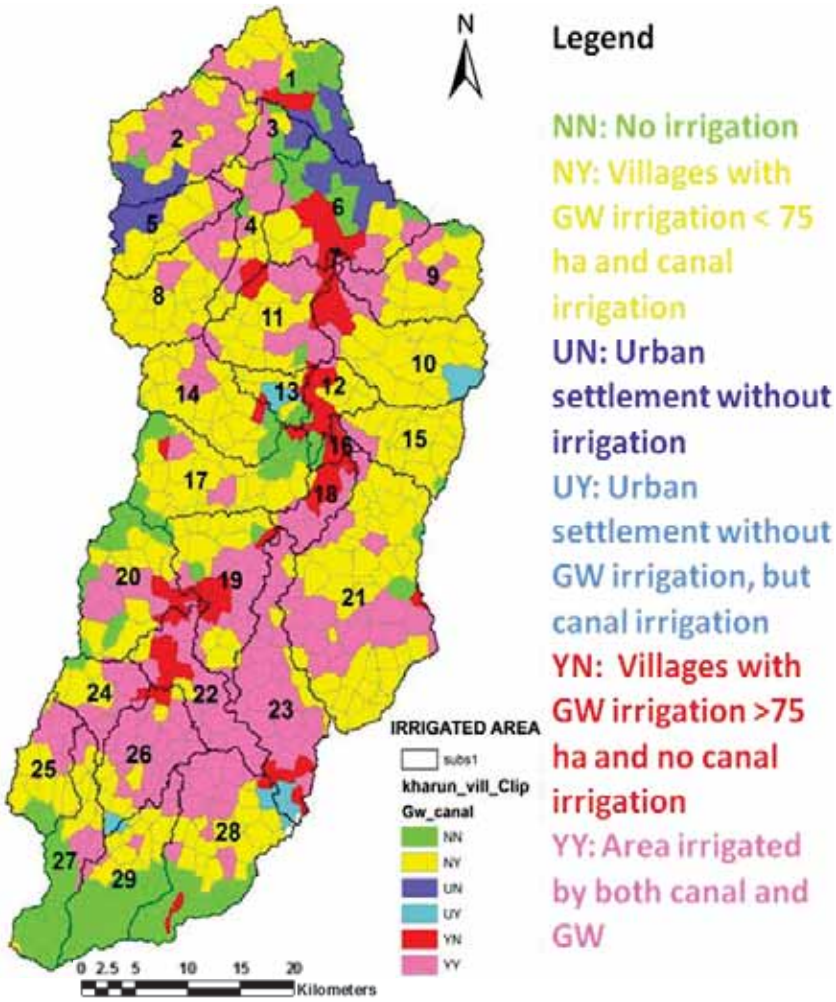

Figure 5.7: Irrigated and non-irrigated areas (all water sources) in 2011

In 2011, the area irrigated by canal and/or groundwater and non-irrigated areas in the UKC is shown in Figure 5.7.

NY: These areas receive canal irrigation water that comes from outside the UKC and use less groundwater for irrigation. They thus receive groundwater recharge other than rainfall.

YN: These are the hotpot areas where groundwater withdrawal is high (irrigation area more than 75 ha per village) and there is no canal irrigation. They do not receive additional recharge from canal irrigation. Thus, these hotspots areas should be examined in terms of sustainable management of groundwater resources.

CHAPTER 6: SWAT MODEL SETUP, CALIBRATION AND VALIDATION

6.1 Introduction

The Soil and Water Assessment Tool (SWAT) model 2012 was used for hydrological modeling and impact analysis of climate change and land-use change on the water resources of the Upper Kharun Catchment (UKC). Input data was prepared according to the SWAT manual 2012 (Arnold, 2012). The model was set up for three time steps representing the three decades 1990s, 2000s and 2010s. The relevant management practices (crop rotation and irrigation) and land-use maps (1991, 2001 and 2011) of the representative decades were considered during the model setup.

SWAT CUP 2012 was applied for sensitivity analysis of hydrological parameters, uncertainty analysis, calibration and validation of the SWAT model. Global sensitivity analysis was used to identify the relative sensitivities of the hydrological parameters for the model discharge. The SUFI 2 program was employed for model uncertainty analysis, calibration and validation.

Observed discharge at the UKC outlet was used for calibration. Five iterations with 1000 simulations each (5000 simulations) were performed separately for the three model runs. After each iteration, the new suggested parameter ranges were used as the initial parameter range for the next iteration, and finally after the fifth iteration the model was found to be reasonably calibrated. The model was further validated using the final calibrated parameter ranges and single iteration of 500 simulations.

The calibrated and validated model was used to analyse the impacts of climate and land-use change in terms of the water balance components namely discharge, percolation (groundwater recharge), surface runoff, groundwater contribution to streamflow, water yield and actual evapotranspiration.

6.2 Hydrological models

Management of water resources and the need for models

The management of water resources basically consists of conceiving strategies and designing infrastructure to coordinate water uses/users taking water availability and the impact on water and linked resources into account.

Conceiving strategies and infrastructure and assessing the impact requires an understanding and quantification of water/matter fluxes and balances under the influence of the alternative conceptions for strategies/infrastructure. Considering alternative conceptions needs simulations based on modeling approaches, analyzing monitored data is required, but alone not sufficient, because these data sets obviously do not include the effect of planned strategies and infrastructure. A further task necessitating the application of models is the estimation of the impacts on water fluxes and balances caused by future trends of influential factors (e.g., impact

of changing rainfall patterns under the influence of climate change on future water balances and effect of land-use change on water fluxes). Especially while taking the lifetime of water management infrastructure to be conceived into account; it is important to consider the impact of future trends on the design situation as far as possible.

However, all modeling approaches need data input gained from monitoring, and it is advantageous to support the modeling of future scenarios by understanding gained from analyzing processes in the past.

The literature reviews presented in the following concentrates on modeling approaches which are appropriate to detect the impacts of climate and land-use changes on the water fluxes and balances in the UKC and contribute thereby to support water management in this catchment.

SWAT in the context of hydrological models

Models can be used to represent the real world processes and their interaction. The natural system can be either represented by physical or mathematical models. A physical model represents all the processes occurring in a system directly, whereas a mathematical model simulates the real situation indirectly by means of relevant equations and algorithms that depict the relevant physical processes occurring in the system. Hydrological models represent the processes in the hydrological system in order to quantify water fluxes and balances covering the hydrological cycle or part of it.

Hydrological models can be grouped into deterministic and stochastic types (Abbott and Refsgaard, 1996). Deterministic models explain the cause and effect relations and are based on physical principles like conservation of energy, mass and momentum (Konikow and Reilly, 1998). However, stochastic models may also consider the physical processes, but because of uncertainty in input variables, the possible outcome from stochastic models also contains a certain degree of randomness and uncertainty (Beven, 2001).

Deterministic hydrological models are further grouped into lumped conceptual models and distributed physical models. Lumped models cannot consider the spatial variability, and treat the entire watershed as a single unit where the parameters and variables represent a single average value for the entire watershed (Abbott and Refsgaard, 1996). In contrast, distributed hydrological models estimate the water flow directly from the governing partial differential equations and consider the spatial as well as temporal behavior of the variables in the model and hence come closer to reality (Konikow and Reilly, 1998).

Surface water models are used to simulate the surface water fluxes at different scales and also to simulate the impact of climate change and land-use change on the surface water hydrology. For that purpose, these models need to be linked with or need to use the output of stochastic models (e.g., analysis of the relationship between magnitude of rainfall and respective probability with stochastic models, and using this information as an input to (deterministic)

surface hydrology models to estimate probability of discharges; this has a rather high degree of uncertainty.

A number of surface water models have been developed and employed for the purpose of investigating the impacts of land-use / land cover change and climate change on the available water resources. These hydrological models have proved to be useful, as they can analyze past as well as future impacts. For instance, MIKE-SHE (e.g., Refsgaard and Storm 1995; Im et al., 2009) HBV (Bergström and Forsman, 1973), SWAT (Arnold et al., 1998; Fohrer et al., 2001), or WaSiM-ETH (Schulla, 1997; Niehoff et al., 2002).

The Soil and Water Assessment Tool (SWAT) was selected for the current study. The characteristics of SWAT that provide the arguments to choose this model for the research are described in the following sections.

SWAT is a physically based, semi-distributed hydrological model, which is quite flexible and can be integrated with GIS. It is capable of running on a daily time step, and effectively stimulates hydrological processes and water balance components of small catchments to large river basins (Arnold et al., 1998). It is freely available and has a strong network support.

Basically, hydrological models face three challenges namely, deficient data, spatial heterogeneity of catchment characteristics, and the complex issues present in natural system. However, because of the semi-distributed nature of SWAT, it is able to handle all the mentioned challenges well (Gassman et al., 2007). As a consequence of its advantages compared to other models, SWAT achieves a high level of recognition all around the world. At present, there are over 1000 articles available based on this model (Douglas et al., 2010).

Some of the studies include Ndomba et al. (2008); Stehr et al. (2008); Bosch et al. (2005); Qiu and Prato, 2001; Santhi et al. (2001); Van Liew and Garbrecht, 2001; Fontaine et al. (2001); Spruill et al. (2000); Chu and Shirmohammadi, 2004; Singh et al. (2005); Rosenthal et al. (1995); Rosenthal and Hoffman, 1999; Pohlert et al. (2005 and 2006).

Based on various literature reviews, it was found that SWAT is quite efficient in simulating the impact of climate change and land-use changes on surface-water resources in different parts of the world and the respective environmental conditions.

According to Gassman et al. (2007), SWAT is known for its worldwide multi-objective applications including analyses on the impacts of land-use and climate changes. It is considered to be a versatile model that is flexible enough to integrate multiple environmental processes and effectively handle the watershed management practices and provide the informational base for sound policy decisions.

World-wide examples of studies on climate change impacts on water resources using SWAT

A number of studies have been done so far using SWAT for simulating the impact of climate change on the hydrology of complex watersheds at basin scale over a long period of time. Some examples are: Impacts of climate change on groundwater recharge and streamflow in a central European low mountain range (Eckhardt et al., 2003), climate change impact on SWAT simulated streamflow in western Kenya (Githui et al., 2009), hydrologic responses to climate change from forested watershed in Mississippi (Parajuli, 2010), impact on water yield in upper Wind river basin (Stonefelt et al., 2000), streamflow response to climate change (Xu et al., 2009), Hondu River of Kenya (Jayakrishnan et al. 2005). Verbeeten et al. (2007) conducted research in a semi-arid region of West Africa and concluded that SWAT is an effective tool for evaluation of impacts of climate change on the water balance.

Studies on climate change impacts on water resources using SWAT in India

Lakshmanan et al. (2009) in their study for Bhavani basin of India concluded that the SWAT model can be employed as a decision tool for developing adaption strategies to sustain rice production under different climate change and management scenarios. Gosain et al. (2006) used SWAT to study the climate change impact on the hydrology of Indian River basins. Dhar et al. (2009) applied the model to study the impacts of climate change under the threat of global warming for an agricultural watershed of the Kangsabati River. A study on climate change response in Krishna Basin using SWAT was carried by Kulkarni et al. (2014).

World-wide examples for studies on land-use change impacts on water resources using SWAT

SWAT has been widely used in every corner of the world to investigate the potential impact of land-use changes on water resources. Some of the work includes impacts of land-use change on different watersheds of Ethiopia (Tadele et al., 2007; Fohrer et al., 2001), impacts in the Heihe River basin in China (Nian et al., 2014), and in a watershed in eastern Africa (Baker et al., 2013). The model was used for studying the impacts of land-use changes on the hydrology of Zanjanrood basin, northwest Iran (Ghaffari et al., 2010).

SWAT predictions have been found to be acceptable for evaluating the impacts of land management practices on the hydrology of complex watersheds with different scales over long periods of time (Neitsch et al. 2001; Santhi et al. 2001).

A study related to Indian scenarios is an assessment of land-use change impacts on the water resources of the Mula and Mutha rivers catchment upstream of Pune, India by Wagner et al. (2013).

6.3 Soil Water Assessment Tool (SWAT)

The Soil and Water Assessment Tool (SWAT) was developed by Jeff Arnold (1998) for the Agricultural Research Service (ARS), United States Department of Agriculture (USDA). It is a physical, time-continuous and a river-basin or watershed-scale distributed hydrological model, which was developed to simulate the impact of land management practices on rainfall-runoff processes with varying soil, land-use and management practices over a long period of time. It is freely available software with strong user support.

SWAT consists of the following main components: Weather, surface runoff, return flow, percolation, evapotranspiration, transmission losses, pond and reservoir storage, crop growth and irrigation, groundwater flow, reach routing, nutrient and pesticide loading, and water transfer.

SWAT is considered as a watershed hydrological transport model. The quantification of the hydrologic cycle in SWAT is based on the water balance equation:

$$SWt = SW0 + \sum_{i=1}^{t} (\text{Rday} - \text{Qsurf} - \text{Ea} - \text{Wseep} - \text{Qgw}) \quad (6.1)$$

where SWt = final soil water content (mm), SW0 = initial soil water content on day i (mm), Rday = amount of precipitation on day i (mm), Qsurf = amount of surface runoff on day i (mm), Ea = amount of evapotranspiration on day i (mm), Wseep= amount of water entering the vadose zone from the soil profile on day i (mm), Qgw = amount of return flow on day i (mm).

The basic principle behind SWAT modeling is to partition a watershed into a number of sub-units using a two-step approach. First, a topographic discretization is performed by dividing the watershed into a number of sub-catchments or sub-basins that will serve as the basis of determining the routing structure of water and pollutants through the watershed. These partitioned sub-basins are beneficial for simulation when the watershed has different land-use or soil properties that might impact the hydrology differently. In the second step, the input information for each sub-basin is grouped or organized into the following categories: climate, hydrological response units (HRUs), ponds/wetlands, groundwater and the main channel or reach draining the sub-basin. HRUs are obtained by overlaying the soil and land-use maps and slope, and are the lumped areas within the sub-basin that are comprised of a unique combination of land cover, soil type, slope and management practices.

6.4 Materials and methods

The SWAT model was selected to study the impact of climate change and land-use change on water resources (surface runoff, evapotranspiration and groundwater recharge) of the UKC.

As described in Chapter 3, climate change trend detection analysis and PRECIS climate change scenarios were bias corrected using the simple mean monthly average technique (2011-2098). The impact analysis of bias-corrected climate change scenarios is presented below.

Satellite imageries, remote sensing techniques, field surveys and census book reports were used to prepare the land-use maps of 1991, 2001 and 2011. Expert interviews, government policies, trends derived from past land-use changes, and future urban and agricultural expansion information were employed to generate the potential land-use change map for the year 2021 (see Chapter 4 and 5). The impact analysis of land-use change is discussed below.

6.4.1 SWAT basic data requirements

Digital Elevation Model (DEM): This provides the elevation / contour information in grid format, and is used for delineation of basin boundaries, streamflow network, reaches and sub-catchments. The latest updated version 4.0 of SRTM DEM with 90-m resolution is used in the current study. It was downloaded from CGIAR consortium for spatial information (CGIAR-CSI) website (http://srtm.csi.cgiar.org/). The elevation difference in the UKC is only 192 m from south to north (Figure 2.5).

Land-use maps: Land-use maps are used for HRU delineation in SWAT. Maps were prepared for four different time steps and representing the decadal years 1991, 2001, 2011 and 2021. LANDSAT satellite imageries of the same time periods were used. The spatial resolution of the land-use maps is 30 m. (see Chapter 4.0).

Soil map: A detailed soil map with 64 soil attribute types was prepared at 1:50,000 scale. Field surveys, reports of soil survey departments and previous soil maps were analyzed and the desired and missing soil physical properties required for running SWAT model were estimated using Soil Par 2.0 software. The major soil types are Alfisols (loam also known as Dorsa), Vertisols (clay also known as Kanhar), Entisols (sandy loam also known as Bhata) and Inceptisols (sandy clay loam also known as Matasi) (Section 2.3 and Figures 2.7 and 2.8).

Climate data: The climate parameters required to run SWAT are rainfall (mm), maximum temperature (°C), minimum temperature (°C), relative humidity (%), wind speed (km/h), evapotranspiration (mm) and sunshine (hr) at daily time steps.

Daily rainfall measurements from 14 rainfall stations covering the entire study area were obtained from the State Data Centre, Department of Water Resources, Raipur, Council of Science and technology, Raipur and Indian Meteorological Department, Pune. The locations of the stations are shown in Figure 3.1 and Thiessen-polygons representing the covered areas are depicted in Figure 3.2. Other climate parameters were collected from Raipur Agriculture University, meteorological station, Raipur (Figure 3.3).

The daily climate parameters from 1990 – 2008 were fed into the SWAT model as weather input data. The data were prepared in text format as given in the SWAT 2012 user manual.

Crop rotation: In the UKC, there are three different crop growing seasons. Depending on the water availability, farmers produce one to three crops in a year. The information about crop

rotation and types of crops grown was collected from the census books 1991 and 2001. Information on the year 2011 was gathered from field visits and block agriculture offices (Chapter 5). This information was fed into SWAT by editing the management files of the HRU.

Irrigation: Irrigation water in the UKC is supplied by a well developed network of canal systems and groundwater sources (Chapter 5). Detailed information on the amount of irrigation water supplied by different sources was prepared and fed as an input into the SWAT model by writing the HRU management file. The pothole functionality of SWAT 2012 was applied and examined for rice irrigation.

Discharge: The daily gauge – discharge data from 1990 to 2010 were obtained from the Central Water Commission, Bhubaneswar, Orissa. The discharge data were used for model calibration and validation. The availability of discharge data from 1990 onwards is the reason for starting the first SWAT model run from 1990.

The detailed methodology of the SWAT model setup is presented in Figure 6.0.

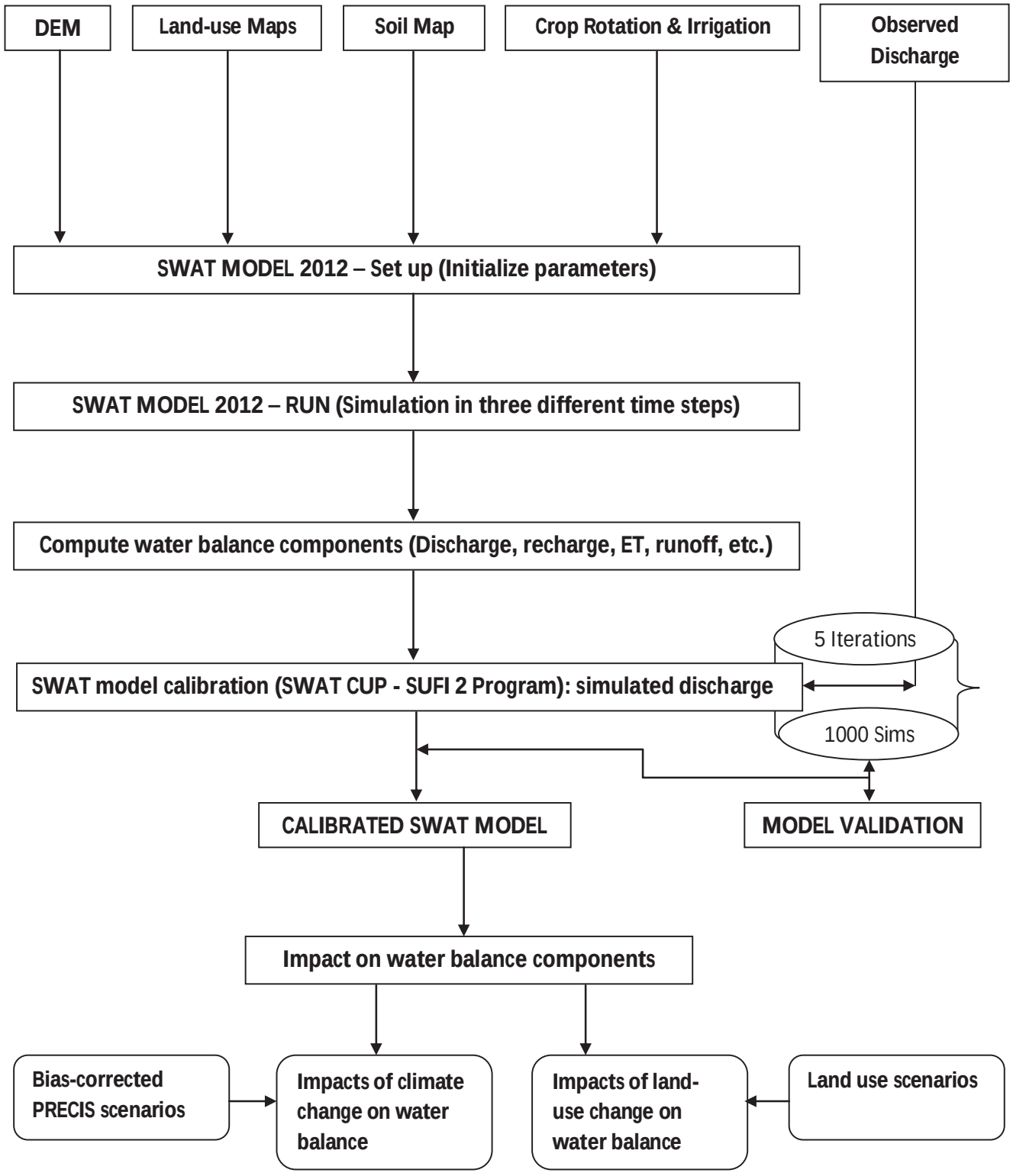

Figure 6.0: Flow diagram of SWAT setup for UKC

6.4.2 SWAT model setup for Upper Kharun Catchment

The SWAT model was initiated by feeding the input data into the model and followed a stepwise procedure (Figure 6.1).

Step 1: The UKC boundary was delineated based on the SRTM DEM (90-m resolution) and drainage network in Arc SWAT 2012. A raster mask file was used to provide the boundary condition. The discharge river gauging station Patharidih was added as the catchment outlet. The UKC was further delineated into 29 sub-catchments, and their parameters were calculated (Figure 6.2),

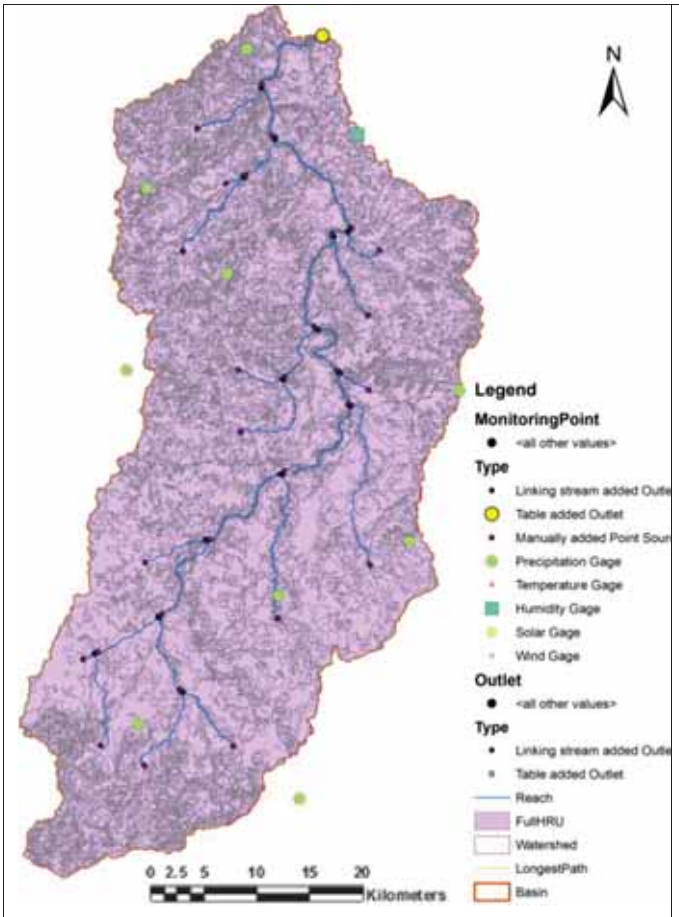

Figure 6.1: SWAT-delineated catchment, reach and HRUs with the input data locations

Figure 6.2: SWAT-delineated sub-catchments for UKC

Step 2: HRU analysis: The land-use map, soil map and slopes with associated attribute properties were used as input, and HRU definition was set in the model. Based on the overlay of these inputs, 2978 HRUs were generated with the 1991 land-use map, 3605 HRUs with the 2001 map, and 3468 HRUs with the 2011 map.

Step 3: Meteorological data were loaded as input with the help of the weather input interface.

Step 4: Management files were written for annual irrigation and crop rotation using the edit management input files option.

Step 5: The SWAT input files were built, and finally the model was set for run, sensitivity analysis, calibration, validation and impact assessment study.

6.5 Model sensitivity analysis

SWAT CUP 2012 software was used for SWAT model sensitivity analysis, calibration and validation. This software has been applied in a number of studies and is gaining popularity worldwide. Its advantageous features are a user-friendly interface, linkage with the Arc SWAT model run results, simplicity regarding execution, and semi-automated process for the selection of best basin parameter ranges.

Prior to model calibration, a sensitivity analysis was performed for the selection of the most sensitive hydrological parameters for discharge generation in the UKC. Global sensitivity analysis was used for the current study.

Global sensitivity analysis

The global sensitivity analysis for the UKC was performed in SWAT CUP 2012. This program is used to judge the relative sensitivity of the parameters with respect to basin hydrology.

A multiple regression analysis was made between the objective function values (defined in file goal.sf2) and Latin hypercube-generated parameters.

A t-test is used to identify the relative significance of each parameter compared to others on the basin hydrology. A t-stat summary provides a measure of relative sensitivities of the parameters. Larger absolute values indicate greater sensitivity of the given parameter.

The p-value is an indicator to judge the level of significance of the sensitivities. Smaller values indicate higher level of statistical significance for the measured sensitivity. A detailed description of global sensitivity analysis is dealt with in the SWAT CUP 2012 manual.

Fifteen hydrological parameters (curve number, groundwater delay, soil evaporation compensation factor (ESCO), plant uptake compensation factor (EPCO), channel effective hydraulic conductivity, soil available water capacity, hydraulic conductivity, surface runoff lag time, soil bulk density, soil depth, bio-mixing efficiency, groundwater revap coefficient, threshold depth of water in the shallow aquifer required for return flow to occur, deep aquifer percolation fraction and base flow alpha factor) based on expert knowledge were considered for the sensitivity analysis (Figure 6.3 and Table 6.1).

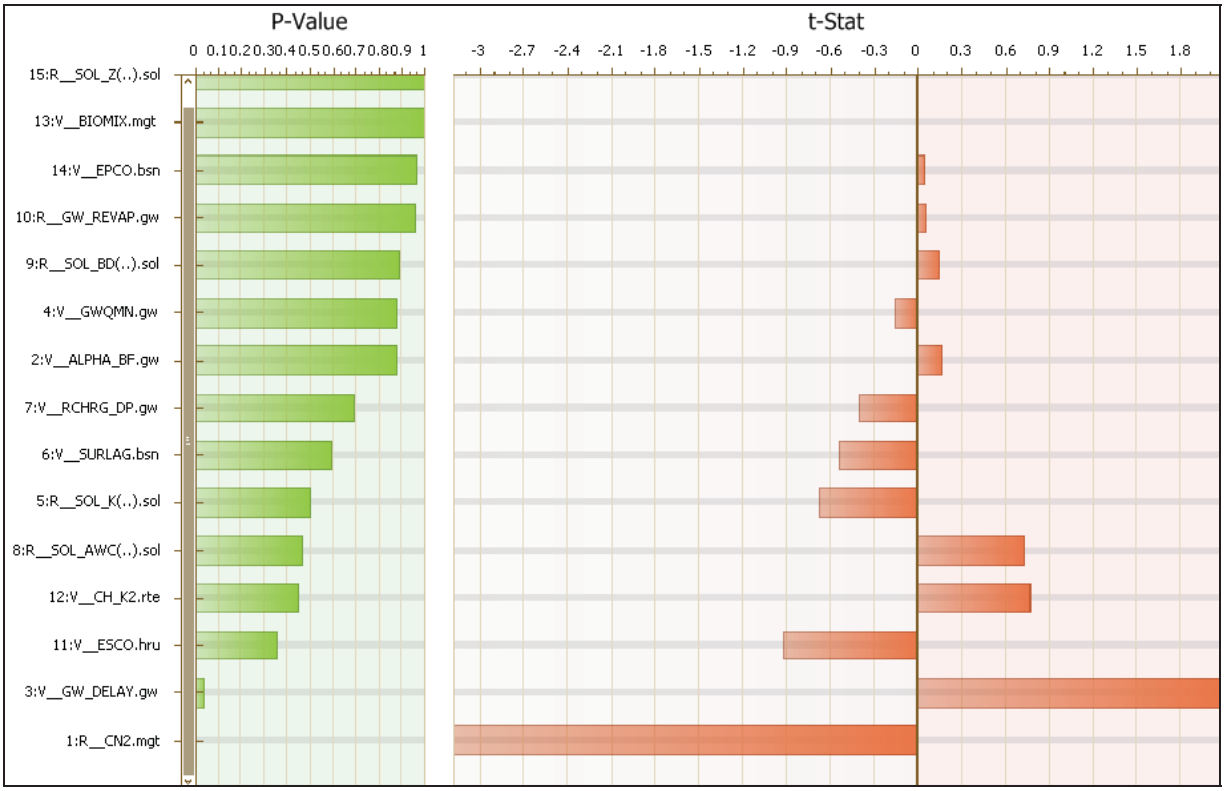

Figure 6.3: Global parameter sensitivity analysis for UKC

The curve number is the most sensitive parameter followed by groundwater delay, soil evaporation compensation factor (ESCO) and channel effective hydraulic conductivity (Figure 6.3 and Table 6.1).

Table 6.1: Global sensitivity analysis of parameters

Parameter name	**t-Stat**	**P-Value**	**Ranking**
R - SOL_Z(..).sol	0.00	1.00	**15**
V - BIOMIX.mgt	0.00	1.00	**14**
V - EPCO.bsn	0.04	0.97	**13**
R - GW_REVAP.gw	0.05	0.96	**12**
R- SOL_BD(..).sol	0.14	0.89	**11**
V- GWQMN.gw	-0.16	0.88	**10**
V- ALPHA_BF.gw	0.16	0.87	**9**

V- RCHRG_DP.gw	-0.40	0.69	**8**
V- SURLAG.bsn	-0.54	0.59	**7**
R- SOL_K(..).sol	-0.68	0.50	**6**
R- SOL_AWC(..).sol	0.73	0.47	**5**
V- CH_K2.rte	0.76	0.45	**4**
V- ESCO.hru	-0.93	0.36	**3**
V- GW_DELAY.gw	2.07	0.04	**2**
R- CN2.mgt	-3.18	0.00	**1**

6.6. Uncertainty analysis

Sequential Uncertainty Fitting version 2 (SUFI 2) of SWAT CUP 2012 was applied. The uncertainty analysis routine of SUFI 2 accounts for a wide sources of model parameter uncertainties and input measured data uncertainties. The uncertainty in model prediction is given by the 95PPU band and quantified by P-factor and R-factor.

The P-factor is the percentage of measured data bracketed by the 95% prediction uncertainty (95PPU). It is a good measure to assess the strength of an uncertainty analysis. The 95PPU is calculated at the 2.5% and 97.5% levels of the cumulative distribution of an output variable obtained through Latin hypercube sampling, and eliminates 5% of the very bad simulations. The % error in the model is given by the 1-P factor, as these are the data points not captured or accounted for by the 95PPU.

The R-factor is another measure for quantifying the strength of a model calibration/uncertainty analysis. It is the average thickness of the 95PPU band divided by the standard deviation of the measured data. With SUFI-2, the smallest possible uncertainty band for the measured data is achieved.

The P-factor theoretically lies between 0 and 100%, while the R-factor ranges between 0 and infinity. A P-factor of 1 and R-factor of zero is an ideal simulation that exactly corresponds to measured data. These factors are used to measure the strength of the uncertainty analysis and calibration of the model.

During the model calibration, one should expect the 95PPU band to get smaller at each iteration, and the P-factor and R-factor to get smaller. The P-factor should not get too small while the R-factor remains too large. Hence, often a balance between the two must be maintained. Finally, an analyst has to make the decision as to when to stop the iterations. Once

the P factor and R factor in the subsequent iterations are not changing, the point is reached where the parameter uncertainties are the desired model parameter ranges. Further, the goodness of model fit can be quantified by the R^2 and/or Nash-Sutcliff (NS) coefficient between the observations and the final "best" simulation. However, the best simulation is just one of many acceptable solutions within the 95PPU, and in such a stochastic procedure the best solution is actually the final parameter ranges.

A detailed description of SUFI 2 uncertainty analysis is provided by the SWAT CUP 2012 user manual.

6.7. Model calibration and validation

SWAT model calibration and validation performance for the UKC for different climate and land-use scenarios was assessed. Three models with different time steps (land-use, climate variables and management practices) were applied. The observed discharge values were used for model calibration and validation. This was to check the performance and acceptability of the model under different conditions for the UKC.

The first model setup was for the period between 1990 and 1993 (4 years) representing the decade 1990s. This period was further split into 2 years (1990 – 1991) for calibration and another 2 years (1992-1993) for validation. The climate variables and management operations were considered for the same periods and the land-use map of 1991 was used.

The second model was setup for the period between 1998 and 2001 (4 years) representing the decade 2000s. All relevant management practices were considered and the land-use map of 2001 was used. Calibration was based on the 1998-1999 data, and 2000–2001 data were used for validation.

The third model setup represents the decade 2010s, and was built for the period 2000–2008. The land-use map of 2010-2011 and management practices during the period were considered. The period 2000–2006 was used for calibration and 2007–2008 for validation.

The third model setup is considered as the reference model for estimating the impacts of future climate and land-use changes, because it represents the most recent land-use scenario (2010-11). The calibrated parameter values of this model were used for model setup for impact analysis of different climate and land-use change scenarios.

Model calibration and validation with different land-use and climate scenarios

SWAT was calibrated and validated with different land-use and climate data for the study area to assess its performance and acceptability for the study area under different conditions.

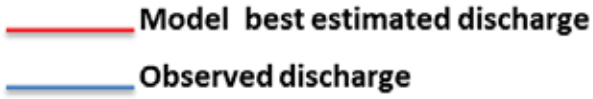

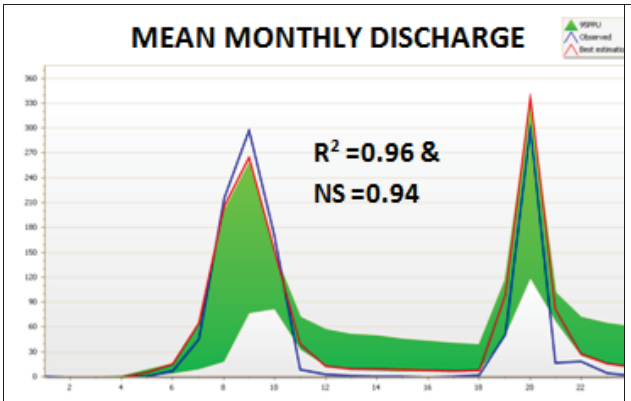

Figure 6.5: Observed versus simulated mean monthly discharge – calibration period: 1990-1991 (land-use 1991)

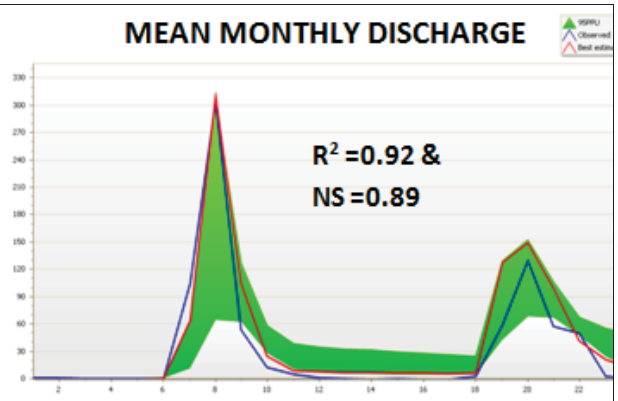

Figure 6.6: Observed versus simulated mean monthly discharge – validation period: 1992-1993 (land-use 1991)

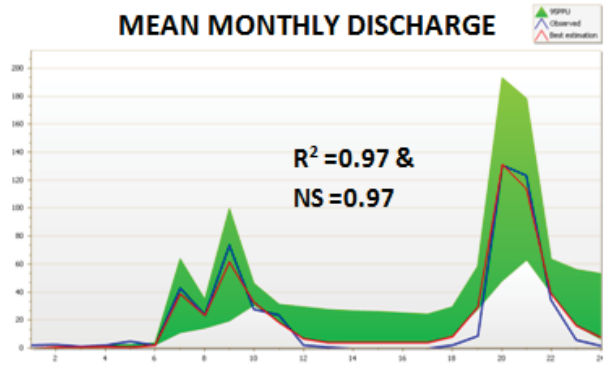

Figure 6.7: Observed versus simulated mean monthly discharge – calibration period: 1998-1999 (land-use 2001)

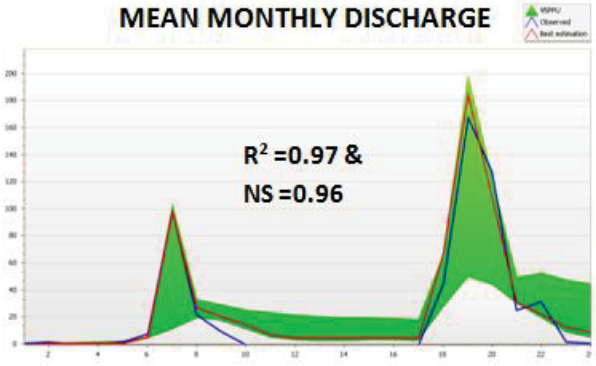

Figure 6.8: Observed versus simulated mean monthly discharge – validation period: 2000-2001 (land-use 2001)

Figures 6.5 – 6.8 show that the SWAT model is well calibrated and validated for the different time steps under different land-use and climate conditions in the UKC. It confirms and justified the selection and use of SWAT for this study.

The third model calibration is considered as a reference model calibration; the calibrated parameter range was used for further impact analysis. Calibration was performed for land-use in 2011 and climate between 2000 and 2006; validation was performed for 2007-2008.

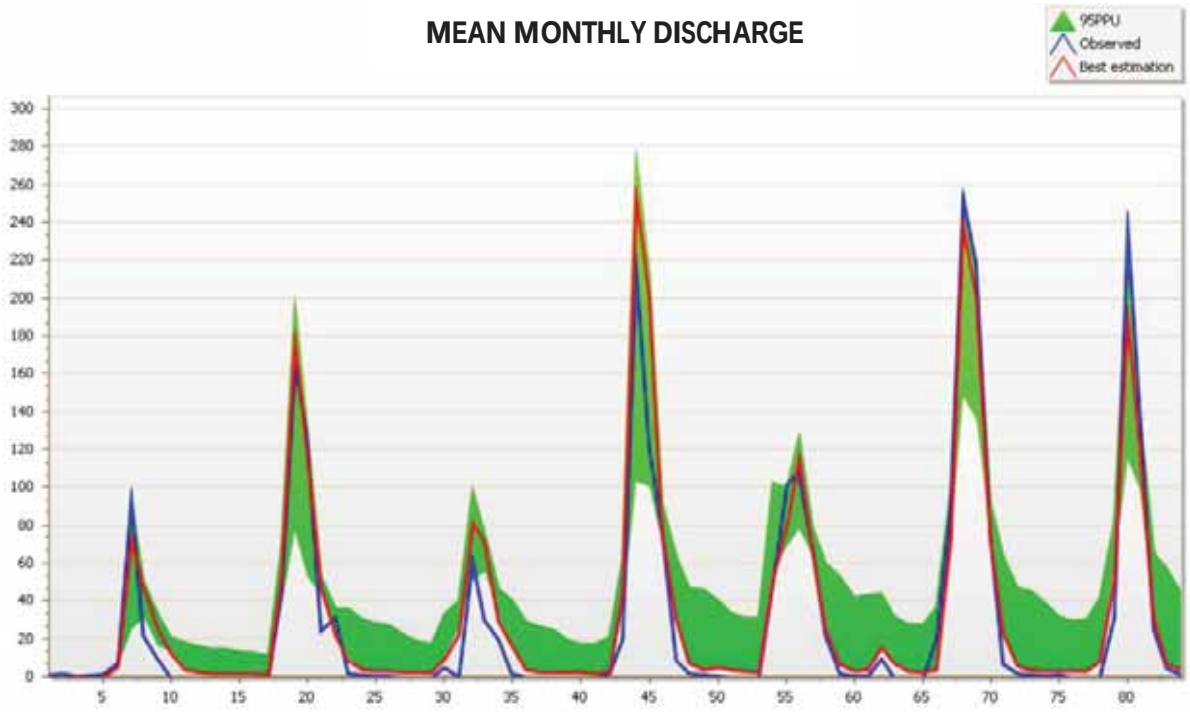

Fig. 6.9: Comparison between simulated and observed mean monthly streamflow for calibration period 2000-2006

Table 6.2: Model evaluation statistics for calibration period 2000-2006

Calibration (2000-2006)	Mean (m^3/s)	Standard deviation	R^2	NS (Nash-Sutcliff)	P factor	R factor
Observed	**31.13**	**59.18**	**0.94**	**0.93**	**0.29**	**0.55**
Simulated	**35.45**	**58.12**				

A tendency of the model to over-estimate discharge in the calibration period was observed (Figure 6.9). The standard deviation of observed and model simulation is close, and the R^2 and NS value of model calibration show a good agreement between simulated and observed values (Table 6.2). The P and R factors of the model uncertainty analysis are in the desired range. This leads to the conclusion that the model is well calibrated for the study area.

There is a tendency of the model to over-estimate and under-estimate discharge for different years in the validation period (Figure 6.10). The standard deviation of observed and model simulation is close, and the R^2 and NS values show a good agreement between simulated and observed value (Table 6.3). The P and R factor of model uncertainty analysis are in the desired range. Thus, it is concluded that the model is satisfactorily validated and can be used further for impact analysis studies for the study area.

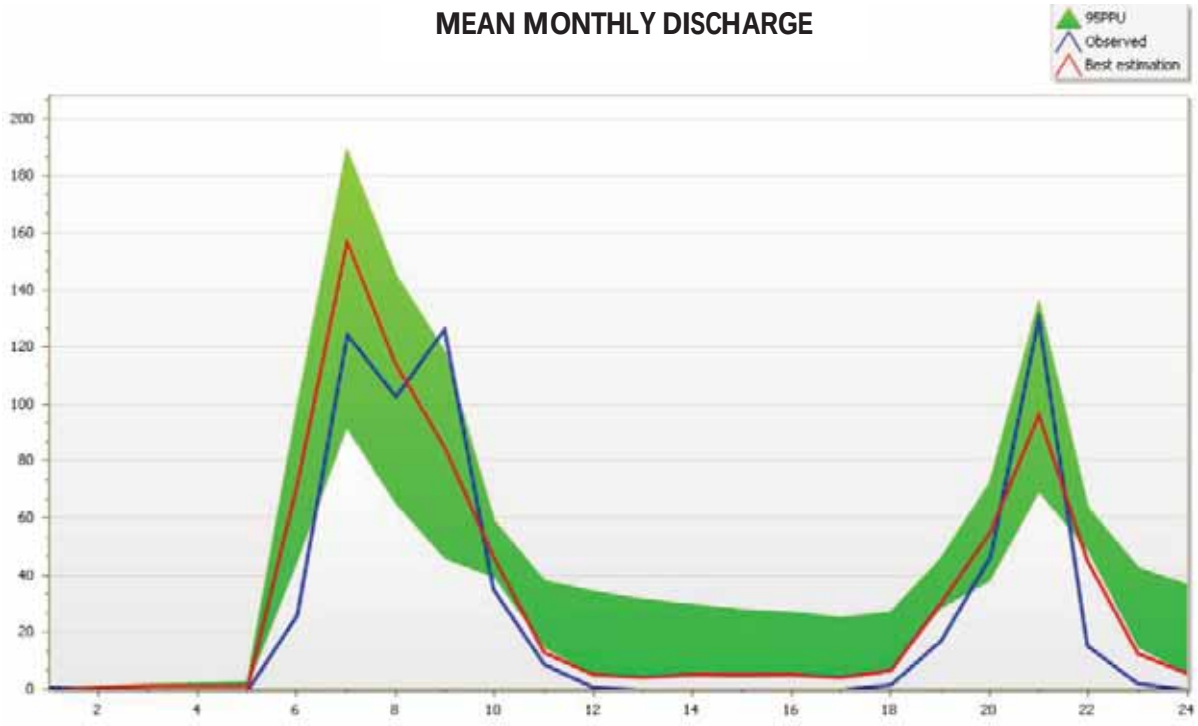

Fig. 6.10: Comparison between simulated and observed mean monthly streamflow for the validation period 2007-2008

Table 6.3: Model evaluation statistics for the validation period 2007-2008

Validation (2007-2008)	Mean (m^3/s)	Standard deviation	R^2	NS (Nash-Sutcliff)	P factor	R factor
Observed	**26.80**	**44.35**	**0.85**	**0.83**	**0.25**	**0.67**
Simulated	**32.53**	**42.60**				

The difference in simulated and observed mean discharge (Table 6.2 and Table 6.3) might be due to the following reasons:

(1) No discharge measurements were carried out in the dry season (January to June), so the model simulation might over-estimates the base flow in this season.

(2) Precision in discharge measurement varies between 5-8% (current meter)

(3) Daily discharge measurement at 8:30 am (only once a day)

6.8 Linkage between SWAT and MODFLOW

Groundwater recharge is an important issue, as it links surface and groundwater resources and can be used as a starting point to conceive options for surface water management aiming at sustainable use of surface and groundwater resources.

Recharge dominates the input into groundwater systems, and is therefore an essential input parameter in groundwater modeling. Most of the groundwater models use approaches like water balancing for estimating groundwater recharge. However, these estimates are limited when considering spatial variability, and thus do not deliver representative estimates, which further leads to errors in groundwater modeling. However, surface water models are efficient in estimating spatial groundwater recharge.

SWAT, as discussed in section 6.2, is recognized world-wide as an accepted and efficient surface water model for studying the impact of climate change and land-use change on water balance components. However, there are certain limitations of the model which restrict its use for groundwater modeling.

Limitations of SWAT

SWAT is a semi-distributed hydrological model. Although it is physically based and computationally efficient for surface water modeling and groundwater recharge estimation, it has limited capabilities for groundwater modeling and as a consequence restricted capabilities as a tool for groundwater management. The model has its own module for groundwater components but it is lumped and not distributed. Thus, the distributed parameters like hydraulic conductivity distribution, which is an influential component for groundwater modeling, cannot be represented. Additionally, the model faces difficulties in estimating the spatial distribution of groundwater levels.

Groundwater models quantify the spatio-temporal behavior of groundwater levels, resulting velocities, flows and water balances. They are applied to simulate the present and future scenarios of groundwater flow and its interaction with various factors, and have been extensively employed in various water resources planning worldwide.

MODFLOW is a standard groundwater flow model frequently used world-wide. When applied appropriately, MODFLOW is considered to be a standard model by regulatory agencies, universities, consultants and industry. The model has been integrated with climate models in a number of studies to examine the possible impacts of climate change on groundwater resources, e.g., Yusoff et al. (2002), Scibek et al. (2006) and Christy et al. (2009). The impact of land-use change on groundwater resources is analyzed by MODFLOW in a number of studies, e.g., Reeves et al. (2010) and Dams et al. (2008).

Limitation of MODFLOW

MODFLOW is physically based and is capable of modeling spatial distribution and movement of groundwater. However, it has limitations because of its dependence on the input data such as groundwater recharge, aquifer-stream flow interaction and evaporation.

Groundwater flow analyses using MODFLOW often do not consider the accuracy of the recharge rate, which is one of the most important components of groundwater models. This may result in considerable uncertainty in the simulated groundwater flow. The groundwater recharge rate is frequently determined through trial and error during calibration.

Since recharge is the basic input parameter to the groundwater system, improving the precision of the recharge estimation will improve the results of groundwater modeling. SWAT is a surface water model which is effective in modeling spatio-temporal distribution of groundwater recharge, and linking SWAT with MODFLOW may thus improve the results of groundwater modeling.

Some research has been done towards developing tools for sustainable management of groundwater resources explicitly based on linking surface water and groundwater models. Chung et al. (2010) integrated the surface water model SWAT with the groundwater model MODLOW and found that the groundwater modeling was improved by using the developed tool as compared to using the groundwater model alone. Hence, there is an urgent need to develop such tools which can be employed for sustainable management of groundwater resources.

Integrated SWAT – MODFLOW

The most widely used hydrological models for studying the impacts of climate change and land-use / land cover change on surface and groundwater resources are SWAT and MODFLOW, respectively. Despite having a number of advantages, both models have some limitations as discussed earlier. Yet the advantages and disadvantages of these models are complementary, and linking the models has therefore the potential to foster the development of a tool that can effectively support integrated analysis and management for both groundwater and surface water.

Nevertheless, linking the above-mentioned models has to take into account the different features of the models. SWAT divides the study area in HRUs (hydrologic response units) by overlaying the soil and land-use maps. HRUs are the functional units in SWAT, and for each HRU the water balance equation is applied. MODFLOW divides the study area in blocks called as cells; these cells are the functional units in MODFLOW, and for each cell the flow equation is established and solved. In order to implement an effective flow of data between the HRUs in SWAT and the cells in MODFLOW, a HRU-cell interface is developed. The main purpose is to replace the groundwater module of SWAT with MODFLOW. Basically, the groundwater recharge is estimated by SWAT as a function of hydrological processes, and is supplied as input to MODFLOW for computing the groundwater level and flow. By doing so, the advantages of

both models are used to compensate their limitations. Hence, SWAT-MODFLOW is a fully combined modeling program, which is able to form a linkage in each time step. It considers both the surface and groundwater interaction and depicts a realistic picture of hydrological processes (Figure 6.11).

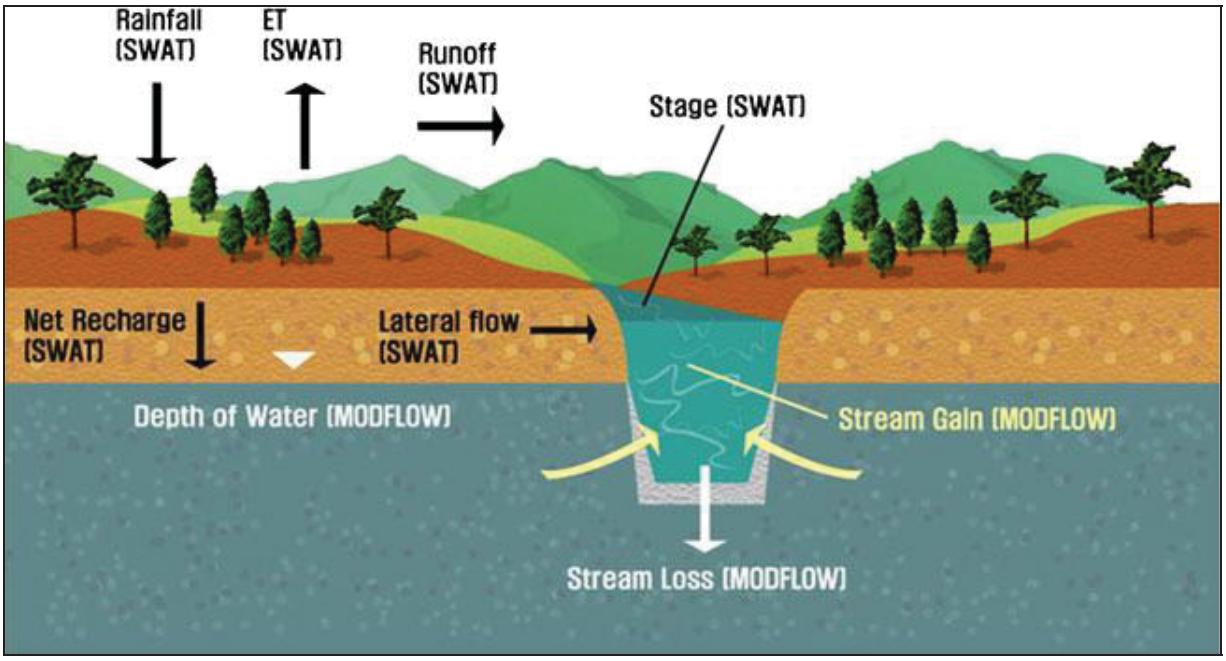

Figure 6.11 Schematic diagram of integrated SWAT-MODFLOW (Kim et al., 2008)

In the current study, a linkage interface was prepared, which converts the recharge estimation of the HRU format in the SWAT to the grid/cell format of MODFLOW.

6.8.1. Methodology

SWATmf is a user-friendly interface prepared by the Agriculture Research Station, USDA, Oklahoma, USA. It provides an integration of the SWAT and the MODFLOW based on differences in their physical discretization and representation.

The overall integration process runs in SWATmf interface and requires three files:

(1) The textinout folder of SWAT model run

(2) Input data for MODFLOW modeling

(3) Linkage file: HRU-ID raster map

The current study focuses on the preparation of the linkage file as a step to improve groundwater modeling. The latter is subject to further research and beyond the scope of this study.

The input data for SWAT and MODFLOW were prepared separately. First, the SWAT model was run independently for spatial recharge estimation, and then the textinout folder of SWAT was used as an input in MODFLOW using the SWATmf interface.

Preparation of the linkage file (HRU-ID map)

The linkage file is used as another input in the SWATmf interface to convert the HRU (SWAT format) to an ASCII grid file (MODFLOW format).

The concept note of the linkage file is prepared by the Agriculture Research Station, USDA, Oklahoma, USA. This concept is applied in the present study.

During the ArcSWAT model set up, the "Create the HRU Feature Class" option of "Land-Use/Soil/Slope definition" menu should be checked. The HRU re-classification option is not supported while preparing the linkage file and should be avoided.

Second, in ArcGIS a unique HRUCODE is assigned for each HRU within the FullHRU table created by the ARCSWAT project, and then the HRU is converted to a raster with a cell size equal (recommended) to the input DEM file. The HRUCODE field should be considered for feature to raster conversion. The resulting HRU-ID grid map in ASCII format is termed as the linkage file. This file is used as an input in the SWATmf interface, which further facilitates the conversion of HRU-based percolation (inputted as textinout folder of SWAT) in the grid/cell format of MODFLOW while running the SWATmf interface.

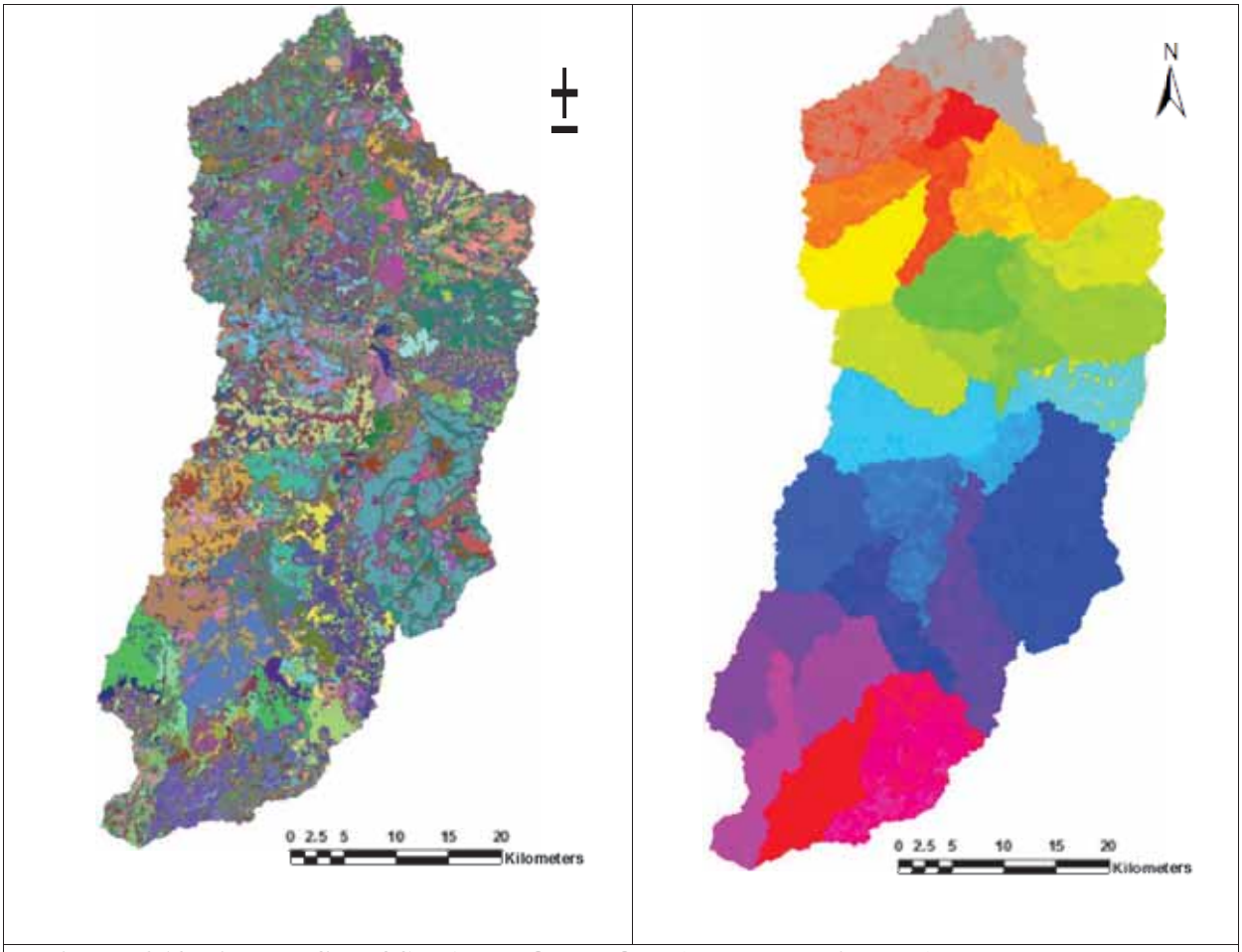

Figure 6.12 Linkage file of SWAT-MODFLOW (HRU-ID grid map)

CHAPTER 7: ANALYSES ON THE IMPACT OF CLIMATE CHANGE AND LAND-USE CHANGES ON WATER RESOURCES IN THE UPPER KHARUN CATCHMENT

7.1 Introduction

As described in Chapter 6, the SWAT model was setup, calibrated and validated for the study area. The calibrated parameter values referring to the period 2000 to 2006 were further used for a model setup (reference situation) to study the impact of climate change and land-use change on the water balance components in terms of discharge, percolation (groundwater recharge), surface runoff, groundwater contribution to streamflow, water yield and actual evapotranspiration. The impact analyses were performed in a three-step approach.

(1) Impacts of land-use change on water resources

This step focuses on the impacts of land-use on the water balance components.

The climatic variables and calibrated parameter ranges were kept constant, whereas the land-use maps of 1991, 2001 and 2021 were introduced one by one and the model was run subsequently to simulate the impacts of land-use change on the above-mentioned components of the water balance.

(2) Impacts of climate change on water resources

The calibrated model for the period 2000–2006 was used. The land-use map of 2011 and the calibrated parameter ranges were kept constant. PRECIS climate change scenarios (q0, q1 and q14) representing the 2020s (2011-2040), 2050s (2041-2070) and 2080s (2071-2098) were introduced in the model one by one, and their impact on the water resources was analyzed.

(3) Combined impact of climate change and land-use change on water resources

The land-use map of 2021 and the climate of the 2020s were used to analyze the impact on water resources. The calibrated parameter values of the 2000-2006 model provided the reference. Results were compared with the land-use map of 2011 and climate of 1990-2008.

7.2 Impacts of land-use changes on water balance components

The impacts of different land-use scenarios on the water balance components were first analyzed at the level of the entire UKC (catchment scale) (Section 7.2.1 and Table 7.1). In a further step, the spatial resolution of the analyses on land-use impacts was refined by considering in detail the 29 sub-catchments (sub-catchment scale).

7.2.1 Analyses on land-use impact at catchment scale

For detailed analyses of spatio-temporal land-use changes in decadal year steps see Chapter 4. Over the period 1991 to 2021, a decreasing trend for agricultural land, wasteland and water-

bodies was detected in the UKC, whereas an increasing trend for built-up areas and a slight increase in forest areas were found. It is estimated that between 1991 and 2021, the decrease in agriculture land will be 2.4%, in wasteland 4.8%, and in the area covered by water bodies 0.3%. The increase in built-up areas is expected to be 7.3% and an expansion by 0.2% is estimated for forest areas.

Irrigation plays an important role in the UKC. Extended networks of canal systems exist which were developed over the years. Furthermore, advancement in technology and better availability of electricity facilitated a significant increase in groundwater-irrigated areas.

It can be concluded that at the UKC scale, the impact of land-use change on relevant water balance components is small (Table 7.1). There is a decreasing trend of annual discharge, water yield and groundwater contribution to streamflow and an increasing trend of annual surface runoff and actual evapotranspiration over the decades; however, the magnitude of changes is quite low.

For percolation, the land-use change impact is low, i.e., annual percolation is almost constant between 1991 and 2011 with a slight decline of 2.7 mm between 2011 and 2021.

Referring to land-use changes from 1991 to 2011, the annual discharge sum decreased by 11.5 million m^3. Regarding the period 2021, a further decrease of 20.7 million m^3 is indicated as compared to 2011.

Groundwater contribution to streamflow declined significantly over the decades. It is simulated that the decadal decrease is 9.4 mm between 1991 and 2011, and a further decrease of 8.2 mm is expected for the land-use scenario of 2021 compared to the land-use of 2011.

Table 7.1: Impacts of different land-use scenarios on water balance components

DISCHARGE - REACH 01 - m3/s				
UKC	BASELINE	LANDUSE SCENARIOS		
Months	1991	2001	2011	2021
Jan	4.8	3.9	3.8	2.8
Feb	4.5	3.9	3.5	2.5
Mar	4.0	3.5	3.2	2.4
Apr	3.5	3.0	2.9	2.2
May	3.3	2.8	2.8	2.1
Jun	44.5	44.9	45.0	43.5
Jul	157.2	158.6	158.5	158.2
Aug	115.9	115.9	115.6	114.9
Sep	48.9	48.9	48.7	48.5
Oct	23.0	23.3	22.8	22.3
Nov	9.8	9.6	9.2	9.0
Dec	4.9	4.3	3.9	3.6
Ann Sum (mio m*3)	1099.8	1095.5	1088.3	1067.6

SURFACE RUNOFF (mm)				
UKC	BASELINE	LANDUSE SCENARIOS		
Months	1991	2001	2011	2021
Jan	0.0	0.1	0.1	0.1
Feb	0.0	0.0	0.0	0.0
Mar	0.2	0.3	0.2	0.3
Apr	0.1	0.1	0.1	0.2
May	0.0	0.0	0.0	0.1
Jun	77.9	79.9	80.3	79.9
Jul	174.6	176.3	176.4	176.6
Aug	115.7	116.6	116.7	117.0
Sep	14.3	14.9	14.9	15.1
Oct	12.7	13.2	13.1	13.0
Nov	0.0	0.1	0.1	0.1
Dec	0.0	0.0	0.0	0.0
Ann Sum	395.5	401.4	401.8	402.3

PERCOLATION (mm)				
UKC	BASELINE	LANDUSE SCENARIOS		
Months	1991	2001	2011	2021
Jan	0.5	0.6	0.7	0.6
Feb	0.4	0.6	0.7	0.4
Mar	0.7	0.8	0.9	0.5
Apr	0.5	0.6	0.6	0.3
May	0.1	0.1	0.1	0.1
Jun	12.6	12.3	12.4	12.0
Jul	24.4	24.1	24.1	23.7
Aug	22.1	21.8	21.8	21.4
Sep	10.2	10.3	10.2	9.9
Oct	14.3	14.6	14.5	14.1
Nov	1.3	1.4	1.3	1.4
Dec	0.9	0.9	1.0	1.0
Ann Sum	87.9	88.1	88.1	85.4

ACTUAL EVAPOTRANSPIRATION (mm)				
UKC	BASELINE	LANDUSE SCENARIOS		
Months	1991	2001	2011	2021
Jan	23.9	24.8	25.5	26.2
Feb	23.4	24.8	25.8	26.5
Mar	36.7	38.8	40.6	43.1
Apr	37.6	41.2	42.8	45.9
May	29.5	30.2	30.4	26.9
Jun	91.5	91.6	91.4	89.4
Jul	99.7	99.5	99.3	98.6
Aug	91.0	90.8	90.6	90.2
Sep	99.4	100.0	99.8	99.1
Oct	88.8	89.2	88.9	88.1
Nov	41.1	41.9	42.1	42.9
Dec	29.0	29.8	30.1	30.9
Ann Sum	691.8	702.6	707.4	707.9

Ground-water contribution to streamflow (mm)				
UKC	BASELINE	LANDUSE SCENARIOS		
Months	1991	2001	2011	2021
Jan	2.2	1.7	1.3	0.3
Feb	1.6	1.0	0.8	0.1
Mar	1.4	0.8	0.8	0.0
Apr	1.1	0.6	0.7	0.1
May	1.3	1.0	0.8	0.1
Jun	1.6	1.3	1.0	0.5
Jul	1.8	1.2	1.0	0.3
Aug	2.7	2.2	1.8	0.9
Sep	2.7	2.4	1.8	1.7
Oct	2.9	2.5	2.1	1.6
Nov	2.4	1.7	1.4	1.0
Dec	2.5	1.4	1.3	0.2
Ann Sum	24.2	17.8	14.8	6.6

WATER YIELD (mm)				
UKC	BASELINE	LANDUSE SCENARIOS		
Months	1991	2001	2011	2021
Jan	4.6	4.1	3.7	2.7
Feb	3.7	3.1	2.9	2.1
Mar	3.9	3.4	3.3	2.5
Apr	3.3	2.8	2.9	2.3
May	3.4	3.2	2.9	2.2
Jun	81.4	83.0	83.2	82.2
Jul	178.4	179.4	179.4	178.8
Aug	120.5	120.8	120.5	119.8
Sep	19.1	19.4	18.8	18.7
Oct	17.8	18.0	17.4	16.8
Nov	4.6	4.0	3.7	3.2
Dec	4.9	3.8	3.6	2.5
Ann Sum	445.5	444.9	442.2	433.8

The land-use change statistics (Table 4.4) reveal that the groundwater-irrigated areas between 1991 and 2011 increased by 6.05% for the two-season cropped sites and 5.46% for three-season cropped sites. In comparison with the 2011 land-use, the land-use scenario of 2021 predicts a further increase in groundwater-irrigated area by 17.85% for two-season cropped sites and 12.58% for three-season cropped sites.

The declining trend of discharge, water yield and groundwater contribution to streamflow corresponds to the significant increase in groundwater-irrigated areas over the decades. Increasing pumping rates of groundwater for irrigation can be assessed as the main reason for decreasing groundwater contribution to streamflow and subsequently a decrease in discharge and water yield.

On the other hand, annual surface runoff increased by 6.3 mm through changing land-use from 1991 to 2001 with a slight increase of 0.5 mm from 2011 to 2021. As the main reason, the significant increase in built-up areas over the decades is plausible. There was an increase in built-up area by 4.7 % between 1991 and 2011 and a further increase of 2.6% is expected to take place between 2011 and 2021 (Table 4.2).

The simulations indicate an increase in annual actual evapotranspiration by 15.6 mm between 1991 and 2011. A further slight increase (0.5 mm) is expected between 2011 and 2021. This might be explained by an increasing cropping intensification in the crop rotation patterns.

7.2.2 Sub-catchment scale land-use impact analysis

The UKC is divided into 29 sub-catchments (according to SWAT). The impact of land-use change on water resources with a refined resolution (sub-catchment scale) was investigated.

Two comparisons were made: first, between the water balance components changes 1991 and 2011 and second, changes between 2011 and 2021 were predicted by simulations using the respective land-use scenarios (Tables 7.2 and 7.3).

Table 7.2: Impact of land-use change on water balance components (% per unit area)

Impact of Land use Change on Water Balance Components : % Per unit area									
SUB-CATCHMENT	AREA Sq Km	Surface runoff % Change : 1991-2011	Surface runoff % Change : 2011-2021	Percolation % Change : 1991-2011	Percolation % Change : 2011-2021	AET % Change : 1991-2011	AET % Change : 2011-2021	WYLD % Change : 1991-2011	WYLD % Change : 2011-2021
1	100.5	48.3	8.4	-10.4	3.8	-7.4	4.1	27.4	-0.8
2	118.5	17.6	4.7	-4.3	-5.3	3.3	-0.5	5.5	2.3
3	26.9	28.4	38.0	-41.0	23.3	-16.0	3.8	23.6	30.3
4	51.9	4.7	1.0	3.1	0.0	2.6	-0.3	2.9	0.9
5	61.3	9.2	8.8	-11.6	-10.8	-4.1	1.5	10.1	0.5
6	128.2	5.6	10.3	-10.8	-6.1	0.5	-4.2	-8.5	5.5
7	2.0	-20.3	3.7	-21.6	6.3	-3.6	0.4	-20.2	3.8
8	96.8	3.7	0.4	2.5	-0.7	1.5	0.1	2.8	0.1
9	88.2	1.0	2.9	0.5	-22.9	0.9	-4.7	0.8	1.7
10	119.4	3.5	-5.7	10.4	-15.1	4.1	-3.4	3.6	-6.2
11	94.9	1.5	0.0	0.6	-1.0	2.1	-0.3	-1.8	-0.2
12	36.5	-3.9	-0.4	-2.0	0.0	-0.1	0.1	-3.9	-0.4
13	27.1	4.2	-1.7	8.3	-8.5	5.3	-3.1	1.4	-2.0
14	95.8	1.1	1.6	4.8	-1.4	3.0	0.8	1.2	-0.2
15	69.1	0.5	-2.5	2.8	-0.8	1.6	4.0	-0.6	-2.7
16	10.8	-3.2	0.4	-1.5	0.5	-2.6	0.2	-3.1	0.4
17	122.2	4.1	1.0	11.9	-2.7	6.0	0.9	4.1	-0.5
18	36.6	-4.3	-0.3	-5.1	-1.0	-0.5	-0.3	-4.3	-0.3
19	110.6	-2.6	-1.0	-7.2	-1.9	-0.5	0.7	-2.7	-1.0
20	109.5	0.9	-1.3	10.4	-8.0	5.2	-0.5	1.0	-1.6
21	257.5	1.0	-2.2	13.1	-11.0	8.9	-2.1	0.1	-2.3
22	74.9	-0.5	-1.2	-3.9	-2.1	-3.6	0.8	-0.6	-1.2
23	124.6	-4.8	-0.4	-13.6	-1.7	-0.7	0.8	-5.1	-0.4
24	49.7	-1.2	0.3	-5.4	-0.5	-1.6	0.4	-1.3	0.2
25	60.0	0.3	0.0	11.1	-4.6	8.2	-3.0	-1.3	-0.2
26	85.0	0.3	-0.2	-2.7	-1.3	-3.5	0.1	0.2	-0.2
27	80.6	0.4	2.0	1.2	4.8	3.2	12.2	-2.4	-11.4
28	151.1	1.4	-1.5	5.4	-4.2	8.3	-1.1	-7.2	-1.7
29	97.6	-0.3	2.3	1.4	4.3	2.9	10.9	-2.3	-9.6

Table 7.3: Impact of land-use change on water balance components (change in amount: mm)

Impact of Landuse Change on Water Balance Components Amount in mm											
Sub-Catchment	AREA Sq Km	Surface runoff Amount Change : 1991-2011	Surface runoff Amount Change : 2011-2021	Percolation Amount Change : 1991-2011	Percolation Amount Change : 2011-2021	AET Amount Change : 1991-2011	AET Amount Change : 2011-2021	WYLD Amount Change : 1991-2011	WYLD Amount Change : 2011-2021	GWQ Amount Change : 1991-2011	GWQ Amount Change : 2011-2021
1	100.5	37.2	9.6	-6.0	1.9	-40.9	21.1	30.7	-1.1	-4.6	-11.1
2	118.5	29.5	9.2	-3.5	-4.2	21.4	-3.6	12.3	5.4	-15.8	-2.4
3	26.9	22.0	37.8	-16.0	5.4	-100.4	19.9	21.3	33.9	4.0	-5.0
4	51.9	9.7	2.1	2.2	0.0	18.7	-2.2	7.0	2.2	-3.1	0.0
5	61.3	18.4	19.3	-12.4	-10.2	-26.0	8.9	24.9	1.5	10.3	-14.2
6	128.2	17.1	33.2	-16.4	-8.2	3.7	-28.1	-35.5	21.1	-47.5	-9.6
7	2.0	-48.3	7.0	-10.2	2.3	-29.7	3.2	-50.8	7.6	0.0	0.0
8	96.8	8.5	0.9	1.8	-0.5	10.9	1.1	7.3	0.2	-1.5	-0.5
9	88.2	3.6	10.2	0.3	-14.5	7.0	-37.9	3.0	6.4	-0.6	0.0
10	119.4	11.2	-18.7	6.8	-11.0	31.2	-27.0	12.0	-21.3	-0.8	0.0
11	94.9	3.3	0.0	0.4	-0.7	15.8	-2.2	-4.4	-0.5	-8.1	0.0
12	36.5	-10.3	-0.9	-1.1	0.0	-0.7	1.0	-10.8	-1.0	0.0	0.0
13	27.1	8.5	-3.5	5.4	-6.1	39.2	-24.5	3.2	-4.5	-6.6	0.0
14	95.8	2.5	3.7	2.1	-0.6	18.7	4.8	2.8	-0.5	-0.2	-4.1
15	69.1	1.5	-8.1	1.6	-0.5	11.1	27.3	-2.2	-9.2	-4.1	-1.0
16	10.8	-7.3	0.8	-0.7	0.2	-18.6	1.1	-7.4	0.9	0.0	0.0
17	122.2	8.7	2.3	4.4	-1.1	35.4	5.5	9.3	-1.3	-0.5	-3.3
18	36.6	-27.7	-2.1	-3.2	-0.6	-4.2	-1.9	-28.4	-2.2	0.0	0.0
19	110.6	-13.2	-5.0	-5.2	-1.3	-3.8	5.6	-14.6	-5.4	0.0	0.0
20	109.5	4.1	-6.1	5.9	-5.0	38.8	-4.3	4.9	-7.5	-0.8	0.0
21	257.5	7.8	-17.3	7.8	-7.4	61.4	-15.4	0.6	-19.1	-9.2	0.0
22	74.9	-2.7	-5.9	-2.4	-1.3	-28.7	5.8	-3.3	-6.3	0.0	0.0
23	124.6	-29.5	-2.3	-12.2	-1.3	-5.7	6.6	-32.6	-2.6	0.0	0.0
24	49.7	-5.8	1.3	-3.6	-0.3	-10.9	2.5	-6.7	1.1	0.0	0.0
25	60.0	1.6	0.0	8.3	-3.8	52.8	-21.0	-7.5	-1.0	-11.3	0.0
26	85.0	1.6	-1.0	-1.8	-0.8	-25.0	0.9	1.1	-1.2	0.0	0.0
27	80.6	2.1	9.7	3.0	12.5	17.3	68.0	-17.8	-81.5	-20.7	-94.3
28	151.1	7.0	-7.4	8.3	-6.8	57.5	-8.3	-43.2	-9.3	-52.6	0.0
29	97.6	-1.5	11.6	3.9	11.9	15.5	60.0	-17.7	-72.2	-17.3	-86.8

(1) Surface runoff

The main changes in annual surface runoff over the decades are observed for sub-catchments 1, 2, 3, 5 and 6. The land-use change analysis at sub-catchment level was performed to investigate the reason behind the major change in surface runoff.

Sub-catchment 1: The main land-use change between 1991 and 2011 is an increase in built-up areas (urban areas) by 16.62% and a decrease in agricultural land by 13.93%, which resulted in a significant increase in surface runoff by 48%. Similarly for the period 2011 to 2021, there is an increase in built-up area by 5.07% and decrease in agricultural land by 1.89% that corresponds to an increase in surface runoff by 8.4%.

For the other sub-catchments 2, 3, 5 and 6, the increase in built-up areas in combination with a decreasing trend in agricultural land is the reason for an increase in surface runoff.

The physical reason behind the above-mentioned effects is the fact that built-up areas feature a high share of sealed surfaces which hinder or strongly reduce water percolation and groundwater contribution to streamflow and facilitate an increase in surface runoff.

(2) Percolation

The increase in surface runoff in the above-mentioned sub-catchments is characterized by a rising share of built-up areas, which corresponds with the decreasing trend of percolation in these sub-catchments. This is plausible due to the hydrological effect of sealed surfaces on runoff (enhancement) and percolation (reduction).

(3) Actual evapotranspiration

Actual evapotranspiration (AET) increases with the increase in crop intensification (cultivation of two and/or three crops per year instead of one) and decreases with an expansion in built-up areas.

Some of the examples include that of sub-catchment 27, where an increase in two-season cropped area (4.43 km^2 between 1991 and 2011 and 22.12 km^2 between 2011 and 2021) resulted in an increase in AET by 17.3 mm per year and 68 mm per year, respectively. Similarly, the increase in two-season cropped area for sub-catchment number 29 explains the increasing trend.

In the period between 1991 and 2011, sub-catchment 6 features an increase in more than two-season cropped area with paddy as a summer crop. However, the increasing effect on AET is counterbalanced by an expansion of urban areas and thus there is a slight change. For the period between 2011 and 2021, there is no further change in areas with more than two-season cropping with paddy as a summer crop, but an increase in urban area by 14.0 km^2, which resulted in a clear decrease in AET.

(4) Groundwater contribution to streamflow (GWQ)

The increasing trend in built-up areas in some sub-catchments is the reason for declining groundwater contribution to the streamflow components of the water balance. It is evident that for sub-catchment 7, there is an increase in built-up area by 16.1% between 1991 and 2011 and a further increase of 10.9% between 2011 and 2021. This corresponds well with a declining trend of groundwater contribution to streamflow of 47.5 mm between 1991 and 2011 and 9.6 mm between 2011 and 2021.

An increase in groundwater-irrigated areas in some sub-catchments is another reason for the declining groundwater contribution to streamflow. For example, for sub-catchment 29, the increase in groundwater-irrigated paddy crops is the reason for a decline of 17.3 mm between

1991 and 2011 and 86.8 mm between 2011 and 2021. The same reason holds valid for sub-catchment 27.

7.3. Analyses on climate change impact

The climate change impact analysis is based on the bias-corrected PRECIS RCM climate scenarios for the study area. Scenarios were developed for three time periods, i.e., the 2020s (representing the time period 2011 – 2040), 2050s (2041-2070) and 2080s (2071-2098). The baseline period for comparison is the observed climate data for the period 1990-2008.

For the scenarios q0, q1 and q14, PRECIS provides three different climate simulations (ensembles) of IPCC SRES A1B scenario. These scenarios are considered separately for the climate change impact analysis for water balance components. However, q1 scenario shows better agreement with the climate of the study area for the baseline period. Kumar et al. (2011) also advocates that for Chhattisgarh state (the study area is a part of this state) q1 scenario has less biases in rainfall compared to the q0 and q14 scenarios.

The change in climatic parameters indicated by PRECIS was simulated with respect to the following three situations: average, wet and dry climatic conditions in the 2020s, 2050s and 2080s period.

(1) Approach

For average conditions:

- Selection of an average year and application of temporal distribution of rainfall and temperature,
- Extrapolation of daily rainfall and temperature values according to the PRECIS scenarios (2020s, 2050s and 2080s) for all stations (by a factor describing the ratio between predicted and current representative values) and keeping the temporal distribution,
- Simulation of the water balance components with SWAT using the meteo-data of the 2001 (current/representative) and PRECIS scenarios 2020s, 2050s, 2080s.

For wet and dry conditions:

- Selection of a wet/ dry year and keeping the temporal pattern of meteo-parameters but changing the magnitude of rainfall and temperature according to PRECIS scenarios,
- Simulation with SWAT

(2) Justification of approach

The focus of the analyses is on the average (representative) years in terms of rainfall and temperature. In addition, an attempt is made to approximate the changes of major water balance components under wet and dry conditions.

The climate change impact analysis was performed at catchment scale. The land-use of 2011 was kept constant for the reason that this is the most recent land-use scenario, and the calibrated model parameter values for the period 2000-2006 were used.

The impacts of the average climate situation on the water balance components are discussed in detail, while the impacts in years representing high (wet) and low (dry) rainfall conditions are discussed in terms of runoff-rainfall ratios and with respect to changes in surface runoff and percolation.

7.3.1 Climate change impact analysis for q0 scenario: average climate conditions

The results of q0 climate change scenario on water balance components are listed in Table 7.4.

(1) Precipitation: Compared to the baseline period, there is a slight decrease of 10 mm (0.9%) rainfall for the 2020s, an increase of 202 mm (18.2%) for the 2050s and an increase of 323.4 mm (29.1%) for the period 2080s.

(2) Discharge: In comparison with the baseline scenario, the 2020s show a decline in annual discharge sum by 70.8 million m^3 (6.5%). This corresponds well with decreasing rainfall and increasing temperature. For the 2050s, there is an increase of 428.4 million m^3 (39.34%) and in the 2080s an increase by 693.0 million m^3 (63.7 %). The increasing trend in discharge is in good agreement with the increasing rainfall trend.

(3) Surface runoff: The 2020s show a slight decrease of 0.9 mm, the 2050s an increase by 177.1 mm (44.0%), and the 2080s an increase by 279.7 mm (69.6%) of surface runoff as compared to the baseline scenario.

(4) Percolation: Compared to baseline scenario, percolation is slightly increased by 1.6 mm (1.8%) for the 2020s, for the 2050s by 13.6 mm (15.4%), and for the 2080s by 12.1 mm (13.7%).

(5) Actual Evapotranspiration (AET): The simulated increasing trend in AET corresponds well with the rising temperature. There is an average annual increase in AET of 11.9 mm (1.78%) in the 2020s, 52.0 mm (7.4%) in the 2050s and 52.7 mm (7.4%) in the 2080s as compared to the baseline scenario.

(6) Groundwater contribution to streamflow: In comparison with the baseline scenario, the groundwater contribution shows a slight decline by 1.1 mm (7.4%) in the 2020s, an increase by 9.5 mm (64.2%) in the 2050s and an increase by 8.7 mm (58.8%) in the 2080s.

Table 7.4: Climate change impacts (q0 scenario: average climate conditions) on water balance components in amount (mm)

PRECIPITATION (mm)				
UKC	BASELINE	q0 scenarios		
Month	1990-2008	2020s	2050s	2080s
Jan	3.3	2.6	3.7	3.5
Feb	0.0	0.0	0.0	0.0
Mar	9.4	7.7	10.0	7.1
Apr	11.6	12.6	10.4	11.8
May	8.0	6.2	9.3	5.6
Jun	360.1	259.6	346.4	255.1
Jul	352.5	374.5	478.2	577.7
Aug	244.8	287.0	329.4	414.7
Sep	62.0	61.0	56.0	66.4
Oct	56.1	87.5	66.6	89.8
Nov	2.4	1.5	2.2	2.1
Dec	0.0	0.0	0.0	0.0
Annual	1110.2	1100.2	1312.2	1433.6

DISCHARGE - REACH 01 - m3/s				
UKC	BASELINE	q0 scenarios		
Month	1990-2008	2020s	2050s	2080s
Jan	3.8	0.0	3.4	4.1
Feb	3.5	0.0	3.2	3.9
Mar	3.2	0.1	3.3	3.5
Apr	2.9	0.1	2.6	3.2
May	2.8	0.1	2.3	3.0
Jun	45.0	10.5	39.8	11.7
Jul	158.5	139.5	250.5	292.1
Aug	115.6	139.6	184.8	249.3
Sep	48.7	51.8	54.1	59.9
Oct	22.8	32.3	25.1	36.2
Nov	9.2	13.9	11.1	15.0
Dec	3.9	4.6	4.9	5.3
Annual Sum (mio m*3)	1088.3	1017.5	1516.7	1781.3

SURFACE RUNOFF (mm)				
UKC	BASELINE	q0 scenarios		
Month	1990-2008	2020s	2050s	2080s
Jan	0.1	0.1	0.1	0.1
Feb	0.0	0.0	0.0	0.0
Mar	0.2	0.1	0.4	0.2
Apr	0.1	0.1	0.1	0.1
May	0.0	0.0	0.0	0.0
Jun	80.3	33.6	74.1	29.2
Jul	176.4	174.8	284.8	345.6
Aug	116.7	148.3	188.9	259.5
Sep	14.9	14.9	13.4	17.8
Oct	13.1	29.0	16.9	29.0
Nov	0.1	0.0	0.0	0.0
Dec	0.0	0.0	0.0	0.0
Annual	401.8	400.9	578.9	681.5

PERCOLATION (mm)				
UKC	BASELINE	q0 scenarios		
Month	1990-2008	2020s	2050s	2080s
Jan	0.7	0.2	1.5	1.4
Feb	0.7	0.7	1.3	1.0
Mar	0.9	1.3	1.8	1.2
Apr	0.6	1.4	1.5	1.0
May	0.1	0.1	0.1	0.1
Jun	12.4	7.6	12.1	7.1
Jul	24.1	23.5	29.1	29.8
Aug	21.8	24.0	26.5	29.7
Sep	10.2	10.1	9.8	10.2
Oct	14.5	17.5	15.1	16.9
Nov	1.3	1.5	1.2	1.0
Dec	1.0	1.9	1.6	0.9
Annual	88.1	89.7	101.7	100.2

ACTUAL EVAPOTRANSPIRATION (mm)				
UKC	BASELINE	q0 scenarios		
Month	1990-2008	2020s	2050s	2080s
Jan	25.5	25.2	30.9	30.9
Feb	25.8	29.5	33.2	33.3
Mar	40.6	47.2	50.9	48.9
Apr	42.8	47.2	49.5	44.0
May	30.4	31.6	36.8	32.5
Jun	91.4	89.0	99.5	96.2
Jul	99.3	93.0	91.2	93.7
Aug	90.6	89.0	90.6	92.6
Sep	99.8	101.1	104.7	107.8
Oct	88.9	88.2	91.9	99.2
Nov	42.1	43.9	45.3	46.0
Dec	30.1	34.5	35.0	34.9
Annual	707.4	719.3	759.4	760.1

Ground-water contribution to streamflow (mm)				
UKC	BASELINE	q0 scenarios		
Month	1990-2008	2020s	2050s	2080s
Jan	1.3	0.0	2.3	2.2
Feb	0.8	0.0	1.9	1.7
Mar	0.8	0.1	1.8	1.6
Apr	0.7	0.1	1.2	1.4
May	0.8	0.1	1.1	1.2
Jun	1.0	0.2	1.2	1.3
Jul	1.0	0.9	1.7	1.5
Aug	1.8	1.8	2.4	2.4
Sep	1.8	2.4	2.7	2.7
Oct	2.1	2.9	3.1	3.2
Nov	1.4	2.9	2.8	2.4
Dec	1.3	2.4	2.3	2.1
Annual	14.8	13.7	24.3	23.5

WATER YIELD (mm)				
UKC	BASELINE	q0 scenarios		
Month	1990-2008	2020s	2050s	2080s
Jan	3.7	0.1	3.5	4.2
Feb	2.9	0.0	2.9	3.4
Mar	3.3	0.2	3.3	3.6
Apr	2.9	0.2	2.4	3.3
May	2.9	0.1	2.3	3.0
Jun	83.2	33.9	76.3	32.1
Jul	179.4	175.7	287.7	348.7
Aug	120.5	150.4	192.6	263.6
Sep	18.8	17.7	17.5	22.4
Oct	17.4	32.6	21.6	34.3
Nov	3.7	3.8	4.6	4.5
Dec	3.6	3.4	4.2	4.3
Ann Sum	442.2	418.1	618.7	727.3

(7) Water Yield: Compared to the baseline scenario, water yield shows a decrease of 24.1 mm (5.5%) in the 2020s, an increase of 176.5 mm (39.9%) in the 2050s and an increase by 285.1 mm (64.5%) in the 2080s. The water yield trend follows the changes in the dominating surface runoff, which is driven by rainfall patterns over the years.

7.3.2 Climate change impact analysis for q1 scenario: average climate conditions

The results of q1 climate change scenario on water balance components are listed in Table 7.5.

(1) Precipitation: Relative to the baseline period, a significant decrease by 136.4 mm (12.3%) rainfall in the 2020s, a decrease by 74.5 mm (6.7%) in the 2050s and an increase by 128.2 mm (11.5%) in the 2080s.

(2) Discharge: In comparison with the baseline scenario, the 2020s show a decline in the annual discharge sum by 281.6 million m^3 (25.9%) and also for 2050s, where there is a 191.8 million m^3 (17.6%) decrease, which corresponds well with decreasing rainfall and increasing temperature. The 2080s show an increase in the annual discharge sum by 177.0 million m^3 (16.3%).

(3) Surface runoff: For the 2020s, a significant decrease by 115.65 mm (28.8%) is simulated, which remains in tendency amounting to a decrease by 72.1 mm (17.9 %) in the 2050s. For the 2080s, the simulations indicate an increase by 78.3 mm (19.5%) as compared to the baseline scenario.

(4) Percolation: The simulations predict a decrease in percolation for all periods compared to the baseline scenario amounting to 11.3 mm (12.8%) in the 2020s, 9.1 mm (10.3%) in the 2050s and 0.3 mm (0.3%) in the 2080s.

(5) Actual evapotranspiration: All simulations show an increasing trend for AET, which corresponds well with the increasing temperature over the time. The simulations predict an increase by 34.4 mm (4.9%) in the 2020s, 39.0 mm (5.5%) in the 2050s and 69.6 mm (9.8%) in the 2080s as compared to the baseline scenario.

(6) Groundwater contribution to streamflow: In comparison to the base line scenario, groundwater contribution shows an increase by 2.2 mm (14.7%) in the 2020s, a decrease of 2.0 mm (13.3%) in the 2050s, and a decrease of 1.5 mm (10.48%) in the 2080s.

(7) Water yield: Compared to the baseline scenario, water yield shows a decrease by 114.7 mm (26.0%) in the 2020s, a decrease by 77.0 mm (17.4%) in the 2050s, and an increase by 73.8 mm (16.7%) in the 2080s. The water yield trend follows the rainfall change pattern over the years.

Table 7.5: Climate change impacts (q1 scenario: average climate condition) on water balance components in amount (mm)

PRECIPITATION (mm)				
UKC	BASELINE	q1 scenarios		
Month	1990-2008	2020s	2050s	2080s
Jan	3.3	3.5	6.9	6.3
Feb	0.0	0.0	0.0	0.0
Mar	9.4	15.0	10.1	9.3
Apr	11.6	10.6	11.0	7.8
May	8.0	8.6	6.6	7.8
Jun	360.1	285.9	220.4	334.9
Jul	352.5	309.3	368.2	481.1
Aug	244.8	229.7	281.9	270.4
Sep	62.0	47.8	57.7	57.2
Oct	56.1	60.5	69.5	61.7
Nov	2.4	2.9	3.4	1.9
Dec	0.0	0.0	0.0	0.0
Annual	1110.2	973.8	1035.8	1238.4

DISCHARGE - REACH 01 - m3/s				
UKC	BASELINE	q1 scenarios		
Month	1990-2008	2020s	2050s	2080s
Jan	3.8	4.3	3.5	3.3
Feb	3.5	3.9	3.1	3.0
Mar	3.2	4.2	2.9	2.8
Apr	2.9	3.2	2.5	2.4
May	2.8	2.9	2.4	2.3
Jun	45.0	17.9	7.2	29.9
Jul	158.5	96.8	105.2	225.1
Aug	115.6	95.4	130.3	135.8
Sep	48.7	46.0	50.1	48.8
Oct	22.8	22.2	24.3	22.5
Nov	9.2	10.4	10.6	8.8
Dec	3.9	4.0	3.8	3.6
Annual Sum (mio m*3)	1088.3	806.6	896.5	1265.3

SURFACE RUNOFF (mm)				
UKC	BASELINE	q1 scenarios		
Month	1990-2008	2020s	2050s	2080s
Jan	0.1	0.1	0.2	0.1
Feb	0.0	0.0	0.0	0.0
Mar	0.2	1.1	0.4	0.3
Apr	0.1	0.2	0.1	0.1
May	0.0	0.1	0.0	0.0
Jun	80.3	39.6	17.8	58.2
Jul	176.4	118.7	143.7	262.5
Aug	116.7	98.8	137.3	133.0
Sep	14.9	10.4	12.5	11.9
Oct	13.1	17.2	17.8	13.9
Nov	0.1	0.1	0.1	0.0
Dec	0.0	0.0	0.0	0.0
Annual	401.8	286.1	329.7	480.1

PERCOLATION (mm)				
UKC	BASELINE	q1 scenarios		
Month	1990-2008	2020s	2050s	2080s
Jan	0.7	1.0	0.9	0.8
Feb	0.7	1.0	0.7	0.7
Mar	0.9	1.2	1.0	0.9
Apr	0.6	0.7	0.7	0.6
May	0.1	0.1	0.1	0.1
Jun	12.4	8.0	5.7	10.0
Jul	24.1	19.5	21.0	27.6
Aug	21.8	20.3	22.9	22.9
Sep	10.2	10.4	9.0	8.5
Oct	14.5	12.5	15.1	13.9
Nov	1.3	1.3	1.2	1.0
Dec	1.0	0.8	0.9	0.7
Annual	88.1	76.8	79.1	87.8

ACTUAL EVAPOTRANSPIRATION (mm)				
UKC	BASELINE	q1 scenarios		
Month	1990-2008	2020s	2050s	2080s
Jan	25.5	27.1	29.3	29.2
Feb	25.8	29.8	29.2	29.3
Mar	40.6	46.2	44.7	45.1
Apr	42.8	44.7	42.7	39.6
May	30.4	31.8	30.4	30.1
Jun	91.4	103.0	93.8	110.1
Jul	99.3	102.6	103.0	106.3
Aug	90.6	92.1	96.0	99.7
Sep	99.8	103.3	108.0	114.3
Oct	88.9	88.7	92.7	95.5
Nov	42.1	42.6	44.4	45.1
Dec	30.1	30.1	32.2	32.6
Annual	707.4	741.8	746.5	777.0

Ground-water contribution to streamflow (mm)				
UKC	BASELINE	q1 scenarios		
Month	1990-2008	2020s	2050s	2080s
Jan	1.3	1.9	1.1	1.1
Feb	0.8	1.4	0.7	0.7
Mar	0.8	1.1	0.6	0.6
Apr	0.7	0.8	0.5	0.5
May	0.8	0.9	0.6	0.6
Jun	1.0	1.0	0.8	0.8
Jul	1.0	1.0	0.8	0.9
Aug	1.8	1.9	1.7	1.8
Sep	1.8	1.9	1.8	1.9
Oct	2.1	2.3	1.8	1.9
Nov	1.4	1.5	1.3	1.3
Dec	1.3	1.3	1.2	1.3
Annual	14.8	16.9	12.8	13.2

WATER YIELD (mm)				
UKC	BASELINE	q1 scenarios		
Month	1990-2008	2020s	2050s	2080s
Jan	3.7	4.2	3.5	3.2
Feb	2.9	3.4	2.6	2.5
Mar	3.3	4.4	3.0	2.8
Apr	2.9	2.9	2.5	2.3
May	2.9	3.0	2.5	2.4
Jun	83.2	42.5	20.2	60.6
Jul	179.4	121.6	146.2	265.1
Aug	120.5	102.6	140.7	136.7
Sep	18.8	14.2	16.0	15.6
Oct	17.4	21.5	21.6	17.9
Nov	3.7	3.6	3.3	3.4
Dec	3.6	3.4	3.3	3.4
Ann Sum	442.2	327.5	365.2	516.0

7.3.3 Climate change impact analysis for q14 scenario: average climate conditions

Based on the results of the impacts of q14 climate scenario on the water balance components of the UKC (Table 7.6), the following trends in the water balance components were simulated.

Table 7.6: Climate change impacts (q14 scenario: average climate conditions) on water balance components in amount (mm)

PRECIPITATION (mm)				
UKC	BASELINE	q14 scenarios		
Month	1990-2008	2020s	2050s	2080s
Jan	3.3	2.5	3.4	4.0
Feb	0.0	0.0	0.0	0.0
Mar	9.4	8.4	8.1	10.5
Apr	11.6	15.0	11.8	13.7
May	8.0	9.5	5.2	9.6
Jun	360.1	346.9	312.4	254.2
Jul	352.5	456.2	419.5	502.2
Aug	244.8	239.8	289.4	340.2
Sep	62.0	68.4	64.4	78.6
Oct	56.1	88.4	73.1	117.9
Nov	2.4	2.1	3.3	6.7
Dec	0.0	0.0	0.0	0.0
Annual	1110.2	1237.1	1190.4	1337.5

DISCHARGE - REACH 01 - m3/s				
UKC	BASELINE	q14 scenarios		
Month	1990-2008	2020s	2050s	2080s
Jan	3.8	3.4	3.6	3.6
Feb	3.5	3.1	3.2	3.4
Mar	3.2	2.9	3.0	3.1
Apr	2.9	2.6	2.7	2.8
May	2.8	2.5	2.7	2.7
Jun	45.0	39.7	25.2	11.6
Jul	158.5	237.3	191.0	231.3
Aug	115.6	123.5	151.0	192.4
Sep	48.7	50.7	55.5	59.3
Oct	22.8	33.1	29.2	46.2
Nov	9.2	15.5	13.2	19.7
Dec	3.9	4.6	4.3	5.5
Annual Sum (mio m*3)	1088.3	1344.6	1256.4	1507.3

SURFACE RUNOFF (mm)				
UKC	BASELINE	q14 scenarios		
Month	1990-2008	2020s	2050s	2080s
Jan	0.1	0.0	0.1	0.1
Feb	0.0	0.0	0.0	0.0
Mar	0.2	0.3	0.2	0.3
Apr	0.1	0.2	0.2	0.1
May	0.0	0.1	0.0	0.1
Jun	80.3	72.6	52.2	27.7
Jul	176.4	270.9	225.0	280.9
Aug	116.7	117.2	152.7	196.6
Oct	14.9	18.6	18.3	23.3
Nov	13.1	29.9	23.8	45.5
Nov	0.1	0.0	0.1	0.3
Dec	0.0	0.0	0.0	0.0
Annual	401.8	509.7	472.6	574.9

PERCOLATION (mm)				
UKC	BASELINE	q14 scenarios		
Month	1990-2008	2020s	2050s	2080s
Jan	0.7	0.7	0.8	0.7
Feb	0.7	0.7	0.7	0.6
Mar	0.9	0.9	0.7	0.8
Apr	0.6	0.7	0.6	0.6
May	0.1	0.1	0.1	0.2
Jun	12.4	11.7	9.6	6.9
Jul	24.1	28.1	25.9	27.8
Aug	21.8	22.3	24.4	26.7
Sep	10.2	10.6	11.9	10.9
Oct	14.5	17.8	13.8	19.3
Nov	1.3	1.3	1.1	1.1
Dec	1.0	0.9	0.6	0.7
Annual	88.1	95.8	90.2	96.2

ACTUAL EVAPOTRANSPIRATION (mm)				
UKC	BASELINE	q14 scenarios		
Month	1990-2008	2020s	2050s	2080s
Jan	25.5	25.9	28.9	27.5
Feb	25.8	26.9	30.2	28.6
Mar	40.6	41.5	44.2	44.7
Apr	42.8	42.5	40.3	40.2
May	30.4	31.1	29.0	31.0
Jun	91.4	92.8	96.4	92.4
Jul	99.3	89.4	91.9	93.0
Aug	90.6	88.9	92.0	91.7
Sep	99.8	101.8	105.3	107.7
Oct	88.9	90.0	93.4	101.7
Nov	42.1	43.8	45.3	46.6
Dec	30.1	31.6	32.2	33.0
Annual	707.4	706.0	729.0	738.1

Ground-water contribution to streamflow (mm)				
UKC	BASELINE	q14 scenarios		
Month	1990-2008	2020s	2050s	2080s
Jan	1.3	1.2	1.3	1.3
Feb	0.8	0.7	0.8	0.7
Mar	0.8	0.6	0.7	0.7
Apr	0.7	0.5	0.6	0.6
May	0.8	0.7	0.7	0.7
Jun	1.0	0.9	0.9	0.9
Jul	1.0	1.0	0.9	0.9
Aug	1.8	1.9	1.8	1.8
Sep	1.8	2.0	2.0	2.0
Oct	2.1	2.1	2.1	2.2
Nov	1.4	1.5	1.4	1.6
Dec	1.3	1.4	1.3	1.4
Annual	14.8	14.3	14.6	14.7

WATER YIELD (mm)				
UKC	BASELINE	q14 scenarios		
Month	1990-2008	2020s	2050s	2080s
Jan	3.7	3.3	3.6	3.6
Feb	2.9	2.6	2.9	2.8
Mar	3.3	2.9	3.1	3.2
Apr	2.9	2.6	2.8	2.8
May	2.9	2.6	2.7	2.8
Jun	83.2	75.2	54.9	30.4
Jul	179.4	273.6	227.8	283.6
Aug	120.5	120.9	156.5	200.4
Sep	18.8	22.5	22.3	27.2
Oct	17.4	34.1	28.1	49.9
Nov	3.7	3.7	3.7	4.1
Dec	3.6	3.6	3.7	3.8
Ann Sum	442.2	547.7	512.2	614.6

(1) Precipitation: In comparison with the baseline period, the scenario assumes significant increases in precipitation by 126.9 mm (11.4%) in the 2020s, by 80.2 mm (7.2%) in the 2050s and by 227.2 mm (20.5%) in the 2080s.

(2) Discharge: Relative to the baseline scenario, the 2020s show an increase in the annual discharge sum by 256.3 million m^3 (23.6%), for the 2050s an increase by 168.2 million m^3 (15.5%), and for the 2080s an increase by 419.0 million m^3 (38.5%). The increase in discharge is driven by the trend towards higher rainfall.

(3) Surface runoff: The simulations indicate an increasing trend of surface runoff throughout the time periods under consideration as compared to the baseline scenario: for the 2020s an increase by 107.9 mm (26.8%), for the 2050s by 70.8 mm (17.6 %), and for the 2080s by 173.1 mm (43.1%).

(4) Percolation: Compared to the baseline scenario, the simulations show increasing percolation by 7.7 mm (8.7%) in the 2020s, by 2.1 mm (2.3%) in the 2050s, and by 8.1 mm (9.1%) in the 2080s.

(5) Actual evapotranspiration: The model predicts a slight decline in AET of 1.4 mm (0.2%) in the 2020s, whereas in the 2050s an increase by 21.6 mm (3.1%) and in the 2050s by 30.7 mm (4.3%) is simulated as compared to the baseline scenario.

(6) Groundwater contribution to streamflow: In comparison to the baseline scenario, a very slight decline in groundwater contribution of 0.5 mm and 0.1 mm for the 2020s and 2050s respectively, and almost no change for 2080s is predicted.

(7) Water yield: Compared to the baseline scenario, water yield shows an increase by 105.5 mm (23.8%) in the 2020s, by 69.9 mm (15.8%) in the 2050s and by 172.4 mm (39.0%) in the 2080s. The water yield trend follows the rainfall change pattern over the years.

7.4. Climate change impacts considering q0, q1 and q14 scenarios together

Based on the different PRECIS scenarios (q0, q1 and q14), a range of probable changes in water balance components is discussed.

Table 7.7: Percentage change in rainfall in PRECIS scenarios (q0, q1 and q14) compared to baseline

PRECIPITATION (mm)										
UKC	BASELINE	Q0	Q1	Q14	Q0	Q1	Q14	Q0	Q1	Q14
Month	1990-2008	% 2020s			% 2050s			% 2080s		
Jan	3.29	-22.49	5.78	-23.40	13.07	110.03	3.95	6.38	91.79	22.49
Feb	0	0.00	0.00	0.00	0.00	0.00	0.00	0.00	0.00	0.00
Mar	9.4	-18.51	59.79	-10.43	6.70	7.34	-13.62	-24.68	-0.96	11.38
Apr	11.61	8.70	-8.70	28.77	-10.51	-4.91	1.29	1.46	-32.90	17.92
May	8.03	-22.67	6.85	17.93	15.44	-18.43	-35.87	-30.01	-2.49	19.05
Jun	360.12	-27.91	-20.62	-3.67	-3.80	-38.79	-13.26	-29.17	-7.01	-29.41
Jul	352.48	6.25	-12.24	29.43	35.67	4.46	19.00	63.88	36.48	42.49
Aug	244.82	17.24	-6.17	-2.07	34.54	15.15	18.20	69.39	10.43	38.95
Sep	61.97	-1.55	-22.83	10.41	-9.68	-6.89	3.84	7.12	-7.63	26.77
Oct	56.14	55.84	7.77	57.46	18.63	23.82	30.21	59.90	9.98	109.94
Nov	2.39	-35.56	22.59	-13.81	-9.62	43.10	37.66	-12.97	-19.67	179.50
Dec	0	0.00	0.00	0.00	0.00	0.00	0.00	0.00	0.00	0.00
Annual	1110.24	-0.90	-12.29	11.4	18.19	-6.71	7.2	29.13	11.54	20.5

(1) Precipitation

The q0, q1 and q14 scenarios indicate different trends in annual precipitation in the 2020s and 2050s. Regarding the 2020s, q0 and q1 predict a decrease by 0.9% (q0) and 12.3% (q1), whereas q14 assumes an increase by 11.4% compared to the baseline (1110.24 mm). For the 2050s, predictions vary from a 6.7% decrease to 18.1% increase. For 2080s, all scenarios indicate an increase ranging between 11.5% and 29.1% relative to the baseline. In all scenarios, there is a decrease in rainfall in June.

(2) Actual evapotranspiration

An increase in actual evapotranspiration (AET) is predicted in all scenarios for different time steps except for the q14 scenario for the 2020s where a very slight decrease is predicted.

Table 7.8: Percentage change in actual evapotranspiration in PRECIS scenarios (q0, q1 and q14) compared to baseline

ACTUAL EVAPOTRANSPIRATION (mm)										
UKC	BASELINE	Q0	Q1	Q14	Q0	Q1	Q14	Q0	Q1	Q14
Month	1990-2008	% 2020s			% 2050s			% 2080s		
Jan	25.52	-1.25	6.07	1.37	21.16	14.77	13.17	21.24	14.38	7.88
Feb	25.79	0.00	0.00	0.00	0.00	0.00	0.00	0.00	0.00	0.00
Mar	40.63	16.15	13.76	2.17	25.28	10.07	8.74	20.45	11.05	10.07
Apr	42.77	10.24	4.42	-0.63	15.69	-0.16	-5.89	2.81	-7.44	-5.94
May	30.43	3.94	4.40	2.27	20.87	0.00	-4.57	6.74	-1.25	2.00
Jun	91.4	-2.66	12.71	1.49	8.85	2.66	5.43	5.26	20.48	1.12
Jul	99.29	-6.32	3.33	-9.96	-8.19	3.75	-7.40	-5.61	7.10	-6.38
Aug	90.57	-1.70	1.63	-1.84	0.02	6.02	1.57	2.27	10.10	1.25
Sep	99.81	1.29	3.47	2.02	4.92	8.22	5.54	7.97	14.49	7.87
Oct	88.93	-0.85	-0.27	1.17	3.38	4.25	4.98	11.50	7.42	14.39
Nov	42.14	4.13	0.97	3.84	7.55	5.36	7.48	9.18	7.05	10.49
Dec	30.12	0.00	0.00	0.00	0.00	0.00	0.00	0.00	0.00	0.00
Annual	707.39	1.69	4.86	-0.2	7.36	5.53	3.1	7.45	9.83	4.3

Compared to the baseline, the expected changes in the AET vary between a very slight decrease by 0.2% and a 4.86% increase. For the 2050s and 2080s, the scenarios show an increasing trend of 3.1% to 7.36% in the 2050s and 4.3% to 9.83% in the 2080s. The least increase is for the q14 scenario, while q1 features the highest increase.

(3) Discharge

Table 7.9: Percentage change in discharge for PRECIS scenarios (q0, q1 and q14) compared to baseline

DISCHARGE (m3/s)										
UKC	BASELINE	Q0	Q1	Q14	Q0	Q1	Q14	Q0	Q1	Q14
Month	1990-2008	% 2020s			% 2050s			% 2080s		
Jan	3.81	-98.85	11.71	-11.92	-9.64	-6.91	-5.04	8.04	-13.58	-5.09
Feb	3.51	0.00	0.00	0.00	0.00	0.00	0.00	0.00	0.00	0.00
Mar	3.19	-96.61	32.19	-10.02	1.97	-9.17	-4.66	10.71	-13.53	-3.13
Apr	2.89	-95.92	12.05	-11.50	-8.73	-13.50	-5.47	12.40	-17.24	-4.61
May	2.78	-94.89	4.96	-10.64	-18.48	-14.81	-4.10	8.38	-18.34	-4.46
Jun	45.02	-76.79	-60.15	-11.75	-11.59	-83.97	-43.98	-73.99	-33.65	-74.14
Jul	158.50	-11.99	-38.95	49.72	58.04	-33.63	20.50	84.29	42.02	45.93
Aug	115.60	20.76	-17.45	6.83	59.86	12.72	30.62	115.66	17.47	66.44
Sep	48.69	6.33	-5.59	4.03	11.07	2.81	14.03	23.06	0.14	21.77
Oct	22.78	41.88	-2.72	45.22	10.36	6.58	28.27	58.74	-1.19	102.77
Nov	9.21	51.18	12.87	68.01	20.69	14.72	43.15	62.47	-4.91	113.59
Dec	3.87	0.00	0.00	0.00	0.00	0.00	0.00	0.00	0.00	0.00
Annual	419.86	-6.51	-25.88	23.6	39.36	-17.62	15.5	63.68	16.26	38.5

For the 2020s and 2050s, the simulations indicate opposite trends of discharge compared to the baseline depending on the PRECIS scenario used. For the 2020s, there is a decrease from 25.9% to an increase of 23.6%, and for the 2050s there is a 17.6% decrease to a 39.4% increase. The simulations of 2080s agree on an increasing trend in the range of 16.3% to 63.7% depending on the PRECIS scenario used.

(4) Surface runoff

Table 7.9: Percentage change in surface runoff for different PRECIS scenarios (q0, q1 and q14) compared to baseline

SURFACE RUNOFF (mm)										
UKC	BASELINE	Q0	Q1	Q14	Q0	Q1	Q14	Q0	Q1	Q14
Month	1990-2008	% 2020s			% 2050s			% 2080s		
Jan	0.06	-16.67	-16.67	-50.00	133.33	233.33	0.00	66.67	100.00	0.00
Feb	0	0.00	0.00	0.00	0.00	0.00	0.00	0.00	0.00	0.00
Mar	0.23	-47.83	391.30	21.74	56.52	60.87	4.35	-13.04	34.78	26.09
Apr	0.1	40.00	50.00	60.00	40.00	-10.00	50.00	40.00	-50.00	30.00
May	0.04	-50.00	25.00	50.00	0.00	-25.00	-50.00	-50.00	0.00	75.00
Jun	80.33	-58.16	-50.69	-9.65	-7.74	-77.89	-35.01	-63.71	-27.56	-65.48
Jul	176.35	-0.91	-32.67	53.59	61.51	-18.51	27.56	95.95	48.86	59.26
Aug	116.67	27.13	-15.33	0.45	61.93	17.64	30.92	122.38	14.01	68.54
Sep	14.88	0.40	-30.04	24.87	-9.81	-16.33	22.92	19.62	-20.16	56.25
Oct	13.06	121.90	31.32	128.79	29.33	36.06	82.47	122.28	6.66	248.32
Nov	0.05	-60.00	20.00	-40.00	-20.00	100.00	20.00	-60.00	-60.00	580.00
Dec	0	0.00	0.00	0.00	0.00	0.00	0.00	0.00	0.00	0.00
Annual	401.78	-0.21	-28.78	26.8	44.08	-17.94	17.6	69.61	19.48	43.1

Simulations on surface runoff show opposite trends in the 2020s and 2050s depending on the PRECIS scenario. As surface runoff is the main contribution to discharge, a similarity with the discharge pattern (see above) can be observed. For the 2020s, surface runoff is found in the range of 28.8% decrease to 26.8% increase. For the 2050s, the predictions vary between 17.9% decrease to 44.1% increase, and for the 2080s all scenarios lead to an increasing trend in the range of 19.5% to 69.6%.

(5) Percolation

Table 7.10: Percentage change in surface runoff for different PRECIS scenarios (q0, q1 and q14) compared to baseline

PERCOLATION (mm)										
UKC	BASELINE	Q0	Q1	Q14	Q0	Q1	Q14	Q0	Q1	Q14
Month	1990-2008	% 2020s			% 2050s			% 2080s		
Jan	0.71	-70.42	33.80	0.00	115.49	26.76	5.63	94.37	15.49	-5.63
Feb	0.66	0.00	0.00	0.00	0.00	0.00	0.00	0.00	0.00	0.00
Mar	0.86	53.49	40.70	6.98	108.14	12.79	-17.44	43.02	5.81	-4.65
Apr	0.58	143.10	15.52	13.79	158.62	12.07	-3.45	68.97	6.90	0.00
May	0.09	-22.22	33.33	44.44	11.11	0.00	-22.22	-33.33	33.33	66.67
Jun	12.37	-38.97	-35.41	-5.66	-2.10	-54.16	-22.72	-43.01	-19.08	-44.54
Jul	24.05	-2.12	-18.92	16.67	20.96	-12.72	7.78	23.83	14.72	15.68
Aug	21.75	10.11	-6.57	2.30	21.89	5.20	12.37	36.37	5.38	22.67
Sep	10.23	-1.76	2.05	4.01	-4.01	-11.83	16.23	-0.20	-16.72	6.45
Oct	14.48	20.51	-13.47	22.72	4.28	4.42	-4.90	16.99	-3.94	33.29
Nov	1.32	11.36	-3.03	-0.76	-8.33	-10.61	-13.64	-25.76	-25.00	-17.42
Dec	0.98	0.00	0.00	0.00	0.00	0.00	0.00	0.00	0.00	0.00
Annual	88.10	1.76	-12.81	8.7	15.43	-10.27	2.3	13.69	-0.34	9.1

For the 2020s, annual percolation is found in the range of 12.8% decrease to 8.7% increase compared to the baseline. Predictions for the 2050s vary between 10.3% decrease and 15.4% increase, and for the 2080s from 0.3% decrease to 13.7% increase. Scenario q1 shows a decrease in all the time steps compared to the baseline.

(6) Groundwater contribution to streamflow:

Table 7.11: Percentage change in groundwater contribution to streamflow for PRECIS scenarios (q0, q1 and q14) compared to baseline

GROUND-WATER CONTRIBUTION TO STREAMFLOW (GWQ) : mm										
UKC	BASELINE	Q0	Q1	Q14	Q0	Q1	Q14	Q0	Q1	Q14
Month	1990-2008	% 2020s			% 2050s			% 2080s		
Jan	1.30	-100.00	48.46	-11.54	73.08	-13.08	-1.54	69.23	-18.46	-3.85
Feb	0.84	0.00	0.00	0.00	0.00	0.00	0.00	0.00	0.00	0.00
Mar	0.76	-90.79	44.74	-19.74	139.47	-22.37	-11.84	106.58	-27.63	-10.53
Apr	0.68	-88.24	10.29	-20.59	73.53	-27.94	-10.29	101.47	-30.88	-11.76
May	0.82	-90.24	10.98	-19.51	35.37	-23.17	-12.20	51.22	-28.05	-10.98
Jun	1.01	-78.22	2.97	-11.88	15.84	-23.76	-9.90	28.71	-23.76	-14.85
Jul	0.99	-13.13	-3.03	-4.04	66.67	-22.22	-5.05	49.49	-14.14	-10.10
Aug	1.82	-1.10	6.04	2.75	33.52	-7.14	-0.55	29.12	1.10	-1.65
Sep	1.84	27.72	3.26	8.15	46.20	-4.35	10.87	48.37	2.72	8.15
Oct	2.06	40.78	10.68	2.43	49.51	-11.17	1.94	52.91	-5.83	7.28
Nov	1.40	109.29	7.14	4.29	101.43	-9.29	2.14	71.43	-4.29	10.71
Dec	1.27	0.00	0.00	0.00	0.00	0.00	0.00	0.00	0.00	0.00
Annual	14.77	-6.97	14.69	-3.2	64.73	-13.27	-0.9	59.11	-10.43	-0.3

Predictions on the groundwater contribution to streamflow strongly depend on the PRECIS scenario as indicated by different trends compared to the baseline. For the 2020s, annual groundwater contribution to streamflow is in the range of 7.0% decrease to 14.7% increase. The simulations for the 2050s predict 13.3% decrease to 64.7% increase, and for the 2080s the range is 10.4% decrease to 59.1% increase. Scenario q1 shows a decrease in all the time steps compared to the baseline.

(7) Water yield

Table 7.12: Percentage change in water yield for PRECIS scenarios (q0, q1 and q14) compared to the baseline

WATER YEILD (mm)										
UKC	BASELINE	Q0	Q1	Q14	Q0	Q1	Q14	Q0	Q1	Q14
Month	1990-2008	% 2020s			% 2050s			% 2080s		
Jan	3.72	-98.66	13.71	-11.02	-7.26	-6.99	-2.96	12.63	-13.17	-2.96
Feb	2.94	0.00	0.00	0.00	0.00	0.00	0.00	0.00	0.00	0.00
Mar	3.25	-93.85	35.38	-10.15	1.54	-8.62	-4.92	11.38	-13.23	-3.08
Apr	2.89	-92.04	1.38	-9.69	-16.96	-14.88	-3.46	12.80	-19.03	-4.50
May	2.94	-95.58	1.02	-11.56	-23.13	-14.63	-6.80	2.38	-17.01	-4.42
Jun	83.21	-59.31	-48.91	-9.69	-8.32	-75.68	-33.97	-61.46	-27.16	-63.42
Jul	179.37	-2.03	-32.21	52.56	60.37	-18.50	27.01	94.40	47.79	58.13
Aug	120.51	24.79	-14.83	0.35	59.85	16.75	29.87	118.70	13.39	66.26
Sep	18.77	-5.54	-24.24	19.87	-6.61	-14.76	18.91	19.18	-16.78	45.07
Oct	17.36	87.50	23.85	96.54	24.54	24.14	61.98	97.35	3.17	187.50
Nov	3.69	2.44	-1.90	-1.08	24.39	-9.76	0.00	23.04	-7.59	11.92
Dec	3.6	0.00	0.00	0.00	0.00	0.00	0.00	0.00	0.00	0.00
Annual	442.23	-5.47	-25.95	23.8	39.91	-17.41	15.8	64.46	16.68	39.0

As water yield is dominated by surface runoff and discharge, the pattern of predicted changes is similar. Compared to the baseline, the annual water yield is in the range of 26.0% decrease to 23.8% increase for the 2020s. For the 2050s, a 17.4% decrease to 39.9% increase is simulated, and for the 2080s, the scenarios follow this increasing trend with magnitudes ranging from 16.7% to 64.5%. Compared to the baseline, q14 shows an increase in all time steps.

7.5 Impact of PRECIS average, high and low rainfall scenarios on water balance components

Runoff-rainfall ratio analyses were carried out for the PRECIS average, high and low rainfall conditions of the q0, q1 and q14 scenarios. The results are discussed (1) with regard to runoff-rainfall ratios (Table 7.13, 7.14 and 7.15), and (2) the effect of increased rainfall on surface runoff and percolation will be considered with respect to the q1 scenario (Tables 7.16, 7.17 and 7.18).

(1) Runoff-rainfall ratio of PRECIS average rainfall conditions

Table 7.13: Runoff-rainfall ratio for PRECIS average rainfall for q0, q1 and q14 scenarios

Baseline	q0 scenarios			Baseline	q1 scenarios			Baseline	q14 scenarios		
1990-2008	2020s	2050s	2080s	1990-2008	2020s	2050s	2080s	1990-2008	2020s	2050s	2080s
0.39	0.37	0.46	0.50	0.39	0.33	0.35	0.41	0.39	0.44	0.42	0.45

(2) Runoff-rainfall ratio of PRECIS high rainfall conditions

Table 7.14: Runoff-rainfall ratio for PRECIS high rainfall for q0, q1 and q14 scenarios:

Baseline	q0 scenarios			Baseline	q1 scenarios			Baseline	q14 scenarios		
1990-2008	2020s	2050s	2080s	1990-2008	2020s	2050s	2080s	1990-2008	2020s	2050s	2080s
0.57	0.56	0.63	0.66	0.57	0.52	0.55	0.59	0.57	0.61	0.60	0.63

(3) Runoff-rainfall ratio of PRECIS low rainfall conditions

Table 7.15: Runoff-rainfall ratio for PRECIS low rainfall for q0, q1 and q14 scenarios

Baseline	q0 scenarios			Baseline	q1 scenarios			Baseline	q14 scenarios		
1990-2008	2020s	2050s	2080s	1990-2008	2020s	2050s	2080s	1990-2008	2020s	2050s	2080s
0.26	0.26	0.35	0.40	0.26	0.20	0.24	0.30	0.26	0.31	0.29	0.34

The results indicate larger/smaller runoff-rainfall ratios for the scenarios based on high/low rainfall conditions. This means that the model in a plausible way simulates an over-proportional relationship between runoff and rainfall level.

(2) Effect of high and low rainfall conditions on surface runoff and percolation

Table 7.16: q1 scenario impact on water resources: average climate conditions

PRECIPITATION (mm)				
UKC	BASELINE	q1 scenarios		
Month	1990-2008	2020s	2050s	2080s
Jan	3.3	3.5	6.9	6.3
Feb	0.0	0.0	0.0	0.0
Mar	9.4	15.0	10.1	9.3
Apr	11.6	10.6	11.0	7.8
May	8.0	8.6	6.6	7.8
Jun	360.1	285.9	220.4	334.9
Jul	352.5	309.3	368.2	481.1
Aug	244.8	229.7	281.9	270.4
Sep	62.0	47.8	57.7	57.2
Oct	56.1	60.5	69.5	61.7
Nov	2.4	2.9	3.4	1.9
Dec	0.0	0.0	0.0	0.0
Annual	1110.2	973.8	1035.8	1238.4

SURFACE RUNOFF (mm)				
UKC	BASELINE	q1 scenarios		
Month	1990-2008	2020s	2050s	2080s
Jan	0.1	0.1	0.2	0.1
Feb	0.0	0.0	0.0	0.0
Mar	0.2	1.1	0.4	0.3
Apr	0.1	0.2	0.1	0.1
May	0.0	0.1	0.0	0.0
Jun	80.3	39.6	17.8	58.2
Jul	176.4	118.7	143.7	262.5
Aug	116.7	98.8	137.3	133.0
Sep	14.9	10.4	12.5	11.9
Oct	13.1	17.2	17.8	13.9
Nov	0.1	0.1	0.1	0.0
Dec	0.0	0.0	0.0	0.0
Annual	401.8	286.1	329.7	480.1

PERCOLATION (mm)				
UKC	BASELINE	q1 scenarios		
Month	1990-2008	2020s	2050s	2080s
Jan	0.7	1.0	0.9	0.8
Feb	0.7	1.0	0.7	0.7
Mar	0.9	1.2	1.0	0.9
Apr	0.6	0.7	0.7	0.6
May	0.1	0.1	0.1	0.1
Jun	12.4	8.0	5.7	10.0
Jul	24.1	19.5	21.0	27.6
Aug	21.8	20.3	22.9	22.9
Sep	10.2	10.4	9.0	8.5
Oct	14.5	12.5	15.1	13.9
Nov	1.3	1.3	1.2	1.0
Dec	1.0	0.8	0.9	0.7
Annual	88.1	76.8	79.1	87.8

Table 7.17: q1 scenarios impact on water resources: wet climate conditions

PRECIPITATION (mm)				
UKC	BASELINE	q1 scenarios		
Month	1990-2008	2020s	2050s	2080s
Jan	0.6	0.5	1.1	0.8
Feb	1.7	1.1	1.3	1.5
Mar	0.0	0.0	0.0	0.0
Apr	1.8	1.3	1.3	0.9
May	3.1	4.3	2.9	3.9
Jun	286.6	230.5	176.2	268.7
Jul	638.8	559.9	666.8	871.4
Aug	402.0	374.6	461.3	443.0
Sep	232.7	175.0	211.3	214.5
Oct	36.0	39.7	45.2	40.7
Nov	1.0	1.5	1.7	1.0
Dec	0.0	0.0	0.0	0.0
Annual	1604.3	1388.4	1569.1	1846.4

SURFACE RUNOFF (mm)				
UKC	BASELINE	q1 scenarios		
Month	1990-2008	2020s	2050s	2080s
Jan	0.0	0.0	0.1	0.0
Feb	0.1	0.1	0.1	0.1
Mar	0.0	0.0	0.0	0.0
Apr	0.1	0.0	0.0	0.0
May	0.1	0.2	0.1	0.2
Jun	50.0	26.3	11.3	38.7
Jul	429.2	330.0	396.7	612.9
Aug	241.0	212.7	285.1	269.1
Sep	139.1	98.8	119.8	118.2
Oct	9.3	9.7	13.0	11.0
Nov	0.0	0.0	0.1	0.0
Dec	0.0	0.0	0.0	0.0
Annual	869.0	677.9	826.2	1050.3

PERCOLATION (mm)				
UKC	BASELINE	q1 scenarios		
Month	1990-2008	2020s	2050s	2080s
Jan	0.8	1.0	0.9	0.8
Feb	0.8	1.2	0.9	0.8
Mar	0.7	0.9	0.8	0.8
Apr	0.6	0.7	0.7	0.6
May	0.2	0.3	0.2	0.3
Jun	9.3	6.2	4.3	7.6
Jul	28.4	24.1	26.2	32.5
Aug	29.8	28.7	31.5	31.3
Sep	24.4	22.5	22.4	22.3
Oct	11.7	9.8	11.9	11.6
Nov	1.3	1.5	1.4	1.3
Dec	1.1	1.0	1.0	0.9
Annual	109.2	97.8	102.1	110.8

Table 7.18: q1 scenarios impact on water resources: dry climate conditions

PRECIPITATION (mm)				
UKC	BASELINE	q1 scenarios		
Month	1990-2008	2020s	2050s	2080s
Jan	1.5	1.6	3.0	3.5
Feb	15.8	10.9	10.8	13.8
Mar	0.0	0.0	0.0	0.0
Apr	0.0	0.0	0.0	0.0
May	28.2	28.8	22.0	26.3
Jun	194.4	153.9	117.8	179.6
Jul	291.1	256.4	304.2	396.6
Aug	143.8	133.4	164.4	158.0
Sep	58.6	43.9	52.7	54.0
Oct	3.0	3.4	3.8	3.5
Nov	0.0	0.0	0.0	0.0
Dec	0.0	0.0	0.0	0.0
Annual	736.4	632.4	678.5	835.4

SURFACE RUNOFF (mm)				
UKC	BASELINE	q1 scenarios		
Month	1990-2008	2020s	2050s	2080s
Jan	0.1	0.2	0.4	0.5
Feb	0.5	0.4	0.3	0.4
Mar	0.0	0.0	0.0	0.0
Apr	0.0	0.0	0.0	0.0
May	0.2	0.3	0.2	0.2
Jun	10.9	4.5	2.5	6.6
Jul	113.8	71.8	88.6	176.2
Aug	29.3	20.0	35.9	35.4
Sep	17.1	7.0	13.5	14.0
Oct	0.5	0.5	0.8	0.7
Nov	0.0	0.0	0.0	0.0
Dec	0.0	0.0	0.0	0.0
Annual	172.5	104.6	142.0	234.0

PERCOLATION (mm)				
UKC	BASELINE	q1 scenarios		
Month	1990-2008	2020s	2050s	2080s
Jan	0.6	0.9	0.7	0.7
Feb	0.8	1.2	0.9	0.9
Mar	0.6	0.9	0.8	0.8
Apr	0.4	0.6	0.6	0.5
May	0.1	0.2	0.1	0.2
Jun	5.8	3.5	1.9	4.6
Jul	15.5	11.6	12.8	18.8
Aug	10.9	9.1	12.1	12.2
Sep	13.0	12.1	11.2	11.3
Oct	9.1	7.2	8.7	8.7
Nov	1.0	1.0	0.8	0.7
Dec	0.8	0.7	0.6	0.5
Annual	58.7	48.8	51.1	59.9

As an example, these analyses were performed for the scenario q1, because this scenario is less biased with regard to the study area. The surface runoff and the percolation are driven by changes in rainfall (Table 7.16, 7.17 and 7.18). Yet the magnitude of the effect is high in terms

of surface runoff and very low for percolation. With respect to groundwater management, it can be concluded that recharge is expected to remain nearly constant (despite increase in rainfall) whereas at least in parts of the catchment the groundwater withdrawals for intensifying cropping pattern will increase and, as a consequence, the risk of over-exploitation needs to be considered and counterbalanced by management measures. With respect to the rather strong effect of the predicted increase in rainfall on surface runoff, it makes sense to (i) think about additional facilities and strategies to increase the storage capacity of the landscape, and (ii) carry out more detailed runoff-rainfall analyses with higher temporal resolution in order to assess a potentially increasing risk of floods.

7.6 Impacts of combined climate change and land-use change on water resources for the 2020s

The land-use map of 2021 and the PRECIS climate scenarios (q0, q1 and14) for the 2020s were used to analyze the combined impact on water balance components. The reference-calibrated parameter values of the 2000-2006 model were used. The results of these PRECIS scenarios are compared with the baseline scenario (2011 land-use and climate of 1990-2008). The results are expressed as percentage change in water balance components (Table 7.19).

Table 7.19: Combined impact of climate and land-use change on water balance for the 2020s (% change between 2011 and 2021)

PRECIPITATION (mm)				
UKC	BASELINE	SCENARIOS		
Scenario	LULC 2011	LULC 2021 & Climate 2020s		
Month	1990-2008	%q0	%q1	%q14
Jan	3.3	-22.5	5.5	-23.4
Feb	0.0	0.0	0.0	0.0
Mar	9.4	-18.6	59.7	-10.5
Apr	11.6	8.6	-8.8	28.7
May	8.0	-22.7	6.8	17.8
Jun	360.1	-27.9	-20.6	-3.7
Jul	352.5	6.2	-12.3	29.4
Aug	244.8	17.2	-6.2	-2.1
Sep	62.0	-1.6	-22.8	10.4
Oct	56.1	55.8	7.7	57.4
Nov	2.4	-35.6	22.6	-13.8
Dec	0.0	0.0	0.0	0.0
Annual	1110.2	-0.9	-12.3	11.4

DISCHARGE - REACH 01 - m3/s				
UKC	BASELINE	SCENARIOS		
Scenario	LULC 2011	LULC 2021 & Climate 2020s		
Month	1990-2008	%q0	%q1	%q14
Jan	3.8	-97.7	-21.6	-34.4
Feb	3.5	0.0	0.0	0.0
Mar	3.2	-93.6	5.5	-31.8
Apr	2.9	-93.7	-18.5	-31.6
May	2.8	-93.2	-22.3	-30.1
Jun	45.0	-68.3	-59.7	-14.9
Jul	158.5	-4.5	-38.4	49.1
Aug	115.6	23.3	-17.2	6.2
Sep	48.7	6.5	-5.6	3.7
Oct	22.8	37.4	-3.1	43.9
Nov	9.2	40.2	9.3	66.3
Dec	3.9	0.0	0.0	0.0
Annual Sum (mio m*3)	1088.3	-2.8	-27.0	21.7

SURFACE RUNOFF (mm)				
UKC	BASELINE	SCENARIOS		
Scenario	LULC 2011	LULC 2021 & Climate 2020s		
Month	1990-2008	%q0	%q1	%q14
Jan	0.1	66.7	50.0	-16.7
Feb	0.0	0.0	0.0	0.0
Mar	0.2	-17.4	521.7	26.1
Apr	0.1	140.0	40.0	120.0
May	0.0	-25.0	125.0	150.0
Jun	80.3	-50.2	-49.4	-10.2
Jul	176.4	5.5	-31.9	53.4
Aug	116.7	29.2	-14.6	0.7
Sep	14.9	2.9	-29.2	26.2
Oct	13.1	121.2	30.9	128.1
Nov	0.1	20.0	80.0	20.0
Dec	0.0	0.0	0.0	0.0
Annual	401.8	4.9	-27.9	26.8

PERCOLATION (mm)				
UKC	BASELINE	SCENARIOS		
Scenario	LULC 2011	LULC 2021 & Climate 2020s		
Month	1990-2008	%q0	%q1	%q14
Jan	0.7	11.3	67.6	-28.2
Feb	0.7	0.0	0.0	0.0
Mar	0.9	209.3	47.7	-44.2
Apr	0.6	351.7	5.2	-56.9
May	0.1	44.4	44.4	33.3
Jun	12.4	-36.0	-37.0	-8.6
Jul	24.1	3.8	-19.3	15.0
Aug	21.8	9.7	-7.6	0.6
Sep	10.2	-3.9	-0.4	0.7
Oct	14.5	17.7	-15.6	20.0
Nov	1.3	40.9	5.3	3.0
Dec	1.0	0.0	0.0	0.0
Annual	88.1	10.6	-13.3	5.0

ACTUAL EVAPOTRANSPIRATION (mm)				
UKC	BASELINE	SCENARIOS		
Scenario	LULC 2011	LULC 2021 & Climate 2020s		
Month	1990-2008	%q0	%q1	%q14
Jan	25.5	27.3	13.6	2.9
Feb	25.8	0.0	0.0	0.0
Mar	40.6	76.4	30.2	10.0
Apr	42.8	69.0	11.6	1.6
May	30.4	39.8	-3.3	-13.6
Jun	91.4	0.8	10.7	-1.2
Jul	99.3	-6.9	2.7	-10.6
Aug	90.6	-2.3	1.2	-2.2
Sep	99.8	0.5	2.6	1.3
Oct	88.9	-1.3	-1.1	0.4
Nov	42.1	9.8	3.8	5.8
Dec	30.1	0.0	0.0	0.0
Annual	707.4	15.2	6.3	-0.6

Ground-water contribution to streamflow (mm)				
UKC	BASELINE	SCENARIOS		
Scenario	LULC 2011	LULC 2021 & Climate 2020s		
Month	1990-2008	%q0	%q1	%q14
Jan	1.3	-99.2	-56.9	-70.0
Feb	0.8	0.0	0.0	0.0
Mar	0.8	-90.8	-92.1	-97.4
Apr	0.7	-92.6	-89.7	-94.1
May	0.8	-95.1	-63.4	-90.2
Jun	1.0	-85.1	-29.7	-76.2
Jul	1.0	-43.4	-60.6	-75.8
Aug	1.8	-40.1	-27.5	-50.0
Sep	1.8	-25.5	-1.6	0.0
Oct	2.1	-21.4	-13.1	-4.9
Nov	1.4	15.0	-37.9	-28.6
Dec	1.3	0.0	0.0	0.0
Annual	14.8	-44.3	-42.9	-51.9

WATER YIELD (mm)				
UKC	BASELINE	SCENARIOS		
Scenario	LULC 2011	LULC 2021 & Climate 2020s		
Month	1990-2008	%q0	%q1	%q14
Jan	3.7	-97.0	-20.7	-32.3
Feb	2.9	0.0	0.0	0.0
Mar	3.3	-91.4	13.8	-29.5
Apr	2.9	-88.6	-20.8	-27.0
May	2.9	-95.6	-17.0	-31.6
Jun	83.2	-51.6	-48.0	-11.0
Jul	179.4	4.1	-31.7	52.0
Aug	120.5	26.2	-14.6	-0.3
Sep	18.8	-8.4	-23.8	19.8
Oct	17.4	80.0	20.8	94.8
Nov	3.7	-30.6	-17.3	-14.4
Dec	3.6	0.0	0.0	0.0
Annual	442.2	-1.9	-26.9	22.0

(1) Precipitation: As mentioned in section 7.4, annual rainfall for the 2020s decreases by 0.9% according to the q0 scenario, decreases by 12.3%, according to the q1 scenario, whereas the rainfall in the q14 scenario increases by 11.4% as compared to the baseline.

(2) Actual evapotranspiration (AET): Simulation results in section 7.6 show that for the 2020s, annual AET increases by 15.2% in the q0 scenario and by 6.3% in the q1 scenario, and shows a slight decrease by 0.6% in the q14 scenario as compared to the baseline.

(3) Discharge: Compared to the baseline, annual discharge sum for the 2020s decreases by 2.8% and 28.0% for the q0 and q1 scenarios, respectively, whereas it increases by 21.7% in the q14 scenario.

(4) Surface runoff: In comparison to the baseline scenario, annual surface runoff decreases by 27.9% for the q1 scenario, whereas it increases by 4.9% and 26.8 % for the q0 and q14 scenarios, respectively.

(5) Percolation: Compared to the baseline, annual percolation decreases by 13.3% for the q1 scenario. In contrast, it increases by 10.6% and 5.0% for the q0 the q14 scenarios, respectively.

(6) Groundwater contribution to streamflow: Compared to the baseline, the groundwater contribution to streamflow decreases significantly by 44.3%, 42.9% and 51.9% for the q0, q1 and q14 scenarios, respectively. It corresponds well with an increasing share of groundwater-irrigated areas in 2021 which result in a reduction in groundwater available for contribution to the streamflow.

(7) Water yield: In comparison to the baseline, the water yield decreases by 1.9% and 26.9% in the q0 and q1 scenarios, respectively, whereas it is predicted to increase by 22.0% in the q14 scenario.

7.7 Groundwater level and irrigation

The groundwater levels are regularly monitored by the Central Groundwater Board (CGWB) and State Groundwater Board (SGWB), Chhattisgarh. Monitoring is carried out four times per annum, i.e., in the first week of January (winter), May (before monsoon), August (during monsoon) and November (post monsoon).

In the present study, the historic groundwater level measurements of the SGWB from 1993 to 2011 were considered for trend analysis of groundwater levels. There are 27 spatially well distributed observation stations over the entire study area. Mann Kendall test with Theil-Sen's slope estimate was used for trend analysis and judged at $p \leq 0.1$ level of significance (Table 7.20).

A further groundwater level trend detection analysis of different groundwater levels with data from stations monitored at varying observation dates by the Central Groundwater Board was carried out separately (Table 7.21).

For the Mann Kendall test, the groundwater level data for more than 10 periods are a prerequisite, so only the stations fulfilling the required criteria were selected for the analysis.

Table 7.20: Trend detection analysis of groundwater levels 1993-2011 (data from State Ground Water Board)

S.No.	Obs. Station	Groundwater level change (m/annum)				Significance level (p≤0.1)
	DHAMTARI	January	May	August	November	
1	Bhakara	0.001	-0.303	0.097	0.077	May (p=0.01), Aug (p=0.001) & Nov (p=0.1)
2	Bhatagaon	0.033	0.050	-0.010	-0.018	No significance level
3	Jamgaon	-0.122	0.000	-0.001	-0.007	Jan (p=0.01)
4	Kurud	-0.115	0.000	0.038	0.050	Jan (p=0.1)
5	Chhati	-0.092	0.012	0.040	0.028	Jan (p=0.05) & Aug (p=0.05)
	DURG	January	May	August	November	
6	Armari Kalan	-0.020	0.148	0.015	-0.020	No significance level
7	Belhari	-0.004	0.150	-0.013	0.007	No significance level
8	Funda	0.025	0.073	-0.001	0.005	No significance level
9	Gadadih	0.015	-0.087	-0.037	0.003	Aug (p=0.1)
10	Gurur	-0.027	0.047	-0.014	0.005	No significance level
11	Jagtara	0.019	0.074	-0.035	0.110	Nov (p=0.05)
12	Jamgaon	0.075	-0.122	-0.050	0.088	May (p=0.1) & Aug (p=0.1)
13	Jamul	-0.060	-0.052	-0.030	-0.017	Jan (p=0.1) & May (p=0.1)
14	Karahibadar	0.044	0.195	0.048	0.060	May (p=0.1) & Aug (p=0.01)
15	Kuliya	0.033	0.191	0.018	0.008	No significance level
16	Kumhari	-0.150	-0.025	-0.036	-0.094	Jan (p=0.05) & Nov (p=0.01)
17	Murmunda	-0.085	-0.178	-0.013	-0.104	Jan (p=0.1), May (p=0.001) & Nov (p=0.01)
18	Palari	-0.075	-0.081	-0.121	-0.068	Jan (p=0.1), May (p=0.1) & Nov (p=0.1)
19	Patan	-0.297	-0.250	-0.025	-0.066	Jan (p=0.01), May (p=0.05) & Nov (p=0.05)
20	Patora	0.106	0.155	-0.020	0.055	Jan (p=0.05), May (p=0.05) & Nov (p=0.01)
21	Purur	-0.020	-0.044	-0.025	0.039	No significance level
22	Tarra	0.081	0.025	0.000	0.072	No significance level
23	Urla	-0.046	-0.020	-0.027	0.030	No significance level
	RAIPUR	January	May	August	November	
24	Abhanpur	-0.142	0.025	-0.044	-0.054	Jan (p=0.01) & Aug (p=0.1)
25	Dharsiwa	-0.100	-0.006	-0.086	-0.115	Aug (p=0.1) & Nov (p=0.05)
26	Mana	-0.065	-0.008	0.026	0.006	Jan (p=0.01)
27	Raipur	0.275	0.176	0.013	0.096	Jan (p=0.001), May (p=0.001) & Nov (p=0.05)

Table 7.21: Trend detection analysis of groundwater levels (data from Central Ground Water Board)

S.No.	Obs. Station	Period of Observation	Groundwater level change (m/annum)				Significance level (p≤0.1)
			January	May	August	November	
1	Bhilai nagar	1989-2002	-0.040	-0.038	0.051	0.006	Aug (p=0.1)
2	Funda	1995-2011	0.056	0.215	-0.008	0.070	May (p=0.001) & Nov (p=0.01)
3	Gurur	1987-2011	-0.065	-0.143	-0.014	-0.028	Jan (p=0.01)
4	Gurur_HP	2001-2011	0.234	0.350	0.450	0.368	Aug (p=0.05)
5	Kumhari	2001-2011	-0.285	-0.384	-0.020	0.041	No significance level
6	Motipur	1988-2011	0.016	0.042	-0.015	-0.004	Aug (p=0.01)
7	Patan	1987-2011	-0.196	-0.061	-0.052	-0.148	Jan (p=0.05), Aug (p=0.05) & Nov (p=0.1)

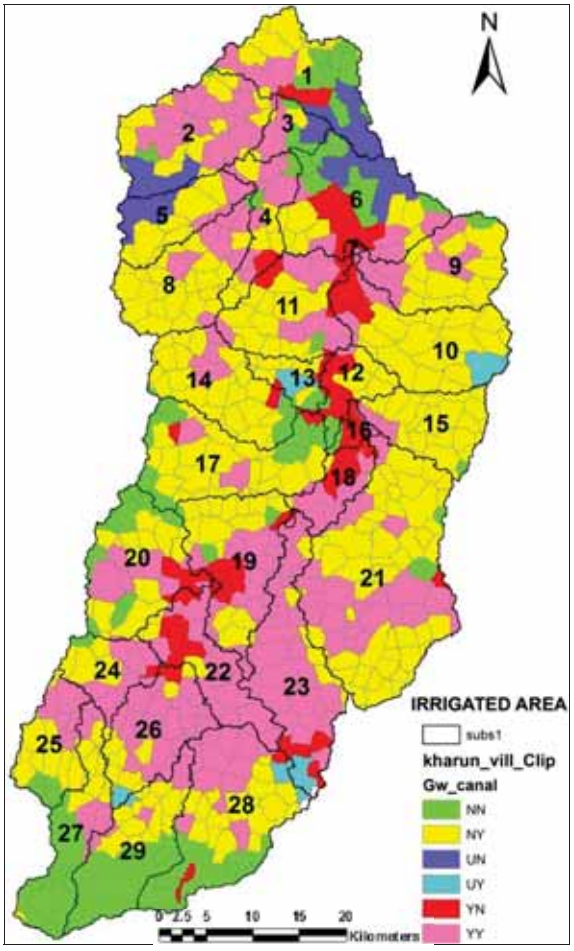

Figure 7.1: Annual canal and groundwater irrigated areas of UKC in 2011

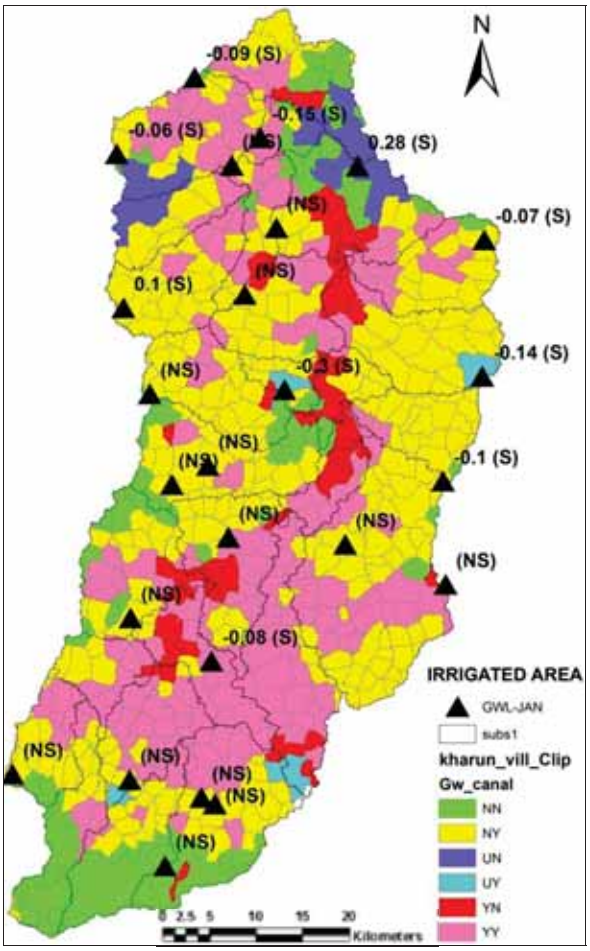

Figure 7.2: Groundwater level trend for January (1993-2011)

Legend
S: Significant trend (p≤0.1)
NS: Non-significant trend
NN: No irrigation
NY: Villages with groundwater-irrigated areas less than 75 ha and irrigated by canal water.

UN: Urban settlement without irrigation
UY: Urban settlement without groundwater irrigation, but with canal irrigation of urban vegetation area
YN: Villages with groundwater-irrigated areas more than 75 ha and no canal irrigation (non-command area)
YY: Area irrigated by both canal and groundwater resources

YN: sites without access to canal networks and irrigated extensively by groundwater irrigation only. These are hotspot areas, which should be examined in terms of sustainable management of groundwater managements. These areas may suffer less groundwater recharge compared to the amount of groundwater withdrawal.
YY: Area irrigated by both canal and more than 75 ha area by groundwater resources. These areas are also considered as hotspot areas and should be considered for sustainable management of water resources.

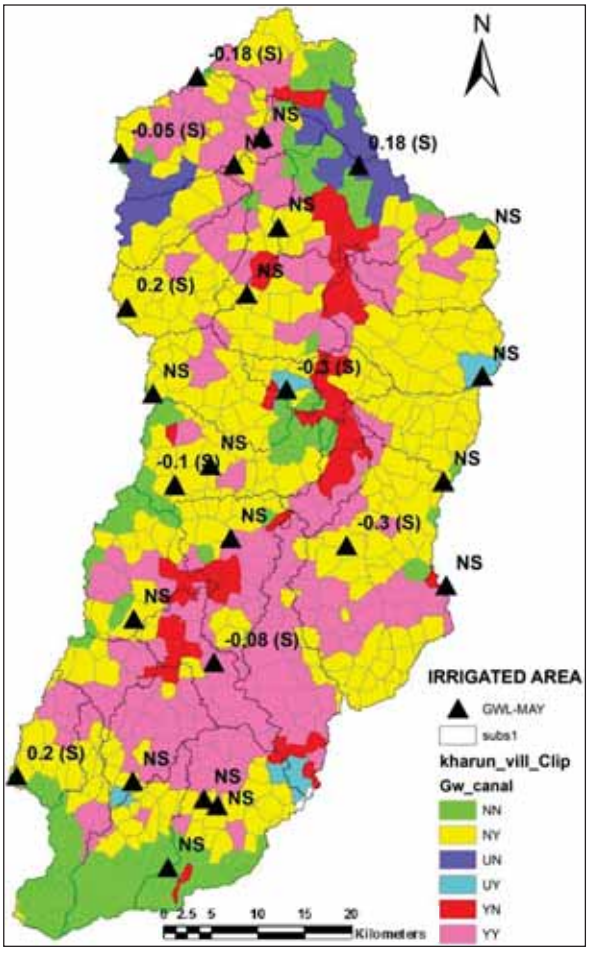

Figure 7.3: Groundwater level trend for May (1993-2011)

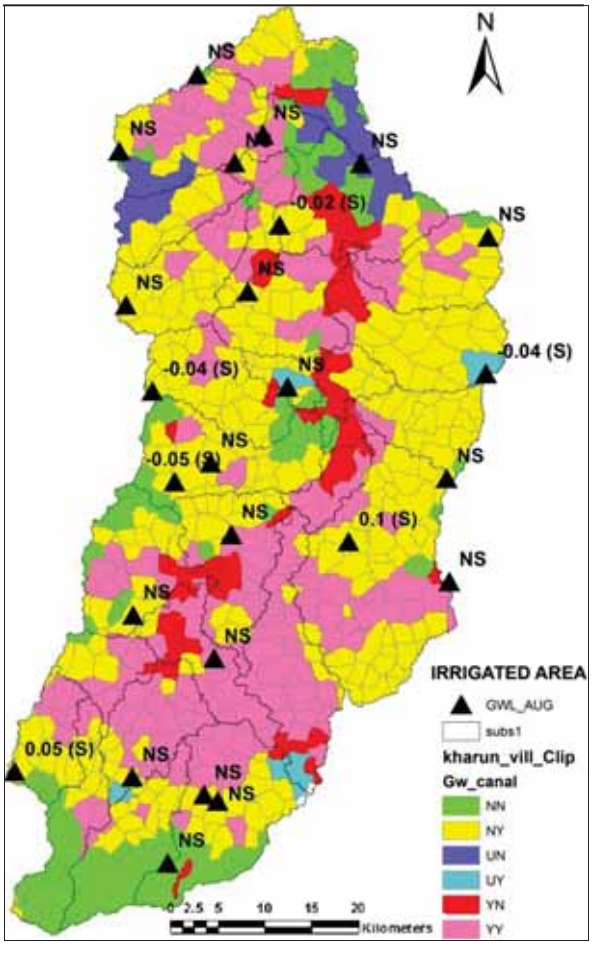

Figure 7.4: Groundwater level trend for August (1993-2011)

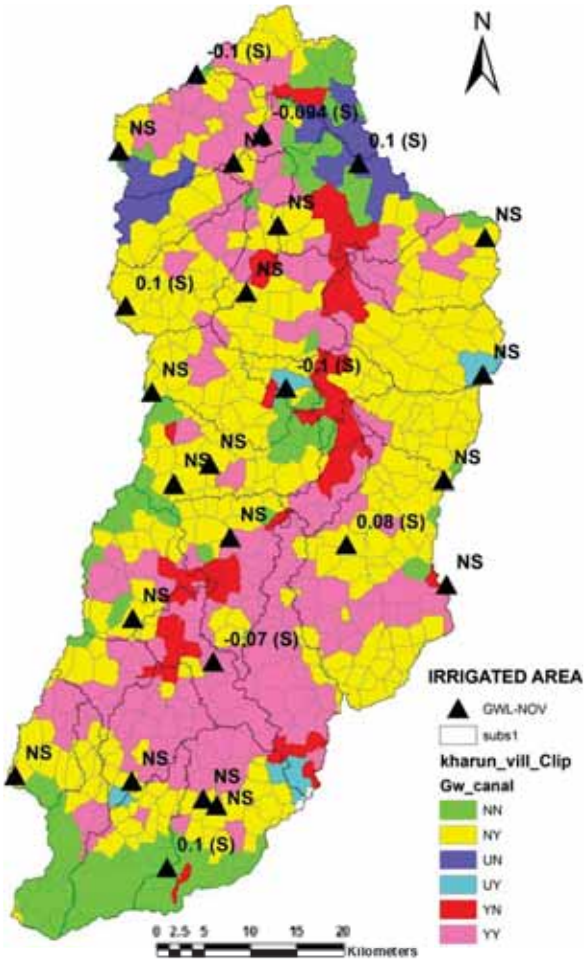

Figure 7.5: Groundwater level trend for November (1993-2011)

As the number of groundwater monitoring stations in or close to the hotspot areas is very limited, it is not possible to clearly prove the relationship between the trend of groundwater level and the withdrawals. Yet the appropriately located stations (see Figures 7.1 to 7.5) indicate such a relationship. Therefore, these sites should be priority areas for intensifying the monitoring network in order to support sustainable water management.

As the maps indicate, the hot-spot areas (sites with high withdrawals from groundwater for intensifying cropping) are located close to the Kharun River. To counterbalance these withdrawals, it would make sense to consider measures on water level management related to the Kharun river which support a shift from surface runoff to percolation, especially while taking the findings regarding a strong effect of rainfall on surface runoff and low effect on percolation into account (section 7.5).

CHAPTER 8: CONCLUSIONS AND RECOMMENDATIONS FOR FURTHER RESEARCH

8.1 Introduction

SWAT 2012 was used in this study to analyze the impacts of climate change and land-use change on the water balance components of the Upper Kharun Catchment (UKC), Chhattisgarh, India. The major findings of the study consist of (i) the results from model simulations (water balance components under the influence of several climate and land-use scenarios), (ii) data sets collected and compiled for input into SWAT, and (iii) data describing the drivers of land-use changes necessary for understanding land-use dynamics and their impact on the water balance. The findings according to (ii) and (iii) include detailed land-use maps, bias-corrected regional climate change scenarios, trend detection analysis of observed rainfall and temperature, different land-use and climate change scenarios, population dynamics and surface and groundwater irrigated area changes over the decades, and impact analysis of climate change and land-use change on the hydrology of the study area. Furthermore, an approach to transfer HRU-related groundwater recharge from SWAT into grid-based MODFLOW is also subject of the study.

This chapter summarizes the main findings and contributions of this study to (i) issues of climate and land-use (change) parameters (trends, bias-corrected scenarios, land-use change), (ii) simulated changes in water resources in the UKC, (iii) recommendations for water management in the UKC, and (iv) recommended research related to the modeling approach. It also includes a discussion on some of the limitations of SWAT and recommendations for future research.

8.2 Summary of results

8.2.1 Historical trends of observed climate

The climate in the study region is analyzed in terms of observed rainfall variations from 1961 to 2011 and temperature data from 1971 to 2011 for trend detection analysis. Twelve rainfall stations (with varying observation dates) and one temperature observatory, all located inside the study area, were considered. The trend detection methods (parametric and non-parametric approaches) were applied. The seasonal effects were removed by smoothening techniques to determine the trend.

(1) Rainfall: trend detection analysis at UKC scale

Based on the average value (representative value) from all stations in the UKC, simple linear regression and Prais–Winsten AR (1) trend detection analysis over the period 1961-2011 for the UKC reveals that mean annual rainfall amounts increased by 0.33 mm/annum with a significance level of $p=0.04$.

The simple linear regression for maximum annual rainfall in a year detected an increase at the rate of 1.18 mm per year at $p = 0.09$ level of statistical significance and an increase in the

maximum monthly rainfall in monsoon at the rate of 1.22 mm per annum at p = 0.07. However, the Prais–Winsten AR (1) analysis found that the increasing trend is not significant. Furthermore, an straightforward approach termed as the Gaussian linear regression trend analysis is introduced, which reveals that there is an increasing trend for maximum annual rainfall in a year at a rate of 1.94 mm per annum at p=0.033, which confirms the increasing trend of the simple linear regression. It also shows that there is no statistically significant change in the month of peak rainfall. Mid July remains the period of peak rainfall over the years (1961 – 2011). Simple regression and the Prais–Winsten AR (1) analysis found no statistically significant trend for minimum monthly rainfall in a year and minimum monthly rainfall in the monsoon season.

The correlation tests (Spearman and Mann Kendall test) did not detect significant trends in any rainfall variable.

(2) Rainfall: trend detection analysis for each station

Based on both linear regression and Prais–Winsten AR (1) test, the statistically significant trend in rainfall (for all variables) is found only for Bhilai station out of 12 stations in the UKC.

The increase in mean annual rainfall in a year for Bhilai station is 0.5 mm per annum at p = 0.02 level of significance for linear regression test and p = 0.007 (high) level of significance for Prais–Winsten AR (1) test. Correlation tests (Kendall tau, Spearman and Pearson test), confirm the results of the regression analysis.

The increase in maximum monthly rainfall in a year is 3.48 mm per annum at p = 0.0005 (very high) for the linear regression test, and p = 0.00016 (very high) for Prais–Winsten AR (1) test. Correlation tests (Kendall tau, Spearman and Pearson test) support the results of regression analysis.

The probable reasons for the significant increase in rainfall for Bhilai station might be its location in an industrial area, i.e., the increase in pollution and dust particles that favors condensation may lead to an increase in rainfall amount. Another reason might be an increase in urbanization around the rainfall station.

(3) Major findings of correlation test (Mann Kendall test with Theil-Sen's slope) applied to each station and month

Balod rainfall station: A very small increase in monthly rainfall at the rate of 0.0001 mm per annum for May at p =0.05 level of significance was detected and a decreasing trend for October at the rate of 0.5 mm per annum; however the significance level noticed here is less than p = 0.1.

Bhilai rainfall station: The test revealed an increase in monthly rainfall at the rate of 2.43 mm per annum (p=0.1) for August.

Chhati rainfall station: The test detected an increase in monthly rainfall at the rate of 0.22 mm per annum (p=0.1) for April.

Dhamtari rainfall station: The test shows a slight increase in monthly rainfall at the rate of 0.0001 mm per annum (p=0.05) for March.

Patharidih rainfall station: The test detects an increase in monthly rainfall at the rate of 5.56 mm per annum (p=0.1) for September.

Raipur rainfall station: The test indicates an increase in monthly rainfall at the rate of 2.32 mm per annum for September at p = 0.08.

Gangral, Banbarod, Gurur and Kondapar and Charama rainfall stations: No statistically significant changes were found.

The maximum monthly rainfall in a year for the UKC shows an increasing trend of 1.94 mm per annum (p=0.33). However, the research by Guhathakurta and Rajeevan (2008) and Kumar et al. (2010) reveal that monsoon rainfall is decreasing in Chhattisgarh. The study area is a part of Chhattisgarh state.

Chakraborty et al. (2013) observed a decreasing trend in annual and seasonal rainfall for the Seonath river basin (the UKC is a catchment of the Seonath river basin).

Rao (1993) used linear regression time series analysis for Mahanadi basin and found no significant trend in monsoon or annual rainfall during the period 1901–1980.

The trend detection analysis in the present study opens a new discussion and contradicts the findings of the earlier few studies on the study area, which show a decreasing trend in rainfall. However, the earlier studies were on a larger scale. Furthermore, the increase in rainfall trend investigated in the present study is only small.

(4) Temperature: mean annual trend detection analysis

Simple linear regression, Prais–Winsten AR (1) test, auto-segmented linear regression and correlation tests (Spearman and Mann Kendall test) show no significant changes in mean annual maximum, mean annual minimum and mean annual average and decadal temperature in the study area from 1971 to 2011.

(5) Temperature: mean monthly trend detection analysis

The analysis of the actual observed temperature (with the seasonal variations) shows a small increasing trend for specific months. A slight increase in mean monthly maximum temperature was observed for November and December. For mean monthly minimum temperature, a small increase was detected for March, July and August and for mean monthly average temperature a slight increase was observed for July, August, November and December.

After removing the seasonal variations using the smoothening method, it can be seen that the mean monthly maximum, minimum and average temperatures show no significant changes (based on both parametric and non-parametric tests).

8.2.2 Analysis of bias-corrected future climate scenarios

The PRECIS regional climate model scenarios (q0, q1 and q14) were bias corrected at station level. Fourteen rainfall stations in and around the UKC were considered and Thiessen weights were applied to determine future rainfall scenarios representative for the UKC in the periods 2020s (2011-2040), 2040s (2041-2070) and 2080s (2071-2098) compared to the baseline scenarios (1971-2010). Similarly, maximum and minimum temperature of one meteorological station (Raipur) is considered as representative of the UKC and used for the bias correction of temperatures of future scenarios of the above periods.

q0 rainfall scenarios: The mean annual rainfall for the UKC compared to the baseline (1989-2008) will increase by 6.45% by the 2020s; 23.48% by the 2050s, and 41.53% by the 2080s.

q1 rainfall scenarios: Mean annual rainfall for the UKC compared to the baseline (1989-2008) for the 2020s will decrease by 9.96% and increase by 2.72% by the 2050s and 13.74% by the 2080s.

q14 rainfall scenarios: It can be concluded that the mean annual rainfall for the UKC compared to the baseline (1989-2008) will increase by 13.15% by the 2020s; 11.82% by the 2050s and 25.72% by the 2080s.

Note: For all future rainfall scenarios, the rainfall in the month of June decreases significantly for all the future scenarios compared to the baseline.

In contrast, for the other months rainfall shows an increase (except for q1 scenario, for which the month of July and August show a decrease).

q0 maximum temperature scenarios: The results reveal that the mean annual maximum temperature for the UKC compared to the baseline (observed values, 1971-2005) will increase by 1.5 ^{0}C by the 2020s, 2.5 ^{0}C by the 2050s and 3.7 ^{0}C by the 2080s.

q1 maximum temperature scenarios: The mean annual maximum temperature for the UKC compared to the baseline (observed values, 1971-2005) will increase by 1.1 ^{0}C by the 2020s, 2.5 ^{0}C by the 2050s and 3.6 ^{0}C by the 2080s.

q14 maximum temperature scenarios: it is concluded that the mean annual maximum temperature for the UKC compared to baseline (observed values, 1971-2005) will increase by 1.1 ^{0}C for the 2020s, by 3.0 ^{0}C for the 2050s, and by 3.5 ^{0}C for the 2080s.

Note: It can also be observed that the mean monthly maximum temperature in all months in all scenarios (q0, q1 and q14) increases compared to the baseline.

q0 minimum temperature scenarios: The mean annual minimum temperature for the UKC based on q0 compared to the baseline observed values (1971-2005) will increase by 2.0 ^{0}C by the 2020s, 3.6 ^{0}C by the 2050s and 6.7 ^{0}C by the 2080s.

q1 minimum temperature scenarios: It can be expected that the mean annual minimum temperature for the UKC compared to the baseline observed values (1971-2005) will increase by 1.4 ^{0}C for the 2020s, by 2.8 ^{0}C for the 2050s, and by 4.0 ^{0}C for the 2080s.

q14 minimum temperature scenarios: It can be concluded that the mean annual minimum temperature for the UKC compared to the baseline observed values (1971-2005) will increase by 1.4 ^{0}C for the 2020s, by 3.3 ^{0}C for the 2050s, and by 4.5 ^{0}C for the 2080s (Table 3.65).

Note: It can also be observed that the mean monthly minimum temperatures of all months and all scenarios (q0, q1 and q14) are increasing compared to the baseline scenarios.

8.2.3 Land-use change analysis

Land-use maps were prepared for 4 time steps (1991, 2001, 2011 and 2021) representing the decades 1990s, 2000s, 2010s and 2020s. The land-use is classified in two scales: broad land-use classification (5 classes) and detailed land-use classification (19 classes). The land-use change analysis focused on comparing the land-use of different decades with the baseline scenario (1991).

The broad land-use classification change analysis revealed that there is a slight declining trend in agricultural land in the UKC. It shows a significant increase in the proportion of built-up areas by almost 4.67% between 1991 and 2011. It also indicates a significant population growth and rapid development of the study area. This further leads to an increase in sealed areas leading to generation of surface runoff and lowering of the groundwater recharge in the respective areas. It is expected that there will be an increase in built-up areas by 2.6% in UKC between 2011 and 2021. The share of land under forest declined between 1991 and 2001 by 0.3%, but showed an increasing trend between 2001 and 2011 by 0.49%. The decrease in wasteland was 3.76% between 1991 and 2011 and can be interpreted as an indication for high pressure on land resources involving the use of an increasing area of waste land for other purposes. Wasteland in the UKC is expected to decrease by 1.1% between 2011 and 2021. Decadal land-use statistics reveal a slight decline in the area covered by water bodies during 1991 to 2001 by 0.2% and during 2001 to 2011 a further slight decline by 0.02%. It is expected that the area of water bodies will remain constant between 2011 and 2021 in spite of increasing water demand by different sectors.

The detailed land-use classification indicates an intensification of groundwater-irrigated land over the decades. A significant increase of 5.43 % area under two-season crops was observed between 1991 and 2011. Due to the development of irrigation infrastructure and the increasing demand for food, it is expected that there will be a significant conversion of one-season crops

(AKHA) to two-season crops (ADOR). Between 2011 and 2021, the expected increase in the area of two-season crops (ADOR) is 24.25% of the total study area, which is quite high compared to the other classes.

Cropping in more than two seasons with paddy as a summer crop is the land-use class that shows a significant increase by 5.67% of the study area from 1991 to 2011. A significantly high increase by 12.57% under this class is expected between 2011 and 2021. This indicates an excessive increase in groundwater irrigation in some villages, and indicates the limits of sustainable use of the precious groundwater resources.

The decrease in area with only one crop (AKHA) and the increase in areas with two (ADOR) or three crops (ATRS) is considered as an indication for high pressure on land (and water resources), i.e., towards intensification driven by population growth.

In Chapter 5, the analysis regarding the development of irrigation schemes and practices based on field records and census book reports further supports the findings derived from satellite data on land-use map and statistics, which indicate intensification in groundwater-irrigated area in the study area over the decades.

8.2.4 Climate change impacts on water balance components

(1) The rainfall pattern of the scenarios is clearly the dominating impact on water balance components,

(2) Due to the simulated over-proportional relationship between runoff and rainfall, a rather high increase in discharge can be expected,

(3) It is obvious that the high uncertainty of expected changes in rainfall (marked differences in the PRECIS scenarios) is translated in high uncertainty of simulated changes in discharge and further water balance components,

(4) Actual evapotranspiration basically shows an increasing trend of different magnitude depending on the PRECIS scenario (driven by temperature),

(5) A decreasing trend in groundwater contribution to streamflow is simulated,

(6) Detecting hotspot leads to identifying priority areas for advancing groundwater monitoring and management.

8.2.5 Land-use change impacts on water balance components

The impact of land-use change on the water balance is small at the catchment scale due to compensation of different effects (e.g., urbanization versus intensification of cropping) (section

7.2.1 and 7.2.2). Yet, an effect of land-use change becomes influential at the sub-catchment level at sites with relevant land-use dynamics.

8.2.6 Water management in the UKC

Surface runoff and percolation is under the clear influence of changes in rainfall. Nevertheless, the magnitude of the effect is high in terms of surface runoff and very low for percolation (section 7.5). As a consequence, groundwater recharge is expected to slightly increase (despite significant increase in rainfall), whereas at least in parts of the catchment the withdrawals for intensifying cropping patterns will increase. This leads to the conclusion that the risk of over-exploitation may occur and needs to be considered and counterbalanced by management measures. With respect to the strong effect of the predicted increase in rainfall on surface runoff, it can be concluded that (i) additional facilities and strategies to increase the storage capacity of the landscape should be considered, and that (ii) it is recommended to carry out more detailed runoff-rainfall analyses with higher temporal resolution in order to assess a potentially increasing risk of floods.

The groundwater stations in or close to the hotspot areas are limited; therefore, it was not possible to clearly prove the relationship between the trend in groundwater level and the withdrawals. As the few appropriately located stations (see Figures 7.1 to 7.5) indicate a trend towards declining groundwater tables, an impact of increasing withdrawals on the hotspot areas seems to exist (section 7.7). Therefore, these sites would be priority areas for intensifying the monitoring network in order to support sustainable water management.

The hot-spot areas (sites with high withdrawals from groundwater for intensifying cropping) are located close to the Kharun River. To counterbalance these withdrawals, it would make sense to consider measures on water level management related to the Kharun River which support a shift from surface runoff to percolation (especially when considering the findings regarding the strong effect of rainfall on surface runoff and low effect on percolation (section 7.5).

8.3 Contribution of the study

(1) The bias-corrected climate scenarios at high spatial station level resolution prepared in this study can be used for further impact analysis on agriculture and other sectors of the study area.

(2) The detailed basic data prepared on demography, irrigation and land-use scenarios can be used by the officials (stakeholders) for better resource management in the UKC.

(3) A straightforward approach of trend detection analysis termed as Gaussian regression method is introduced and practiced.

(4) The approach of linking SWAT and MODLOW using a linkage file is introduced and explored.

8.4 Recommendations for future research

(i) The linkage file prepared in the current study could be further used to transfer the spatial estimated recharge from HRUs to the grid format of MODFLOW, and has the potential to facilitate integrated surface and sub-surface hydrological modeling in the study area.

(ii) The POTHOLE functionality of SWAT was tested in the current study, and it was observed that this functionality does not sufficiently supports the hydrological modeling for irrigated paddy fields. The development of irrigation modules in SWAT that efficiently handle the irrigated paddy field hydrology is strongly recommended.

(iii) Apart from land-use mapping, remote sensing offers wide possibilities to derive various hydrological parameters, like evapotranspiration, soil moisture, surface temperature and TRMM rainfall estimates, etc., which can be use in calibration and validation of hydrological models in data-scarce areas. The GRACE satellite mission of water balance estimation is another path-breaking innovative study to be used. It is highly recommended to explore the potential of remote sensing in hydrological modeling for future research.

(iv) The multi-criteria approach in uncertainty analysis and model calibration should be explored where sediments, remote sensing-derived evapotranspiration, etc., other than discharge could be used.

(v) For hydrological modeling of the UKC, the performance of other hydrological models should be compared with SWAT in terms of catchment behavior and impact statistics.

(vi) Research on coupling of SWAT with socioeconomic models is recommended. This would yield an overall integrative assessment of water availability, demand and supply analysis in the UKC.

REFERENCES

- Abbott MB, Refsgaard JC (1996) Distributed Hydrological Modelling. Kluwer Academic Publishers, Dordrecht, The Netherlands, pp. 255-278
- Acutis M, Donatelli M (2003) *SOIL*PAR 2.00: software to estimate soil hydrological parameters and functions. Eur. J. Agron., 18:373-377
- Allen RG, Pereira LS, Raes D, Smith M (1998) Crop evapotranspiration - Guidelines for computing crop water requirements - FAO Irrigation and drainage paper 56
- Anttila P (2002a) Updating stand level inventory data applying growth models and visual interpretation of aerial photographs. Silva Fenn.36: 549–560
- Anttila P (2002b) nonparametric estimation of stand volume using spectral and spatial features of aerial photographs and old inventory data. Can. J. For. Res. 32: 1849–1857
- Arnold JG, Srinivasan R, Muttiah RS, Williams JR (1998) Large area hydrologic modelling and assessment Part 1: Model development. J. American Water Resour. Association 34 (1):73-89
- Arnold JG, Kiniry JR, Srinivasan R, Williams JR, Haney EB, Neitsch SL (2012) SWAT input/output documentation version 2012 at http://swat.tamu.edu/media/69296/SWAT-IO-Documentation-2012.pdf
- Asian Development Bank (2003) Water Resources Development in India: Critical Issues and Strategic Options (Manila:ADB, n.d.) at http://www.adb.org/Documents/Assessments/Water/IND/Water-Assessment.pdf.
- Asner GP, Keller M, Pereira R, Zweede, JC (2002) Remote based on detailed field observations, Landsat ETM+, and textural analysis. Remote Sensing of Environment 80: 483–496
- Back AJ, Bruna ED, Vieira HJ (2012) Climate trends and grape production in the region of the Valley of Uva Goethe. Brazilian Agricultural Research, 47:497-504
- Baker TJ, Miller SN (2013) Using the Soil and Water Assessment Tool (SWAT) to assess land use impact on water resources in an East African watershed. Journal of Hydrology, Volume 486, pp 100–111. DOI: 10.1016/j.jhydrol.2013.01.041
- Benderev AD, Orehova TV, Bojilova EK (2008) Some aspects of ground-water regime in Bulgaria with respect to climate variability. Geological Society, London, Special Publications 288: 13-24
- Bergström S, Forsman A (1973) Development of a conceptual deterministic rainfall-runoff model. Nordic Hydrol., 4:147-170
- Beven KJ (2001) On stochastic models and the single realisation, Hydrological Processes (HPToday), 15:895-896
- Bhadwal S (2003) Coping with global change: vulnerability and adaptation in Indian agriculture. Teri Report. Venema, H. et al. (eds), IG Printers: New Delhi.

- Blain GC, Pires (2011) RCM temporal evapotranspiration and the ratio of actual evapotranspiration and potential in Campinas, State of Sao Paulo. Variability Bragantia 70(2):460-470
- Bosch DD, Potter TL, Truman CC, Bednarz C, Strickland TC (2005) Surface runoff and lateral subsurface flow as a response to conservation tillage and soil-water conditions. Trans. ASAE 48(6): 2137-2144
- Bosch JM, Hewlett JD (1982) A Review of Catchment Experiments to Determine the Effect of Vegetation Changes on Water Yield and Evapotranspiration. Journal of Hydrology, 55: 3-23
- Buffoni L, Brunetti M, Mangianti F, Maugeri M, Nanni T (2002) Bollettino Geofisico Anno. Variazioni Climatiche in Italia Negli Ultimi 130 Anni, Bollettino Geofisico Anno XXIII
- Burn, DH (1994) Hydrologic effects of climatic change in West Central Canada. J. Hydrol. 160 :53–70
- Burn, DH, Hag Elnur, MA (2002) Detection of hydrologic trends and variability. Journal of Hydrology 255:107–122
- Cailas MD, Cavadias G, Gehr R (1986) Application of a nonparametric approach for monitoring and detecting trends in water quality data of the St. Lawrence River. Can. Water Poll. Res. J. 21 2:153–167
- Carvalho JR, Assad ED, Evangelista SRM, Pinto HS (2013) Estimation of dry spells in three Brazilian regions - Analysis of extremes. Atmospheric Research, 132-133:12-21
- CWC (Central Water Commission) and NIH (National Institute of Hydrology) (2008) Preliminary Consolidated Report on Effect of Climate Change on Water Resources. Ministry of Water Resources, Government of India, New Delhi.
- CGWB (2012) Dynamic ground water resources of Chhattisgarh, North Central Chhattisgarh Region (NCCR), Raipur, Ministry of Water Resources, Govt. of India.
- CGWB (2004) Report of the ground water resource estimation committee, Ground water resource Estimation Methodology-1997 (GEC'97)
- CGWB (2006) State Report: Hydrogeology of Chhattisgarh, NCCR, Raipur
- Chakraborty Shiulee , Mishra SK, Pandey RP, Chaube UC (2013) Long-term Changes of Irrigation Water Requirement in the Context of Climatic Variability, ISH Journal of Hydraulic Engineering 19(3)
- Chase TN, Pielke RA, Kittel TGF, Nemani RR, Running SW (2000) Simulation impacts of historical land cover changes on global climate in northern winter, Climate Dynamics, 16:93 – 105
- Chaudhary A, Abhyankar VP (1979) Does precipitation pattern foretell Gujarat climate becoming arid. Mausam, 30:85–90
- Chiew FHS, McMahon TA (1993) Detection of trend or change in annual flow of Australian rivers. Int. J. Clim. 13:643–653

- Christy BA, Weeks G, O'Leary, Beverly C (2009) Separating the impact of climate change from land-use change in local and regional ground-water systems. 18th World IMACS / MODSIM Congress, Cairns, Australia 13-17
- Christensen JH, Christensen OB (2003) Severe summertime flooding in Europe, Nature, 421:805–806
- Christensen JH, Christensen OB (2004) Intensification of extreme European summer precipitation in a warmer climate, Global Planet. Change, 44:107–117
- Christensen JH, Hewitson B, Busuioc A, Chen A, Gao X, Held I, Jones R, Kolli RK, Kwon WT, Laprise R, Magaña RV, Mearns L, Menéndez G, Räisänen J, Rinke A, Sarr A, Whetton P (2007) Regional Climate Projections. The Physical Science Basis
- Chu TW, Shirmohammadi A (2004) Evaluation of the SWAT model's hydrology component in the piedmont physiographic region of Maryland. Trans. ASAE 47(4):1057-1073
- Chung M, Kim NW, Lee J, Sophocleous M (2010) Assessing distributed ground-water recharge rate using integrated surface water-ground-water modelling: application to Mihocheon watershed, South Korea. Hydrogeology Journal 18: 1253–1264
- Cohen WB, Spies TA, Fiorella, M (1995) Estimating the age and structure of forests in a multi-ownership landscape of western Oregon, U.S.A. Int. J. Remote Sensing 16: 721–746
- Costa MH, Botta A, Cardille J (2003) Effects of large-scale changes in land cover on the discharge of the Tocantins River, South eastern Amazonia. Journal of Hydrology 283: 206-217
- Crawford CG, Slack JR, Hirsch RM (1983) Nonparametric tests for trend in water quality data using the statistical analysis system. Open Report no. 83-550, US Geological Survey, USA
- Crist EP, Cicone RC (1984) Application of the tasseled Cap Concept to Simulated Thematic Mapper Data. Photogrammetric Engineering and Remote Sensing 50:343-352
- Crist, EP, Kauth RJ (1986) The tasseled Cap De-Mystified. Photogrammetric Engineering and Remote Sensing 52:81-86
- Cruz RV et al. (2007) Asia. Climate Change 2007: Impacts, Adaptation and Vulnerability. Contribution of Working Group 2 to the 4th Assessment Report of the Intergovernmental Panel on Climate Change. Parry, M. L. (eds), Cambridge University Press: Cambridge
- Dams J, Woldeamlak ST, Batelaan O (2008) Predicting land-use change and its impact on the ground-water system of the Kleine Nete catchment, Belgium. Hydrol. Earth Syst. Sci 12:1369-1385
- Dash SK, Jenamani RK, Kalsi SR, Panda SK (2007) Some evidence of climate change in twentieth-century India, Climatic change 85: 299-321
- DeFries R, Eshleman KN (2004). Land-use change and hydrologic processes: a major focus for the future. Hydrological Processes 18: 2183-2186

- Delude (2010) Minor changes in precipitation may have major impact on groundwater supplies in arid regions, Department of Civil & Environmental Engineering, MIT. https://cee.mit.edu/news/releases/2010/groundwater-recharge
- Demaree GR, Nicolis C (1990) Onset of Sahelian drought viewed as fluctuation-induced transition. Q J Roy Meteor Soc 116:221–238
- Dhar S, Mazumdar A (2009) Impacts of climate change under the threat of global Warming for an agricultural watershed of the Kangsabati River. International Journal of Civil and Environmental Engineering 1(3)
- Dibike YB, Coulibaly P (2005) Hydrologic impact of climate change in the Saguenay watershed: comparison of downscaling methods and hydrologic models, J. Hydrol 307:145–163
- Douglas EM, Vogel RM, Kroll CN (2000) Trends in floods and low flows in the United States: impact of spatial correlation. J Hydrol 240:90–105
- Douglas-Mankin KR, Srinivasan R, Arnold JG (2010) Soil and Water Assessment Tool (SWAT) Model: Current developments and applications. Transactions of the ASABE. 53(5):1423-1431
- Dragoni W (1998) Water, Environment and Society in Times of Climatic Change, Some considerations on climatic changes, water resources and water needs in the Italian region south of the 43°N, eds Issar A. S., Brown N. (Kluwer), 241–271
- Durman CF, Gregory JM, Hassell DC, Jones RG, Murphy JM (2001) A comparison of extreme European daily precipitation simulated by a global and a regional climate model for present and future climates, Q. J. R. Meteorol. Soc 127:1005–1015
- Dymond CC, Mladenoff DJ, Radeloff VC (2002) Phonological differences in tasseled cap indices improves deciduous forest classification. Remote Sens. Environ. 80: 460-472
- Eckhardt K and Ulbrich U (2003) Potential impacts of climate change on groundwater recharge and streamflow in a central European low mountain range. Journal of Hydrology, 284(1-4): 244-252
- El-Shaarawi, AH, Esterby, SR, Kuntz, KW (1983) A statistical evaluation of trends in the water quality of the Niagara River. J. Great Lakes Res. 9, 234–240.
- Farley KA, Jobbagy EG, Jackson RB (2005) Effects of afforestation on water yield: a global synthesis with implications for policy. Global Change Biology, 11: 1565-1576
- Fei Y, Kali ES, Brian CL, Marvin EB (2005) Land cover classification and change analysis of the Twin Cities (Minnesota) Metropolitan Area by multitemporal Landsat remote sensing, Remote Sensing of Environment 98:317 – 328
- Fohrer N, Haverkamp S., Eckhardt K, Frede HG (2001) Hydrologic response to land use changes on the catchment scale, Physics and Chemistry of Earth 26: 577–582
- Fontaine TA, Klassen JF, Hotchkiss RH (2001) Hydrological response to climate change in the Black Hills of South Dakota, USA. Hydrological Sciences 46 (1): 27–40
- Franklin JF, Lindenmayer D, MacMahon, JM, McKee A, Magnuson JJ, Perry DA, Waide RB, Foster DR (2000) Threads of continuity. Conserv. Biol. Pract. 1:9–16

- Franklin SE, Michael BL, Michael AW, Thomas M. McCaffrey (2002) Large-area forest structure change detection: an example. Canadian Journal of Remote Sensing 28 (4):588-592
- Frei C, Christensen JH, De´que´ M, Jacob D, Jones RG, Vidale PL (2003) Daily precipitation statistics in regional climate models:Evaluation and intercomparison for the European Alps, J. Geophys. Res.,108 (D3):4124
- Gassman PW, Reyes M, Green CH, Arnold JG (2007) The Soil and Water Assessment Tool: Historical development, applications, and future directions. Trans. ASABE 50(4):1211-1250
- GEC (1997) Report of the Ground-water Resource Estimation Committee-Ground-water resource estimation methodology. Central Ground-water Board, Ministry of Water Resources, Govt. of India, New Delhi 107
- Geethalakshmi V, Lakshmanan A, Bhuvaneswari K, Rajalakshmi D, Sekhar NU, Anbhazhagan R, Gurusamy L (2011) Climate and Agriculture: Model Inter-Comparison for Evaluating the Uncertainties in Climate Change Impact Assessment American Geophysical Union, Fall Meeting
- Ghaffari G, Keesstra S, Ghodousi J, Ahmadi H (2010) SWAT simulated hydrological impact of land-use change in the Zanjanrood basin, Northwest Iran. Hydrological Processes, Volume 24, Issue 7, pp 892–903
- Githui F, Gitau W, Mutua F, Bauwens W (2009) Climate change impact on SWAT simulated streamflow in western Kenya, International Journal of Climatology 29:1823b-1834
- Goodess CM, Anagnostopoulou C, Bárdossy A, Frei C, Harpham C, Haylock MR, Hundecha Y, Maheras P, Ribalaygua J, Schmidli J, Schmith T, Tolika K, Tomozeiu R Wilby RL (2005) An inter comparison of statistical downscaling methods for Europe and European regions – assessing their performance with respect to extreme temperature and precipitation events. Climatic Research Unit Research Publication 11
- Gosain AK, Rao S, Basuray D (2006) Climate change impact assessment on hydrology of Indian river basins. Current Science 90 (3)
- Gosain AK, Rao S, Arora A (2011) Climate change impact assessment of water resources of India. Current Science, Vol. 101, No. 3, 10
- Guhathakurta P, Rajeevan M (2008) Trends in the rainfall pattern over India. Int. J. Climatol 28:1453–1469
- Haan CT (1977) Statistical methods in hydrology. The Iowa University Press, Iowa, U.S.A
- Hayes DJ, Sader SA (2001) Comparison of change-detection techniques for monitoring tropical forest clearing and vegetation regrowth in a time series. Photogrammetric Engineering and Remote Sensing 67: 1067-1075

- Healey SP, Cohen WB, Zhiqiang Y, Krankina, ON (2005) Comparison of TasseledCap-based Landsat data structures for use in forest disturbance detection. Remote Sensing of Environment, 97:301−310
- Helsel DR, Hirsch RM (1988) Discussion of Applicability of the t-test for detecting trends in water quality variables by Montgomery RH and. Loftis JC: Water Resources Bulletin 24 (1): 201-204
- Hingane LS, Rupa K, Murty VR (1985) Long-term trends of surface air temperature in India. Int. J. Climatol 5: 521–528
- Hipel KW, McLeod AI (1994) Time series modelling of water resources and environmental systems. Developments in Water Science45, Elsevier, Amsterdam
- Hipel KW, McLeod AI, Weiler RR (1988) Data analysis of water quality time series in Lake Erie. Water Resour. Bull. 24 (3):533–544
- Hirsch RM, Slack JR, Smith RA (1982) Techniques of trend analysis for monthly water quality data. Water Resources Research 18:107–12
- Houghton RA, Hackler JL (2003) Sources and sinks of carbon from land-use change in China. Global Biogeochemical Cycles 17: 1034
- Huang H, Legarsky J, and Othman M (2007) Land-cover Classification Using Radarsat and Landsat Imagery for St. Louis, Missouri, Photogrammetric Engineering & Remote Sensing 73(1) : 037–043
- Huntingford C, Jones RG, Prudhomme C, Lamb R, Gash HHC, Jones DA (2003) Regional climate-model predictions of extreme rain- fall for a changing climate, Q. J. R. Meteorol. Soc., 129:1607–1621
- Huntingford C, Lambert FH, Gash JCH, Taylor CM, Challinor AJ (2005) Aspects of climate change prediction relevant to crop productivity. Phylos. T. Roy. Soc. B 360:1999-2009
- Huntington TG (2006) Evidence for intensification of the global water cycle: Review and synthesis. Journal of Hydrology 319:83–95
- Huth R, Pokorná L (2004) Parametric versus non-parametric estimates of climatic trends. Theor. Appl. Climatol 77: 107-112
- Im S, Kim H, Kim C, Jang C (2009) Assessing the impacts of land-use changes on watershed hydrology using MIKE SHE, Environmental geology, 57(1): 231-239
- IPCC TAR WG3 (2001). Metz, B.; Davidson, O.; Swart, R.; and Pan, J., ed., Climate Change 2001: Mitigation, Contribution of Working Group III to the Third Assessment Report of the Intergovernmental Panel on Climate Change, Cambridge University Press, ISBN 0-521-80769-7 (pb: 0-521-01502-2)
- IPCC (2007) The physical science basis – summary for Policymakers. Contribution of WG1 to the Fourth assessment report of the Intergovernmental Panel on Climate Change. http://www.ipcc.ch/ipccreports/ar4-wg1.htm
- Jagannathan P, Parthasarathy B (1973) Trends and periodicities of rainfall over India. Monthly Weather Review 101:371–375

- Jarosz N, Beziat P, Bonnefond JM, Brunet Y, Calvet JC, Ceschia E, Elbers JA, Hutjes RWA, Traulle O (2009) Effect of land use on carbon dioxide, water vapour and energy exchange over terrestrial ecosystemsin Southwestern France during the CERES campaign. Biogeosciences Discuss 6: 2755–2784
- Jat ML, Gathala MK, Ladha JK, Saharawat YS, Jat AS, Kumar V, Sharma SK, Kumar V, Raj G (2009) Evaluation of precision land leveling and double zero-till systems in the rice-wheat rotation: Water use, productivity, profitability and soil physical properties, Soil and Tillage Research, 105:112–121
- Jayakrishnan R, Srinivasan R, Santhi C, Arnold JG (2005) Advances in the application of the SWAT model for water resources management. Hydrological Processes. 19(3):749-762
- Jensen JR (1996) Introductory digital image processing: a remote sensing perspective. Prentice-Hall, Upper Saddle River, NJ, 318
- Jha M, Pan Z, Takle ES, Gu R (2004) Impacts of climate change on streamflow in the Upper Mississippi River basin: A regional climate model perspective. J. Geophys. Res. 109
- Jonathan AF, Ruth D, Gregory PA, Carol B, Gordon B, Stephen RC, Chapin FS, Michael TC, Gretchen CD, Holly KG, Joseph HH, Holloway T, Erica AH, Christopher JK, Chad M, Jonathan AP, Prentice IC, Ramankutty N, Snyde PK (2005), Global Consequences of Land Use, Science 309:570
- Justice CO, Hiemaux PHY(1986) Monitoring the grasslands of the Sahel using NOAA AVHRR data: Niger 1983: The International Journal of Remote Sensing, November 7(11):1475
- Kanungo DP, Sarkar S (2011) Use of Multi-Source Data Sets for Land Use/Land Cover Classification in a Hilly Terrain for Landslide Study, Disaster & Development 5(1)
- Kahya E, Kalayci S (2004). Trend analysis of streamflow in Turkey. Journals of Hydrology 289: 128-144
- Kauth RJ, Thomas GS (1976) The tasseled Cap – A Graphic Description of the Spectral-Temporal Development of Agricultural Crops as Seen by LANDSAT. Proceedings of the Symposium on Machine Processing of Remotely Sensed Data, Purdue University of West Lafayette, Indiana : 4B-41 to 4B-51
- Kendall MG (1975) Rank Correlation Methods. Griffin, London, UK
- Keil M, Kiefl R, Strunz G (2005) Final report on CORINE Land Cover 2000 – Germany. German Aerospace Center, available at http://www.umweltbundesamt.de/sites/default/files/medien/publikation/long/3212.pdf
- Kim NW, Chung M, Won YS, Arnold JG (2008) Development and application of the integrated SWAT–MODFLOW model. Journal of Hydrology 356: 1– 16
- Konikow LF, Reilly TE (1998) Ground-water Modelling. In: The Handbook of Ground-water Engineering 20:1-20.40

- Koteswaram P, Alvi SMA (1969) Secular trends and periodicities in rainfall at west coast stations in India. Current Science 101:371–375
- Kothawale DR, Rupa K (2005) On the recent changes in surface temperature trends over India. Geophys Res Lett 32:L18714
- Kulkarni BD, Deshpande NR, Patwardhan SK, Bansod SD (2014) Assessing Hydrological Response to Changing Climate in the Krishna Basin of India. J Earth Sci Clim Change 5: 211doi: 10.4172/2157-7617.1000211
- Kumar, V., Singh, P. & Jain, S. K. (2005) Rainfall trends over Himachal Pradesh, Western Himalaya, India. In: Development of Hydro Power Projects – A Prospective Challenge (Conf. Shimla, 20–22 April, 2005)
- Kumar V, Jain SK (2010) Trends in rainfall amount and number of rainy days in river basins of India (1951–2004). Hydrol. Res 42(4):290–306
- Kumar V, Jain SK, Singh Y (2010) Analysis of long-term rainfall trends in India. Hydrol. Sci. J 55:484–49
- Kumar KK, Patwardhan SK , Kulkarni A , Kamala K, Rao KK , Jones R (2011) Simulated projections for summer monsoon climate over India by a high-resolution regional climate model (PRECIS), CURRENT SCIENCE 101(3)
- Labat D, Goddéris Y, Probst JL, Guyot JL (2004) Evidence for global runoff increase related to climate warming. Advances in Water Resources 27:631–642
- Lakshmanan A, Geethalakshmi V, Srinivasan R, Sekhar NU, Annamalai H (2009) Climate change adaptation strategies in Bhavani basin using SWAT model
- Lal M, Harasawa H (2001) Future climate change scenarios for Asia as inferred from selected coupled atmosphere–ocean global climate models. J. Meteorol. Soc. Japan 79: 219–227
- Lal M, Singh SK (2001) Global warming and monsoon climate. Mausam 52:245–262
- Lettenmaier DP (1976) Detection of trend in water quality data from records with dependent observations. Water Resour. Res., 12(5):1037-1046
- Lettenmaier DP, Wood EF, Wallis JR (1994) Hydro-climatological trends in the continental United States, 1948–88. J. Clim.7:586–607
- Lins HF, Slack JR. (1999) Streamflow trends in the United States. Geophys. Res. Lett. 26(2): 227–230
- Lunetta RL, Johnson DM, Lyon JG, Crotwell J (2004) Impacts of imagery temporal frequency on land-cover change detection monitoring. Remote Sensing of Environment 89(4): 444–454
- Lyon JG, Yuan D, Lunetta RS, Elvidge CD (1998) A change detection experiment using Vegetation Indices, Photogrammetric Eng. Remote Sens. 64:143–150
- Jianwen M, Bagan H (2005) Land use classification using Aster data and self- organised neutral networks, International journal of applied earth observation and geoinformation 7:183-188

- MacMillan L, Liniger HP (2005) Monitoring and Modelling for the Sustainable Management of Water Resources in Tropical Mountain Basins: The Mount Kenya Example. Global Change and Mountain Regions: An Overview of Current Knowledge: 605-616
- Mall RK, Gupta Akhilesh, Singh Ranjeet, Singh RS, Rathore LS (2006) Water resources and climate change: An Indian perspective, Current Science 90 (12)
- McLeod AI et al. (1991) Trend analysis methodology for water quality time series. Environmetrics, 2: 169–200
- McLeod AI, Hipel KW, Bodo BA (1991) Trend assessment of water quality time series. Water Resour. Bull. 19: 537–547
- Minuzzi RB, Caramori PH, Borrozino E (2011) Trends in seasonal and annual climate variability of maximum and minimum air temperatures in the state of Parana and. Bragantia 70(2):471-479
- Mooley DA, Parthasarathy B (1984) Fluctuations in All-India summer monsoon rainfall during 1871-1978. Climatic Change 6: 287-301
- Morawitz D (2006) Using NDVI to assess vegetative land cover change in central Puget Sound. Environmental Monitoring and Assessment, 114(1): 85−106
- Mudelsee M (2010) Climate time series analysis: Classical Statistical and Boot strap Methods. Springer, Dordrecht. ISBN: 978-90-481-9481-0.
- Mustard J, Fisher T (2004) Land Use and Hydrology. Land Change Science: Observing Monitoring and Understanding Trajectories of Change on the Earth's Surface: 257-276
- Naguer M, Jones R, Hessel D, Hudson D, Wilson S, Jenkins J and Mitchell J (2002) Workbook on generating high res- olution climate change scenarios using PRECIS; Hadley Centre for Climate Prediction and Research, Met Office, Bracknell, UK 43
- Ndomba PM, Birhanu BZ (2008) Problems and Prospects of SWAT Model Applications in Nilotic Catchments: A Review. Nile Basin Water Engineering Scientific Magazine 1:41-52
- Neitsch SL, Arnold JG, Kiniry JR and Williams JR (2005) Soil and Water Assessment Tool. Theoretical Documentation Version
- Nian YY, Li X, Zhou J, Hu XL (2014) Impact of land use change on water resource allocation in the middle reaches of the Heihe River Basin in northwestern China. Journal of arid land, Volume 6, Issue 3, pp 273-286
- Niehoff D, Fritsch U , Bronstert A (2002) Land-use impacts on storm-runoff generation, scenarios of land-use change and simulation of hydrological response in a mesoscale catchment in SW- Germany, Journal of Hydrology, 267(1-2): 80-93
- National Remote Sensing Centre (NRSC) (2012) Technical manual on "National Land Use Land Cover Mapping using Multi-temporal Satellite Data"
- Pant GB ,Kumar KR (1997) Climates of South Asia, John Wiley, Chichester, UK
- Parajuli PB (2010) Assessing sensitivity of hydrological response to climate change from forested watershed in Mississippi. Hydrological processes 24(26) :3785 -3797

- Partal T, Kalya E (2006) Trend analysis in Turkish precipitation data. Hydrological process 20, 2011-2026
- Piao S, Friedlingstein P, Ciais P, N. de Noblet-Ducoudre´, Labat D, Zaehle S (2007) Changes in climate and land use have a larger direct impact than rising CO2 on global river runoff trends. PNAS, 104(39): 15242-15247
- Pilon PJ, Condie R, Harvey KD (1985) User manual of Consolidated Frequency Analysis Package 88. Environment Canada, Ottawa
- Pohlert T, Huisman JA, Breuer L, Frede HG (2005) Modelling of point and non-point source pollution of nitrate with SWAT in the river Dill, Germany. Adv. Geosci. 5: 7-12
- Pohlert T, Breuer L, Huisman JA. Frede HG (2006) Assessing the model performance of an integrated hydrological and biogeochemical model for discharge and nitrate load predictions. Hydrol. Earth Syst. Sci. Discuss 3: 2813-2851
- Qiu Z, Prato T (2001) Physical determinants of economic value of riparian buffers in an agricultural watershed. J. American Water Resources Assoc. 34(3): 531−544
- Raghavendra VK (1974) Trends and periodicities of rainfall in subdivisions of Maharashtra state, Ind. J. Met. Gelphy., 25:197-210
- Rao PG (1993) Climatic changes and trends over a major river basin in India. Climate Research 2:215-223
- Roy PK, Mazumdar A (2013) Water Resources in India under Changed Climate Scenario International Journal of Engineering Research and Applications (IJERA) 3(1) : 954-961
- Reeves HW, Zellner ML (2010) Linking MODFLOW with an Agent-Based Land-Use Model to Support Decision Making. GROUND-WATER 48(5): 649–660
- Refsgaard JC, Storm B (1995) MIKE SHE. In Computer Models of Watershed Hydrology, 809−846
- Rodell M, Velicogna I, Famiglietti JS (2009) Satellite Based Estimates of Ground-water Depletion in India ,Nature 460 :999-1002
- Rosenthal, W. D., and D. W. Hoffman (1999) Hydrologic modelings/GIS as an aid in locating monitoring sites. Trans. ASAE 42(6): 1591−1598
- Rosenthal WD, Srinivasan R, Arnold JG (1995) Alternative river management using a linked GIS−hydrology model. Trans. ASAE 38(3): 783−790
- Rupa K, Pant GB, Parthasarathy B, Sontakke NA(1992) Spatial and sub-seasonal patterns of the long-term trends of Indian summer monsoon rainfall. International Journal of Climatology 12: 257–268
- Saha AK, Arora MK, Csaplovics E, Gupta RP (2005) Land Cover Classification Using IRS LISS III Image and DEM in a Rugged Terrain: A Case Study in Himalayas, Geocarto International, 20(2), 33-40.
- Sahin, V. & M.J. Hall (1996) The effects of afforestation and deforestation on water yields. Journal of Hydrology, 178: 293-309

- Sakai R, Fitzjarrald D, Moraes O, Staebler R, Acevedo O, Czikowsky M,Silva R, Brait E, Miranda V (2004) Land-use change effects on localenergy, water, and carbon balance in an Amazonian agricultural field.Global Change Biology 10: 895–907
- Sansigolo CA, Kayano MT (2010) Trends of seasonal maximum and minimum temperatures and precipitation in southern Brazil for the 1913-2006 period. Theoretical and Applied Climatology 101:209-216
- Santhi C, Arnold JG, Williams JR, Dugas WA, Srinivasan R, Hauck LM (2001) Validation of the SWAT model on a large river basin with point and nonpoint sources. Journal of the American Water Resources Association 37(5):1169-1188
- Sarkar RP, Thapliyal V (1988) Climatic change and variability. Mausam, 39:127–138
- Schott JR, Salvaggio C, Volchok WJ (1988) Radiometric scene normalization using pseudo invariant features, Remote Sensing of Environment, 26:1-16
- Schulla J (1997) Hydrological modeling of river basins to assess the impact of climate change, Zurich Geographical writings 69 :161
- Scibek J, Allen DM, Cannon A, Whitfield P (2006) Ground-water-surface water interaction under scenarios of climate change using a high-resolution transient ground-water model. J Hydrol
- Sen PK (1968) Estimates of the regression coefficient based on Kendall's τ. Journal of the American Statistical Association 63:1379-1389
- Shanahan P, Jacobs BL (2007) Ground-water and cities. In Novotny, V. & P.R. Brown (Eds.), Cities of the Future: Towards Integrated Sustainable Water and Landscape Management: 122-140. IWA Publishing, London
- Singh J, Williams JD, Kolpin DW, Knapp HV, Arnold JG, Demissie M (2005) Hydrological Modeling of the Iroquois River Watershed Using HSPF and SWAT. Journal of the American Water Resources Association. 41 (2):343-360
- Singh N, Sontakke NA (2002) On climatic fluctuations and environmental changes of the Indo-Gangetic Plains, India. Climatic Change 52(3):287–313
- Singh P, Kumar V, Thomas T, Arora M (2008) Basin-wide assessment of temperature trends in the north-west and central India. Hydrol. Sci. J 53:421–433
- Song K, Wang Z, Liu Q, Liu D , Ermoshin VV, Ganzei SS , Zhang B , Ren C , Zeng L, Du Jia (2011) Land use/land cover (LULC) classification with MODIS time series data and validation in the Amur River Basin, Geography and Natural Resources 32(1):9-15
- Spruill CA, Workman SR, Taraba JL (2000) Simulation of daily and monthly stream discharge from small watersheds using the SWAT model. Trans. ASAE 43(6): 1431-1439
- Srivastava HN, Sinha Ray, KC, Dikshit SK, Mukhopadhaya RK (1998) Trends in rainfall and radiation over India. Vayu Mandal 41–45
- Steele TD, Gilroy EJ, Hawkinson RO (1974) Techniques for the assessment of areal and temporal variations in streamflow quality. Open File Report, US Geological Survey, Washington, DC

- Stefanski J, Mack B, Waske B (2013) Superpixel segmentation for object-based land use / land cover classification of RapidEye data, 5th RESA Workshop
- Stehr A, Debels P, Romero F, Alcayaga H (2008) Hydrological modelling with SWAT underlimited conditions of data availability: evaluation of results from a Chilean case study, J.Hydrol. Sci., 53:588–601
- Still DA, Shih SF (1985) Using Landsat to classify land use for assessing the basin-wide runoff index.Water Resources Bulletin. 21:931-939
- Stonefelt MD, Fontaine TA, Hotchkiss RH (2000) Impacts of Climate Change on Water Yield in the Upper Wind River Basin. Journal of the American Water Resources Association (JAWRA) 36(2):321-336
- Streck NAL, Oliveria I, Heldwein FB, Avila AB, Bosco LA, LC (2011) Modeling the development of cultivated rice and weedy red rice. Transactions of the American Society of Agricultural and Biological Engineering 54:371-384
- SWAT CUP (2012) user manual, available at: http://www.neprashtechnology.ca/Downloads/SwatCup/Manual/Usermanual_Swat_Cup.pdf
- Tabari H, Talaee PH (2011) Recent trends of mean maximum and minimum air temperatures in the western half of Iran. Meteorology and Atmospheric Physics, 11:121-131
- Thapliyal V, Kulshrestha SM (1991) Climate changes and trends over India. Mausam 42:333–338
- Schulthess U, Weichelt H, Grundner S, Stein C, Schelling K, Reigber S, Höber E, Grüner V, Rothenhäusler FJ (2006) Multi Temporal Land Cover Classification Approach With New Rapideye Imagine, Center for Remote Sensing of Land Surfaces, Bonn
- Van BG, Hughes JP (1984) Nonparametric tests for trends in water quality. Water Resour. Res., 20(1):127-136
- Van Liew MW, Garbrecht J (2001) Sensitivity of hydrologic response of an experimental watershed to changes in annual precipitation amounts. ASAE Paper No. 012001. St. Joseph, Mich.: ASAE
- Venkata Reddy K , Eldho TI ,Rao EP , Kulkarni AT (2011) FEM-GIS based channel network model for runoff simulation in agricultural watershed using remotely sensed data, International journal of River Basin Management 9(1) :17-30
- Verbeeten E, Barendregt A (2007) Assessing the Impact of Climate Change on the Water Balance in SemiArid West Africa: a SWAT Application young researchers forum proceedings of the 5th Geographic Information Days, 10-12. Münster, Germany. 309-12
- Verhoef W (1996) Application of Harmonic Analysis of NDVI Time Series (HANTS). In Fourier Analysis of T emporal NDVI in the Southern African and American Continents, edited by Azzali S ,Menenti M, DLO Winand Staring Centre, Wageningen, The Netherlands, Report 108:19–24

- Verhoef W, Menenti M, Azzali S (1996) A colour composite of NOAA-AVHRR- NDVI based on time series (1981–1992). International Journal of Remote Sensing 17:231–235
- Villarreal ML, Norman LM, Webb RH, Boyer DE ,Turner RM (2011) Unravelling long-term vegetation change patterns in a binational watershed using multitemporal land cover data and historical repeat photography. Proceedings of MULTITEMP 2011, 6th International Workshop on the Analysis of Multitemporal Remote Sensing Images. Bruzzone, L. and F. Bovolo (Eds.). IEEE Geoscience and Remote Sensing Society, IEEE Xplore:101-104
- Volcani A, Karnieli A, Svoray T (2005) The use of remote sensing and GIS for spatio-temporal analysis of the physiological state of a semi-arid forest with respect to drought years, Forest Ecology and Management, vol 215, pp. 239–250
- Von Storch H (1995) Misuses of statistical analysis in climate research, in Analysis of Climate Variability Applications of Statistical Techniques
- Wang S, Feng J, Liu G (2013) Mathematical and Computer Modelling 58:677–683
- Wagner PD, Kumar S, Schneider K (2013) An assessment of land use change impacts on the water resources of the Mula and Mutha Rivers catchment upstream of Pune, India. Hydrol. Earth Syst. Sci., 17, 2233–2246. doi:10.5194/hess-17-2233-2013
- Weng S (2010) Changes of Diurnal Temperature Range in Taiwan and Their Large-Scale Associations: Univariate and Multivariate Trend Analyses. Journal of the Meteorological Society of Japan, 88:203-226
- Wilby RL, Charles SP, Zorita E, Timbal B, Whetton P, Mearns LO (2004) Guidelines for use of climate scenarios developed from statistical downscaling methods: supporting material of the Intergovernmental Panel on Climate Change. Task Group on Data and Scenario Support for Impacts and Climate Analysis, Rotherham
- Winter TC, Harvey JW, Franke OL, Alley WM (1998) Ground-water and Surface Water: A Single Resource. US. Geological Survey, Circular 1139, Denver, Colorado, USA
- Xie Y, Sha Z, Yu M (2008) Remote sensing imagery in vegetation mapping: a review. Journal of Plant Ecology, 1(1):9-23
- Xu ZX, Takeuchi K, Ishidaira H (2003) Monotonic trend and step changes in Japanese precipitation. Journal of Hydrology; 279:144-150
- Xu ZX, Zhao FF, Li JY (2009) Response of streamflow to climate change in the headwater catchment of the Yellow River basin. Quaternary International, Volume 208, Issues 1–2, Pages 62–75
- Yang T, Zhang Q, Chen Y, Tao X, Xu C, Chen X (2008) A spatial assessment of hydrologic alteration caused by dam construction in the middle and lower Yellow River, China, Hydrol. Process. 22:3829–3843
- Young MD, Evans R (1998) Right opportunity — Using right markets to manage diffuse ground-water pollution. Occasional Paper Land and Water Resources Research and Development Corporation Australia 19:97

- Yuan F, Sawaya KE, Loeffelholz BC, Bauer ME (2005) Land cover classification and change analysis of the Twin Cities (Minnesota) Metropolitan Area by multi-temporal Landsat remote sensing. Remote sensing of Environment, 98 (2&3): 317-328. http://dx.doi.org/10.1016/j.rse.2005.08.006.
- Yue S, Hashino M (2003) Long term trends of annual and monthly precipitation in Japan. Journal of the American Water Resources Association. 39, 587-596
- Yue S, Pilon P, Phinney B, Cavadias G (2002) The influence of autocorrelation on the ability to detect trend in hydrological series. Hydrol Process 16:1807– 1829
- Yue S, Pilon P, Cavadias, G. (2002) Power of the Mann–Kendall and Spearman's rho tests for detecting monotonic trends in Hydrological series. Journal of Hydrology 259 (1-4): 254-271
- Yüksel A, Akay AE, Gundogan JC (2008) Using ASTER Imagery in Land Use/cover Classification of Eastern Mediterranean Landscapes According to CORINE Land Cover Project, Sensors 8: 1237-1251
- Yulianti JS, Burn DH (1998) Investigating links between climatic warming and low streamflow in the Prairies Region of Canada. Can. Water Resour. J. 23 (1):45–60
- Yusoff I, Hiscock KM, Conway D (2002) Simulation of the impacts of climate change on ground-water resources in eastern England. In Sustainable Ground-water Development. Eds. K. M. Hiscock, M. O. Rivett, R.M. Davidson. The Geological Society Publishing House, Bath. 325-344
- Zetterqvist, L. (1991) Statistical estimation and interpretation of trends in water quality time series. Water Resour. Res. 27(7), 1637–1648.
- Zhang Q, Ban Y (2010) Monitoring impervious surface sprawl using Tasseled Cap transformation of Landsat data. Wagner W and Székely, B (eds), ISPRS TC VII Symposium – 100 Years ISPRS.XXXVIII, Part 7A
- Zhang X, Harvey KD, Hogg WD, Yuzyk TR (2001) Trends in Canadian streamflow. Water Resour. Res. 37(4):987–998
- Zhu G, Blumberg DG (2001) Classification using ASTER data and SVM algorithms; The case study of Beer Sheva, Israel Remote Sensing of Environment 80:233–240

ACKNOWLEDGMENTS

During the journey of my Ph.D. study, I have been supported by numerous people including my well-wishers, supervisors, friends and family. It is a great pleasure to show my gratitude to all these people who made this thesis possible.

First of all I would like to express my deepest gratitude towards German Academic Exchange Service (DAAD) for their financial assistance in the form of a scholarship, which allowed me to undertake this study. I gratefully acknowledge the financial support of the Dr. Hermann Eiselen Doctoral Program of the Foundation Fiat Panis during my field research that also enabled me to attend several conferences and workshops.

At this moment of accomplishment, I owe my gratitude to my supervisor Prof. Dr. Janos J Bogardi, who supported me at every phase of my studies and provided his crucial time. Without his constant encouragement and guidance, this dissertation would not have materialized.

I am most grateful to my tutor, Dr. Bernhard Tischbein, for his constant guidance, support and personal attention. His invaluable advice and in-depth subject knowledge have always provided me with confidence and strength to accomplish my task. Despite his busy schedule, he always had time for the fruitful discussions and suggestions on my research. I will never forget his help all my life. I would also like to extend my greatest appreciation to my second supervisor Prof. Dr. Jürgen Kusche, who offered me his constructive advice and warm encouragement during my Ph.D. research.

I am extremely grateful to the entire ZEF community especially Dr. Günther Manske, the coordinator of ZEF's Doctoral program, Frau Rosemary Zabel and Frau Maike Retat-Amin who have been always kind, caring and supportive to me during my Ph.D. research.

I would like to thank Dr. Laux Patrick, Karlsruhe Institute of Technology, Germany, for his guidance on bias correction of PRECIS future rainfall and temperature scenarios of my study area. I am also grateful to Dr. Guido Luechters for providing his expertise on statistical trend detection analysis of climate data.

I should also like to sincerely thank Prof. Dr. Mukund Hambarde, Director General, and Mr. M.K. Beg, Senior Scientist, Chhattisgarh Council of Science and Technology (CGCOST), Raipur, India, for supporting collaboration and for facilitating the primary and secondary data collection for this study. Without their tremendous support, this study would not have been possible. I would also like to express my thanks to Mr. J.R. Verma, senior geo-hydrologist, CGWB, for providing me with his in-depth knowledge about the study area and helping me in conducting the field visits. I pay my deepest regards to all the Indian agencies that provided data for this study as well as to all the people involved for their cooperation.

I would also like to thank Dr. Daniel Moriasi and Dr. Jorge Gunzman, Agriculture Research Station, USDA, Oklahoma, USA, for providing their practical expertise and training on the coupling of SWAT and MODFLOW models.

I expand my thanks to my parents, brothers and wife who were always there as a supporting pillar beside me. Their support and encouraging words have helped me to endure all the dark phases of this journey. Over and above all, I thank God for his showers of blessings throughout my research work to complete the research successfully.